

**An *in vivo* anti-staphylococcal drug screen
using a zebrafish infection model implicates
host autophagy in *Staphylococcus aureus*
survival**

By

Lore Marie P.R. Lambein

A thesis submitted for the degree of Doctor of Philosophy

**Department of Chemistry
University of Sheffield**

May 2015

Summary

An established larval zebrafish model of staphylococcal infection has enabled us to develop and optimise an *in vivo* drug screening assay to identify small molecules with curative potential against *S. aureus* infection. One-day old zebrafish embryos were infected intravenously with *S. aureus*. At 70 hours post-infection, larvae survival was $45.3 \pm 6.2\%$ (mean \pm SEM) in the untreated control, and $96 \pm 8\%$ (mean \pm SEM) in the positive control (penicillin G treated 6.4 mg/L). Test compounds were dissolved in the fish water and hits were detected by their ability to promote the survival of the infected zebrafish. Hit compounds might act directly on the pathogen, or enhance the ability of immune cells to control infection.

Screening of 660 compounds from the Johns Hopkins clinical compound collection has identified 99 potential 'hits' that have been retested on a larger number of fish. Of these compounds, 22 showed an interesting effect after the secondary screening and have been tested in dose-response assays. One early hit was fusidic acid, a known anti-staphylococcal compound, demonstrating the ability of this method to identify anti-infective compounds.

Autophagy is a catabolic mechanism that degrades dysfunctional cellular components via the lysosomal machinery, and intracellular pathogens can be eliminated in this process. However some microorganisms have developed strategies to subvert autophagy to stay alive. Some evidences show that *S. aureus* is a facultative intracellular pathogen and that autophagy is essential for its survival within the host. Therefore, inhibition of autophagy would reduce *S. aureus* killing of the host. This hypothesis has been tested on the *S. aureus*-zebrafish infection model using several technical strategies.

Acknowledgments

I would first and foremost like to thank my 2 supervisors, Simon Jones and Steve Renshaw, for their support and expert advice throughout my PhD. I would also like to thank the members of the Infectious Disease Network for listening to my progress every 2 months and providing advice to the problems I was facing. In particular, I'd like to thank my 2 fellow PhD students Jamil Jubrail and John Connolly, as well as all the supervisors (Simon Foster, Moira Whyte, David Dockrell and Helen Marriott).

I would like to thank several people for their technical advice enabling me to perform experiments. My thanks go to Tomek Prajsnar, Alex Williams and Gareth McVicker for their advice with all the *S. aureus* aspect of the project and the associated infection techniques into zebrafish embryos; to Anne Robertson for her technical advice on drug screen with zebrafish larvae; to Catherine Loynes and Katy Henry for their advice with molecular biology techniques; to Tomek Prajsnar and Nik Ogryzko for their help with microscopy; to Pranvira Sadiku, Tida Tong and Stone Elworthy for their advice with the TALEN technique to generate zebrafish mutant line. My thanks also go to the aquarium staff, the screening facility of the Bateson centre and all the people that I have met during my PhD.

I finally would like to thank all my family and friends outside the lab for their moral support, especially in the difficult times.

I am grateful to the University of Sheffield for funding this project and enabling me to perform my research.

List of abbreviations

agr	Accessory gene regulator
Akt	Protein Kinase B
AMP	Antimicrobial peptide
AMPK	AMP-activated protein kinase
ATG	Autophagy related proteins
ATP	Adenosine triphosphate
BVC	<i>Brucella</i> -containing vacuole
Beclin-1	Bcl-2-interacting protein 1
BHI	Brain Heart Infusion
bp	base pair
CA	Community-acquired
Ca²⁺	Calcium ion
cAMP	Cyclic adenosine monophosphate
CFP	Cyan fluorescent protein
CFT-1	Cystic fibrosis tracheal epithelial cells
CFU	Colony Forming Unit
CHIPS	Chemotaxis inhibitory protein of staphylococci
Cif	Clumping factor
CNS	Coagulase-negative staphylococci
°C	Degrees Celsius
dAdo	2'-deoxyadenosine
DIC	Differential interference contrast
DMSO	Dimethyl sulfoxide
DNA	Deoxyribonucleic acid
dNTPs	Deoxyribonucleoside-5'-phosphate
dpf	Day post fertilisation
dpt	Day post treatment
DNA	Deoxyribonucleic acid
DSB	Double strand break
EGFP	Enhanced GFP
ER	Endoplasmic reticulum
FACS	Fluorescence-activated cell sorting
FAD	Flavin adenine dinucleotide
fMLP	Formyl-methionyl-leucyl-phenylalanine
FnBPs	Fibronectin-binding proteins
GABARAP	g-aminobutyric-acid-type-A-receptor-associated protein
GAS	Group A <i>Streptococcus</i>
GATE-16	Golgi-associated ATPase enhancer of 16 kDa
GcAVs	GAS-containing autophagosome-like vacuoles
GFP	Green fluorescent protein
h	Hours
HA	Hospital-acquired
HCV	Hepatitis C virus
HDR	Homology directed repair
HeLa	Human epithelial cells
Hla	Alpha-hemolysin

hpf	Hours post fertilisation
hpi	Hours post infection
hpt	Hours post treatment
IFN	Interferon
IgG	Immunoglobulin G
IL-	Interleukin
IMPase	Inositol monophosphatase
IP3	Myoinositol-1,4,5-triphosphate
LAMP-1	Lysosomal-associated membrane protein 1
LB	Luria-Bertani
LCFSN	Complemented counterpart of cystic fibrosis tracheal epithelial cells
LC3	Microtubule-associated protein 1A/1B-light chain 3
LIR	LC3-Interacting Region
LLO	Listeriolysin O
LPS	Lipopolysaccharide
LWT	London wild-type
MAPK	Mitogen-activated protein kinase
MEF	Mouse embryonic fibroblasts
MHC II	Major histocompatibility complex class II
min	Minutes
MO	Morpholino oligonucleotide
MPO	Myeloperoxidase
MPX	Myeloid specific peroxidase
mRNA	Messenger RNA
MRSA	Methicillin-resistant <i>S. aureus</i>
MSCRAMM	Microbial-Surface Components Recognising Adhesive Matrix Molecules
MSSA	Methicillin-sensitive <i>S. aureus</i>
mTOR	Mammalian target of rapamycin
Myd88	Myeloid differentiation factor 88
NA	Numerical aperture
NAC	N-acetyl cysteine
NBR1	NBR1 neighbor of BRCA1 gene 1
NDP52	Nuclear dot protein 52 kDa
NET	Neutrophil extracellular trap
NF-κB	Nuclear factor kappa-light-chain-enhancer of activated B cells
NHEJ	Non-homologous end-joining
NH₄Cl	Ammonium chloride
NLRP3	NOD-like receptor family, pyrin domain containing 3
NOD	Nucleotide-binding oligomerisation domain
OD	Optical density
OPTN	Optineurin
PAMP	Pathogen-associated molecular pattern
PBP	Penicillin-binding protein
PBS	Phosphate buffered saline
PCR	Polymerase chain reaction
PE	Phosphatidylethanolamine
PI3K	Phosphatidylinositol-3-kinase
PI3P	Phosphatidylinositol-3,4,5-triphosphate

PLC	Phospholipase C
PRRs	Pattern recognition receptors
PSM	Phenol soluble modulins
PVL	Panton-Valentine Leukocidin
RFP	Red fluorescent protein
RNA	Ribonucleic acid
ROS	Reactive oxygen species
rpm	Revolutions per minute
RVD	repeat-variable di-residue
SCCmec	Staphylococcal Cassette Chromosome mec
SCV	Small colony variant
SEM	Standard error of the mean
SLO	Streptolysin O
SLRs	Sequestome 1/p62-like receptors
SpA	Staphylococcal protein A
TAL	Transcription activator-like
TALEN	Transcription activator-like effector nuclease
TCRS	Two-component regulatory system
TLR	Toll-like receptor
TNF-α	Tumor necrosis factor alpha
T3SS	Type III secretion system
UAS	Upstream activation sequence
UV	Ultra violet
VDR	Vitamin D receptor
Vps34	Vacuolar protein sorting 34
v/v	Volume for volume
WT	Wild-type
w/v	Weight for volume
ZFN	Zinc-finger nuclease

Table of contents

Summary	2
Acknowledgments	3
List of abbreviations	4
Table of contents	7
List of Figures	10
List of Tables	13
Chapter 1: Introduction	14
1.1. <i>Staphylococcus aureus</i> (<i>S. aureus</i>)	14
1.1.1. Microbiology of <i>S. aureus</i>	14
1.1.2. <i>S. aureus</i> carriage and disease.....	16
1.1.3. <i>S. aureus</i> pathogenesis and virulence factors	18
1.1.4.2. Immune evasion strategies by <i>S. aureus</i>	26
1.1.5. Preventive strategies of staphylococcal infections	29
1.1.6. Antibiotic strategies and staphylococcal resistance	32
1.1.7. <i>S. aureus</i> as an intracellular pathogen.....	36
1.1.8. Animal models to study staphylococcal disease	36
1.2. <i>Danio rerio</i> as an animal model for infection	39
1.2.1. Zebrafish as a model organism	39
1.2.2. The zebrafish immune system	41
1.2.3. Zebrafish as an infection model for several pathogens.....	47
1.2.4. Zebrafish as an infection model for <i>S. aureus</i>	50
1.3. Zebrafish use in drug screening	52
1.3.1. Drug screening assays in zebrafish	52
1.3.2. Zebrafish-based drug screen assay	53
1.3.3. Zebrafish drug screen for antimicrobials	56
1.4. Thesis aims	58
Chapter 2 Materials and methods	59
2.1. Materials	59
2.1.1. <i>Staphylococcus aureus</i>	59
2.1.2. Zebrafish <i>Danio rerio</i>	60
2.1.3. Drugs.....	62
2.1.4. Molecular biology	63
2.1.5. Disposables.....	65
2.1.6. Instruments.....	65
2.1.7. Softwares	65
2.2. Methods	67
2.2.1. Culture of <i>S. aureus</i>	67
2.2.2. Direct cell counts (CFU.ml ⁻¹)	67
2.2.3. Zebrafish husbandry.....	67
2.2.4. Zebrafish marbling or pair mating.....	68
2.2.5. Zebrafish fin clip	68
2.2.6. Morpholinos injection into zebrafish eggs	69
2.2.7. Microinjection of <i>S. aureus</i> into zebrafish larvae.....	69

2.2.8. Determination of zebrafish larvae mortality following infection.....	71
2.2.9. Drug modulation by immersion on infected zebrafish	71
2.2.10. Mounting zebrafish larvae for microscopy	72
2.2.11. RNA extraction from zebrafish embryos.....	72
2.2.12. cDNA transcript from RNA samples	73
2.2.13. Polymerase Chain Reaction	73
2.2.14. Agarose gel	74
2.2.15. Sequencing	74
2.2.16. Construction of TALENs.....	75
2.2.17. Genotyping of mutation generated by TALENs.....	80
2.2.18. Genotyping of zebrafish mutant <i>apg3l</i> , <i>atg5</i> and <i>atg10</i>	84

Chapter 3 : An *in vivo* drug screen assay for novel anti-staphylococcal compounds..... 86

3.1. Introduction	86
3.1.1. Aims and hypotheses	88
3.2. Optimisation of experimental parameters of the screening assay..... 88	88
3.3. Identification of putative ‘hit’ compounds by primary screening..... 98	98
3.4. Further testing of putative ‘hit’ compounds in a secondary screen 99	99
3.5. Detailed analysis of effects of potential hits on <i>S. aureus</i> infection.... 107	107
3.5.1. Dose-response assays	107
3.5.2. Redosing assays	111
3.5.3. Retesting the newly purchased compounds in a survival assay	111
3.6. Examination of the effects of zinc sulfide on <i>S. aureus</i> infection 114	114
3.7. Examination of the properties of potential ‘anti-hits’ 115	115
3.8. Testing an immunomodulatory compound 120	120
3.9. Discussion	121

Chapter 4: The implication of autophagy in *S. aureus* infection 128

4.1. Introduction: Host autophagy in pathogenesis of infectious disease .128	128
4.1.1. Autophagy	128
4.1.2. Roles of autophagy during bacterial infections.....	133
4.1.3. Importance of autophagy in <i>S. aureus</i> pathogenesis	139
4.1.4. Autophagy in zebrafish.....	146
4.1.5. Aims and hypotheses	148
4.2. The <i>frozen</i> zebrafish strain and <i>S. aureus</i> infection 149	149
4.2.1. The <i>frozen</i> zebrafish strain	149
4.2.2. <i>S. aureus</i> infection in <i>frozen</i> fish	149
4.2.3. Mimicking the slow circulation of the <i>frozen</i> fish with tricaine	158
4.2.4. Distribution of <i>S. aureus</i> in the <i>frozen</i> fish compared to the siblings....	159
4.3. Modulation of autophagy using a pharmacochemical approach 159	159
4.3.1. Chemical enhancers of autophagy.....	160
4.3.2. Chemical inhibitors of autophagy	162
4.4. Modulation of autophagy by interfering at the transcription level 172	172
4.5. Utilisation of a transgenic zebrafish line to visualise autophagy..... 184	184
4.5.1. Transgenic zebrafish lines.....	184
4.5.2. Selection of the transgenic zebrafish lines	186
4.5.3. Expression of LC3 proteins exclusively in zebrafish macrophages.....	190
4.5.4. Expression of LC3 proteins exclusively in zebrafish neutrophils.....	199
4.5.5. Autophagosome formation in the <i>frozen</i> mutant	200
4.6. Discussion	210
4.6.1. <i>Frozen</i> mutant	210
4.6.2. Pharmacological approach	211
4.6.3. Morpholino approaches	217
4.6.4. Autophagy visualisation.....	219
4.6.5. Conclusions	221

Chapter 5: Generation of zebrafish <i>apg3l</i> mutants by genome editing with TALENs.....	223
5.1. Introduction	223
5.1.1. Genome editing with TALENs	223
5.1.2. The importance of ATG3 in the autophagy pathway	226
5.1.3. Aims and hypotheses	226
5.2. Generation of an <i>apg3l</i> mutant zebrafish line	227
5.2.1. Construction of the TALENs targeting exon 4 of the <i>apg3l</i> gene	227
5.2.2. Testing the efficiency of the TALENs targeting exon 4 of the <i>apg3l</i> gene	228
5.2.3. Effects of genomic polymorphism in <i>apg3l</i> locus	229
5.2.4. Screening potential founder fish for a defective mutation in exon 4 of the <i>apg3l</i> gene.....	230
5.2.5. Analysis of the <i>apg3l</i> mutation carried by the founder fish.....	236
5.2.6. Generation of heterozygous fish carrying a defective mutation in exon 4 of the <i>apg3l</i> gene.....	237
5.3. Screening <i>atg5</i> mutant zebrafish line.....	247
5.4. The <i>atg10</i> mutant zebrafish line.....	252
5.5. <i>S. aureus</i> infection into zebrafish mutant lines.....	254
5.5.1. Abscess formation precedes the death of <i>S. aureus</i> infected zebrafish embryos.....	254
5.5.2. Bacterial virulence in <i>apg3l</i> mutant zebrafish line	255
5.5.3. Bacterial virulence in <i>atg5</i> mutant zebrafish line	259
5.5.4. Bacterial virulence in <i>atg10</i> mutant zebrafish line	259
5.6. Discussion	263
Chapter 6: Conclusion and perspectives	269
6.1. The potential of an <i>in vivo</i> drug screen for the discovery of antistaphylococcal compounds.....	269
6.2. The <i>frozen</i> zebrafish mutant is resistant to <i>S. aureus</i> pathogenesis...	270
6.3. Autophagy.....	271
6.4. Generation of targeted mutation in zebrafish.....	271
6.5. Concluding remarks.....	271
References	273
Appendix 1	301

List of Figures

Figure 1.1. Regulation of virulence determinants in <i>S. aureus</i> by global regulatory loci.....	22
Figure 1.2. Schematic depiction of anatomical sites (a) and approximate durations (b) of hematopoietic activity in developing zebrafish.....	43
Figure 1.3. Injection methods used for establishing systemic or local infections in zebrafish embryos.....	49
Figure 2.1. <i>S. aureus</i> infection into zebrafish larvae.....	70
Figure 3.1. Visual detection of the alive or dead status of zebrafish embryos.....	92
Figure 3.2. Effect of 3 different staphylococcal doses on the survival of zebrafish embryos.....	93
Figure 3.3. Effect of freshly prepared and defrosted staphylococcal injection on the survival of zebrafish embryos.....	94
Figure 3.4. Increase in survival of infected zebrafish embryos treated with antibiotic.....	95
Figure 3.5.A. A zebrafish <i>in vivo</i> screen protocol for new anti-staphylococcal compounds.....	96
Figure 3.5.B. Flow chart of the antistaphylococcal screening strategy and the compounds tested.....	97
Figure 3.6. Heat map representing the 660 compounds screened with the systemic <i>S. aureus</i> infection model in zebrafish embryos.....	101
Figure 3.7. Survival curves of infected larvae treated with 3 highly effective potential hits.....	102
Figure 3.8. Survival curves of infected larvae treated with intermediate effective potential hit compounds.....	103
Figure 3.8. Survival curves of infected larvae treated with intermediate effective potential hit compounds.....	104
Figure 3.8. Survival curves of infected larvae treated with intermediate effective potential hit compounds.....	105
Figure 3.9. Effect of the delayed compounds on infected zebrafish embryos.....	106
Figure 3.10. Dose-response assays of potential 'hits'.....	109
Figure 3.11. Dose-response assays of potential 'hits'.....	110
Figure 3.12. Redosing assays of the potential 'hits'.....	112
Figure 3.13. Retest of of the potential 'hits' in secondary screen – like assay.....	113
Figure 3.14. <i>in vitro</i> effect of zinc sulfide on <i>S. aureus</i> growth.....	116
Figure 3.15. Testing other zinc derivatives compounds on <i>S. aureus</i> infected zebrafish larvae.....	117
Figure 3.16. Toxicity test of some 'antihit' compounds.....	118
Figure 3.17. Survival tests of some 'anti-hit' compounds.....	119
Figure 3.18. Testing the known immunomodulatory compound nicotinamide.....	122
Figure 4.1. Scheme of autophagy pathway.....	134
Figure 4.1. Scheme of autophagy pathway.....	135
Figure 4.2. Infection of <i>frozen</i> mutant zebrafish larvae with <i>S. aureus</i>	151
Figure 4.3. Tricaine treated zebrafish embryos.....	153
Figure 4.4. Survival curves of tricaine treated zebrafish embryos.....	154
Figure 4.5.A. Tails of zebrafish larvae infected with GFP-SH1000 at 2 hpi.....	155
Figure 4.5.B. Phagocytosis of GFP-SH1000 in the <i>frozen</i> mutant at 2 hpi.....	156
Figure 4.5.C. Whole body of zebrafish larvae infected with GFP-SH1000 at 2 hpi.....	157
Figure 4.6. Toxicity test of autophagy enhancing and inhibiting drugs.....	164
Figure 4.6. Toxicity test of autophagy enhancing and inhibiting drugs.....	165

Figure 4.7. Effect of the autophagy enhancer rapamycin on zebrafish embryos infected with <i>S. aureus</i>	166
Figure 4.8. Effect of the autophagy enhancer rilmenidine on zebrafish embryos infected with <i>S. aureus</i>	167
Figure 4.9. Effect of the autophagy enhancer carbamazepine or verapamil on zebrafish embryos infected with <i>S. aureus</i>	168
Figure 4.10. Effect of the PI3K inhibitors wortmannin or LY294001 on zebrafish embryos infected with <i>S. aureus</i>	169
Figure 4.11. Effect of the autophagy inhibitor +/- Bay K8644 on <i>S. aureus</i> infected zebrafish embryos	170
Figure 4.12. Effect of the autophagy inhibitor NAC or vitamin E acetate on <i>S. aureus</i> infected zebrafish embryos	173
Figure 4.13. Effect of the autophagy inhibitor NH ₄ Cl on <i>S. aureus</i> infected zebrafish embryos.....	174
Figure 4.14. Effect of the microtubule inhibitor nocodazole on <i>S. aureus</i> infected zebrafish embryos	175
Figure 4.15. Infection of autophagy knockdown zebrafish embryos	180
Figure 4.16. Infection of autophagy knockdown zebrafish embryos	181
Figure 4.17. Structure and mechanism of morpholinos	182
Figure 4.18. Efficacy of splice morpholinos <i>atg7</i> and <i>atg5</i>	183
Figure 4.19. Schematic representation of the RFP-GFP-LC3 tandem fluorescent system	188
Figure 4.20. Screening transgenic fish.....	189
Figure 4.21. Rapamycin induces the expression of autophagy LC3 proteins in zebrafish macrophages	192
Figure 4.22. A zebrafish infected macrophage containing a high number of <i>S. aureus</i> expresses autophagy LC3 proteins	193
Figure 4.23. <i>S. aureus</i> bacteria are localised in a LC3 proteins positive vacuole inside a zebrafish macrophage	194
Figure 4.24. Several <i>S. aureus</i> bacteria phagocytosed in a zebrafish macrophage are also colocalised with autophagy LC3 proteins	195
Figure 4.25. A large vacuole containing a few <i>S. aureus</i> bacteria expresses the autophagy LC3 proteins in an infected zebrafish macrophage at 6 h after infection	196
Figure 4.26. Colocalisation of autophagy LC3 proteins and a high number of <i>S. aureus</i> bacteria in an infected zebrafish macrophage at 6 h after infection ...	197
Figure 4.27. Colocalisation of autophagy LC3 proteins and <i>S. aureus</i> bacteria in a zebrafish macrophages 6 h after infection	198
Figure 4.28. Rapamycin induces the expression of autophagy LC3 proteins in zebrafish neutrophils	201
Figure 4.29. Rapamycin induces the expression of autophagy LC3 proteins in zebrafish neutrophils	202
Figure 4.30. Colocalisation of autophagy LC3 proteins and <i>S. aureus</i> bacteria inside a zebrafish neutrophil	203
Figure 4.31. <i>S. aureus</i> bacteria are localised in a LC3 proteins-decorated autophagosome inside a zebrafish neutrophil	204
Figure 4.32. Colocalisation of autophagy LC3 proteins and <i>S. aureus</i> bacteria in an infected zebrafish neutrophil	205
Figure 4.33. Colocalisation of autophagy LC3 proteins and <i>S. aureus</i> bacteria in a zebrafish neutrophil 6 h after infection	206
Figure 4.34. Colocalisation of autophagy LC3 proteins and <i>S. aureus</i> bacteria in an infected macrophage of the zebrafish <i>frozen</i> mutant	207
Figure 4.36. Colocalisation of autophagy LC3 proteins and 2 <i>S. aureus</i> bacteria in an infected neutrophil of the zebrafish <i>frozen</i> mutant	209

Figure 5.1. BLAST alignment of zebrafish Apg3l protein sequence and human Atg3 protein sequence	231
Figure 5.2. Design of the TALENs targeting the exon 4 of the zebrafish <i>apg3l</i> gene	232
Figure 5.3. TALEN plasmid construction and the mRNA synthesis	233
Figure 5.4. Testing the efficacy of <i>apg3l</i> TALEN after mRNA injection into 1-cell stage zebrafish egg	234
Figure 5.5. Effects of genomic polymorphism in <i>apg3l</i> locus	235
Figure 5.6. Screening the progeny of founder fish carrying an Atg3 mutation	238
Figure 5.7. Sequencing result of founder 1 around the TALEN spacer region.....	239
Figure 5.8. Sequencing result of founder 2 around the TALEN spacer region.....	240
Figure 5.9. Sequencing result of founder 3 around the TALEN spacer region.....	241
Figure 5.10. Sequencing result of founder 4 around the TALEN spacer region.....	242
Figure 5.11. BLAST alignment between Apg3l zebrafish protein sequence and the hypothesised protein sequence due to the TALEN mutation	243
Figure 5.12. BLAST alignment between Apg3l zebrafish protein sequence and the hypothesised protein sequence due to the TALEN mutation	244
Figure 5.13. BLAST alignment between Apg3l zebrafish protein sequence and the hypothesised protein sequence due to the TALEN mutation	245
Figure 5.14. BLAST alignment between Apg3l zebrafish protein sequence and the hypothesised protein sequence due to the TALEN mutation	246
Figure 5.15. Genotyping of the <i>apg3l</i> mutants	249
Figure 5.16. The 23 bp mutation in exon 3 of the <i>atg5</i> gene.....	250
Figure 5.17. The 23 bp mutation in exon 3 of the <i>atg5</i> gene.....	251
Figure 5.18. Genotyping of the <i>atg10</i> ^{Δ2} mutants	253
Figure 5.19. Late stage of staphylococcal infection can be recorded via mortality or abscesses formation	256
Figure 5.20. <i>S. aureus</i> infection of the <i>apg3l</i> ^{ΔCTATCTGCCC} mutant zebrafish line	257
Figure 5.21. <i>S. aureus</i> infection of the <i>apg3l</i> ^{ΔCTATCTGCCC} mutant zebrafish line	258
Figure 5.22. <i>S. aureus</i> infection of the <i>atg5</i> ^{Δ23} mutant zebrafish line	260
Figure 5.23. <i>S. aureus</i> infection of the <i>atg10</i> ^{Δ2} mutant zebrafish line	261
Figure 5.24. <i>S. aureus</i> infection of the <i>atg10</i> ^{Δ2} mutant zebrafish line	262
Figure Appendix 1: BLAST alignment of zebrafish and human protein sequences of A) Atg5, B) Atg7, C) Atg10 and D) Atg16L1	302

List of Tables

Table 1.1. Various toxins and enzymes produced by <i>S. aureus</i> with their physiological action on the host	21
Table 4.1. Observations of the state of the circulation of LWT zebrafish embryos treated with tricaine at the indicated concentration.	152

Chapter 1: Introduction

The pathogenic bacteria *S. aureus* causes multiple diseases and is a global challenge to human health, especially due to problems of antibiotic resistance. Alternative treatment strategies are required to treat staphylococcal infections, for example immune system enhancement, or targeting *in vivo* bacterial virulence factors to avoid rapid evolutionary resistant bacterial strains. An *in vivo* drug screen is one approach to identify this kind of treatment. The zebrafish, *Danio rerio*, is a convenient vertebrate animal model with a similar innate immune system as humans at their early stage of development. Zebrafish embryos have been established as a good infection model for systemic *S. aureus* pathogenesis (Prajsnar, Cunliffe et al. 2008). In addition, they are suitable for drug screen assays due to their small size that can be contained in a well of a 96-well plate and their permeability to small molecules.

The first anti-infective *in vivo* drug screen assay to be performed using the *S. aureus*-zebrafish infection model is discussed in chapter 3. Further investigations on a mechanistic host pathway subverted by *S. aureus* to survive and replicate is discussed in chapters 4 and 5.

1.1. *Staphylococcus aureus* (*S. aureus*)

1.1.1. Microbiology of *S. aureus*

S. aureus was first discovered in pus of surgical abscess, in 1880 by the surgeon Sir Alexander Ogston in Aberdeen, Scotland (Ogston 1984). Among the huge community of bacteria, staphylococci are part of the Gram-positive bacteria subset. Gram-positive bacteria can retain the violet stain used in the Gram staining method, which is due to their cell wall architecture. Gram-positive bacteria are usually composed of a cytoplasmic lipid membrane

surrounded by a thick peptidoglycan layer, in which lipoteichoic acids are attached and the peptidoglycan chains are cross-linked by DD-transpeptidases. On an agar plate, staphylococci appear as large round colonies. At high magnification under a microscope, staphylococci appear as small cocci about 1 μm in diameter and they are usually assembled in clusters resembling grapes, due to the division pattern of the cells in 3 perpendicular planes while the sister cell remains attached to the other sister cell (Turner, Ratcliffe et al. 2010). Staphylococci are facultative anaerobes, growing by both aerobic respiration and fermentation. The catalase test is a common identification test to distinguish staphylococci that are catalase positive, from bacteria belonging to the genus streptococci that are catalase negative. The catalase test is performed by flooding an agar slant or broth culture with several drops of 3% hydrogen peroxide. The catalase-positive cultures are recognised by their bubbling aspect. Staphylococci are oxidase negative, salt tolerant and usually haemolytic. The capability of staphylococcal strains of clotting blood plasma depends on the presence of the coagulase enzyme, leading to a differentiation between coagulase negative strains and coagulase positive strains. The pigmentation colour produced by staphylococci lead to subcategories between yellow-producing staphylococcus, called “golden staph” in English, or *S. aureus* in latin; and the white-producing staphylococcus, initially called *S. albus*, and now called *S. epidermidis*. Even though coagulase-negative staphylococci (CNS) were considered as apathogenic at the time of their discovery, several studies have detected *S. epidermidis* infections among immunocompromised patients carrying indwelling or implanted devices (Keys and Hewitt 1973). The main virulence factor of these CNS is their biofilms, which enable their attachment and persistence on foreign materials, and act as protection against antibiotics or immune defences (Piette and Verschraegen 2009). The *Staphylococcus* genus comprises more than 40 species, which belong in one of the 11 clusters. The taxonomy is usually determined with the 16S rRNA sequences. Other genotyping methods have been developed, such as *sodA*, *gap*, *rpoB*, *hsp60* and *tuf* gene sequencing (Ghebremedhin, Layer et al. 2008). Staphylococci are found worldwide, but only *S. aureus* and *S.*

epidermidis have potential pathogenic interactions with humans (Foster 1996; Prescott, Harley et al. 1999).

1.1.2. *S. aureus* carriage and disease

S. aureus is a commensal bacteria that is also the main pathogenic staphylococcal strain that can cause several forms of infections. *S. aureus* is responsible for some superficial skin lesions such as boils, furuncles, styes or impetigo. *S. aureus* is also a causative agent of more serious diseases such as pneumonia, mastitis, phlebitis, meningitis, and urinary tract infections, or even life-threatening diseases localised in deep-seated organs, such as osteomyelitis and endocarditis. *S. aureus* can be acquired in hospitals, and is the second most common source of nosocomial bloodstream infections coming from surgical wounds. *S. aureus* can also cause food poisoning and toxic shock syndrome. Food poisoning is caused by the release of enterotoxins by the bacteria into the food, while the toxic shock syndrome is due to the release of superantigens into the blood stream by *S. aureus*.

The primary ecological niche of *S. aureus* in humans is the nasal vestibule. The nares microbial population may vary between hospitalised and healthy populations. Longitudinal studies showed that about 20% of the healthy people persistently carry *S. aureus* in their nose, 30% are intermittent carriers and 50% of the population are never or rarely colonised (Wertheim, Vos et al. 2004). In the anterior nares, which are histologically described as stratified keratinised squamous non-ciliated epithelium, *S. aureus* competes with other microbial species. By culture-based and molecular studies, it was demonstrated that healthy people carry mainly members of the phylum Actinobacteria (e.g. *Propionibacterium spp.* and *Corynebacterium spp.*), but also Firmicutes (e.g. *Staphylococcus spp.*) and Proteobacteria (e.g. *Enterobacter spp.*). The number of Actinobacteria is reduced in the bacterial population of *S. aureus* carriers. In addition, the carriage of *S. aureus* is negatively associated with species such as *S. epidermidis* (Frank, Feazel et al. 2010). A study compared the microbiota of 3 special areas of the nasal environment: anterior nares, middle meatus and sphenoethmoidal recess,

and exposed the slightly different microbial community in function of the site epithelium type. *Corynebacterium accolens* and *Corynebacterium pseudodiphtheriticum* were identified as being an important factor in determining the presence or absence of *S. aureus*. Cocultures of these species *in vitro* showed that *C. accolens* and *S. aureus* are promoting each other growth, while *C. pseudodiphtheriticum* and *S. aureus* are in competition, interfering with the growth of the other bacteria (Yan, Pamp et al. 2013).

The risk of developing nosocomial infections for hospitalised patients is higher in *S. aureus* carriers compared to non-carriers. *S. aureus* carriers have a three-fold higher susceptibility to contracting staphylococcal infections, which is clonally identical to their nasal isolate in more than 80% of the cases. However, the outcome of nosocomial bacteraemia is more dramatic for non-*S. aureus* carriers, as they have a higher chance of mortality following bacteraemia. This could illustrate that *S. aureus* carriers that develop bacteraemia, which is usually the same endogenous strain they carry, might be immunologically adapted to that strain. Another possibility is that exogenous strains attacking non-carriers patients are more virulent (von Eiff, Becker et al. 2001; Wertheim, Vos et al. 2004). Nosocomial MRSA (methicillin-resistant *S. aureus*) bacteraemia induce greater infections and increase the mortality risk of the patients of about 2 times compared to MSSA (methicillin-sensitive *S. aureus*) bacteraemia (Wang, Chen et al. 2008). The risk of getting nosocomial *S. aureus* infections is higher for hospitalised patients for surgery, on haemodialysis, on continuous ambulatory peritoneal dialysis, HIV-infected or in intensive care units. In an attempt to prevent *S. aureus* infection, mupirocin prophylaxis is the most common strategy used, even though it is not routinely applied in hospitals. This strategy involves an intranasal treatment of patients with an ointment of the antibiotic mupirocin to eliminate the nasal carriage of *S. aureus*. Several randomised trials in different hospitalised units have tested the effectiveness of mupirocin treatment among *S. aureus* carriers. The authors conclude that mupirocin treatment of *S. aureus* carriers results in a statistically significant reduction in staphylococcal infections (van Rijen, Bonten et al. 2008).

An increased proportion of the population that has not been hospitalised or received a surgical procedure in the past year gets infected by *S. aureus*. This type of staphylococcal infection is called community-acquired *S. aureus* infection (CA-*S. aureus*). These community outbreaks have been reported in sports teams, child care attendees, prison inmates, and diverse populations where habitation is relatively concentrated. CA-*S. aureus* strains are usually methicillin-resistant, and therefore called CA-MRSA, which increases the public-health problem. CA-MRSA are infecting healthy people, causing skin and soft tissue disease in the vast majority of the cases (Fridkin, Hageman et al. 2005). Due to environmental pressures, CA-MRSA isolates have evolved different characteristics to hospital-acquired MRSA (HA-MRSA), such as virulence factors, fitness attributes and resistance traits (Zetola, Francis et al. 2005). CA-MRSA have acquired some toxic genes such as the one encoding Panton-Valentine leukocidin (PVL). CA-MRSA have also adapted the expression pattern of some genome-encoded genes such as alpha-toxin and phenol-soluble modulins (PSM) (Otto 2013). An example of very successful and epidemic CA-MRSA is the USA300 strain, which has acquired genes present on the arginine catabolic mobile element, including the *speG* gene encoding a spermidin N-acetyltransferase that detoxifies host-derived polyamines (Joshi, Spontak et al. 2011).

1.1.3. *S. aureus* pathogenesis and virulence factors

The pathogenicity of *S. aureus* strains is associated with their virulence determinants, which are accessory gene products non-essential for growth and cell division, but which provide an advantage in some circumstances. They are usually encoded on mobile genetic elements such as plasmids, transposons, prophages and pathogenicity islands. Virulence factors are expressed at different stage of infection depending on their specific actions. Some of them promote the adherence to host surface, other help the invasion of the tissues or the avoidance of host immune system, and finally some other cause harmful toxic effects to the host. The combined effects of these virulence determinants influence the pathogenicity of the staphylococcal strains. The virulence factors include antigens, enzymes and

toxins. The adherence of *S. aureus* to host proteins is mediated by surface proteins and “adhesins”. These molecules recognise components of the extracellular matrix or blood plasma, including fibrinogen, fibronectin, and collagens. Typical members of the family of adhesins called MSCRAMM (Microbial-Surface Components Recognising Adhesive Matrix Molecules) are staphylococcal protein A (SpA), fibronectin-binding proteins A and B (FnbpA and FnbpB), collagen-binding protein, and clumping factor (Clf) A and B proteins. Other types of toxins can penetrate into host cells and are called “invasins”. They often have a cytolytic action that can cause breakdown and lysis of host cells. These cytolytic toxins are divided into 3 classes: the amphiphilic peptides such as phenol soluble modulins and delta-toxins, the single component toxins such as alpha-toxin and the bicomponent leukotoxins such as leukocidins and gamma haemolysins. The infectious symptoms are usually caused by exotoxins that damage host tissues. Exotoxins include toxic shock syndrome toxin, exfoliative toxins A and B, and different staphylococcal enterotoxins. The major staphylococcal toxins and enzymes and their physiological actions on the host are reported in Table 1.

The expression of staphylococcal virulence determinants is timely regulated by a complex network of interacting regulatory factors. Two major groups of global regulatory elements exist in *S. aureus*: the two-component regulatory systems (TCRSs) and the SarA protein family. There are 16 putative TCRSs that are composed of a membrane sensor histidine kinase and a response regulator protein. The most important TCRS is the *agr* (accessory gene regulator) locus that activates the expression of most exoproteins while represses the synthesis of cell wall associated proteins during the postexponential phase. Other TCRSs would include *saeRS*, *srrAB*, *arlSR* or *lytRS* systems (Bronner, Monteil et al. 2004). The SarA protein family is a collection of DNA binding proteins that are divided into three subfamilies: the single domain proteins, the double domain proteins and the MarR homologs. The SarA protein family members bind DNA through the attachment of the helix-turn-helix binding domain to the major groove of DNA while the winged region interacts with the minor groove. Even though the binding domains are conserved, the activation domains are different for the different SarA protein

family members, reflecting their divergent functions. The mechanism of gene regulation by the SarA protein family acts via direct binding to the target gene promoter, via binding to general regulons such as *agr*, or via the stabilisation of mRNA during log phase. In particular, the expression of the prototype member of this family, SarA, starts at the end of the exponential phase. SarA enhances the synthesis of fibronectin, fibrinogen binding protein and toxins (α , β and δ) and represses the expression of protein A and proteases (Cheung, Nishina et al. 2008). Next to the global regulatory elements, staphylococcal virulence genes are also modulated by alternative sigma factors such as SigA or SigB. SigA controls the expression of house-keeping genes (Deora and Misra 1996), while SigB is activated by environmental stress, stimuli and energy depletion (Chan, Foster et al. 1998), and is regulated by RsbU (Horsburgh, Aish et al. 2002). The SH1000 *S. aureus* strain has a restored active RsbU gene.

All these regulatory systems modulate the timing for the expression or repression of the different virulence factors, which is determined by the growth stage, infection stage and the local environment such as the concentration of autoinducing peptides, bacterial density, pH, CO₂ and host signals. It is a highly complex regulatory system that controls the pathogenicity of *S. aureus*, generating a variety of diseases. For example, attachment and surface proteins are important at the early stages of infection whereas exoproteins must be secreted during tissue invasion, which has to be nicely regulated (Figure 1.1.). Transcriptional analyses of virulence regulators performed in *in vivo* models do not always correlate to the results of similar analyses performed *in vitro*, highlighting the importance of the role of staphylococcal virulence factors *in vivo* (Pragman and Schlievert 2004). Indeed, the *in vivo* conditions experienced by *S. aureus* inside a host are different than the conditions created in a flask culture *in vitro*. The expression pattern of the virulence factors is influenced by these different conditions (Novick 2003; Cheung, Bayer et al. 2004).

Bacterial product	Physiological action
β-lactamase	Induction of a break in β-lactam antibiotics such as penicillins
Catalase	Conversion of hydrogen peroxide into water and oxygen and reduction of killing by phagocytosis
Coagulase	Coagulase interacts with prothrombin to form a complex that enable the enzyme protease to cleave fibrinogen in fibrin, resulting in clotting of the blood. Coagulase causes the formation of a fibrin coat on the surface of staphylococci upon contact with blood, which protects the bacteria from phagocytosis.
DNase	Destruction of DNA
Enterotoxins	Family of 9 serological types of heat-stable toxins, causing gastroenteritis following the ingestion of contaminated food
Exfoliative toxins A and B	Causing the loss of the surface layers of the skin in scalded-skin syndrome (SSSS)
Haemolysins	α Haemolysin destroys erythrocytes and causes skin destruction β Haemolysin destroys erythrocytes and sphingomyelin around nerves γ Haemolysin destroys erythrocytes δ Haemolysin destroys erythrocytes
Hyaluronidase	Hyaluronidase catalyses the hydrolysis of the extracellular matrix component hyaluronan, facilitating the spread of the bacteria between the tissues.
Panton-valentine leukocidin (PVL)	PVL creates pores into the membranes of infected cells
Lipases	Digestion of lipids
Nucleases	Breakdown of nucleic acids
Protein A	Disruption of phagocytosis and opsonisation through the binding to the Fc portion of most immunoglobulins
Proteases	Breakdown of proteins
Staphylokinase	Activation of plasminogen to form plasmin, which dissolves fibrin clots Inhibition of phagocytosis
Staphyloxanthin	Carotenoid pigment with an antioxidant action to avoid death by reactive oxygen species
Toxic shock syndrome toxin-1 (TSST-1)	Induction of the toxic shock syndrome, with symptoms such as high fever, low blood pressure, malaise and confusion, rash

Table 1.1. Various toxins and enzymes produced by *S. aureus* with their physiological action on the host

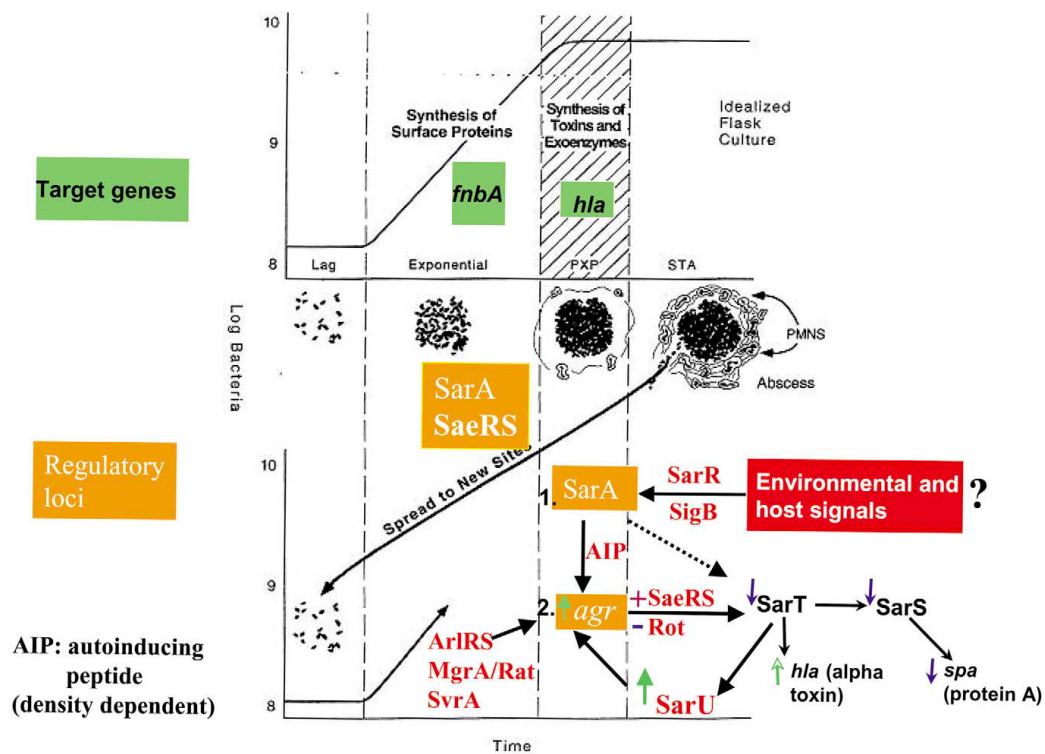


Figure 1.1. Regulation of virulence determinants in *S. aureus* by global regulatory loci.

Normally, the synthesis of cell surface adhesins such as fibronectin binding protein A during the exponential phase coincides with the expression of SarA and Sae, suggesting regulation of fibronectin A (*fnbA*) by these two loci. And in transition from exponential to postexponential phase, the synthesis of cell wall proteins is disrupted and the production of extracellular toxins such as alpha-toxin would begin. This transition corresponds to the maximal expression of SarA and the ensuing activation of *agr*. SarA expression is controlled by SarR, a SarA protein homolog, and SigB, a stress-induced transcription factor. On the other hand, *agr* is controlled by SarA, a quorum sensing AIP, a TCRS called ArIRS, MgrA/Rat/NorR and also a novel membrane protein called SvrA. Activation of *agr* would lead to up-regulation of another TCRS system called Sae and down-regulation of a SarA protein homolog called Rot. This will eventually lead to repression of two gene products called SarT and SarS. SarT is a repressor of alpha-toxin and SarS is an activator of protein A synthesis, thus explaining the elevated production of alpha-toxin and repression of protein A upon *agr* activation. Activation of *agr* would also result in the amplification of the original signal by activating SarU, which is a positive regulator of *agr*.

With permission, image and description from (Cheung, Bayer et al. 2004)

S. aureus bacteria in direct contact with plasma trigger the complement system, leading to a first battle between the bacteria and the host immune system. Complement can be activated by 3 different pathways: classical, lectin or alternative. The classical pathway involves the presence of antibody attached to the microbe, while the lectin and alternative pathways are components of the innate immunity by their direct recognition of the pathogen. The opsonisation process, in which complement molecules bind bacterial antigens, promotes phagocytosis by immune effector cells.

Circulating *S. aureus* are cleared by neutrophils and macrophages in a healthy individual, but in case of damaged endothelium, bacteria can adhere and invade endothelial cells (Hamill, Vann et al. 1986). Following contact with staphylococci, white blood cells, epithelial cells, endothelial cells and platelets are stimulated to release cytokines. It was shown that serums of *S. aureus* infected patients exhibiting toxic shock syndrome contain high levels of interleukin-6, interleukin-10, tumour necrosis factor-alpha (TNF- α) and interferon-gamma (IFN γ) (Seishima, Kato et al. 2009). Chemokines are recognised by G protein-coupled receptors at the surface of leukocytes, which respond by migrating from the blood to the site of infection, especially neutrophils that are the first responders to *S. aureus* infection (Verdrengh and Tarkowski 1997), followed by macrophages.

Following bacterial degradation, host cells can detect bacterial molecules called pathogen-associated molecule patterns (PAMPs) via specific receptors called pattern recognition receptors (PRRs). For example, innate host defences are triggered by the presence of staphylococcal diacylglycerol lipoproteins, which was demonstrated via the decrease of immune detection of the *lgt* *S. aureus* mutant lacking diacylglycerol-modified lipoproteins, leading to the formation of lethal abscesses in mice (Bubeck Wardenburg, Williams et al. 2006). PRRs include toll-like receptors (TLR), nucleotide-binding oligomerisation domain (NOD) proteins, TNF- α receptor 1 or peptidoglycan recognition proteins (Fournier and Philpott 2005). TLR family members are expressed on cell membranes of innate, adaptive and non-immune cells, but also in intracellular compartments such as phagosomes

and endosomes. TLRs function mainly to sense microbes and regulate proinflammatory signalling cascades, which can use a MyD88-dependent or MyD88-independent pathway. The use of MyD88 pathway in *S. aureus* infection seems to depend on the infected tissue. The MyD88-dependent signalling pathway is the most important and requires prior *S. aureus* phagocytosis, followed by complete acidified phagosome maturation to be active (Ip, Sokolovska et al. 2010). The acidification step of the phagosome requires the NOD-like receptor family, pyrin domain containing 3 (NLRP3) inflammasome and an active caspase-1 (Sokolovska, Becker et al. 2013). Among the TLR family, the TLR2 recognition pathway plays an important role in *S. aureus* infection control, as mice deficient for this receptor are highly susceptible to systemic infection. MyD88-deficient mice infected with *S. aureus* showed an even higher mortality rate than TLR2-deficient mice, and were lacking the production of several cytokines such as IL-1, IL-18, TNF- α and IL-6. This highlights the essential role of the MyD88 signalling pathway in immune response against *S. aureus* and the contribution of other receptors signalling via MyD88 (Takeuchi, Hoshino et al. 2000). A staphylococcal skin infection model in mouse showed that MyD88-dependent pathway is also required for neutrophils recruitment at the site of infection, which is initiated by IL-1R signalling by the resident skin cells (Miller, O'Connell et al. 2006). Once stimulated, TLR2 pathway activates the transcription factor NF- κ B and c-Jun N-terminal kinase. Internal rearrangement processes of the targeted immune cells are taking place in order to activate mechanisms involved in pathogen elimination such as transcription of proinflammatory cytokine genes. Also, antigen-presenting cells carrying bacterial products move to lymph nodes where B-cells are stimulated to differentiate and release antibodies to neutralise toxins and promote bacterial opsonisation.

Neutrophils usually uptake bacteria through phagocytosis, forming an isolated compartment containing the bacteria called the phagosome. Activated neutrophils can initiate their pathogen destruction mechanisms via 3 main pathways: production of NADPH oxidase-derived ROS (reactive oxygen species), degranulation of azurophilic and specific granules containing neutrophil antimicrobial peptides (AMPs) and antimicrobial

proteins such as α -defensins, cathelicidins, azurocidin, cathepsins, lactoferrin, lysozyme, proteinase-3, and elastase, and release of neutrophil extracellular traps (NETs) (Rigby and DeLeo 2012). The ingestion of bacteria by neutrophils induces a global change in neutrophil gene expression, followed by neutrophil apoptosis differentiation program, a process known as phagocytosed-induced cell death (Kobayashi, Braughton et al. 2003). Macrophages are subsequently recruited to ingest apoptotic neutrophils in order to resolve the infection site and inflammatory response. This is the normal immunological system to clear staphylococcal infection in healthy conditions (Rigby and DeLeo 2012). However, in some cases of *S. aureus* infection, the neutrophil-pathogen interaction leads to neutrophil lysis-induced by the bacteria such as pyroptosis or oncosis, or a delay of neutrophil apoptosis, which contribute to host tissue damage or bacterial survival, and therefore long-lasting disease (Kennedy and DeLeo 2009).

Macrophages are more long-lived cells than neutrophils, have high phagocytic capabilities, combined with great bacteria digestion skills, and produce various pro-inflammatory mediators required for recruitment and activation. Influenced by the cytokine milieu, macrophages can be polarised towards a classical M1 or an alternatively activated M2 phenotype, which have opposite properties. Classically activated macrophages of M1 type express opsonic receptors, produce IL-1, IL-6 and TNF- α and the arginine metabolism is characterised by high levels of inducible nitric oxide synthase. M1 macrophages have antimicrobial properties (Mantovani, Sica et al. 2004). However, in case of staphylococcal biofilm, macrophages seem skewed into M2 phenotypes, generating a pro-inflammatory and pro-fibrosis innate immune response, which is ideal for bacterial survival and persistence (Thurlow, Hanke et al. 2011). The M2 macrophage polarisation is regulated by a MyD88-dependent signalling (Hanke, Angle et al. 2012).

Upon the detection of pathogen, tissue macrophages secrete several molecules such as CXCL8, CXCL1/2/3, CCL2 and CCL3/4, that attract inflammatory cells. Recruited neutrophils become activated and participate in the recruitment of more neutrophils and macrophages. The infection site

becomes filled with activated neutrophils and inflammatory macrophages that work cooperatively to eradicate the pathogen via phagocytosis and release of antimicrobial granules (Silva 2010).

1.1.4.2. Immune evasion strategies by *S. aureus*

The host immune system is composed of several components to fight invading *S. aureus*, as described previously. However, this system does not work properly all the time, leading to disease. Indeed, *S. aureus* has evolved throughout the years of interaction with the human immune system, developing several passive and active defence strategies to counteract the immune system. Passive strategies include the prevention of recognition, binding and phagocytosis by the immune cells, as well as the protection against microbicides released into the cell and/or the phagosome. Active strategies involve the secretion of cytotoxic molecules that damage immune cells (Foster 2005).

Chemotaxis inhibitory protein of staphylococci (CHIPS) is released by 60% of *S. aureus* strains. CHIPS binds C5a receptor and formyl peptide receptor, blocking the binding of cognate agonist and therefore reducing the chemotaxis of inflammatory cells to the site of infection (Postma, Poppelier et al. 2004). Other complement inactivation strategies of *S. aureus* are the release of *Staphylococcus* complement inhibitor, which interferes with the C3 convertase assembly (Rooijackers, Ruyken et al. 2005), and the release of staphylokinase, a secreted plasminogen activator protein that inactivates complement factor C3b bound to the bacterial surface (Rooijackers, van Wamel et al. 2005). These strategies inactivate the complement, and therefore reduce bacterial phagocytosis. Expression of surface proteins such as clumping factor A (ClfA) and second immunoglobulin-binding protein interferes with the attachment of antibodies to the bacteria, therefore compromising the phagocytosis of *S. aureus* by phagocytes (Higgins, Loughman et al. 2006; Smith, Visai et al. 2011). Another phagocytosis inhibition strategy is the expression of a thin microcapsular layer composed

of serotype 5 or serotype 8 capsular polysaccharides (Thakker, Park et al. 1998; Luong and Lee 2002).

In case of phagocytosis by neutrophils, *S. aureus* has developed strategies to survive inside the phagosome. Survival mechanisms include natural modifications to wall teichoic acid, lipoteichoic acid and to a membrane phospholipid. For example, attachment of Dlt proteins and MprF proteins neutralise the negative charge of the bacterial membrane, which reduce the affinity of cationic antimicrobial peptides secreted into the neutrophil phagosomes or repel positively charged proteins in serum such as lactoferrin (Collins, Kristian et al. 2002; Kristian, Durr et al. 2003). Secreted proteins inhibiting charged antimicrobials also exist, such as staphylokinase (Jin, Bokarewa et al. 2004) or aureolysin (Sieprawska-Lupa, Mydel et al. 2004). *S. aureus* resists to the lysozyme by modifying the C6 hydroxyl group of muramic acid of their cell-wall peptidoglycan via a membrane-bound O-acetyltransferase (Bera, Herbert et al. 2005). Other intraphagosomal survival strategies include scavenging oxygen free radicals generated by neutrophils, through the expression of superoxide dismutase enzymes.

S. aureus can also survive intracellularly in a semi-dormant form referred to as small colony variants (SCV). These SCVs grow slowly and present a smaller colony size compared to normal phenotype. They have a reduced carbohydrate metabolism, a lack of pigment and altered virulence factor expression. The two major groups are the electron transport defective SCRs and the thymidine-auxotrophs (von Eiff 2008).

Next to the avoidance of recognition or binding by innate immune cells, *S. aureus* secretes several polypeptides that perforate the cytoplasmic membranes of target cells, causing leakage and ultimately lysis. The α -hemolysin is the archetype of β -barrel pores forming toxin (Valeva, Walev et al. 1997), while leukotoxins are formed of 2 components and include γ -toxin, Panton-Valentine leukocidin (PVL), leukocidin E/D and leukocidin M/F-PV-like (Yoong and Torres 2013).

S. aureus also uses several immunomodulatory molecules to modulate the host immune response. *S. aureus* secretes protein A that binds the V_{H3} region of IgM molecules exposed at the surface of B lymphocytes. This interaction leads to proliferation and apoptosis of B lymphocytes, depleting the spleen and the bone marrow stocks (Goodyear and Silverman 2004). The MHC class II analogue protein Map can bind T cell receptors, resulting to an alteration of T-cell function and a reduction of T-cell proliferation (Lee, Miyamoto et al. 2002). *S. aureus* can also bind to platelets and stimulate their activation via the immune receptor FcγIIA, integrin αIIbβ₃, and platelet factor 4. In endocarditis disease, *S. aureus* grow in platelet-fibrin thrombi, escaping from the attention of neutrophils (Arman, Krauel et al. 2014).

Biofilms often grow on implanted medical devices and are composed of bacteria and a matrix made of extracellular DNA, proteins and polysaccharides. The gene expression and metabolic activity of biofilm cells depend on the environment. Biofilms are a conserved bacterial strategy that circumvent immune response and is usually resistant to antibiotics. In presence of biofilms, host immunity seems often skewed towards an antiinflammatory and profibrosis status, promoting bacterial persistence. It has been shown that contact with macrophages alters the biofilm transcriptome, while the presence of neutrophils does not seem to influence the gene expression profile of the biofilm. The biofilm microenvironment is also modified compared to single or few bacteria, such as a modification in oxygen level and pH, which influence the immune response. Several *in vivo* factors are also secreted by biofilms to evade immune recognition and clearance (Scherr, Heim et al. 2014).

Recent evidence have shown that *S. aureus* can turn the host immune system against itself, for example by degrading NETs into leukotoxic deoxyadenosine. In staphylococcal abscesses, macrophages are excluded from the immune cells cuff surrounding the abscesses. This phenomenon involves a mechanism requiring nuclease and AdsA secretion by the bacteria. Indeed, AdsA produces 2'-deoxyadenosine (dAdo) that induces apoptosis of macrophages via activation of caspase-3, while nuclease facilitates the

production of dAdo through the degradation of NET DNA into deoxyadenosine monophosphate, a substrate for AdsA (Thammavongsa, Missiakas et al. 2013).

1.1.5. Preventive strategies of staphylococcal infections

Prevention of *S. aureus* dissemination in hospitals is economically favourable compared to treating patients acquiring nosocomial infections during their stay in hospital. Although comparisons between prevention costs and therapeutic costs are limited (Korczak and Schoffmann 2010), a few studies in Dutch hospitals evaluated that a “Search and Destroy” policy resulted in an annual saving of € 427,356 and 10 lives in a hospital of a country with a low endemic MRSA incidence (van Rijen and Kluytmans 2009). This policy remains cost-effective for a MRSA prevalence up to 8% (Nulens, Broex et al. 2008). In order to reduce the propagation of pathogenic bacteria, some prophylactic approaches have been developed focussing on control strategies. Specific guidelines have been drafted for health-care facilities to help controlling *S. aureus* infections and spreading. One of them is the early screening of patients to identify MRSA carriers, followed by application of usual methods such as isolation, nasal or skin decontamination if needed. Another important aspect of prevention involves the education of healthcare workers about *S. aureus* in order to re-enforce hand hygiene, for example (Coia, Duckworth et al. 2006). Prevention strategies are an efficient way to limit the dissemination of *S. aureus* among patients and therefore to reduce the risk of nosocomial infections (Vos, Behrendt et al. 2009), even if it does not eradicate the pathogen.

Some decolonisation strategies have been tested in hospitals, but these practices remain controversial as it may contribute to stimulate the appearance of antibiotic resistance. Some studies have tested to reduce *S. aureus* infections of hospitalised patients by screening at the usual bacterial carriage sites like the anterior nares or the skin, followed by anti-staphylococcal treatment. A review has compared the data of several studies using single treatment with mupirocin ointment in the nares of patients and

revealed the improvement in the reduction of nosocomial infections (van Rijen, Bonten et al. 2008). However this approach is mostly beneficial for patients with a weaker immune system. Combinational therapy seems to provide better results to eliminate the pathogen, such as using oral antibiotics and rifampicin, or the association of topical antibacterial agents like mupirocin with germicides. Full body decontamination involving mupirocin nasal ointment, mouth rinse and full-body washes with chlorhexidine, associated with vaginal, intestinal and urinary-tract decolonisation gave a successful rate of decontamination among patients (Buehlmann, Frei et al. 2008). Another study used a 7-day course combining chlorhexidine gluconate washes, intranasal 2% mupirocin ointment, oral rifampin and doxycycline as treatment for hospitalised patients in Canada and showed the efficacy of MRSA decolonisation of these patients for at least 3 months (Simor, Phillips et al. 2007). However, the relevance of *S. aureus* decolonisation as routine practice in hospitals remains questionable. Such methods might be an additional inducing factor of drug resistance development, as a high-level mupirocin resistance gene (*mupA*) has already been discovered on a plasmid and could become a significant problem if spread among the staphylococcal community (Patel, Gorwitz et al. 2009). In addition, the temporary eradication of *S. aureus* in patients may lead to a later recolonisation by more virulent bacterial strains. Next to the chemical antistaphylococcal strategy, another possibility to reduce the number of *S. aureus* in the nares is the substitution of *S. aureus* population for an Esp-secreting *S. epidermidis* population. Indeed, their presence seems to inhibit biofilm formation and destroys pre-existing *S. aureus* biofilms (Iwase, Uehara et al. 2010).

In the world of vaccine development, 2 types of immunisation exist: active and passive immunisation, depending on the target population. Active immunisation would target people at risk of contracting staphylococcal disease due to their environment (school, care facility, prison) or a long-lasting disease (HIV, diabetes, drug addiction), while passive immunisation is suitable for persons who are already immunocompromised (neonates) or at immediate risk of infection with time constraint for another approach (trauma

victims, patients in intensive care units or undergoing emergency surgery). To date, no vaccine against *S. aureus* infections is available on the market, despite all the efforts of academia and pharmaceutical companies to develop one. In the last decade, all completed trials based upon opsonic and/or neutralising antibodies have failed. Nabi's StaphVAX® is a vaccine designed using type 5 and 8 capsular polysaccharides conjugated to the nontoxic recombinant *Pseudomonas aeruginosa* exotoxin A. The initial phase III clinical trial on hemodialysis patients was promising with a protective effect lasting up to 40 weeks postvaccination (Fattom, Horwith et al. 2004). However, it was found ineffective in the confirmatory phase III clinical trial (Bienfait 2005). The Merck's V710 vaccine targeting the cell-wall-anchored IsdB antigen went to phase II/III of clinical trials, but failed to provide efficacy for patients undergoing cardiothoracic surgery (Fowler, Allen et al. 2013). Among the passive immunisation therapy strategies, AltaStaph was developed as an adjunctive therapy for people at high risk of staphylococcal disease. AltaStaph is a polyclonal investigational human immunoglobulin G (IgG) with high levels of opsonising *S. aureus* CPS types 5 and 8 IgG. In the pilot trial, it was shown that AltaStaph was well tolerated by very low birth weight neonates, but it did not prevent the incidence of *S. aureus* bacteremia in the treated group (Benjamin, Schelonka et al. 2006). Similar results were observed in a phase II trial on 40 subjects having *S. aureus* bacteremia (Rupp, Holley et al. 2007). Another example is the human immunoglobulin G preparation known as INH-A21 (Veronate) containing elevated levels of antibodies for staphylococcal surface adhesins ClfA and SdrG. Veronate went into phase III testing, where it failed to reduce the incidence of staphylococcal late-onset sepsis or candidemia in premature infants (DeJonge, Burchfield et al. 2007).

Because *S. aureus* is an extremely well-adapted pathogen to the human immune system with multiple virulence strategies creating a multifactorial pathogenesis, the development of new vaccines must target multiple virulence and bacterial defence mechanisms (Anderson, Miller et al. 2012). Vaccines are now designed against several antigens as it was demonstrated to be more efficient to induce opsonophagocytic antibodies than single

antigen-targeting strategy, using immunisation against IsdA, IsdB, SdrD and SdrE (Stranger-Jones, Bae et al. 2006). In addition, cell-mediated immunity plays a critical role in the protection against *S. aureus* infections. In particular, neutrophils are really important in the control of *S. aureus* infections, as shown by the increased susceptibility to staphylococcal infections by patients with neutrophil disorders such as chronic granulomatous disease (Segal, Leto et al. 2000). Neutrophils can be linked to cell-mediated immunity via the Th17/IL-17 axis. Indeed, the release of IL-17 by Th17 cells induce the mobilisation and activation of neutrophils in a more efficient way than the antibodies only, which give promise for the future development of new types of vaccine (Proctor 2012).

1.1.6. Antibiotic strategies and staphylococcal resistance

1.1.6.1. History of antibiotics and resistant strains

Since the purification of penicillin in early 1940s (Chain, Florey et al. 1940; Abraham, Chain et al. 1941) and its utilisation to treat infections, antibiotics have saved untold numbers of sick people from bacterial disease, bringing a revolution in the medical field. Unfortunately, within decades of widespread antibiotic use, bacteria have developed resistance strategies. One year after the introduction of penicillin to treat bacterial infections, the first case of penicillin-resistant *S. aureus* was reported (Rammelkamp 1942). Since then, the number of penicillin-resistant strains kept increasing. In 1948, a London hospital reported that 59% of patients infected with *S. aureus* were carrying penicillin-resistant strains (Barber and Rozwadowska-Dowzenko 1948), while previous studies in the same hospital recorded an incidence of 14% in 1946 and 38% in 1947, suggesting a selection process of the penicillin-resistant *S. aureus* strains in the hospital over time. Similar situations were soon reported from hospitals from around the world. Other natural antibiotics such as streptomycin, tetracycline or chloramphenicol were used against penicillin-resistant staphylococci, but bacterial resistances to one or several of these antibiotics started to emerge soon after their therapeutic use (Clarke, Dagleish et al. 1952; Rountree and Thomson 1952). To overcome the penicillin resistance problem, a semi-synthetic penicillin antibiotic called

methicillin was designed and introduced in 1959. However, the first MRSA was reported in 1961, the year following its introduction on the market, even though the 3 patients carrying a resistant-*S. aureus* strain had not been treated with methicillin during their hospital stay (Jevons 1961). Soon after that, more MRSA isolates were discovered in other European hospitals, in Japan, in Australia and in the United States. A decade after being recorded only in hospital settings, MRSA isolates emerged in the community, being in most cases also resistant to other antibiotics. At the time, the most reliable therapy for MRSA infections was the treatment with vancomycin. The first case of vancomycin-resistant strain (Mu50) was isolated in 1996 in a Japanese hospital (Hiramatsu, Hanaki et al. 1997). Some vancomycin resistance was predicted, as it was known that some enterococci were resistant to vancomycin when carrying genes *VanA* or *VanB* (Arthur and Courvalin 1993). However, Mu50 did not carry any of these 2 genes and instead had a thicker cell wall enriched with penicillin-binding protein 2 and 2' and murein monomer precursor, suggesting a spontaneous apparition of the resistance (Hiramatsu, Hanaki et al. 1997). Nowadays, the most common antibiotics used to treat antibiotics-resistant *S. aureus* infections are vancomycin, quinupristin-dalfopristin, linezolid, tigecycline, telavancin, ceftaroline, and daptomycin (Rodvold and McConeghy 2014). The choice of one or another antibiotic depends on the type of bacterial disease and the virulence of the strain. However, no real novel structural classes of compounds have emerged in the recent years, questioning how long will it last until bacteria become extensively resistant to them.

Recent studies showed that the genes coding for the resistance to beta-lactam, tetracycline and glycopeptide antibiotics have been found in DNA from non-contaminated Late Pleistocene permafrost sediments suggesting these are at least 30,000-years-old (D'Costa, King et al. 2011). Natural antibiotics have been developed to prevent growth of competitor microorganisms in a specific microbiota, but those microbes have co-evolved antibiotic resistance strategies for their own survival. Antibiotics resistance genes are usually located on mobile genetic elements, and can easily be transferred intra or even inter-species. The higher the exposure to antibiotics,

the quickest the transfer of these resistance traits occurs. Synthetic antibiotics could be a solution, but most bacteria express efflux systems that are encoded in their genome to protect themselves against all non-natural products, including synthetic antibiotics. This reveals a fundamental flaw in antibacterial drug discovery: bacteria have already evolved sophisticated strategies to overcome all natural antibiotics, and probably the synthetic ones too - it just needs for these strategies to spread in the bacterial populations.

1.1.6.2. Antibiotic resistance mechanisms

Bacteria have developed a wide diversity of resistance mechanisms to antibacterial drugs, and often use a combination of resistance mechanisms to protect themselves against a specific antibiotic. Nowadays, at least one mechanism of resistance is known against each class of commonly used antibiotics.

There are 3 general types of resistance mechanisms, even though the diversity of resistance mechanism is quite broad. The first type is the reduction of intracellular concentration of antibiotics inside the cell to avoid toxic concentration, either by decreasing the cell wall permeability or through the expression of specific or multidrug efflux pumps that export the drug outside the cell. There is a large variety of efflux pumps encoded either in the chromosome or in bacterial plasmids. For example, the resistance to hydrophilic fluoroquinolones can be conferred by the expression of the *norA* gene, encoding a membrane-associated protein that actively expulses these drugs outside the cell (Kaatz, Seo et al. 1993; Neyfakh, Borsch et al. 1993). The second resistance mechanism is the inactivation of the drug by enzymatic degradation. A historical example of drug inactivation mechanism is the expression of the *blaZ* gene coding for the β -lactamase by *S. aureus*. The β -lactamase enzyme deactivates β -lactam antibiotics by hydrolysing the β -lactam ring of the drugs. Finally, the third resistance mechanism is the alteration of the antibiotics molecular target via a genetic mutation, or an overexpression of the drug target. An example of drug target alteration resistance mechanism is the resistance to penicillinase-resistant beta-lactam antibiotics such as methicillin. The resistance to these antibiotics is conferred

through the acquisition of the *mecA* gene carried on a mobile genetic element called the Staphylococcal Cassette Chromosome *mec* (SCC*mec*), which can be transferred to other bacteria. The *mecA* gene encodes a transpeptidase designated penicillin-binding protein 2' (PBP 2' or PBP 2a) that is involved in cell wall synthesis. In normal conditions, *S. aureus* produce penicillin-binding proteins (PBP) that tightly cross-link the cell wall peptidoglycans. In presence of a β -lactam antibiotic, the transpeptidase function of the intrinsic PBP is inhibited due to a covalent bond between the antibiotic and the D-alanyl-D-alanine-binding pocket site of the enzyme (Tipper and Strominger 1965). In contrast, PBP 2' has less affinity for the antibiotics and is therefore not inhibited. PBP 2' can recognise the peptidoglycan residues, enabling the formation of the cross-link reaction with the peptidoglycan to form the cell wall. The resistance gene *mecA* is regulated by the factors *fem* (factor essential for methicillin resistance) and *aux* (auxiliary) (Chambers 1997). To date, eleven different SCC*mec* allotypes (I-XI) have been described, with some of them being divided into different subtypes, on the basis of the cassette chromosome recombinases gene complexes and the *mec* gene complexes (Turlej, Hryniewicz et al. 2011).

An intrinsic drug resistance mechanism is the formation of biofilms, which are composed of microcolonies encased in extracellular polysaccharide material (slime). Biofilms are particularly resistant to antibiotics due to a limited diffusion of the drug in the biofilm structure, a repulsion of the antibacterial drug, or a reduced efficacy of the drug targeting active cell processes (Otto 2008). The Calgary biofilm device has been developed to experimentally form biofilms, subsequently enabling to test the efficacy of antibiotics on bacterial biofilms (Ceri, Olson et al. 1999; Olson, Ceri et al. 2002).

1.1.6.3. Strategies to find new antimicrobials

It is clear that novel approaches are required to find new anti-microbial therapies. All current antibiotics have been found or developed using a target-based biochemical screening for inhibitors of bacterial growth, which has failed to develop new products in the recent years. It should also be reminded that bacteria have evolved anti-microbial strategies and “intrinsic”

resistance mechanisms such as the formation of biofilm and the expression of multidrug efflux pumps. Today's antimicrobial strategy should focus on a combination of bacteriocidal and immunostimulatory treatment.

In the mean time, while new antimicrobials are still searched for, judicious use of antibiotics is indispensable to protect our current antibiotics from bacterial resistance. Because microorganisms develop resistance as a response upon exposure to antimicrobials, better antimicrobial management should include optimal duration of therapy and combination of drugs from different classes to limit resistance appearance. In addition, a continuous education of prescribing doctors and patients on antibiotics is also important to avoid unnecessary utilisation of antibiotics (Dixon and Duncan 2014).

1.1.7. *S. aureus* as an intracellular pathogen

S. aureus was initially thought to be an extracellular pathogen, but the presence and survival of the bacteria within several cell types has reevaluated *S. aureus* as a facultative intracellular pathogen. Indeed, the survival of *S. aureus* has been demonstrated into endothelial cells, epithelial cells, keratinocytes, fibroblasts and osteoclasts (Garzoni and Kelley 2009); but also its survival in professional phagocytes such as neutrophils (Gresham, Lowrance et al. 2000) and macrophages (Kubica, Guzik et al. 2008). Intracellular survival is a good strategy to avoid the host immune system and extracellular concentrations of antibiotics. Intracellular survival enables the bacteria to persist long-term and induce relapses and chronic infections.

1.1.8. Animal models to study staphylococcal disease

A bacterial infection involves a complex interaction between 2 partners: the pathogen and the host. Animal models are useful tools to study the infectious process and increase the understanding of bacterial pathogenesis in an *in vivo* context, exposed to the host immunological response. Animal models are commonly used in drug development, sometimes at early screening stage to identify new antibacterial compounds, but more often at the clinical

trial level, before the tests on humans. Rats, rabbits and mice have had a central role in modelling human *S. aureus* diseases.

The mouse is the usual animal of choice to study *S. aureus* pathogenesis as i) it is a natural host of the bacteria, ii) the murine immune and inflammation systems are closely related to humans, iii) many inbred and genetically well-characterised murine strains are available, and iv) a large number of knock-out and transgenic murine strains are available. Consequently several staphylococcal diseases have been modelled in murine models such as sepsis, skin abscess and septic arthritis. Skin abscesses are usually modelled by subcutaneous injection of the pathogen into mice, along with a foreign material such as microbeads (Bunce, Wheeler et al. 1992). Superficial skin infections have also been modelled in mouse by partially removing the epidermal layer and applying the pathogen. It is a topical route of infection, which is biologically relevant (Kugelberg, Norstrom et al. 2005). Septic arthritis can be induced in mice through intravenous administration of *S. aureus*. Similar to the spreading pattern in humans, bacteria proliferate first in the blood until they reach a critical level and invade the bone and synovial tissue 24 h after the inoculation (Bremell, Lange et al. 1991; Tarkowski, Collins et al. 2001). Infection mouse models can provide useful information on staphylococcal pathogenesis and to evaluate the response to antimicrobial treatment.

Rats used to be the preferred models of experimental staphylococcal endocarditis. Practically, a catheter was introduced into the left ventricle through the right carotid artery of the heart, then bacteria were injected 1 or 2 days after catheterisation (Santoro and Levison 1978). Nowadays, rats are still used to model *S. aureus* endocarditis disease (Ulphani and Rupp 1999), but the use of other animals have also been developed in mice (Gibson, Kreuser et al. 2007) and guinea pigs (Maurin, Lepidi et al. 1997). Toxic shock syndrome is quite difficult to reproduce in animals but has been successfully induced by using subcutaneous infection chambers in rabbits (Scott, Kling et al. 1983). Even though they are less commonly used in research, other

animal models of staphylococcal infection include chicken, baboon, guinea pig, dog, sheep and cow (Collins and Tarkowski 2000).

The use of living vertebrate animals for scientific research purpose is restricted and evaluated by law in the UK under the Animals (Scientific Procedures) 1986 Act. Every experiment requires the application of the 3 R principles: refinement, reduction and replacement. The aim of these principles is to minimise the adverse effects caused to animals, improve their welfare and enhance the quality of science. For ethical reasons, intensive use of mammals is restricted, without mentioning the financial and logistical reasons limiting the use of large numbers of mammals. Therefore, alternative strategies to study *S. aureus* infection *in vivo* are required.

Because invertebrates are not protected under the Animals (Scientific Procedures) 1986 Act, they can be used as animal models without restriction. Invertebrate animal models include the fruit fly *Drosophila melanogaster* (*D. melanogaster*), the roundworm *Caenorhabditis elegans* (*C. elegans*) or the silkworm *Bombyx mori* (*B. mori*). Orthologous proteins between humans and these invertebrates belong to core processes with conserved functions throughout evolution. Despite their lack of adaptive immune system, studying *S. aureus* pathogenesis in these invertebrates can give valuable information about staphylococcal virulence determinants and humoral and cellular responses of the host (Garcia-Lara, Needham et al. 2005).

D. melanogaster has been developed as a model to study host-pathogen interaction in the case of a systemic staphylococcal disease. The infection was induced via pricking the dorsal thorax of the fly with a needle dipped in bacterial suspension. The starting infecting dose was 1×10^4 CFU and the death-determining CFU number was 2×10^7 - 2×10^9 . *S. aureus* infected flies could be cured by treating them with antibiotics-enriched food (Needham, Kibart et al. 2004). The *S. aureus*-*C. elegans* infection model is initiated by plating the worms on agar medium inoculated with bacteria for 48 to 72 h. Microscopic observation showed the colonisation of growing *S. aureus* in the host intestine, and the accumulation of live bacteria induced the killing of the

nematodes. 70% of the infected roundworms died within the course of the 5-day experiment, which could happen at any larval-stages of the nematode development. The killing efficiency is function of the bacterial strains and their virulence determinants (Sifri, Begun et al. 2003). This *S. aureus*-nematode killing assay has allowed the identification of several bacterial virulence genes using random transposon-mutant bacteria method (Bae, Banger et al. 2004; Begun, Sifri et al. 2005). The silkworm *Bombyx mori* is another invertebrate model used to study bacterial infection caused by pathogenic *S. aureus* (Kaito, Akimitsu et al. 2002). Infection of silkworm larvae with *S. aureus* by dorsal injection provides a useful *in vivo* tool to evaluate the efficacy of antimicrobial strategies such as antibiotics (Fujiyuki, Imamura et al. 2010) or bacteriophage therapy (Takemura-Uchiyama, Uchiyama et al. 2013), before being tested in a mammalian model. The *S. aureus*-*B. mori* infection model is also useful to study important bacterial virulence factors (Miyazaki, Matsumoto et al. 2012).

1.2. *Danio rerio* as an animal model for infection

1.2.1. Zebrafish as a model organism

Zebrafish (*Danio rerio*) are small tropical freshwater teleost fish of approximately 3-4 cm long, belonging to the Cyprinidae family. Zebrafish were originally named after their 5 horizontal black/blue stripes visible on the side of their body from the head to the tail. The stripes phenotype is present in wild-type zebrafish, but some zebrafish strains are lacking these stripes due to some pigmentation defects. The male is torpedo-shaped, with pinker lines between the dark stripes, while the female has a larger belly and a silver colour between the dark stripes. Zebrafish are native from the Ganges and Brahmaputra river basins of south-eastern Asia in India, Nepal and Bangladesh, and still found naturally in these regions.

Zebrafish have become a popular animal model for research due to the following characteristics: they are cheap and easy to maintain, they have a high fecundity producing about 100 to 200 eggs per mating and they reach their adulthood in 3 months. The zebrafish embryos develop externally, and

their transparency is an advantage for *in vivo* microscopy. Transgenic, mutagenesis and cloning techniques are easily performed on zebrafish. Indeed, DNA or RNA constructs can be injected into zebrafish eggs immediately after fertilisation, leading to the generation of transgenic zebrafish lines or mutants. The zebrafish genome is 1.7 gigabases in size, diploid and divided up into 25 chromosomes. Many zebrafish genes are orthologues with mammalian genes, and the syntenic relationship has been studied between the two genomes (Barbazuk, Korf et al. 2000). The complete sequencing of the reference Tübingen zebrafish genome has demonstrated that approximately 70% of human genes have a zebrafish orthologous gene, and reciprocally. However, there are about 2.28 zebrafish genes for each human gene, reflecting the teleost-specific genome duplication that occurred 340 million years ago in the ancestor (Howe, Clark et al. 2013).

Several characteristics of the zebrafish prove its qualification as a good animal model, bridging the gap between the invertebrate fruit fly model *D. melanogaster* and the mammalian murine models. As zebrafish are vertebrate animals, their organs and tissues such as brain, heart, liver, pancreas, kidneys, intestines, bones or muscles are quite similar to their human counterparts at the anatomical, physiological and molecular levels. Therefore, studying vertebrate biological processes is possible in zebrafish, which can provide useful information about the same processes in higher vertebrates. In addition, zebrafish have an innate immune system closely related to the higher evolutionary vertebrates, which is non-existent in lower organisms. Compared to mammalian models, young zebrafish are transparent allowing real-time visualisation *in vivo* of internal organs and structures. From the ethical point of view, using living protected animals such as mammals causes more moral issues than using zebrafish in a research project. Although zebrafish are also protected animals in the UK under the Animals (Scientific Procedures) Act 1986, embryos up to 5.2 days are not yet restricted in their use for scientific studies.

Zebrafish have potential for studies in a very broad range of research areas. Zebrafish was initially widely used as an organism model for developmental biology (Grunwald and Eisen 2002), but its research possibilities have then expanded to model human diseases such as cancers (Liu and Leach 2011), neurodegenerative disorders (Bandmann and Burton 2010) or muscular dystrophies (Gibbs, Horstick et al.). Zebrafish embryo heart starts beating at 24 hours post fertilisation (hpf) but they can survive without cardiac function up to 5 days due to simple oxygen diffusion. For that reason, studies of severe developmental defects in heart morphology and physiology is possible in early living embryos. Many cardiovascular diseases have been modelled in zebrafish, including arteriogenesis, thrombosis, cardiomyopathy or inflammation (Chico, Ingham et al. 2008).

1.2.2. The zebrafish immune system

There are 2 major systems that help vertebrates fighting against external and foreign organisms: the innate immunity and the adaptive immunity. The first one is composed of cells that recognise and respond to pathogens in a generic way, while the second is usually activated when pathogens overcome the innate immune response. These 2 systems do crosstalk and interact for a better immune response. The key link between these 2 systems is the dendritic cells in mammals, and similarly, antigen-presenting cells have been identified in zebrafish (Lugo-Villarino, Balla et al. 2010).

The primitive wave of haematopoiesis starts in the lateral plate mesoderm at 12 hpf. The anterior part of the lateral plate mesoderm differentiates into myeloid cells via the expression of *spi1/pu.1*, while the posterior part specifies erythroid cells, which are driven by *gata1* expression. There is a cross-antagonism between *pu.1* and *gata1* transcription factors that controls the fate decision of myeloid vs erythroid cells production (Rhodes, Hagen et al. 2005). Both *pu.1* and *gata1* are positively regulated by *tif1γ* (Monteiro, Pouget et al. 2011). A transient wave of haematopoiesis occurs in the caudal hematopoietic tissue (also called posterior blood island) from 26 to 48 hpf and gives rise to erythromyeloid progenitor cells, the first multipotent

hematopoietic progenitor cells (Bertrand, Kim et al. 2007). The definitive haematopoiesis starts in the aorta-gonadmesonephros, similarly to mammals. Blood cell precursors from the aorta-gonadmesonephros replace the erythromyeloid progenitor cells in the caudal hematopoietic tissue (Bertrand, Chi et al. 2010; Kissa and Herbomel 2010), and subsequently migrate to the thymus and pronephros from 3 dpf and 4 dpf respectively (Bertrand, Kim et al. 2008; Kissa, Murayama et al. 2008) (Figure 1.2.). The pronephros develops into the kidney marrow in adult fish, which is the equivalent of the mammalian bone marrow.

Haematopoiesis and lymphopoiesis take place in the kidney and the thymus of the adult zebrafish, and these organs are seeded by dorsal aorta hematopoietic stem cells having undergone an endothelial to hematopoietic transition (Murayama, Kissa et al. 2006). A lymphatic system is developed in the zebrafish at 3-5 dpf (Yaniv, Isogai et al. 2006).

The 2 major types of phagocytic leukocytes of the innate immune system are macrophages and neutrophils, both of which have been well characterised in the zebrafish.

From the stage of 13-somite, a population of motile and phagocytically active macrophages can be seen emigrating from the anterior lateral mesoderm to the anterior surface of the yolk. Macrophages appear from 24 hpf in the yolk sac, and then quickly get disseminated in the mesenchyme of the head and the blood. The initial function of the macrophages is the elimination of apoptotic corpses. When challenged with bacteria, macrophages become activated and phagocytose foreign pathogens, as well as engulfing erythroblasts (Herbomel, Thisse et al. 1999). Macrophages can engulf large numbers of bacteria located either in body fluids or on tissue surfaces (Le Guyader, Redd et al. 2008; Colucci-Guyon, Tinevez et al. 2011). Macrophages can be studied and tracked using transgenic reporter lines possessing fluorescently marked myelomonocytic compartments, through the *fms* (Gray, Loynes et al. 2011) or *mpeg* (Ellett, Pase et al. 2011) promoters.

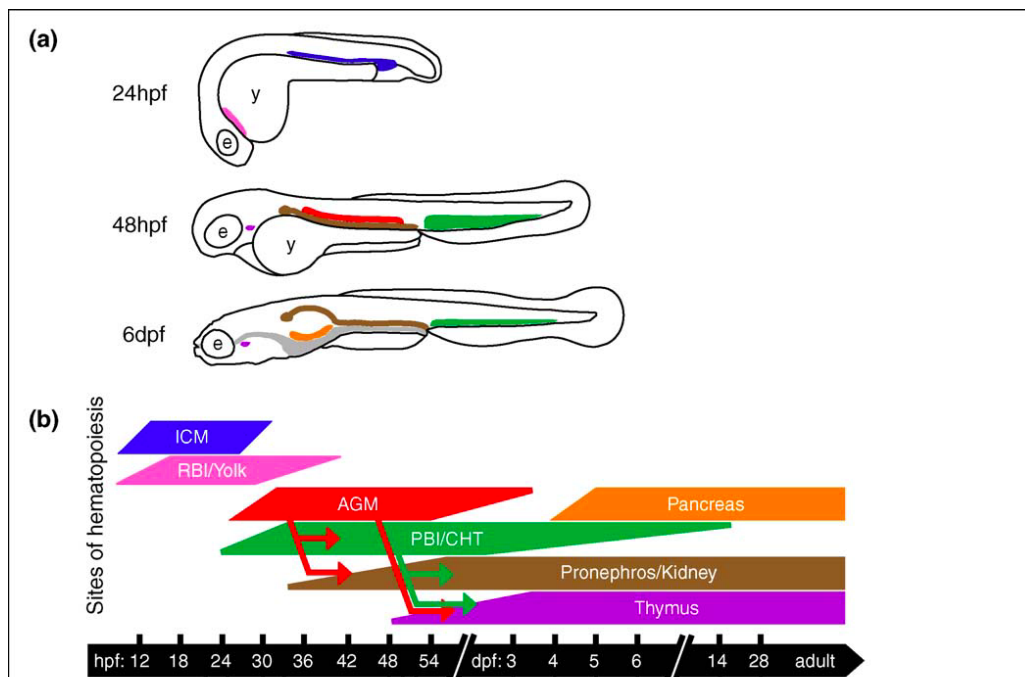


Figure 1.2. Schematic depiction of anatomical sites (a) and approximate durations (b) of hematopoietic activity in developing zebrafish.

The eye (e), yolk (y) and gastrointestinal tract (grey) are indicated in a. Relocation of definitive hematopoietic stem cells (HSCs) between sites is represented by arrows in b. Primitive erythropoiesis occurs in the intermediate cell mass (ICM, blue) which is active 11–30 hpf, whereas primitive myelopoiesis begins in the rostral blood island (RBI) and later the yolk (pink) from 12 to 40 hpf. HSCs appear in the aorta-gonad-mesonephros region (AGM, red) 26 hpf until 3 dpf. These HSCs are mobilised to seed the caudal hematopoietic tissue (PBI/CHT; green) and pronephros (brown) as early as 32 hpf, and the thymus (purple) as early as 48 hpf. Definitive hematopoiesis in the CHT begins de novo 24 hpf and continues until at least 14 dpf. Cells from the CHT contribute to the pronephros and thymus as early as 48 hpf. B cell development initiates in the pancreas (orange) starting 4 dpf, although the hematopoietic origins of these cells remain unknown. The thymus, pancreas, and pronephros/kidney subsequently serve as sites of definitive hematopoiesis into adult stages.

With permission, image and description from (Kanther and Rawls 2010)

Zebrafish neutrophils resemble to their human counterparts, morphologically with their segmented nuclei, and cytochemically with their myeloperoxidase-positive cytoplasmic granules (Bennett, Kanki et al. 2001; Lieschke, Oates et al. 2001). Granulocitic neutrophils can be observed from 33 hpf, using Sudan Black B staining or through video-enhanced differential interference contrast microscopy. Peroxidase activity, which is expressed by neutrophils, can be detected from 24 hpf in the yolk sac, the head mesenchyme and the ventral tail by using Cy3-tyramide labelling. By 2 dpf, neutrophils are the most abundant leukocytes and move rapidly in the mesenchyme and epidermis of zebrafish embryos (Le Guyader, Redd et al. 2008). Circulating neutrophils can respond to infection and injury, as they migrate towards site of infection or wounding. Neutrophils have limited phagocytic activity, to a lesser degree than macrophages. Neutrophils can engulf tissue-associated bacteria as they move over them, but are inefficient at phagocytosing microbes in blood or other fluid-filled cavities (Colucci-Guyon, Tinevez et al. 2011). Zebrafish neutrophils can be studied via the utilisation of transgenic lines generated by coupling fluorescent proteins marking neutrophils driven by specific promoters such as *mpx* (Mathias, Perrin et al. 2006; Renshaw, Loynes et al. 2006) or *lysC* (Hall, Flores et al. 2007).

Among other immune cell types, another granulocytic cell has been identified in the zebrafish, resembling eosinophils, from 5 dpf (Lieschke, Oates et al. 2001). Mast cells have also been identified in zebrafish through the expression of the specific and conserved feature of these cells, *cpa5*. The zebrafish mast cells have similar morphological features than mammalian mast cells, which was demonstrated via histological staining on tissue sections and via cells following FACS after fluorescent in situ hybridization (Dobson, Seibert et al. 2008). Zebrafish mast cells possess a FcεRI-like receptor and are functionally competent to participate in innate and adaptive immunity (Da'as, Teh et al. 2011). Cells with cytotoxic activity carrying novel immune-type receptors (NITR) could be related to natural killer-like cells in the zebrafish (Yoder 2009).

Key components of the complement belonging to the classical pathway,

alternative pathway, lectin pathway or lytic pathway have been identified in the developing zebrafish. Only the alternative pathway seems competent in the early-hatched embryo as seen by its response to LPS challenge (Wang, Zhang et al. 2008). A recent study suggests that the lectin pathway may be active before the full maturity of the zebrafish immune system. Resistance to *Aeromonas hydrophila* infection is increased in zebrafish embryos injected with recombinant mannose-binding lectin (rMBL), while zebrafish embryos co-injected with rMBL and anti-MBL antibody are more sensitive to infection (Yang, Bu et al. 2014).

Microbes are detected through the recognition of specific pathogen-associated molecular patterns (PAMPs) by pattern recognition receptors (PRRs) in zebrafish, similarly to mammalian mechanisms. Several conserved PRRs present in zebrafish have been described, among the families of Toll-like receptors, NOD-like receptors, RIG-I like receptors, scavenger receptors, C-type lectins (van der Vaart, Spaik et al. 2012). Following pathogen recognition, a cascade of signalling pathways leads to an inflammatory response.

Zebrafish infected with virus induce the production of zebrafish virus-induced IFN, which are orthologs of the mammalian IFN- λ (Levraud, Boudinot et al. 2007). Homologs of mammalian genes encoding cytokines have also been identified in the zebrafish, even though they can have some differences in their bioactivity. For example the proinflammatory properties of zebrafish TNF- α are mediated through the activation of endothelial cells (Roca, Mulero et al. 2008). Other cytokines produced by zebrafish include the interferon gamma (IFN- γ) (Lopez-Munoz, Sepulcre et al. 2011), granulocyte colony-stimulating factor (GCSF) (Stachura, Svoboda et al. 2013), interleukin 1 (Ogryzko, Hoggett et al. 2014), interleukin 6, interleukin 8, interleukin 10 and interleukin 12.

Neutrophils are recruited to a wound via a gradient of hydrogen peroxide (Niethammer, Grabher et al. 2009), while bacterial infection with *Pseudomonas aeruginosa* or *Streptococcus iniae* does not require hydrogen

peroxide to be detected by neutrophils. PI3K signalling is involved in neutrophil response to both injury and infection (Deng, Harvie et al. 2012). The zCxcl8 chemokine guides neutrophil recruitment to infection site, as well as neutrophil retention at the infection site, through a tissue-bound gradient binding to heparan sulfate proteoglycans (Sarris, Masson et al. 2012).

The lymphoid cells start developing from 4 dpf, but T-cells from transgenic zebrafish line can be tracked outside the thymus only from 3 weeks post fertilisation (Langenau, Ferrando et al. 2004). The immunocompetence of zebrafish, measured by the humoral response to T-independent and T-dependent antigens, is not fully reached before 4-6 weeks post fertilisation (Lam, Chua et al. 2004). Therefore, the innate immunity can be studied separately from the adaptive immunity in the zebrafish embryos.

Deep sequencing analysis techniques can reveal a large amount of information about RNA transcripts up or downregulated following *in vivo* infection in zebrafish, as shown with *M. marinum* infecting adult zebrafish (Hegedus, Zakrzewska et al. 2009) and *Salmonella typhimurium* infecting zebrafish larvae (Ordas, Hegedus et al. 2011). The results from these studies link the immune system to a large panel of expressed proteins during infection, stressing the complexity of the process. The transcriptomic profiles are also dynamic and evolve with the progression of infection such as adhesion, invasion and damage, as shown with a *Candida albicans* infection of zebrafish larvae study (Chen, Chao et al. 2013). The transcriptional signature of the innate immune response of zebrafish embryos infected with microbes resembles the response observed in mammalian or cell culture systems. Upregulated genes include receptors involved in pathogen recognition, signaling intermediates, their downstream transcription factors and inflammatory mediators (van der Vaart, Spaik et al. 2012).

The acute phase response is the immediate set of host inflammatory reactions following tissue injury, infection and trauma. The acute phase response of the host upon *S. aureus* infection is similar in the adult zebrafish than in mammals. Key components of the acute phase response are

upregulated such as the pro-inflammatory cytokine IL-1, or acute phase proteins such as fibrinogen, haptoglobin, complement components and hepcidin. Some differences such as the upregulation of LECT2 in the zebrafish might highlight a specific immune strategy of the fish species (Lin, Chen et al. 2007).

1.2.3. Zebrafish as an infection model for several pathogens

The use of zebrafish at the embryonic and adult stage has emerged as a powerful tool to model *in vivo* infectious disease of pathogenic bacteria, virus or fungi in a vertebrate host. The first 3-4 weeks of zebrafish development are suitable to study the interaction between a pathogen and the innate immune system of the host. In particular, the zebrafish innate immune cells such as neutrophils and macrophages are fully active from the first days of embryogenesis (Herbomel, Thisse et al. 1999; Le Guyader, Redd et al. 2008). The adaptive immune system becomes fully functional from 4-6 weeks post fertilisation (Lam, Chua et al. 2004), hence the response of the adaptive immune cells such as T and B-cells to pathogens can be studied in adult zebrafish.

Natural routes of infection in adult zebrafish are the gastrointestinal tract, gills or damaged fish surface. Experimentally, infection can be induced by coincubation of the pathogen in the fish water, which is more efficient if the fish is stressed and injured (Neely, Pfeifer et al. 2002). In order to avoid fish trauma, a bacterial suspension can be injected directly into anaesthetised fish. The fish can be injected intramuscularly, intraperitoneally or intravenously. The injection method allows infecting a more accurate dose of pathogen into fish (van der Sar, Appelmelk et al. 2004). To study infectious disease in the zebrafish embryo or zebrafish larvae, coincubation of the desired pathogen in the fish water can be performed (Davis, Clay et al. 2002; O'Toole, Von Hofsten et al. 2004). However, the more common experimental induction of infection is the micro-injection. The site of bacterial micro-injection into the zebrafish larvae determines the type of infection obtained: either the infection becomes systemic or it remains localised, at least at the

beginning. Intravenous injection leading to systemic infection can be performed in the blood island of 1 dpf embryo or in the Duct of Cuvier of 2-3 dpf larvae (Figure 1.3.A. and B.). Injections into the hindbrain ventricle of 1 dpf zebrafish, the tail muscle of 1-2 dpf zebrafish or the otic vesicle of 2-3 dpf zebrafish (Figure 1.3.C., D. and E.) are used for localised infection in which leukocytes chemotaxis can be studied. These injection sites were illustrated using *Salmonella typhimurium* and *Mycobacterium marinum* (Benard, van der Sar et al. 2012).

The zebrafish larvae as an infection model has been used to study several infections caused by pathogenic bacteria such as *Burkholderia cenocepacia* (Vergunst, Meijer et al. 2010), *Enterococcus faecalis* (Prajsnar, Renshaw et al. 2013), *Listeria monocytogenes* (Levraud, Disson et al. 2009), *Mycobacterium marinum* (Davis, Clay et al. 2002), *Pseudomonas aeruginosa* (Clatworthy, Lee et al. 2009), *Salmonella enterica* serovar Typhimurium (van der Sar, Musters et al. 2003), *Shigella flexneri* (Mostowy, Boucontet et al. 2013), *Streptococcus iniae* (Harvie, Green et al. 2013) or *Streptococcus pneumoniae* (Rounioja, Saralahti et al. 2011). Several fungal infections have also been modelled in zebrafish larvae, such as *Candida albicans* (Brothers, Newman et al. 2011) or *Cryptococcus neoformans* (S. A. Johnston, personal communication). The last category of pathogens that have been studied in the zebrafish larvae are the human virus herpes simplex virus type 1 (HSV-1) (Burgos, Ripoll-Gomez et al. 2008) and the chikungunya (Palha, Guivel-Benhassine et al. 2013).

Figure 1.3. Injection methods used for establishing systemic or local infections in zebrafish embryos.

(A-B) Intravenous injections for establishing a rapid systemic infection are performed into the caudal vein at the posterior blood island at 1 dpf (A) or into the Duct of Cuvier at 2-3 dpf (B). (C-E) Local injections for studying macrophage and neutrophil chemotaxis are performed into the hindbrain ventricle at 1 dpf (C), the tail muscle at 1-2 dpf (D) or the otic vesicle at 2-3 dpf (E).

Image and description from (Benard, van der Sar et al. 2012)

The adult zebrafish has been used to model infections as well, for example *Mycobacterium marinum* is a natural fish pathogen that mimics the human tuberculosis caused by *Mycobacterium tuberculosis* (Parikka, Hammaren et al. 2012), and is used to study the implication of the adaptive immune response to granuloma, the hallmark of tuberculosis. Diseases caused by the following pathogens have also been studied in the adult zebrafish: *Aeromonas hydrophila* (Rodriguez, Novoa et al. 2008), *Candida albicans* (Chao, Hsu et al. 2010), *Edwardsiella ictaluri* (Pressley, Phelan et al. 2005), *Staphylococcus aureus* (Lin, Chen et al. 2007), *Streptococcus iniae* (Neely, Pfeifer et al. 2002), *Streptococcus pyogenes* (Neely, Pfeifer et al. 2002) and *Streptococcus agalactiae* (Patterson, Saralahti et al. 2012).

1.2.4. Zebrafish as an infection model for *S. aureus*

S. aureus can be micro-injected at different sites into the zebrafish embryos, such as the pericardial cavity, the eye, the fourth hindbrain ventricle, the yolk circulation valley, the caudal vein, the yolk body or the Duct of Cuvier. The different bacterial entry routes model different type of staphylococcal infection, and influence the mortality rate of the host. Localised *S. aureus* infection into the zebrafish eye showed the initial recruitment of neutrophils, engulfing a few bacteria, followed by a high recruitment of macrophages around 5-6 hpi, which phagocytose many bacteria (Li and Hu 2012). In adult zebrafish, intraperitoneal injection of *S. aureus* leads to symptoms such as distended abdomens and peri-anal oedema and large lesions at and near the site of injection (Lin, Chen et al. 2007).

The *in vivo* systemic staphylococcal infection model into the zebrafish embryos using the yolk circulation valley as entry route has been well established. In practice, a *S. aureus* suspension is injected in the bloodstream of anaesthetised 30 hpf embryos, inducing a fatal infection over time. The survival pattern of the larvae is dose-dependent: a high dose induces a fast mortality rate, while a low dose induces a slower mortality rate. The growth of *S. aureus* within the embryos follows a logarithmic curve reaching a plateau at 10^6 CFU per embryo. A zebrafish embryo containing

more than 10^6 CFU does not survive, while lower number of bacteria can be contained by the zebrafish immune system. The systemic staphylococcal infection model into zebrafish embryos has shown that both pathogen and host exhibit factors involved in the fight. On one side, several virulence determinants of *S. aureus* are expressed and required to induce infection, such as *perR*, *pheP* and *saeR*. On the other side, the zebrafish innate immune system is activated for the recruitment of neutrophils and macrophages that phagocytose the bacteria (Prajsnar, Cunliffe et al. 2008). The lesions induced by *S. aureus* into the zebrafish embryos are mostly created by a single (or very few) bacterium, which was demonstrated with experiments using marked and isogenic strains. Staphylococcal abscesses are clonal, which is a consequence of an immunological bottleneck. Both types of phagocytes are containing the bacteria after the staphylococcal micro-injection. However, neutrophils seem to be responsible for the bottleneck of infection observed with experiments using marked and isogenic staphylococcal strains. This suggests a 'Trojan Horses' function of the neutrophils carrying *S. aureus* (Thwaites and Gant 2011), responsible for bacterial dissemination and therefore causing overwhelming and fatal infection (Prajsnar, Hamilton et al. 2012). Other experiments using the *S. aureus*-zebrafish embryo infection model have shown that sub-curative doses of antibiotics can cause a skewing towards a pre-existing resistant staphylococcal strain population. Host phagocytes are playing a role in this phenomenon (McVicker, Prajsnar et al. 2014).

This *S. aureus* infection model in zebrafish embryos may be used to develop a novel chemical screening method, aiming to identify curative agents of *S. aureus* infection. Indeed, zebrafish embryos are good candidate for small molecules screening as they are permeable to small molecules. In addition, it is an *in vivo* model of infection, bringing the advantages of being in real infection conditions. All the actors involved in a real-time infection are activated: innate immune system of the host and bacterial virulence factors are both activated during infection.

1.3. Zebrafish use in drug screening.

1.3.1. Drug screening assays in zebrafish

Finding new bioactive molecules to treat bacterial infections is a current challenge, especially with the rise of antibiotics-resistant strains. The development of new efficient drugs is a long and costly process. On average, 1 in 5000 discoveries makes it from the bench side to market, taking circa 12 years and costing from 500 million to 2 billion dollars for a single pharmaceutical agent (Williams and Hong 2011).

Modern drug discovery process is divided into major steps: discovery and screening (high-throughput screening and target validation), lead optimisation involving combinatorial chemistry and structure-based drug design, and finally study the ADMET: absorption, distribution, metabolism, excretion and toxicity properties. Afterwards, the biomolecule is tested in clinical trials, followed by a request for approval of the organism accredited to decide which drug is allowed on the market. If all the previous stages of research and development have been successful, the drug finally reaches the customers.

For the last 50 years, the main approach for drug design was the target-based screening procedure. Even though the knowledge about mechanisms of infectious disease and important bacterial molecular pathways has increased, the traditional way of drug discovery has failed to produce new antibiotics structure. Indeed, these drug screens are designed against specific molecular targets, losing the big picture. However, bacterial diseases are complex processes. Several high-throughput screening assays have been monitored to target essential enzymatic activities of the pathogens, leading to identifying compounds that later appeared to be ineffective against microbes *in vivo*. Therefore, it is important to test the microbe in its cellular environment in the case of anti-infectious drug screening assays.

The characteristics of a good screening assay are its robustness and its reproducibility. Ideally, the steps must be simple in order to be automated

and keeping the manual manipulations to a minimum. To increase the speed of the process, robotics software should provide assisted data analysis that can be interpreted without ambiguity.

1.3.2. Zebrafish-based drug screen assay

An important advantage of a zebrafish based drug screen is that many of the absorption, distribution, metabolism, excretion and toxicity (ADMET) properties are assessed during the initial screen itself. In usual “target-centered” drug screen, many compounds have failed after years of development due to ADMET problems. An *in vivo* zebrafish based drug screen enables to discard cytotoxic compounds at early stage of the drug discovery process, which should reduce long-term costs of compounds development. In addition, the overall viability of the organism can be tested, as well as the organ function, the tissue function and the behaviour. It is a whole organism assessment in an *in vivo* context, which lacks in cell culture drug screen assays. Another important benefit of the zebrafish in drug screen is its small size, enabling to dispose a single zebrafish larvae in a well of a 384-well, or dispose 3 to 6 zebrafish larvae in a single well of a 96-well plate. Therefore, a minimal amount of novel drug is used. Zebrafish larvae up can absorb low molecular weight molecules dissolved in the water through their skin and gills. Fish older than 7 dpf will absorb compounds orally. The transparency of the zebrafish larvae enables to perform phenotypic screen and visualise changes of most internal and external systems caused by the compounds. Four different phenotypic screens have been described: chemical genetic screen, therapeutic screen, transgene assisted screen and pathway reporter screen.

Zebrafish have been successfully used in large-scale genetic screens aiming to identify key-genes of developmental processes of vertebrates. This approach involves a mutagenesis step followed by phenotypic screening. To bypass these early requirements of mutagenesis, chemical screens appeared to be a good alternative to modulate protein function. These screens aiming to rescue or induce a specific phenotype with drugs are

called forward chemical genetic screen. In the 1990s, the first chemical screen in zebrafish was carried out, in which zebrafish were used to discover small molecules modulating the development of the central nervous system, cardiovascular system, pigmentation or ear. The timing of some developmental processes could be determined due to the advantage of using chemical compounds that can be added and removed at any time of choice. Of all compounds tested, 1% of them induced specific defects and about 2% were lethal at early stages (Peterson, Link et al. 2000).

Therapeutic screens involve the identification of new bioactive compounds that can cure human diseases such as tumours or bacterial infections. The human disease can be modelled in the zebrafish, and the screen readout would be the restoration of the wild-type phenotype. Even if zebrafish proteins share only 70% identity with their human orthologues, the conservation of functional domains to which the drugs usually bind is much higher, approaching the 100% similarity. Experiments using known anti-angiogenic drugs, anti-coagulant drugs, vasoactive drugs, anti-cancer drugs or anti-inflammation drugs in zebrafish larvae have shown that responses in zebrafish were comparable to those in mammalian systems (Langheinrich 2003). This supports the relevance in using zebrafish as a model organism to discover new therapeutic compounds for human diseases.

Transgene assisted screen involves the use of transgenic zebrafish line in which a protein of interest is associated to a fluorescent protein such as the green fluorescent protein (GFP). The readout of the screen is the visualisation of an altered anatomy through the transgenic marker. This kind of screen can be either genetic to identify mutants, or pharmacological to identify drugs that modulate the phenotype. For example, the endothelial specific Tg(*flk1*:EGFP) zebrafish transgenic line facilitated the identification of mutants with vascular defects (Jin, Herzog et al. 2007).

A pathway reporter screen enables direct visualisation of a signalling pathway. For example, in the transgenic zebrafish line Tg(*Dusp6*:d2EGFP), the green fluorescent protein is expressed under the *Dusp6* promoter, which

is initiated at 4 hpf in the embryo. The d2EGFP expression is under the control of FGF signalling as treatment with FGF receptors inhibitors abolishes d2EGFP expression (Molina, Watkins et al. 2007). The reporter gene is downregulated by the FGF signalling pathway. Therefore, both inhibitors and enhancers of the pathway can be identified in this kind of screen.

A whole organism screening enables to discover molecules involved in complex and poorly understood pathways. This screening approach does not require extensive previous knowledge about the molecular characteristics of the disease. Molecules identified in the screen could be either intrinsically active or could be pro-drugs activated after metabolisation through host detoxifying enzymes. Compounds with undesirable characteristics such as toxicity or unwanted side effects can also be identified during the screen. It is an important advantage of a whole-organism *in vivo* screen to be able to observe both positive and negative effects of molecules that is usually not possible in cell culture assay. Many potential drugs screened using *in vitro* assays are rejected later during clinical trials using animals because of unexpected side effects or ineffectiveness. Toxic compounds or inducing side effects can be identified and discarded in a zebrafish larvae screen, at an early stage of drug discovery. Therefore, hits identified using a whole-organism screen are more valuable as they have already passed a first animal model step.

Because the molecular pathway affected by hit compounds identified using a phenotypic screen is not known, the target and mechanism of action of the hit compounds need to be investigated, which is a critical step of the process. Several techniques are available for this purpose such as affinity chromatography, expression profiling, yeast 3 hybrid or Drug Affinity Response Target Screening (Williams and Hong 2011).

In recent years, zebrafish has been used in several types of *in vivo* drug screen, as a tool to identify lead compounds aiming to cure human disease. Changes of behavioural phenotype can be monitored in zebrafish embryos,

larvae, juveniles or adults. For example, epilepsy can be modelled in the zebrafish by adding the convulsant agent pentylenetetrazole (PTZ) in the water of 2 dpf embryos, increasing the swimming activity of the fish. As PTZ induces the transcription of the gene *fos* in the brain, a screen of 2000 compounds based on *in situ* hybridisation technique has identified 46 new anticonvulsant compounds that suppress the PTZ-induced expression of the gene *fos* (Baxendale, Holdsworth et al. 2013). Toxicity of drugs on specific organs is a problem often identified late in drug development process. Zebrafish model can identify ototoxic compounds through a screen examining the startle response of zebrafish larvae, representing drug-induced hair damage of the lateral line neuromast hair cells (Buck, Winter et al. 2012). Inflammation can be modelled in the zebrafish larvae by sectioning a portion of the tail. Neutrophils response to the injury can be visualised and monitored using a transgenic zebrafish line such as Tg(*mpx*:GFP) marking neutrophils with a green fluorescent protein. A drug screen using this inflammation model has identified compounds that modulate the neutrophils reverse migration mechanism (Robertson, Holmes et al. 2014).

1.3.3. Zebrafish drug screen for antimicrobials

A live-animal antimicrobial drug screening assay has several advantages over *in vitro* target-based and whole cell screening. Infectious diseases are complex processes involving both bacterial virulence determinants and host response, with a lot of interplay between these 2 systems. Most molecules identified via a target-based screening approach or in cell culture lack efficacy *in vivo* in clinical trials on animals. A high-throughput screening using living *C. elegans* has discovered molecules that cure the worms *in vivo* without inhibiting the *in vitro* growth of *Enterococcus faecalis* (Moy, Ball et al. 2006; Moy, Conery et al. 2009), highlighting the influence of *in vivo* environment in bacterial disease. However, a major drawback of *C. elegans* as a model organism for screening purpose is its thick cuticle limiting the diffusion of small molecules. Zebrafish larvae are a more powerful system for drug screen than roundworms as they are permeable to most small molecules and are evolutionary closer to human, including an innate immune system.

A screening platform in zebrafish offers the advantage of replicating the complexities of *in vivo* treatment at a reduced cost than mice. A screening assay using zebrafish modelling an infectious disease focus on lead compounds that suppress the disease phenotype. This include compounds targeting either host or pathogen factors active *in vivo*. In the case of zebrafish embryos modelling systemic *S. aureus* infection, the disease phenotype is death (Prajsnar, Cunliffe et al. 2008). Therefore, the screening assay must highlight compounds that increase the survival ratio of the infected embryos on a specific time period compared to the untreated embryos. These hit compounds could be either inhibitors of *in vivo* virulence factors of the pathogenic bacteria, or enhancers of zebrafish immune system in order to increase bacterial killing *in vivo* or to prevent subversion of the host response. This type of drug screening assay should be able to identify anti-infective compounds that are not typical antibiotics, but rather acting on important pathways that are activated only in an *in vivo* context.

A few drug screening assays using infectious disease modelled in the zebrafish larvae have been described, confirming the possibility to use this kind of model in drug discovery. Methods of semi-automated drug screen platform of zebrafish larvae modelling *Mycobacterium marinum* infection have been described. Both bacterial burden and host survival can be monitored through imaging and fluorimetry readout. Fluorescent bacteria can be visualised and tracked inside the transparent zebrafish, while larval death can be recorded via the increase of green autofluorescence (Takaki, Cosma et al. 2012). A zebrafish model of hepatitis C virus (HCV) infection was developed by co-injecting 2 DNA constructs (prGC3N and p5BR) into the cell of early stage embryos in order to create a HCV sub-replication zebrafish. After assessing the amplification of the sub-replicon in the zebrafish liver, the effectiveness of 2 water-soluble clinical drugs was tested by incubation in the fish water. The inhibition of the sub-replicon amplification in the drug-treated fish enables future drug screening assay for unknown compounds (Ding, Zhang et al. 2011).

1.4. Thesis aims

The increasing resistance of *S. aureus* strains to antibiotics is a worldwide problem to treat these bacterial diseases. Therefore, alternative ways to treat or prevent staphylococcal infections are required.

The aims of this thesis are:

- to design and perform a screening assay using the *S. aureus*-zebrafish embryo infection model with the hypothesis that this approach will reveal new anti-infectious compounds that would either induce the immune system or inhibit *in vivo* staphylococcal virulence factors
- to perform a robust screen of a diverse compounds library and identify compounds that cure staphylococcal infection in the infected zebrafish embryo
- to further investigate the activity of positive hit compounds in zebrafish
- to explore the mechanisms of host bacterial interaction (introduced in more details in chapter 4)

Chapter 2 Materials and methods

2.1. Materials

2.1.1. *Staphylococcus aureus*

2.1.1.1. Bacterial strains

a) SH1000

The wild-type *Staphylococcus aureus* strain used in the majority of experiments is SH1000 with a functional *rsbU*⁺ derivative of 8325-4 (Horsburgh, Aish et al. 2002).

b) GFP-*S. aureus*

Two different GFP expressing strains were used: one strain carries a plasmid containing a chloramphenicol resistant gene (SJF1219) (Needham, Kibart et al. 2004), the other strain carries the pMV158GFP plasmid containing a tetracycline resistant gene (strain not published yet, plasmid published in (Nieto and Espinosa 2003)).

c) CFP-*S. aureus*

CFP-*S. aureus* (SJF3666) is the JLA371 strain carrying the pTKP004-CFP plasmid, which contains a chloramphenicol resistant gene and expresses the CFP colour (Prajsnar, Hamilton et al. 2012).

2.1.1.2. Storage and utilisation of bacterial strains

S. aureus strains were taken from the -80 °C Microbank (Pro-lab Diagnostics) stocks and plated on BHI agar plates. The plates were stored at 4 °C for less than 1 month. Long-term storage was performed by transferring a single colony from an agar plate into Microbank beads stocks, which were placed into -80 °C freezer.

2.1.1.3. Bacterial media

Brain heart infusion (BHI) (supplier: Oxoid) media was prepared at a concentration of 37 g.l⁻¹.

Oxoid agar No. 1 at 1.5 % (w/v) was used to make BHI agar plates.

Liquid and solid bacterial media were prepared using distilled water (dH₂O) and were sterilised by autoclaving for 20 min at 121 °C and 15 psi.

2.1.1.4. Buffer

Phosphate buffered saline (PBS)

NaCl	8 g.l ⁻¹
Na ₂ HPO ₄	1.4 g.l ⁻¹
KCl	0.2 g.l ⁻¹
KH ₂ PO ₄	0.2 g.l ⁻¹

The pH was adjusted to 7.4 using NaOH. After its preparation using dH₂O, the buffer is sterilised by autoclaving.

2.1.2. Zebrafish *Danio rerio*

2.1.2.1. Zebrafish strains

a) LWT

The London Wild Type (LWT) zebrafish strain was used for the screening experiments.

b) fro^{to27c}/+

The fro^{to27c}/+ zebrafish line is a mutant zebrafish line called *frozen*, as the double mutant lacks motility. Experiments using this strain were performed by crossing heterozygous adults, and the progeny was selected in 2 groups: the *frozen* group (double mutant) and the siblings (hets and wild-type).

c) Tg(*mpx*:GAL4)

The *mpx.gal4* zebrafish line is a transgenic line carrying the *mpx*:GAL4 construct.

d) Tg(*mpeg1*:GAL4)

The *mpeg1.gal4* zebrafish line is a transgenic line carrying the *mpeg1*:GAL4 construct.

e) Tg(UASTFLC3)

The UASTFLC3 zebrafish line is a transgenic line carrying the UAS:RFP-GFP-LC3 construct, and generated by a member of the lab, Katy Henry.

f) Atg5 mutant

The Atg5 zebrafish line is a mutant line carrying a defect of 21 bp in the Atg5 gene. This line was generated in Singapore, in Phil Ingham's lab.

g) Atg10 mutant

The Atg10 zebrafish line is a mutant line carrying a 2 bp deletion in the Atg10 gene. This zebrafish line was generated by a collaborator, Stone Elworthy (University of Sheffield).

h) Apg3l mutant

The Apg3l zebrafish line is a mutant line carrying a defect in the *apg3l* gene. This zebrafish line was generated by Lore Lambein, more details about it can be found in chapter 5 of this thesis.

2.1.2.2. Zebrafish media

E3 medium (x10)

NaCl	50 mM
KCl	1.7 mM
CaCl ₂	3.3 mM
MgSO ₄	3.3 mM

The 10x stock was diluted to 1x solution with distilled water. Besides, E3 medium was supplemented with methylene blue with a final concentration of 0.00005% (w/v) in order to avoid fungal growth for most experiments. However, zebrafish embryos used in autophagy-related experiments or involving microscopy were placed in sterile E3 without methylene blue.

2.1.2.3. Zebrafish anaesthesia

A stock solution of 0.4% (w/v) 3-amino benzoic acid ester (tricaine or MS322, Sigma) was prepared in 20 mM Tris-HCl (pH adjusted to 7) and stored at -20 °C. Working stock was stored at 4 °C in the dark. Zebrafish embryos were anaesthetised in final concentration of 0.02% (w/v) tricaine prior to bacterial injections or mounting for microscopy.

2.1.2.4. Methylcellulose

A solution of methylcellulose (3% (w/v)) was prepared in E3 medium without methylene blue. The suspension was mixed, partially frozen and defrosted several times in order to facilitate the solubilisation. Then the solution was aliquoted in 20 mL syringes and stored in the freezer at -20°C. For short-time storage, methylcellulose solution was kept at 28.5 °C.

2.1.3. Drugs

2.1.3.1. Chemical reagents

Reagent	Manufacturer
DMSO	Sigma-Aldrich
Isopropanol	Sigma-Aldrich
Ethanol	Sigma-Aldrich
Chloroform	Sigma-Aldrich
TRlzol ®	Life technologies
Tris HCl	Sigma-Aldrich

2.1.3.2. Compound libraries

The Spectrum compound collection was obtained from MicroSource Discovery System, Inc. The chemistry compound library was made in the Chemistry Department (University of Sheffield, UK). The Johns Hopkins Clinical compound library collection contains FDA and foreign approved drugs that were assembled by Dr. David Sullivan and collaborators at the Johns Hopkins School of Public Health.

2.1.3.3. Potential hits from the drug screen

Name of compound	Manufacturer
Carsalam (2H-1,3-Benzoxazine-2,4(3H)-Dione, 98%)	Sigma-Aldrich
Vitamine D2 = ergocalciferol 40,000,000 USP units/g	Sigma-Aldrich
Zinc sulfide, Powder, <10 Micron, 99.99%	Sigma-Aldrich
Sydnone compound	Chemistry department
Flavin adenine dinucleotide disodium (FAD)	Sigma-Aldrich
Vitamine E acetate ampule of 100 mg	Sigma-Aldrich
Zoxazolamine (2-Amino-5-Chlorobenzoxazole, 97%)	Sigma-Aldrich
Indium(III) chloride, 98%	Sigma-Aldrich
Zinc oxide Ph Eur	Fluka
Zinc acetate, 99.99% metals basis	Sigma-Aldrich
Zinc citrate dihydrate 97%	Sigma-Aldrich
Zinc iodide 98+%	Sigma-Aldrich
Zinc sulfatate hepathydrate 99.99% metal	Sigma-Aldrich

2.1.3.4. Autophagy compounds

Name	Manufacturer
Rapamycin	Sigma-Aldrich
NH ₄ Cl	Sigma-Aldrich
Verapamil	Sigma-Aldrich
Wortmaninn	Sigma-Aldrich
+/- BayK8644	Sigma-Aldrich
N-acetyl-L-cysteine	Sigma-Aldrich

2.1.4. Molecular biology

2.1.4.1. Molecular biology reagents

Reddymix	Thermo Fisher Scientific
Ethidium bromide	Thermo Fisher Scientific
Superscript	Invitrogen, Paisley, UK
MwoI restriction enzyme	New England Biolabs (NEB), Herts, UK
NotI restriction enzyme	NEB
100 bp ladder	NEB
Phenol red	Sigma-Aldrich
10Beta competent cells	Invitrogen
SOC medium	Invitrogen

2.1.4.2. Molecular biology kits

MiniElute PCR purification kit	Qiagen
Mini kit	Qiagen
HiSpeed Plasmid Midi kit	Qiagen
Nucleobond Midi kit	Macherey-Nagel

2.1.4.3. Morpholinos sequences

The Atg10 start, Atg10 splice, Atg5 splice and Atg7 splice morpholinos were obtained as a kind gift from Sarah Baxendale (University of Sheffield), while the other morpholinos were obtained as a kind gift from Angeleen Fleming (University of Cambridge).

Label	Stock conc	Sequence
<i>atg5</i> - 1	1 mM	CATCCTTGTCATCTGCCATTATCA
<i>atg5</i> -1 MisMatch	1 mM	CATCgTTcTCATCTcCCATaATgAT
<i>atg5</i> - 2	1 mM	GTTCTCCAAGTGACACATATAATGA
<i>atg5</i> – 2 MisMatch	1 mM	GTTCTCgAAcTGAgACATAaAATgA
<i>atg16l1</i> - 1	1 mM	AACACTCCACTCTGCGTCCC GCCAT
<i>atg16l1</i> – 1 MisMatch	1 mM	AAGAgTCCAgTCTGCcTCCCcCCAT
<i>atg16l1</i> - 2	1 mM	CTCCTCCTCACAGCATCAAACGCG
<i>atg16l1</i> – 2 MisMatch	1 mM	CTCgTgCTCACAcCATgAAAACcCG
<i>atg10</i> start	1 mM	TCATGATCTCACACGGCCACTTCCG
<i>atg10</i> splice	1 mM	CTGCCTGGAAAACAAGACCAGAAAC
<i>atg7</i> splice	2 mM	GTCCATCCCTATTACACACAATTA
<i>atg5</i> splice	2 mM	TCAACTCAACCTACCATTTAAGAGG

2.1.4.3. PCR primers

Label	Sequence
Atg7MOF	5' ACCGCTTAGACGAAAGTCCA
Atg7MOR	5' TCAGATCCGCAAATGTCAAG
Atg5MOF	5' TGACAAGGATGTGCTTCGAG
Atg5MOR	5' GGTCGAACAACACACCAATG
Atg10EX5F	5' GTGCTGCGCTATGAATACCA
Atg10EX5R	5' GCTAATTCCAGAGCGGGTTT
Gal4 F3	5' AAGTGCGCCAAGTGTCTGA
Gal4 R3	5' TTGGTTTGGGAGAGTAGCG
Atg3Tal1For	5' CCA TTG TTT TTA TGT AGA GCC AGT T
Atg3Tal1Rev	5' TAT GAT GGC CTC CAG CTC A
Atg5For	5' GCT ATG TCA CGT TGC AGT GG
Atg5Rev	5' ACT CCG CAT AAA ACC AGGTG
Atg5SeqRev	5' CAT TTA AGA GGC GTT CCCTCG TGT T
Atg5For2	5' TTT CTT TCT GTC AAT CTG TCA GC
Atg5Rev2	5' CCT CTG CCT TCA TGA CTT TGA G
Atg10For	5' GTC GTA CCC CAC TTT GTC GT
Atg10Rev	5' CGT CTG TCG GAA GTT CAG TG

2.1.5. Disposables

Petri dishes	Scientific Laboratory Supplies Ltd. (SLS), Coatbridge, UK
96-well plate	SLS
24-well plate	SLS
6-well plate	SLS
Pasteur pipette	StarLab
Pipettor tip Microloader for 65micro- injection capillaries (Eppendorf brand)	Thermo Fisher Scientific
Non-filament glass capillary needles	Kwik-Fil™ Borosilicate Glass Capillaries, WPI, Hitchin, UK
Tips	StarLab
Microscopic slides	Thermo Fisher Scientific
Coverslip (number 0)	SLS
High vacuum grease	Dow Corning, Seneffe, Belgium
96-well PCR plate	StarLab
Clear polyolefin StarSeal (PCR)	StarLab
PCR strips + caps	StarLab
PCR tubes	StarLab
1.5 ml microcentrifuge tube	StarLab
2 ml microcentrifuge tube	StarLab
15 ml centrifuge tube	
50 ml centrifuge tube	
QIAshredder	Qiagen

2.1.6. Instruments

PV820 Pneumatic PicoPump	WPI UK, Hitchin, UK
Micropipette puller	Sutter Instruments Co, Novato, USA
NanoDrop Lite spectrophotometer	Fisher Scientific UK Ltd, Loughborough, UK
PCR machine	Bio-RAD
Dissecting microscope	Leica Microsystems Ltd., Milton- Keynes, UK
Fluorescent dissecting microscope	Leica MZ10F, GFP/CFP plus filter
TE-2000 U microscope connected to an Orca-AG camera	Nikon microscope, Hamamatsu camera
Spinning disk confocal microscope	PerkinElmer, Cambridge, UK

2.1.7. Softwares

2.1.7.1. Graph pad Prism software

Graph pad Prism software (version 5.0d) was used to draw survival curves and analyse the statistical relevance of the data.

2.1.7.2. Heat map

The cluster program (Eisen, Spellman et al. 1998) and JaveTreeView (Saldanha 2004) were used to draw the heat map representing the screening results.

2.1.7.3. ApE, primer3, Seqbuilder, FinchTV, NEBcutter, Expasy, clustal omega

ApE - A plasmid Editor v2.0.45. software
Created by M. Wayne Davis

Primer3

It is an online tool that can be accessed on this website address:
<http://bioinfo.ut.ee/primer3/>

SeqBuilder

Software for sequence editing and annotation, automated virtual cloning and primer design

FinchTV version 1.5.0.

NEBcutter V2.0. software

It is an online tool that can be accessed on this website address:
<http://tools.neb.com/NEBcutter2/>

Expasy translation tool

It is an online tool that can be accessed on this website address:
<http://web.expasy.org/translate/>
(Gasteiger, Gattiker et al. 2003)

Clustal Omega tool

It is an online tool that can be accessed on this website address:
<http://www.ebi.ac.uk/Tools/msa/clustalo/>
(Sievers, Wilm et al. 2011)

2.1.7.4. Volocity® 3D image analysis software

Volocity is the software used to process the images obtained with the confocal microscope or the Nikon microscope (Improvision, Coventry, UK).

2.7.1.5. Statistical analysis

The log rank (Mantel-Cox) test was used to compare survival curves in the GraphPad Prism software (version 5.0d). P-value < 0.05 is considered as statistically significant.

* p < 0.05; ** p < 0.01; *** p < 0.001; **** p < 0.0001

2.2. Methods

2.2.1. Culture of *S. aureus*

S. aureus solution was prepared by inoculating 10 mL BHI liquid media in a sterile flask with a single colony. This culture was grown at 37 °C overnight on a rotary shaker at 250 rpm. A small amount of the overnight pre-culture (500 µL) was then taken to inoculate 50 mL of fresh BHI media in a sterile 250 mL conical flask, and grown at 37 °C on a rotary shaker at 250 rpm for 2 hours. Then, 40 mL of that culture was centrifuged at a speed of 5100 rpm for 10 min at 4°C and the supernatant was discarded. The Optical Density (OD) of a diluted sample at 1:10 of this culture was measured at 600 nm in a spectrophotometer. The pellet of bacterial cells was re-suspended in a calculated amount of sterile PBS in order to get a concentration of circa 2.5×10^9 CFU/ml. The precise bacterial concentration was determined by serial dilutions and plating on BHI agar plate.

When using fluorescence expressing *S. aureus* such as the GFP or CFP strains, the appropriate antibiotics were added in the culture.

2.2.2. Direct cell counts (CFU.ml⁻¹)

Direct cell counts are a method to quantify the number of viable cells. Bacterial sample was serially diluted by 1:10 in sterile PBS by successive transfers of 100 µL of solution in 900 µL PBS. Then 10 µL of each dilution was spotted on a BHI agar plate in triplicate. After overnight incubation at 37°C, the number of colony forming units (CFU) was counted.

2.2.3. Zebrafish husbandry

Adult zebrafish were maintained and raised under standard conditions (Nüsslein-Volhard and Sahm 2002), in a continuous re-circulating closed aquarium system at 28°C with a day/night light cycle of 14/10 hours respectively. The UK Home Office approved aquaria are located in the MRC Centre for Developmental and Biomedical Genetics at the University of Sheffield, UK.

The zebrafish experiments were performed on embryos younger than 5.2 days, which is permitted by the UK Home Office legislation to be outside the Animals (Scientific Procedures) Act 1986.

2.2.4. Zebrafish marbling or pair mating

Tanks of fish can be marbled to get a large amount of eggs. A plastic box containing a plastic insert with a grid bottom and overlaid with several marbles was placed into the chosen tank of fish and left overnight. The following day at 8.00 am, the aquarium lights were switched on after a dark period of 10 hours, mimicking a natural light cycle. Right after the lights came on, the fish are simulated to mate thanks to the box of marbles that mimics the river bed. The eggs released by the fish fall through the mesh bottomed insert into the lower half of the box, and can be collected. The water and eggs from the plastic box were poured through a handheld sieve to collect the eggs. The eggs were then poured from the sieve into a Petri dish. About 30 ml of E3 medium was then added, and the eggs sorted in multiple Petri dishes with a density of 50-60 viable eggs, before being placed in a 28.5°C incubator until required for experiments.

Another technique to get zebrafish eggs from adults is called pair mating. In the afternoon, a pair of adult fish of opposite sex was placed in a small plastic box containing an insert box with ridged bottom. The next morning at 8.00 am, when the light are switched on, the fish are simulated to mate and the eggs fall through the insert box. The eggs can be collected in a sieve and poured in a Petri dish, while the adult fish were put back in their original tanks. The eggs were then put in E3 medium and sorted by 60 in Petri dishes (similarly as the sorting of the eggs collected from the marbling technique).

2.2.5. Zebrafish fin clip

Adult zebrafish were anaesthetised in 3-amino benzoic acid ethyl ester (0.02% (w/v)) referred to as tricaine, until they stop moving and fall on their side. The zebrafish are then scooped out with a teaspoon, with the fin on the side of the spoon. A little portion of the fin is cut with a pair of scissors, and

the fin is taken with tweezers and put in a PCR-tube containing a bit of water. The fish are put back in fresh water for recovery. The scissors and tweezers are rinsed in ethanol, and then water between each sample.

2.2.6. Morpholinos injection into zebrafish eggs

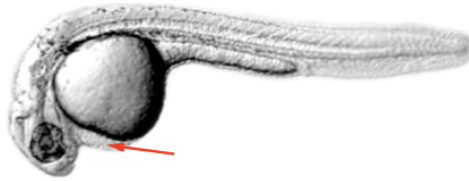
Zebrafish eggs at 1 to 8 cell-stage were collected and viewed under a dissecting microscope. The eggs were aligned against a microscopic slide in a Petri dish, and the excess water was removed. Morpholinos were prepared at the appropriate concentration in sterile water with 10% phenol red to allow visualisation. Injection could start.

2.2.7. Microinjection of *S. aureus* into zebrafish larvae

Zebrafish embryos (30 hpf) were mechanically dechorionated with two pairs of tweezers before being anaesthetized with buffered tricaine by immersion (0.02% (w/v)). Then, they were embedded in 3% (w/v) methylcellulose on a microscopy slide. Embryos were injected using a non-filament glass microcapillary needle (pulled with an electrode puller) filled with the bacterial suspension of known concentration. Microinjection drop sizes were measured on a 0.05 nm graticule in order to get a drop between 1 and 2 nl, depending on the desired dose. Needles were inserted in the yolk sac circulation valley in order to inject directly into the bloodstream (Figure 2.1.A.). The equipment used to perform the injections is a pneumatic micropump (World Precision Instruments PV820) connected to a micromanipulator (WPI), and a dissecting microscope (Leica) (Figure 2.1.B.). After a recovery period of 1h, the fish media was changed in order to remove the dissolved methylcellulose.

For survival assays, every infected fish was dropped in a separate well of a 96-well plate containing E3 media and eventually a chemical compound at a chosen concentration in the case of drug treatment. The total volume in each well was 100 μ L or 200 μ L. The 96-well plate containing zebrafish embryos was placed in an incubator at 28.5°C and the survival of the larvae was recorded at several time points.

A.



B.

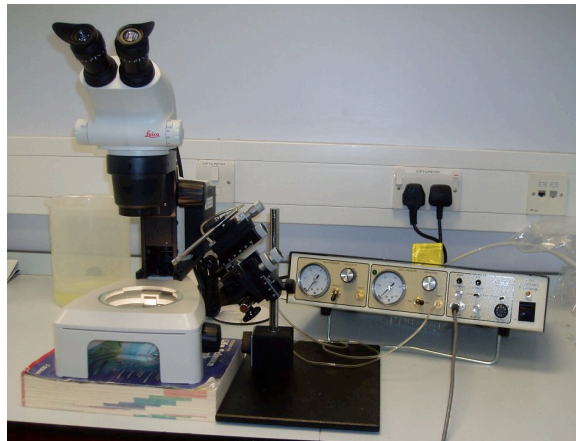


Figure 2.1. *S. aureus* infection into zebrafish larvae

A) Picture of a 30 hpf zebrafish embryo, with the red arrow showing the yolk sac circulation valley, the site of staphylococcal injection to generate systemic infection.

B) Microinjector, micromanipulator and microscope.

The real bacterial dose of each experiment was calculated by injecting 4 times the same volume into 1 ml of sterile PBS. Then, the viable counts were determined by plating 10 μ L of the solution in triplicate on solid BHI agar plates. After an overnight growth at 37 °C, the number of CFU was manually counted and the bacterial dose could be calculated.

2.2.8. Determination of zebrafish larvae mortality following infection

Following infection, embryos were observed for signs of mortality at several time points (up to 120 hpf) and the number of dead embryos was recorded. Mortality was assumed by heart beat cessation.

As the genotyping of dead larvae was required in some experiments (chapter 5), infection was performed using GFP-*S. aureus* in order to check the formation of a big abscess, which is a sign preceding the mortality at about 12 h earlier. This hypothesis was tested in experiment described in paragraph 5.7.1..

2.2.9. Drug modulation by immersion on infected zebrafish

Chemical compounds were dissolved in dimethyl sulfoxide (DMSO), E3 or distilled water, depending on the solubility properties of the compounds. Infected zebrafish embryos were treated by immersion in 96-well plate. A working solution at double the final concentration was prepared by diluting the stock solution in E3 medium. Half of the volume of the working solution was transferred in the wells of a 96-well plate, and the embryos were transferred to the wells with the second half of the volume composed of E3. The chemistry library 2009 (23 compounds) was screened at a final concentration of 10 μ M in a total volume of 200 μ L, the S3 and RF library were screened at a final concentration of 25 μ M in a total volume of 200 μ L, the 95 compounds selected from the Spectrum library were tested at a final concentration of 25 μ M in a total volume of 200 μ L and the 510 compounds issued from the Johns Hopkins library were tested at a final concentration of 10 μ M in a total volume of 100 μ L. Compounds were always tested alongside

the appropriate vehicle control and a positive control. Plates were incubated at 28.5°C.

2.2.10. Mounting zebrafish larvae for microscopy

For microscopy imaging, zebrafish larvae were anaesthetised in tricaine and subsequently transferred to a mounting dish. The mounting dish is composed of a coverslip (number 0) adhering to a 10 mm round opening in a 25 mm Petri dish, using high vacuum grease. Excess water was removed before the addition of a 1% solution of low melting point (LMP) agarose dissolved in transparent E3 and containing 0.02% tricaine. Larvae were manipulated to a flat position with a human hair or a pocking stick.

2.2.11. RNA extraction from zebrafish embryos

2.2.11.1. Preparation of embryos

Pools of 15-20 embryos were collected at several timepoints between 1 and 5 dpf. The embryo water was removed, and the samples were snap frozen in an alcohol/dry ice bath and stored at -80 °C until RNA extraction.

2.2.11.2. Homogenisation of embryos

Embryos were homogenised by adding 500 µL of TRIzol® reagent to each 1.5 mL microcentrifuge tube containing the embryos. Each sample was put through a Qiashreder and centrifuged at full speed for 2 min in order to be homogenised.

2.2.11.3. Purification of embryos RNA

RNA was extracted from homogenised samples through the addition of 100 µL of chloroform. The mixture was shaken vigorously by hand for 15 seconds, then incubated at room temperature for 3 min before being centrifuged at full speed for 5 min to cause triphasic separation. The resultant aqueous phase containing the RNA was transferred to a new 1.5 mL microcentrifuge tube. The purified RNA was subsequently precipitated by the addition of 250 µL of isopropanol, followed by vortexing, incubating at room temperature for 10 min, and then centrifuging at 4 °C for 15 min at full speed. The supernatant

was removed and the remaining RNA pellet was washed with 1 ml of 75% ethanol and centrifuged at 4 °C for 5 min at 7500 rpm. The supernatant was removed and the pellet air-dried before being resuspended in 20 µL of DEPC-dH₂O.

2.2.12. cDNA transcript from RNA samples

The RNA extracted from embryos can be used as a template to get the cDNA transcript.

The following components are added to a nuclease-free microcentrifuge tube:

0.5 µl of random hexamers

10 pg – 5 µg of total RNA

2 µl of 5 mM dNTP mix

sterile distilled water to 13 µl

The mixture was heated to 65 °C for 5 min and incubated on ice for 1 min.

After a brief centrifugation, the following components were added:

4 µl 5X First-Strand Buffer

1 µl 0.1 M DTT

1 µl RNaseOUT™ Recombinant RNase Inhibitor

1 µl of SuperScript™ III RT (200 units/µl)

After a gentle mixing by pipetting up and down, the tube was incubated at 50 °C for 60 min. Then, the reaction was inactivated by heating at 70 °C for 15 min.

2.2.13. Polymerase Chain Reaction

The Polymerase Chain Reaction (PCR) is a biochemical technique that amplifies a single fragment of DNA in multiple copies (thousands to millions).

The ingredients are a DNA template, a pair of primers and Reddymix.

Reddymix is a ready prepared mix that includes a *taq* DNA Polymerase, a mix of nucleotides and salt buffer.

On ice, the following components were mixed in a centrifuge tube:

2 µl cDNA

5 µL reddy mix 2X
2 µl distilled water
0.5 µl primer forward at 10 µM
0.5 µl primer reverse at 10 µM

After a gentle mixing, the tube was put on a PCR machine and the following cycle was performed:

1:94 °C 3 min
2:94 °C 30 sec
3:60 °C 30 sec
4:72 °C 30 sec
5:go to step 2) 34x
6:72 °C 5 min
7:10 °C hold

2.2.14. Agarose gel

Agarose gel electrophoresis is a common way of separating and analysing DNA. Most gels are made between 0.7% and 2% depending on the size of the DNA fragments expected. The higher the percentage agarose, the better the separation of small DNA fragments. For a 2% gel, 1 g of agarose is put in a 250 ml flask with 50 ml of Tris-Acetate-EDTA (TAE) buffer. The flask is heated in the microwave until the agarose is completely melted. After dissolution, a drop of ethidium bromide is added, and the gel is slowly poured in a tank. A comb is inserted on top of the tank to make wells. Once the gel is set, 0.5 X TAE buffer is poured in the gel tank to submerge the gel. A ladder is loaded in the first lane, and the samples are loaded in the following lanes. The gel tank is then closed and the power-source is switched on.

2.2.15. Sequencing

The Exol SAP treatment is performed as a cleanup on the PCR product mix. For 10 samples, a mixture of 32 µL SAP (alkaline phosphatase) + 1.7 µL Exol was prepared. Then 3.2 µL of the above mixture was added to each PCR sample.

The samples were put on the PCR machine, and the cleanup program was run: 37 °C for 2700 sec, 80 °C for 900 sec and 4 °C hold.

10 µL of cleaned PCR sample was mixed with the chosen primer (forward or reverse), and the samples were sent to the GENE group of the University of Sheffield for sequencing.

2.2.16. Construction of TALENs

2.2.16.1. Determination of a target site

The website <https://tale-nt.cac.cornell.edu/node/add/talen-old> was used to determine possible sites for the construction of customised TALENs. The following parameters were changed: a minimum spacer length of 15 bp and a maximum spacer length of 18 bp, while the minimum repeat array length is 15 bp and the maximum repeat array length is 21 bp. It does not require C, G, or T at position 2 (not an A), neither a specific percent composition, neither allowing or not sites to end in G, neither a A, C, or G at position 1 (indeed, we do want a T at position 1), neither a T at position N.

2.2.16.2. Golden gate reactions assembly stage 1

In the first golden gate reactions, the part A was assembled into plasmid pFusA (F5) with the first ten RVD plasmids, while the part B was assembled into the pFusB plasmid appropriate for the TALEN length remembering that the last RVD was not added to the pFusB. So the left TALEN subunit with 15 RVDs used pFusB4 plasmid; and the right TALEN subunit with 16 RVDs used pFusB5 plasmid.

All the plasmids needed for each construct were taken, thawed, mixed and pulse spinned. Then the 4 golden gate reactions were assembled in 0.2 ml tubes on ice.

for each A part :

1 µl each RVD plasmid at 100ng/µl

1 µl pFusA (F5) at 100ng/µl

4 µl H₂O

2 µl T4 ligase buffer NEB

2 µl T4 ligase NEB

1 µl Bsa1 NEB

for each B part :

H₂O to 20 µl

1 µl each RVD plasmid at 100ng/µl

1 µl appropriate pFusB at 100ng/µl

2 µl 10x T4 DNA ligase buffer NEB

2 µl T4 DNA ligase NEB

1 µl Bsa1 NEB

Each reaction was mixed by a gentle up and down pipetting, then went on the PCR machine to be processed with the following cycle with NOT hot-lid option: 10x(37°C/5min+16°C/10min)+50°C/5min+80°C/5min.

When complete, 0.3 µl of 25 mM rATP (thawed and mixed) was added, as well as 1 µl plasmid safe nuclease. Again, each golden gate reaction was mixed by gentle up and down pipetting, then incubated 1 h at 37 °C.

2.2.16.3. Transformation

Each golden gate reaction was transformed into NEB10Beta competent cells. After thawing the cells on ice, 12.5 µl was transferred very gently to ice cold 2 ml tubes, then the NEB protocol was followed exactly using 1 µl of reaction per transformation. Then, 50 µl of each transformation was streaked over a spectinomycin Xgal LB agar plate with flat toothpicks so as to get a wide range of colony densities across the plate. Plates were grown at 37 °C overnight.

2.2.16.4. Miniprep

For each reaction, 3 white colonies were picked and placed in 6 ml of LB spectinomycin in a 25 ml tube with loose lid. The tubes were placed on a shaking incubator at 37 °C overnight. The following day, the cultures were spinned down to discard the supernatant LB and save the bacterial pellet. For each of the 4 components, a Qiagen miniprep was performed (with PB wash) according to the manufacturer's protocol. Only one of the clones was

used, while the other 2 were frozen. The Qiagen minipreps were subsequently eluted into 50 μ l H₂O, before being digested with NheI + XbaI and checked on an agarose gel. For the 4 digests, the following master mix was prepared and assembled on ice:

20 μ l H₂O

5 μ l 10x NEB2 buffer

0.5 μ l 10mg/ml BSA

2 μ l NheI

3 μ l XbaI

6 μ l master mix was transferred to each tube with 4 μ l miniprep. The reaction mix was gently pipetted up and down, then incubated for 1 hour at 37 °C. The reaction mix was run on 1.1% agarose gel alongside 5 μ l, 2 μ l and 1 μ l loadings of 5x diluted NEB 2log DNA ladder. The expected band sizes are 266 bp, 2132 bp and 500 bp-1100 bp (depending on RVD number). The DNA concentration of the minipreps could be estimated with the band intensities.

2.2.16.5. Golden gate reactions assembly stage 2

The A and B parts for each TALEN subunit were combined using a golden gate reaction composed of:

5 μ l H₂O

4 μ l A miniprep (about 150 ng)

4 μ l B miniprep (about 150 ng)

1 μ l 150ng/ μ l the appropriate final RVD plasmid

1 μ l 75ng/ μ l pCAGT7TALEN

2 μ l 10x T4 DNA ligase buffer NEB

2 μ l T4 DNA ligase NEB

1 μ l Esp3I

Each reaction was mixed by gently pipetting up and down, then put on a PCR-machine to be processed with the "TALEN" program choosing the NOT hot-lid option: 10x(37oC/5min+16oC/10min)+50oC/5min+80oC/5min.

2.2.16.5. Transformation

Each golden gate reaction was transformed into NEB10Beta competent cells. After thawing the cells on ice, 12.5 µl was transferred very gently to ice cold 2 ml tubes, and the NEB protocol was followed exactly using 1 µl of reaction per transformation. Then, 50 µl of each transformation was streaked over a carbenecillin Xgal LB agar plate with flat toothpicks so as to get a wide range of colony densities across the plate. Plates were grown at 37 °C overnight.

2.2.16.6. Nucleobond midiprep

For each TALEN subunit, one white colony was picked and grown up in 100 ml LB carbenecillin medium in a flask shaking overnight at 37 °C. Then, a nucleobond midiprep was performed following the manufacturer's booklet. The final precipitation was done in six 1.5 ml tubes. All supernatant was removed after the spin down, pulse spin, liquid removal, wash with 1 ml 70% ethanol, spin, liquid removal, pulse spin, last trace of liquid removal, and finally an air dry with open tubes on bench for one minute. The pellet of each tube was resuspended in 20 µl H₂O, before being mixed and pooled together to get a 120 µl prep. 1 µl of the pooled prep was diluted with 99 µl H₂O to measure the concentration on a big spectrophotometer at A260. A 30 µl stock of 100 ng/µl was prepared and 20 µl was submitted for sequencing using TAL_R2: ggcgacgaggtggtcgttgg and SeqTALEN_5-1 catcgcgcaatgcactgac. The sequences could be checked against the seqbuilder electronic expected constructs.

The midiprep were tested with a BamHI+XbaI digest assembled on ice:

7 µl H₂O

1.5 µl 100 ng/µl DNA

1 µl 10x NEB3 buffer

0.1 µl 100x BSA

0.5 µl BamHI

0.5 µl XbaI

The reaction was mixed by gently pipetting up and down, then incubated for 1 h at 37 °C.

The BamHIXbal digests were run on a 0.7% agarose gel alongside 5 μ l, 2 μ l, and 1 μ l of 5x diluted NEB 1kb DNA ladder. Lanes were loaded with 1 μ l, 3 μ l and 6 μ l. The BamHIXbal digest should give 5322 bp and about 2400 bp (depending on number of RVDs).

2.2.16.7. Linearisation of TALEN plasmids

A linearized pCAGT7TAL constructs was prepared with NotI digestion. The following reaction mix was assembled on ice:

H₂O to 300 μ l

6 μ g L construct

6 μ g R construct

30 μ l 10x NEB3 buffer

3 μ l 10 mg/ml BSA

10 μ l NotI

The reaction mix was mixed by gently pipetting up and down, then incubated for 1 h at 37 °C in water bath. The plasmid was purified using two qiagen PCR clean up columns, eluted with H₂O (30 μ l eluate from one was used to elute the other such that the total elution was 30 μ l).

The purified NotI digest was run on a 0.7% agarose gel alongside 5 μ l, 2 μ l, and 1 μ l of 5x diluted NEB 1kb DNA ladder. After adding 1 μ l to 9 μ l of 15% ficol with loading dye. Lanes were loaded with 1 μ l, 3 μ l and 6 μ l, and the relative band intensities were used to quantitate the 9 kb linearized plasmids.

2.2.16.8. in vitro mRNA synthesis

TALEN mRNA was synthesised from the NotI linearised plasmid using the Epicenter T7 Message Max ARCA kit.

In 0.2 ml tube at room temperature, the following reaction mix was assembled:

5.5 μ l 400 ng/ μ l DNA

2 μ l 10x buffer

8 μ l NTP CAP mix

2 μ l 100 Mm DTT

0.5 µl scriptguard

2 µl enzyme mix

The reaction mix was gently mixed, incubated in PCR machine 30 min at 37 °C. Then 1 µl DNAase was added, mixed and incubated for 15 min at 37 °C.

The TALEN mRNA was subsequent purified with RNeasy Minielute Cleanup kit (Qiagen) following the manufacturer's instruction (elution into 14 µl H₂O). 0.5 µl of elute was checked on an 0.7% agarose gel, while the remaining of the RNA was immediately stored at -80 °C.

2.2.16.9. Injecting fish eggs with TALEN mRNA

On the morning of injection, 3.5 µL of TALATG3 mRNA was mixed with 0.5 µL of phenol red. Then, 0.5 nl, 1 nl and 1.5 nl of the mixture was injected into 1-cell stage LWT zebrafish eggs. Embryos were grown at low density (<50 per petri dish) in a 28 °C incubator up to 5.2 dpf, then in the aquarium system.

2.2.17. Genotyping of mutation generated by TALENs

2.2.17.1. Mutation analysis of TALENs injected embryos

The somatic mutation induced by the TALENs can be assessed by a PCR and digestion test. The PCR amplifies a portion across the target site and the chosen restriction enzyme recognises a portion of the target site. It is important to also do control tests on uninjected embryos when testing the efficiency of the TALEN to generate mutations.

DNA from 72 hpf healthy looking injected embryos was extracted, and a restriction digest test was performed.

2.2.17.2. DNA preps from single embryos

For the first test, individual DNA samples from each of six injected and four uninjected embryos at 72 hpf were prepared. There were 2 options for this step:

EITHER:

The anaesthetized embryos were placed in single 200 µl PCR tubes on ice, and all the water was removed. Then 100 µl of 50 mM NaOH was added to each embryo. The tubes were heated at 95 °C for 20 min on the PCR machine, before adding 10 µl of 1 M Tris HCl (pH 8) to each tube.

OR:

The anaesthetized embryos were placed in single 200 µl PCR tubes on ice, and all the water was removed. Then 50 µl of embryo digestion buffer (10 mM Tris-HCl pH8, 1 mM EDTA, 0.3% Tween 20, 0.3% NP40) was added. On a PCR machine, the samples were heated for 10 min at 98 °C. On ice, 4 µl of 25 mg/ml proteinase K was added. The tubes were then heated for 3 h at 55 °C, then 10 min at 98 °C.

In both cases, a centrifugation of 30 min at full speed at 4 °C immediately before use was performed.

2.2.17.3. PCR and restriction enzyme test

Primers were designed to give an amplicon of between 100 bp and 300 bp. The Atg3Ta1 primers amplify a product of 342 bp.

A PCR mastermix was prepared on ice (usually n+1 or n+2 the amount of samples).

The recipe for 1 sample (if small amount required):

H₂O: 5 µl

Reddymix: 10 µl

F primer at 10 µM: 1 µl

R primer at 10 µM: 1 µl

The recipe for 1 sample (if large amount required):

H₂O: 6.8 µl

Reddymix: 10 µl

F primer at 100 μ M: 0.1 μ l

R primer at 100 μ M: 0.1 μ l

On ice, 17 μ l of mastermix was mixed to 3 μ l of single embryo lysate in a PCR tube. After a gentle mixing, the tube was put on a PCR machine and the following cycle was performed:

1:94 °C 2min
2:94 °C 20sec
3:55 °C 20sec
4:72 °C 45sec
5:go to step 2) 34x
6:72 °C 3min
7:10 °C hold

The amplicon was tested on a 2.5% agarose gel electrophoresis with 3 μ l of the PCR reaction, next to a NEB 100 bp ladder.

On ice, 1 μ l of restriction enzyme was added to the remaining 17 μ l PCR reaction in the 200 μ l PCR tube. After a gentle mixing by pipetting up and down, the tube was incubated at the appropriate temperature for 3 h. The digestion was tested with 15 μ l loaded on a 2.5% agarose gel electrophoresis, with NEB 100 bp ladder.

2.2.17.4. Screening potential founders

Once the TALEN injected embryos were grown to adulthood, the founder fish were identified. Founder fish were defined as fish carrying a mosaic germlines such that some of their offspring are carriers for a TALEN induced mutation. The potential founder adult fish were outcrossed with wild-type fish and put into individual tanks while their progeny embryos was tested using a PCR and restriction enzyme test.

From each potential founder, three 72 hpf embryos were put into each of eight wells of a 96 well PCR plate. After removing all the liquid, 100 μ l of 50 mM NaOH was added to each well. The plate was heated at 95 °C for 20 min on the PCR machine, before adding 10 μ l of 1 M Tris HCl (pH 8) to each well. Then, 100 μ l of milliQ water was added to the zebrafish embryos DNA mixture of each well using a multi channel pipette. The plate was mixed on a

vortex and spinned down at maximum speed for 30 min. Then, 1.5 µl of the mixture of each well was transferred to each well of another 96-well plate to be mixed with the PCR mix. On ice, 18.5 µl of PCR mix was added to each well using a multichannel pipette and pipette up and down to mix.

The PCR mix was composed of:

830 µl H₂O

1 ml reddy mix

10 µl 100 µM left primer

10 µl 100 µM right primer

The plate was put on a PCR machine for the following cycle:

1:94 °C 2 min

2:94 °C 20 sec

3:55 °C 20 sec

4:72 °C 45 sec

5:go to step 2) 34x

6:72 °C 3 min

7:10 °C hold

On ice, 0.5 µl of the appropriate restriction enzyme (MwoI) was added to each well. After a gently mix of the whole reaction by pipetting up and down, the plate was incubated on a PCR machine at 60 °C for 3 h. Each digest was then checked on a 2.5% agarose gel electrophoresis alongside the NEB 100bp ladder. The progeny of the fish that were transmitting a mutation were grown up.

2.2.17.5. Screening F1 fish carriers

The F1 progeny of mosaic germ line founder fish will include fish that are carriers. Once they are old enough, these fish were fin clipped and tested by PCR.

The fin clips were put in wells of a 96 well plate and fish were placed in individual tanks. All the liquid of the wells containing the fin clips was removed, before adding 100 µl of 50 mM NaOH to each well. The plate was heated at 95 °C for 20 min on the PCR machine, before adding 10 µl of 1 M Tris HCl (pH 8) to each well. Then, 100 µl of milliQ water was added to the fin clip DNA mixture of each well using a multi channel pipette. The plate was mixed on a vortex and spinned down at maximum speed for 30 min. Then,

0.5 µl of the fin clip DNA mixture of each well was transferred to each well of another 96-well plate to be mixed with the PCR mix. On ice, 19.5 µl of PCR mix was added to each well using a multichannel pipette and pipette up and down to mix.

The PCR mix was prepared with the following components:

830 µl H₂O

1 ml reddymix

10 µl 100 µM left primer

10 µl 100 µM right primer

The plate was then put on a PCR machine and the following cycle was performed:

1:94 °C 2 min

2:94 °C 20 sec

3:55 °C 20 sec

4:72 °C 45 sec

5:go to step 2) 34x

6:72 °C 3 min

7:10 °C hold

On ice, 0.5 µl of the appropriate restriction enzyme (MwoI) was added to each well. After a gently mix of the whole reaction by pipetting up and down, the plate was incubated on a PCR machine at 60 °C for 3 h. Each digest was then checked on a 2.5% agarose gel electrophoresis alongside the NEB 100bp ladder.

2.2.18. Genotyping of zebrafish mutant *apg3l*, *atg5* and *atg10*

Zebrafish mutants *apg3l* and *atg10* can be genotyped by a PCR and restriction digestion test, while the zebrafish mutant *atg5* can be genotyped with a PCR test only.

In all 3 cases, the first step in the gDNA extraction of zebrafish embryos: The anaesthetized embryos are put in single PCR tubes (or PCR plates) and all the excess water is removed. Then, 100 µl of 50 mM NaOH is added to each embryo, before heating the tubes at 95 °C for 20 min on a PCR machine. An amount of 10 µl of 1 M Tris HCl (pH 8) is added to each embryo, and 3 µl of

this solution is used for PCR genotyping. The tubes can be stored at -20 °C until needed.

The second step is the PCR:

The PCR tubes are centrifuged for 30 min at full speed at 4 °C, and 3 µl of the solution is used for the PCR, with 17 µl of PCR mastermix.

The PCR mastermix consists of:

H₂O: 5 µl

Reddymix: 10 µl

F primer at 10 µM: 1 µl

R primer at 10 µM: 1 µl

The Atg3Tal1For and Atg3Tal1Rev primers are used to genotype *apg3l* zebrafish mutants, the Atg5For2 and Atg5Rev2 primers used to genotype *atg5* zebrafish mutants, and the Atg10For and Atg10Rev primers used to genotype *atg10* zebrafish mutants.

The samples are put in the PCR machine for the following cycle:

1:94oC 2min

2:94oC 20sec

3:55oC 20sec

4:72oC 45sec

5:go to step 2) 34x

6:72oC 3min

7:10oC hold

The third step is the restriction digestion step, which is only performed for *apg3l* and *atg10* samples. On ice 0.5 ul of the restriction enzyme is added to each well. MwoI is used for the *apg3l* genotyping and BanII is used for the *atg10* genotyping. The entire reaction is then gently mixed up and down. The plate is then incubated on a PCR at the appropriate temperature (eg 60 °C for MwoI and 37 °C for BanII) for 3 h.

The fourth step is the agarose gel electrophoresis. The PCR samples or digested PCR samples are checked on a 2.5% agarose gel electrophoresis alongside the NEB 100 bp ladder.

Chapter 3 : An *in vivo* drug screen assay for novel anti-staphylococcal compounds

3.1. Introduction

Antibiotic-resistant *S. aureus* strains have become a worldwide public health concern, as it is difficult to treat people infected with these bacteria carrying one or multiple resistance(s) to current drugs. Therefore, infected patients are subject to chronic disease and potentially death. In presence of high antibiotic drug use, antibiotic-resistant bacteria are selected over non-resistant ones. In addition, susceptible bacteria can develop or acquire antibiotic resistance mechanisms. Indeed, antibiotic resistance genes can spread among bacterial communities due to the plasticity of their genome. Key antibiotics that used to cure infected people - methicillin - have now become insufficient. Analogues of existing antibiotics are synthesised to overcome known antibiotic-resistance mechanisms, but it is only a matter of time for the bacteria to develop new antibiotic resistance mechanisms. There is a cyclic pattern in which the marketing of a new antibiotic is always followed by the emergence of bacterial resistance mechanisms.

The traditional way to discover antibiotics is by testing natural or synthetic molecules in *in vitro* experiments on bacterial colonies growing in liquid or solid media. This approach has produced only 2 new classes of antibiotics (oxazolidinone and cyclic lipopeptide) on the market since 1962, which is extremely low compared to the 20 new antibiotic classes released between 1940 and 1962 (Coates, Halls et al. 2011). New strategies are therefore required to discover new antibacterial drugs, which have become challenging. Even though knowledge of important bacterial pathways has increased immensely, there are some bacterial mechanisms that still need to be discovered and understood. One problem of *in vitro* drug screen is that important bacterial mechanisms active *in vitro* might not be active *in vivo*, and inversely. Indeed, some bacterial virulence determinants are expressed

at specific time of the infection in a host, which could not be detected in *in vitro* assays (Cheung, Bayer et al. 2004).

Thanks to its ease of pharmacological manipulation and its small size, zebrafish larvae have been successfully used in several *in vivo* screening assays modelling human disease (Cao, Semanchik et al. 2009; Robertson, Holmes et al. 2014). A few zebrafish drug screens modelling infectious disease have also been performed in the recent years, illustrating the potential of zebrafish larvae for anti-infective compounds discovery (Carvalho, de Sonnevile et al. 2011; Takaki, Cosma et al. 2012; Veneman, Stockhammer et al. 2013). An *in vivo* antimicrobial screening assay enables to identify molecules acting on new target, offering the physiological context of an infection and combine the screening and animal testing in one single step.

The systemic staphylococcal infection into zebrafish embryos model provides an *in vivo* tool to develop an anti-staphylococcal drug screen. In this infection model, the mortality rate of infected zebrafish embryos is influenced by the initial intravenous *S. aureus* injection – the higher the dose, the faster the infected zebrafish embryos die. The host cellular immune cells such as neutrophils and macrophages phagocytose bacterial cells in the initial 2 h of infection. On the bacterial side, specific virulence factors are expressed during the infection, and knocking out some virulence genes such as *perR*, *pheP* and *saeR* attenuates the virulence of the strains bearing these knockout mutations. The less virulent *S. aureus* strains are, the lower the mortality rate of infected zebrafish larvae is (Prajsnar, Cunliffe et al. 2008; Prajsnar, Hamilton et al. 2012). Infected zebrafish larvae are susceptible to pharmacological manipulation, modulating the survival rate of the infected larvae. Indeed, preliminary tests showed that the addition of an antibiotic compound in the zebrafish media enhances the survival rate of the larvae. The susceptibility of zebrafish larvae to small molecules provided encouraging evidence that the established *S. aureus*-zebrafish infection model would be a suitable platform for high-throughput phenotype-based drug discovery.

3.1.1. Aims and hypotheses

The aim of this chapter is to establish a robust *in vivo* screen for new modulators of *S. aureus* survival using the zebrafish larvae model. I hypothesised that this new screening approach will lead to the discovery of compounds that have a different mechanism than traditional antibiotics. This *in vivo* approach would permit to identify compounds that either inhibit the *in vivo* virulence factors and subversion strategies of the pathogen, or enhance the immune defences of the host.

3.2. Optimisation of experimental parameters of the screening assay

Several experimental parameters of the zebrafish-*S.aureus* infection model were optimised in order to get reproducible conditions between experiments. The chosen variables would also define the cut-off between potential hit compounds and the control. It was a phenotype-based drug screening assay defined by the visual detection of a clear phenotype, which had only two options: dead or alive zebrafish embryos (Figure 3.1.). Therefore, compounds increasing the survival rate of infected zebrafish larvae were candidates as hit compounds.

S. aureus often cause minor skin infections that are local and easily treated. However, bacteria entering blood circulation generate the most severe infections, as they are associated with a high morbidity and mortality. Once in the bloodstream, bacteria can travel in the body and invade organs such as brain, heart, lungs, joints or bones (Corey 2009). These deep-seated infections are the most life-threatening and the most difficult to treat. A systemic infection into zebrafish embryos was chosen to model severe staphylococcal diseases that reach internal organs.

The *S. aureus* strain used in the experiments is the *S. aureus* SH1000 strain. It is a laboratory strain that has an active accessory sigma factor σ^B that transcriptionally regulates several virulence-associated loci. The σ^B is also

active in MSSA1112 and Newman, 2 clinical isolates, and it is known that σ^B influences the expression levels of *agr* and *sar* (Bischoff, Entenza et al. 2001). *S. aureus* SH1000 strain shows a reduction in *agr* (RNA III) and *hla* expression compared to the *rsbU* negative sister strain (8325-4) (Horsburgh, Aish et al. 2002). The low expression level of exoproteins is representative of 2 epidemic MRSA strains (CMRSA-1 and CMRSA-3) in Canada (Papakyriacou, Vaz et al. 2000). This low production of exotoxins phenotype, associated to a high capacity to bind host proteins, is essential and advantageous during the colonisation phase of an infection. Even though SH1000 is not a clinical strain, it has some similar characteristics to some of them such as the low protease production and the lower expression of Hla levels.

Injections were performed into 30 hpf old zebrafish embryos for a few reasons. It has been shown that innate immune cells (neutrophils and macrophages) are already present and active at that developmental stage of the zebrafish embryo. In addition, an early timepoint of bacterial injection enables to monitor the response to the infection for the longest time (96 h) before the zebrafish larvae become protected under the Animals (Scientific Procedures) 1986 Act. Monitoring an infection in zebrafish larvae older than 5.2 dpf requires a special animal licence and is highly regulated. It is thus a compromise between the ability to assess the interaction between the pathogen and the innate immunity and a welfare choice for our animal model.

The mortality rate depended on the initial staphylococcal dose injected into the zebrafish embryos. In order to decide which dose would be optimal for the screening assay, 3 different doses (2500, 3700 and 5000 CFU) were injected intravenously into 30 hpf embryos and the percentage survival of the 3 groups was recorded. At 70 hpi (hours post-infection), zebrafish embryos infected with a dose of 2500 CFU showed a survival of $59.6 \pm 4.7\%$ (mean \pm SEM), while a dose of 3700 CFU showed a survival of $45.3 \pm 6.2\%$ and a dose of 5000 CFU showed a survival of $26.8 \pm 4.2\%$ (Figure 3.2.). A dose of 3700 CFU induced a mortality rate that would allow identification of compounds increasing larval survival due to the positive effect of a drug. This

dose was also low enough to identify compounds reducing larval survival due to a negative effect of the test molecule. A dose of 3700 CFU represented a survivable infectious challenge, preventing overwhelming the host immune system and enabling a functional innate immune response to staphylococcal infection. Therefore, 3700 CFU was the staphylococcal dose chosen to infect zebrafish embryos to screen small molecules in the *in vivo* drug screen assay.

Once the optimal infectious dose to infect zebrafish embryos was chosen, it was important to reliably inject the same dose in every experiment carried out during the drug screening. For this purpose, aliquots of bacterial solution of *S. aureus* SH1000 were frozen and stored in the - 80 °C freezer until utilisation. A zebrafish survival experiment was carried out to test if the utilisation of freshly prepared or defrosted *S. aureus* would influence the virulence of the bacteria. As observed in Figure 3.3., the survival rate of infected zebrafish larvae was not significantly different whether the bacteria were prepared on the day of the experiment or in advance and stored in the freezer.

The drug screen aimed to identify compounds that could cure zebrafish embryos infected with *S. aureus*, and a positive control of the assay would have a similar effect as an antibiotic drug. Three antibiotics - penicillin G, tetracycline and chloramphenicol - were tested to determine their effect on the survival of *S. aureus* injected zebrafish embryos. The infected larvae were immersed in the specified antibiotic dissolved in the E3 medium continuously from 1 h after staphylococcal injection. All 3 antibiotics significantly increased the survival of the infected larvae, but penicillin G required a much lower concentration to protect the larvae against infection compared to tetracycline or chloramphenicol (Figure 3.4.A.). Two different concentrations of penicillin G were tested on infected zebrafish embryos to determine the optimal concentration. The proportion of surviving larvae treated with penicillin G at 6.4 mg/L was 100 % at the end of the experiment against 90.7 ± 4 % (mean \pm SEM) for penicillin G at 3.2 mg/L (Figure 3.4.B.). Therefore, the dose of 6.4 mg/L of penicillin G was chosen as the positive

control for the screening assay. The negative control chosen was dimethyl sulfoxide (DMSO) - the solvent in which most of the compounds tested were dissolved. Prior studies had shown that DMSO at < 1 % had not detrimental effect on larval development and immunity (Hallare, Nagel et al. 2006). I therefore used a final concentration of DMSO of less than 0.5% in the fish water to minimise any negative effect due to the solvent itself.

Based on the Chi-squared statistics (Wilson and Hilferty 1931), 5 infected zebrafish embryos per treatment would allow detection of a large effect increasing survival from 40% to 100%, with a confidence of 80% assuming significance at $p=0.05$. This was the minimum number required to discriminate highly effective potential hit compounds tested in the primary screen from the negative control and to reduce the noise coming from the variability of the model. In addition, a small number of fish allowed us to screen a relatively large amount of different compounds. Five fish per group was a compromise between relatively good discrimination and relatively large number of compounds tested. However, 5 fish per group was only suitable for the detection of significant large effects.

The assay carried out to perform the *in vivo* screening assay is summarised here. A box of marbles was introduced in a tank of London wild-type (LWT) zebrafish, inducing the adult fish to lay eggs on the following day at lights-on. The eggs were then sorted to ensure all embryos were at the same developmental stage and were placed in plates of E3 medium in the 28.5°C incubator. After manual dechoriation, 30 hpf embryos were anaesthetised and microinjected with a defrosted suspension of live *S. aureus* SH1000 strain at a known concentration into the yolk circulation valley in order to access the circulation directly. One hour after injection, infected larvae were distributed in separate wells of a 96-well plate containing screen compounds. A simplified diagram of the *in vivo* *S. aureus* infection screening assay is presented on Figure 3.5.A..



Figure 3.1. Visual detection of the alive or dead status of zebrafish embryos

Scoring alive/dead zebrafish at 70 hours post infection (hpi) of zebrafish infected with *S. aureus* S1000 strain. Alive zebrafish are intact, can swim in the wells and their heartbeats are visible.

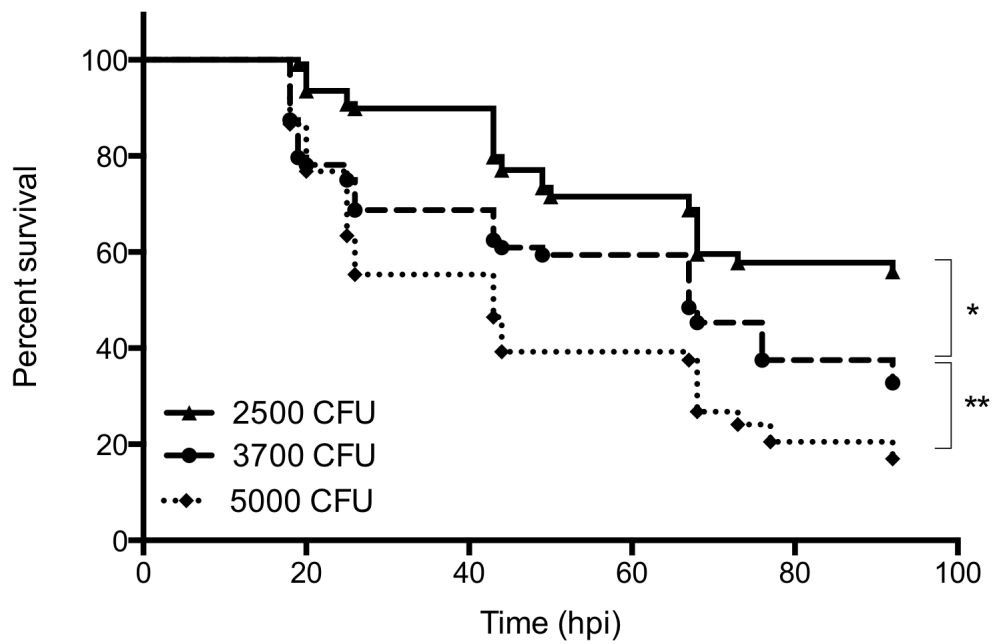


Figure 3.2. Effect of 3 different staphylococcal doses on the survival of zebrafish embryos

LWT zebrafish embryos (30 hpf) were injected with wild-type *S. aureus* (SH1000) into the blood circulation with the 3 doses indicated. n ≥ 64 fish per group (4 to 6 independent experiments).
 * p-value < 0.05; ** p-value < 0.01

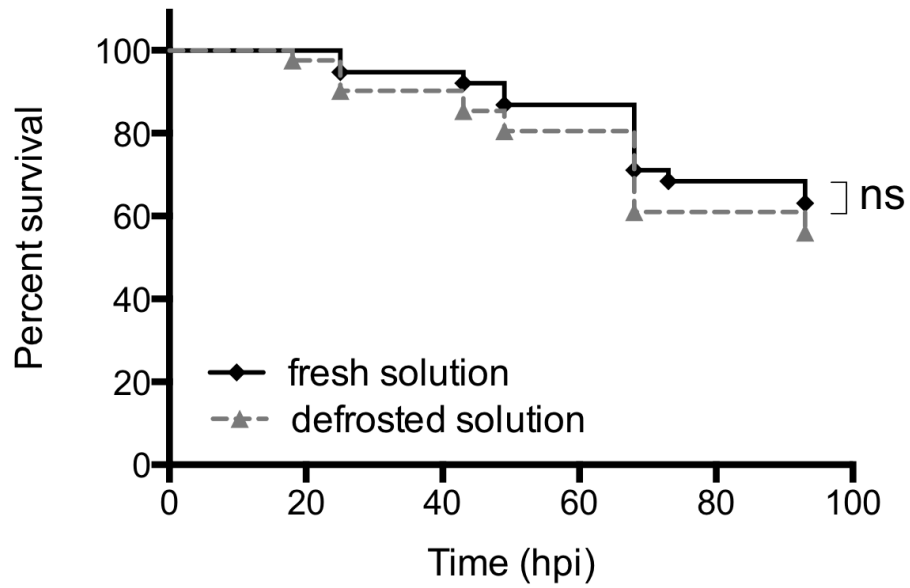


Figure 3.3. Effect of freshly prepared and defrosted staphylococcal injection on the survival of zebrafish embryos

LWT zebrafish embryos (30 hpf) were injected with 2500 CFU of wild-type *S. aureus* (SH1000) into the blood circulation. The bacterial inoculum was either freshly prepared (fresh solution) or defrosted (defrosted solution).

n ≥ 38 fish per group, 1 experiment.

ns = not significant

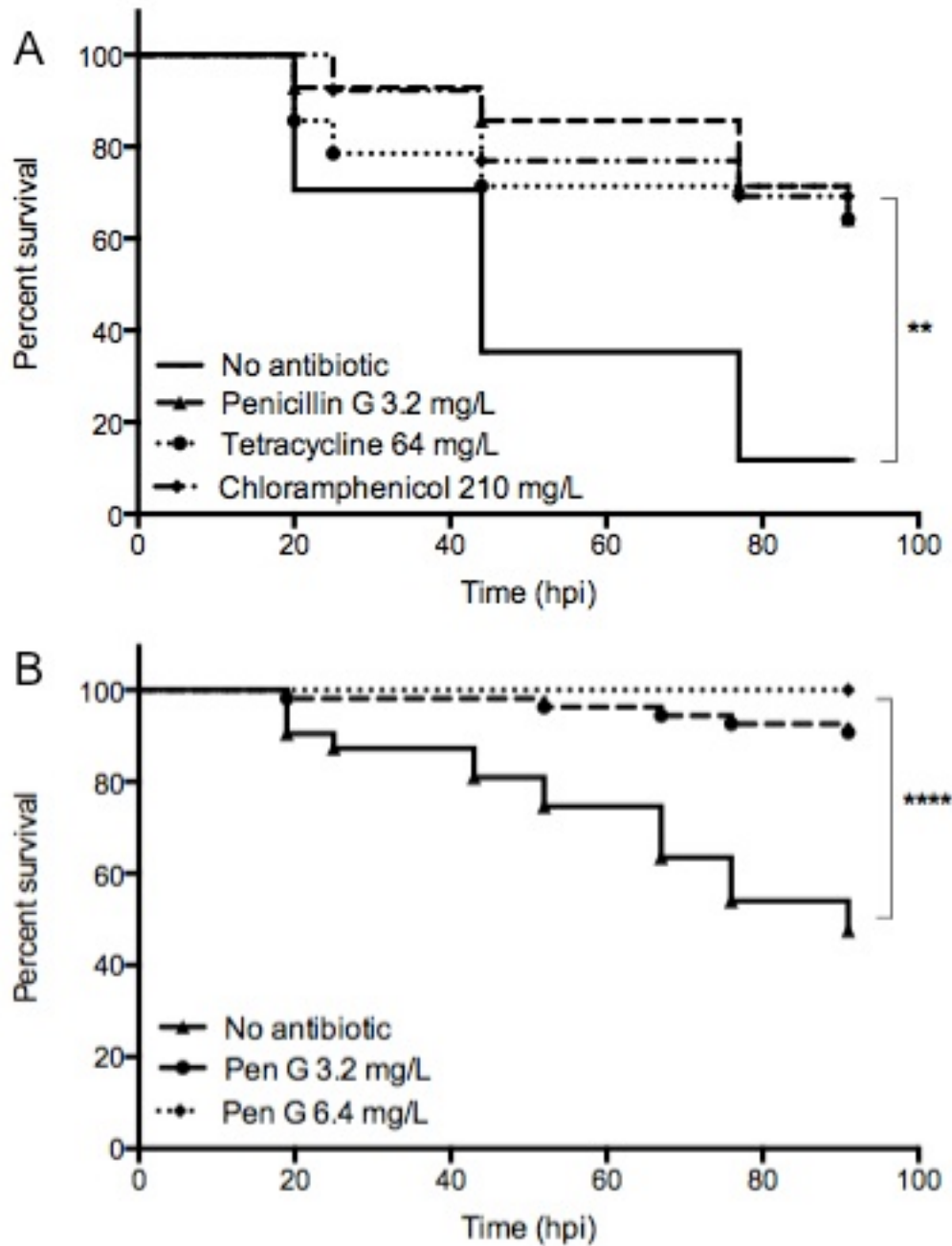


Figure 3.4. Increase in survival of infected zebrafish embryos treated with antibiotic

A) LWT zebrafish embryos (30 hpf) were injected with 5000 CFU of wild-type *S. aureus* (SH1000) into their blood circulation and were treated with the antibiotics indicated by immersion.

n≥13 fish per group, 1 experiment

** p-value < 0.01 for no antibiotic group vs. any other antibiotic group.

B) LWT zebrafish embryos (30 hpf) were injected with 3700 CFU of wild-type *S. aureus* (SH1000) into their blood circulation and were treated with penicillin G (Pen G) at a concentration of 3.2 or 6.4 mg/L by immersion.

n≥54 fish per group (4 independent experiments).

**** p-value < 0.0001 for no antibiotic group vs. pen G group.

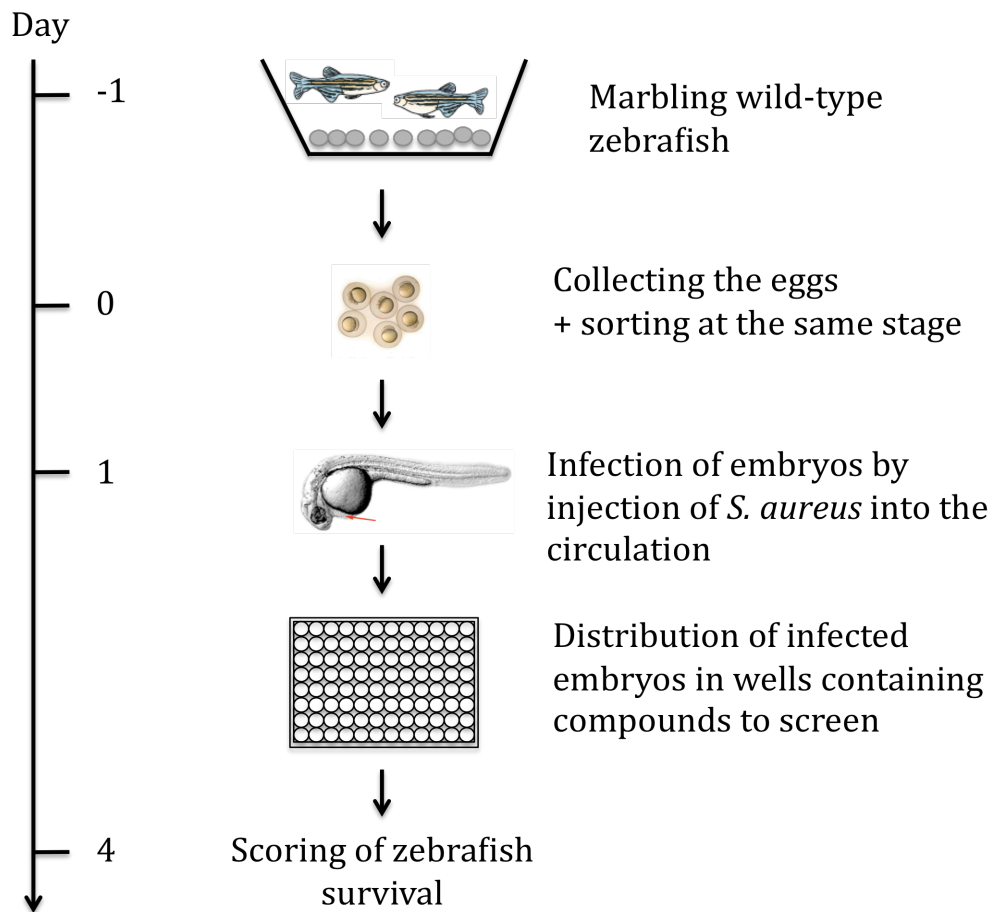


Figure 3.5.A. A zebrafish *in vivo* screen protocol for new anti-staphylococcal compounds

On day -1, a box of marbles is introduced in a tank of London wild-type (LWT) zebrafish, inducing the fish to lay eggs on the following day (day 0). The eggs are then sorted at the same stage and are put in several plates of E3 medium in the 28.5°C incubator. After manual dechoriation, 30 hpf embryos are microinjected with a defrosted suspension of *S. aureus* at a known concentration into the yolk circulation valley in order to reach directly the circulation. One hour after the injection, the infected larvae are distributed in separate wells of a 96-well plate containing the compounds to screen. A few days later, the survival of the infected zebrafish larvae is scored.

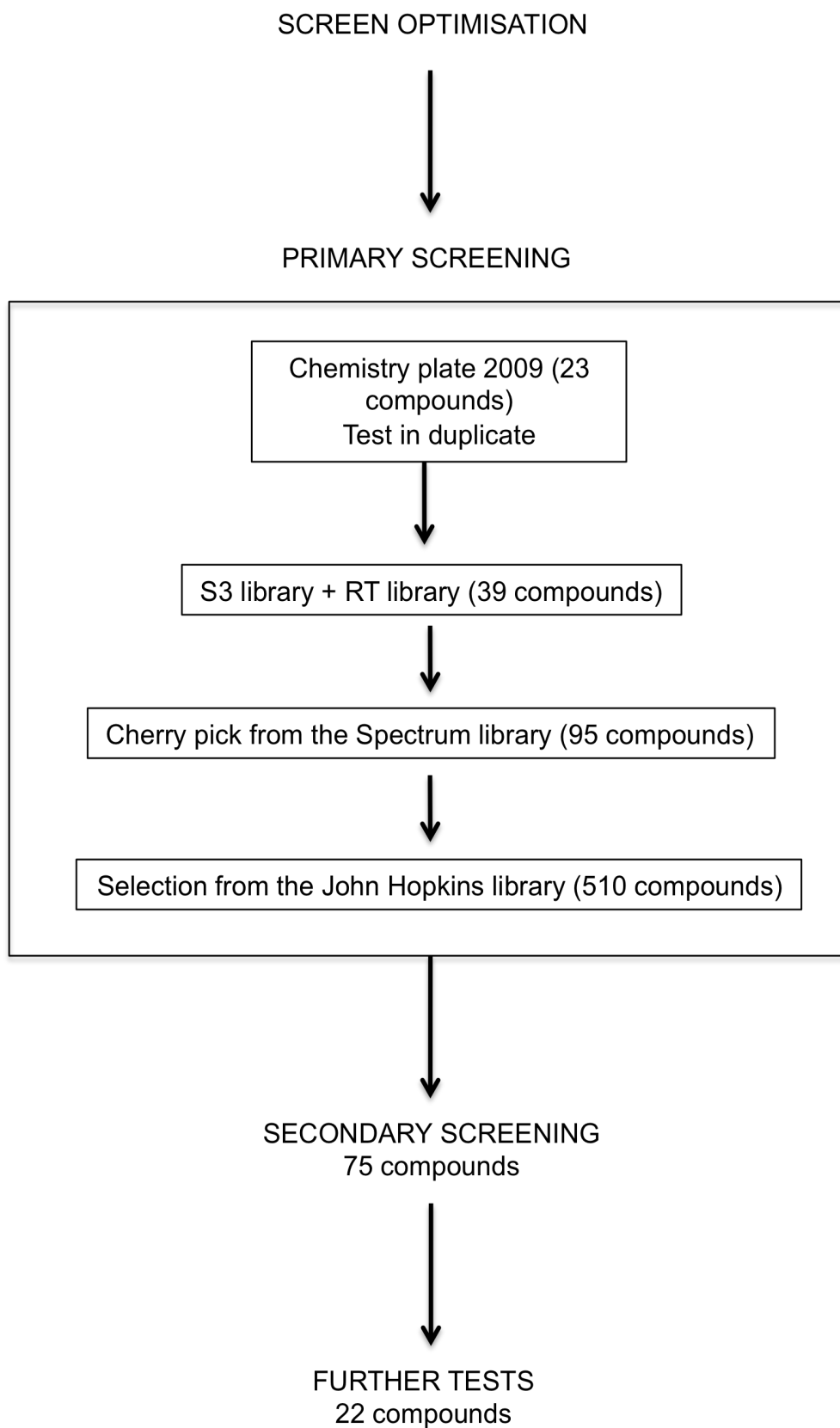


Figure 3.5.B. Flow chart of the antistaphylococcal screening strategy and the compounds tested

3.3. Identification of putative ‘hit’ compounds by primary screening

After optimising the experimental procedure of the screen, some small libraries of compounds were firstly chosen to test the screen. The first library chosen was the Chemistry plate 2009 (23 compounds), which was tested in duplicate with 5 fish each. The survival results were not exactly the same, so by combining the 2 replicates, 5 compounds were chosen for the secondary screening. If the first screening replicate had been performed alone, then 8 compounds would have been chosen for the secondary screen, including the 5 compounds identified with the duplicates. As a compromise, to reduce both time and compound amount, it was decided to test the compounds only once during the primary screening. Further tests would be performed in the later step of secondary screen to distinguish the real hits to the false positives. The S3 library (39 compounds) was subsequently screened, followed by a cherry pick from the Spectrum library (95 compounds). The Spectrum library cherry pick was a selection of anti-inflammatory compounds identified during a zebrafish screen looking at compounds that accelerate the resolution of inflammation resolution. Indeed, after the initial neutrophils recruitment to the site of injury, the number of neutrophils would decrease more quickly after treatment with the compounds (Robertson, Holmes et al. 2014). Similarly to an injury, a bacterial infection induces an inflammatory response by the innate immune cells neutrophils and macrophages. I wanted to test if compounds that have an accelerating effect on neutrophils resolution following an injury would also influence the immune response induced by a staphylococcal infection, and therefore the global survival of the infected fish.

The majority of the screen compounds were issued from the John Hopkins library (510 compounds). The selection of compounds issued from that library were well-characterised U.S. Food and Drug Administration-approved drugs and natural products (vitamins and minerals). Known antibacterial compounds were discarded, as the aim was to detect compounds with currently unknown antistaphylococcal properties. It was hypothesised that

already approved-drugs can have other properties than the ones that have already been identified.

A flow chart of the screening strategy with the number of compounds associated to each step is represented in Figure 3.5.B..

In the primary screen, 30 hpf zebrafish embryos were infected with 3700 CFU of *S. aureus* SH1000, treated with library compounds and then scored as alive or dead at 70 hpi. In the vehicle only negative control (DMSO), 2 or 3 fish died out of the 5 fish tested in every experiment. By comparison to the control group, the compounds promoting the survival of 4 or 5 fish out of the 5 fish tested per treatment were considered as potential 'hits' because they had the ability to enhance zebrafish embryo survival. In contrast to the potential 'hits', molecules inducing 100% mortality in this assay were recorded as 'anti-hits'. These 'anti-hits' could be of scientific interest if they are not toxic and therefore inhibit the innate immune response to the infection, or increase the virulence of the pathogenic bacteria.

Out of the 660 compounds screened in this primary screen, 11% had a score of 4 or 5 and were considered as potential 'hits'; while 15.7% of the compounds tested induced complete killing of the infected embryos, and were described as 'anti-hits'. The potential 'hits' were selected for more investigation in a second round of screening. The effect of all the compounds screened is represented on the heat map on Figure 3.6.

3.4. Further testing of putative 'hit' compounds in a secondary screen

The secondary screen was carried out with compounds selected from the same compound library. In the secondary screen, the number of fish tested per compound was increased from 5 to 24, and the survival of the larvae was recorded regularly to cover the period from the time of the injection up to 4 days later. The number of fish per group (24) was selected to increase statistical significance with a power of 90% and detect a survival percent

increasing from 50% to 90%, assuming significance at $p=0.05$. The resulting survival curves of fish treated with DMSO (control) or with the compounds selected after the primary screen were compared. A compound was deemed effective if it improved survival of the treated fish compared to the control group. The experiments were performed with the observer blinded to the experimental conditions, and the name or structure of the chemicals used was revealed afterwards.

Of the 75 molecules retested on the secondary screen, only 22 showed a positive effect that could treat staphylococcal infection, at least partially. Because of the multiple comparisons used, this assay was not intended to generate statistically significant data, but the aim was to indicate which compounds to focus on for further investigation.

When the effect of multiple comparisons was discounted, three compounds showed a statistically significant effect in the secondary assay compared to the DMSO control: fusidic acid (Figure 3.7.A), carsalam (Figure 3.7.B) and vitamin D2 (Figure 3.7.C). Thirteen compounds seemed to have a small positive effect on the survival of infected larvae, even if they were not statistically significant. The survival curves of these compounds with their structures or name is shown in Figure 3.8.. Six compounds (Figure 3.9.) seemed to have a delayed killing effect. The survival of the treated fish was higher following the initial infection, but then the survival of the treated fish dropped and reached the same level as the DMSO control group at the end of the experiment (around 80 hpi). These results suggest a protective effect of these compounds only during a limited time after the infection.

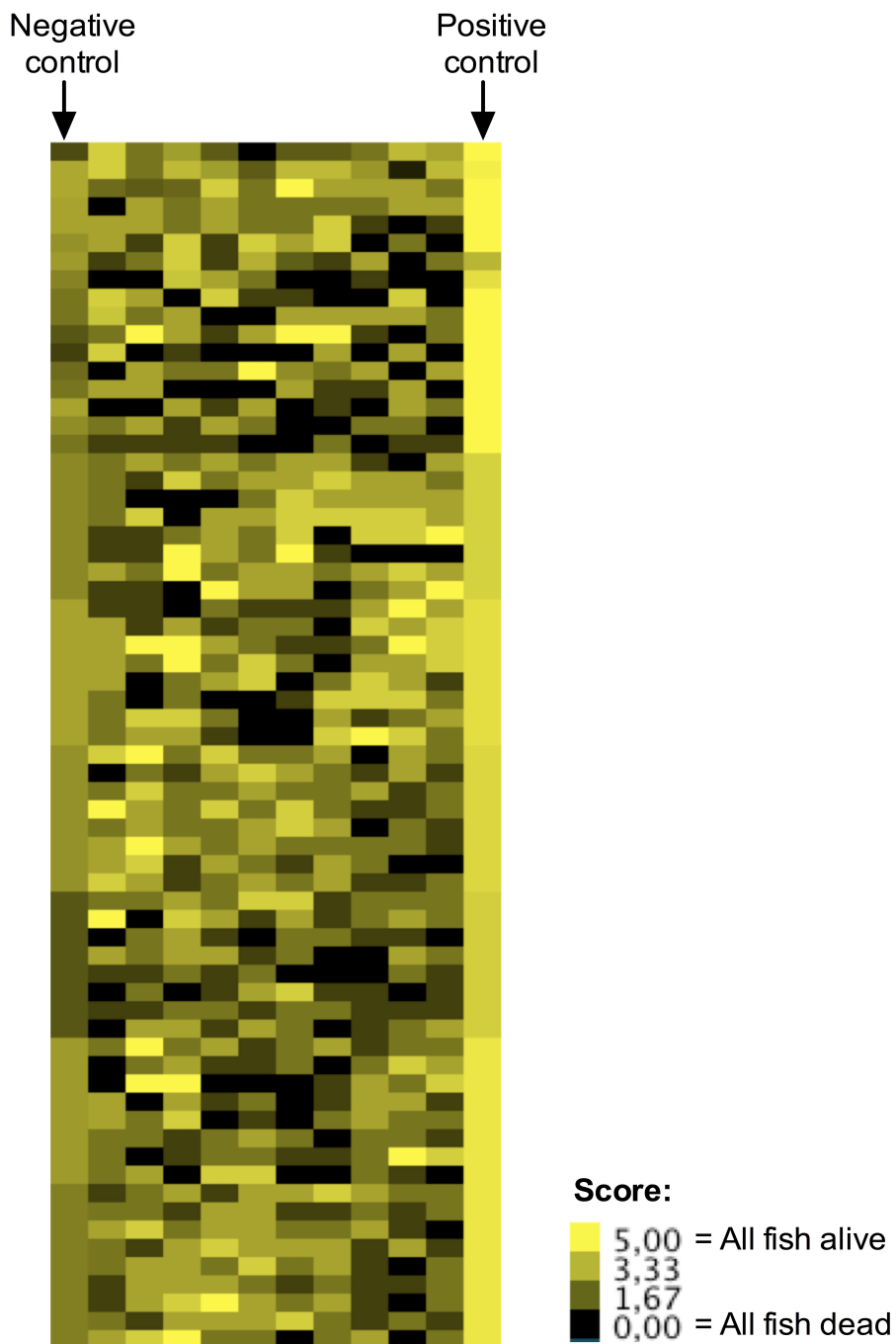


Figure 3.6. Heat map representing the 660 compounds screened with the systemic *S. aureus* infection model in zebrafish embryos.

Each square is a compound and the colour represents the score (see the legend). Positive control (Penicillin G treated zebrafish) is on the right column; negative control (DMSO treated zebrafish) is on the left column.

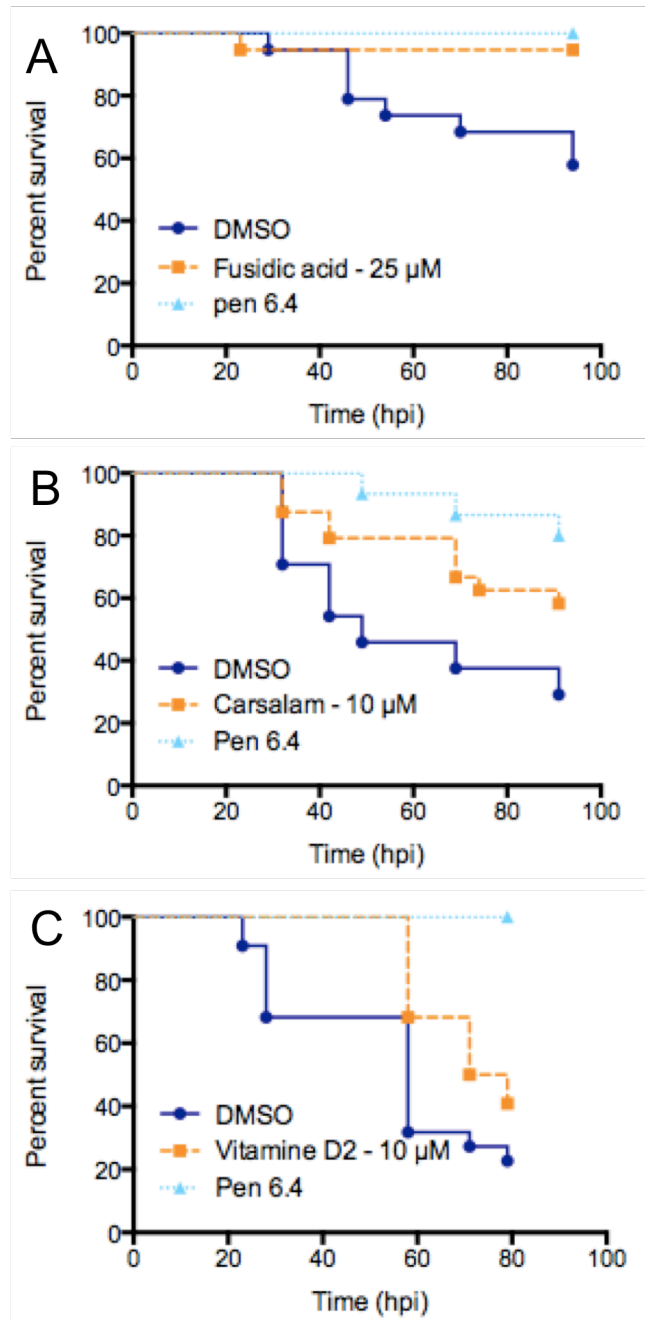


Figure 3.7. Survival curves of infected larvae treated with 3 highly effective potential hits

WT zebrafish embryos (30 hpf) were injected with 3700 CFU of wild-type *S. aureus* (SH1000) into their blood circulation and then were treated with DMSO, Penicillin G (6.4 mg/l) or (A) Fusidic acid (25 μM), n=19. $P = 0.0108$ for DMSO vs. Fusidic acid 25 μM; (B) Carsalam (10 μM), n=24. $P = 0.0291$ for DMSO vs. Carsalam 10 μM; (C) Vitamin D2 (10 μM), n=22. $P = 0.0337$ for DMSO vs. Vitamin D2 10 μM.

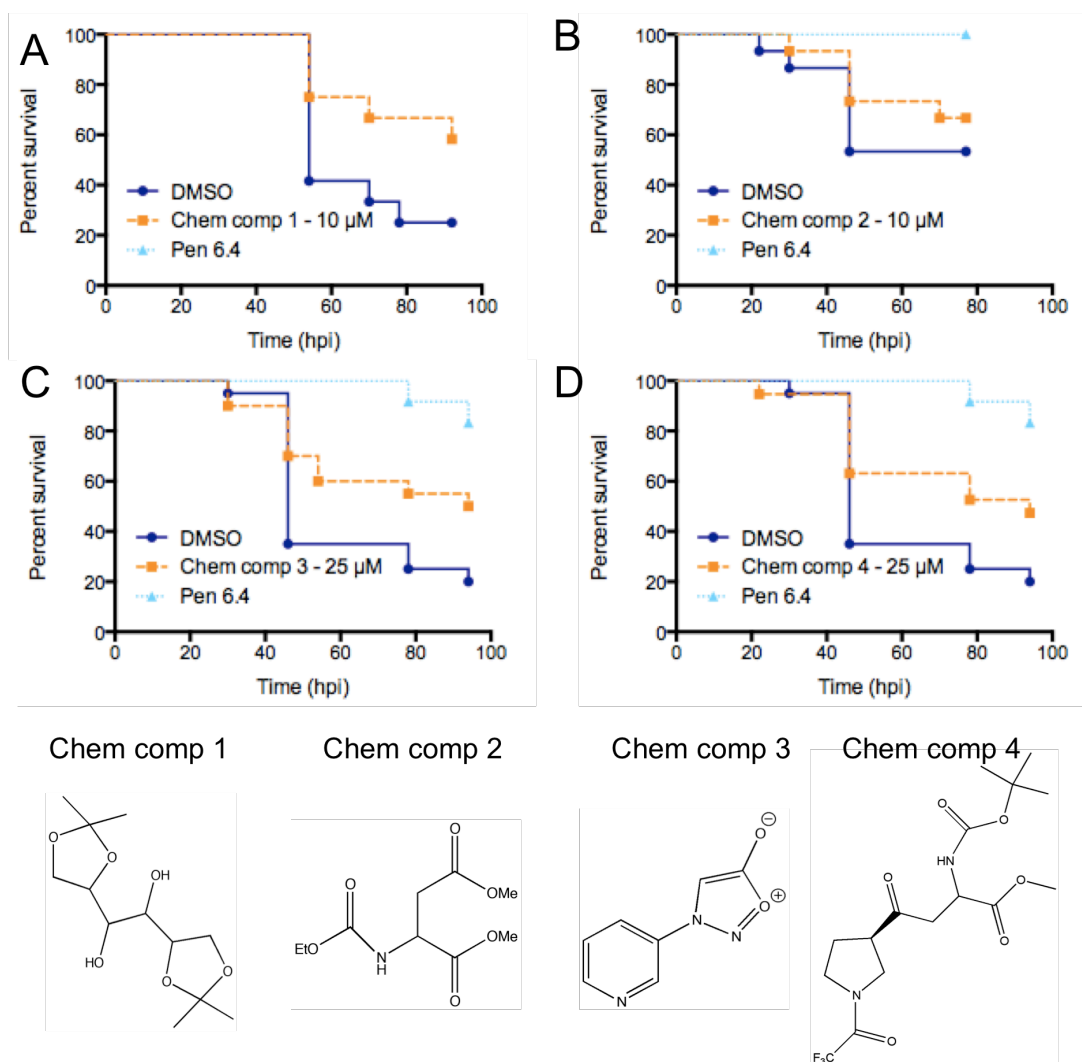


Figure 3.8. Survival curves of infected larvae treated with intermediate effective potential hit compounds

LWT zebrafish embryos (30 hpf) were injected with 3700 CFU of wild-type *S. aureus* (SH1000) into their blood circulation and then were treated with DMSO, Penicillin G (6.4 mg/l) or compounds indicated with their structures: (A) Chem comp 1 (10 μM), $n=12$, $P = 0.08$ for DMSO vs. Chem comp 1 10 μM; (B) Chem comp 2 (10 μM), $n=15$, $P = 0.4188$ for DMSO vs. Chem comp 2 10 μM; (C) Chem comp 3 (25 μM), $n=20$, $P = 0.0665$ for DMSO vs. Chem comp 3 25 μM; (D) Chem comp 4 (25 μM), $n=20$, $P = 0.0759$ for DMSO vs. Chem comp 4 25 μM.

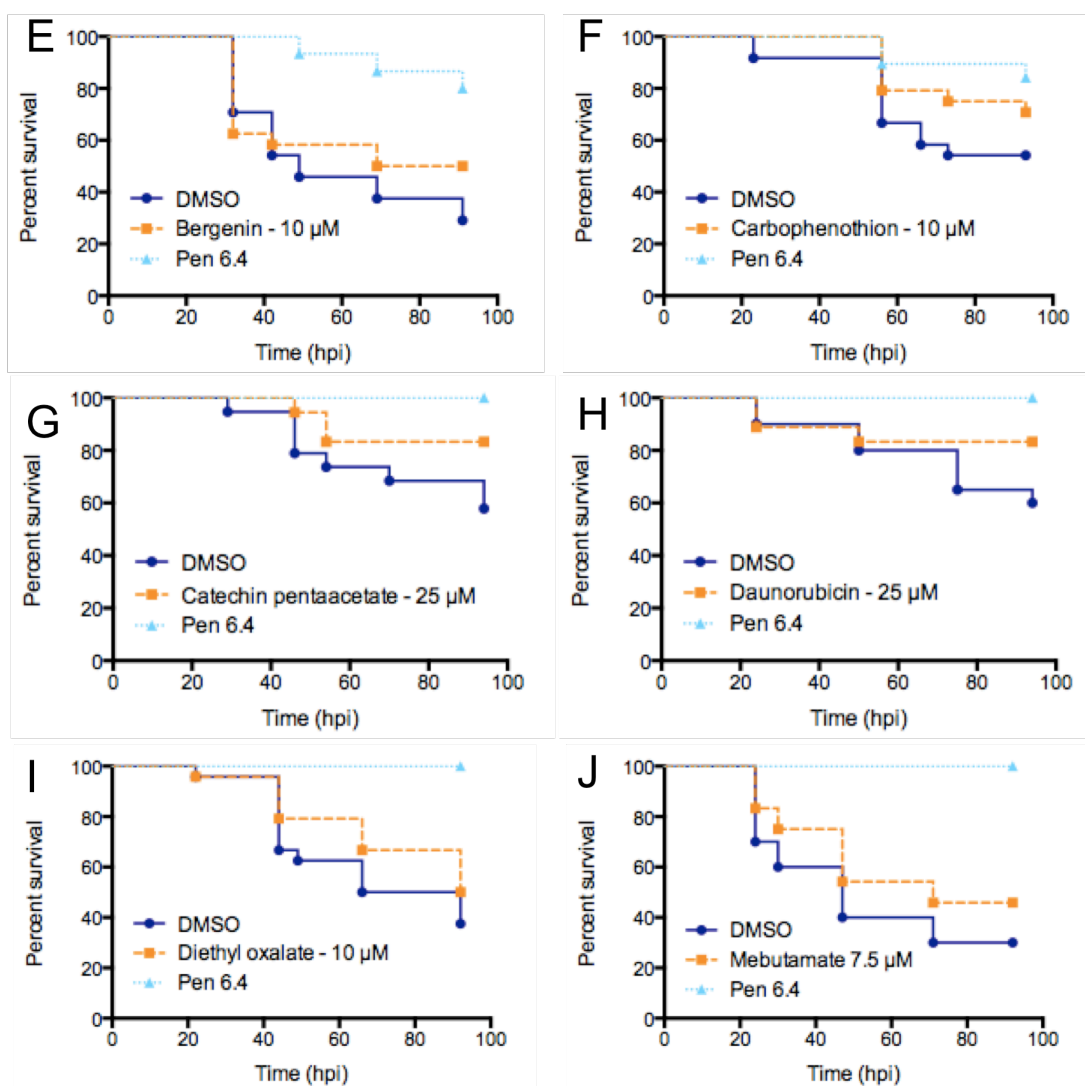


Figure 3.8. Survival curves of infected larvae treated with intermediate effective potential hit compounds

LWT zebrafish embryos (30 hpf) were injected with 3700 CFU of wild-type *S. aureus* (SH1000) into their blood circulation and then were treated with DMSO, Penicillin G (6.4 mg/l) or compounds indicated: (E) Bergenin (10 µM), $n=24$, $P = 0.243$ for DMSO vs. Bergenin 10 µM; (F) Carbophenothion (10 µM), $n=24$, $P = 0.19$ for DMSO vs. Carbophenothion 10 µM; (G) Catechin pentaacetate (25 µM), $n=18$, $P = 0.097$ for DMSO vs. Catechin pentaacetate 25 µM; (H) Daunorubicin (25 µM), $n=18$, $P = 0.152$ for DMSO vs. Daunorubicin 25 µM; (I) Diethyl oxalate (10 µM), $n=24$, $P = 0.305$ for DMSO vs. Diethyl oxalate 10 µM; (J) Mebutamate (7.5 µM), $n=24$, $P = 0.239$ for DMSO vs. Mebutamate 7.5 µM.

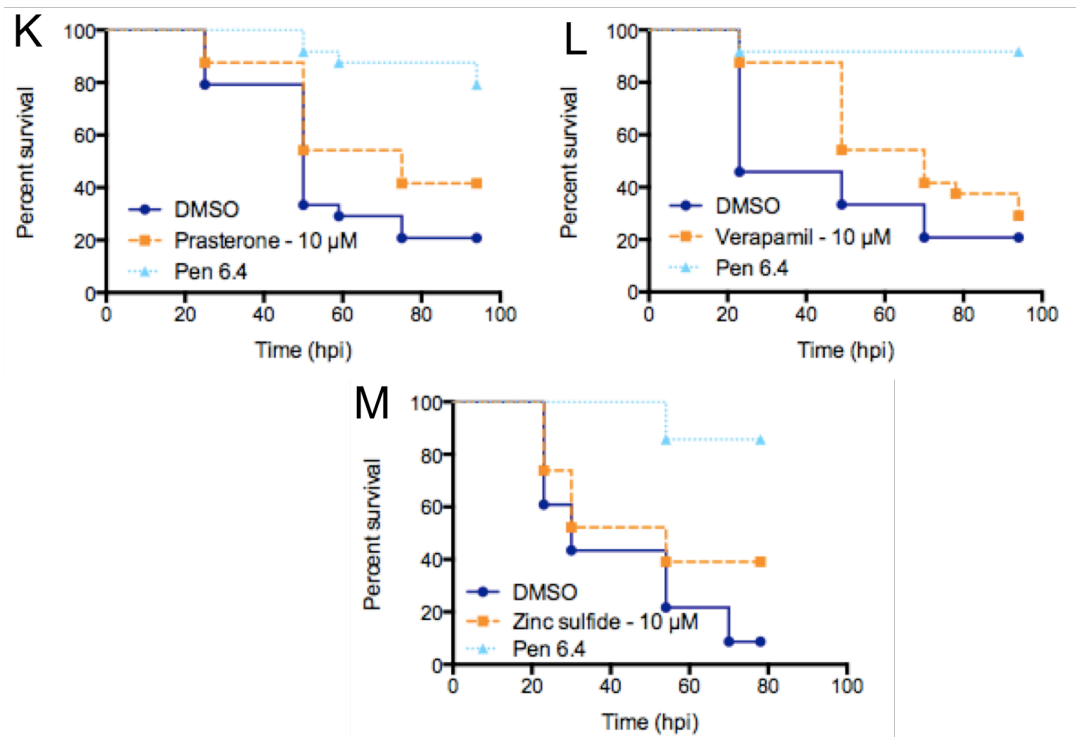


Figure 3.8. Survival curves of infected larvae treated with intermediate effective potential hit compounds

LWT zebrafish embryos (30 hpf) were injected with 3700 CFU of wild-type *S. aureus* (SH1000) into their blood circulation and then were treated with DMSO, Penicillin G (6.4 mg/l) or compounds indicated: (K) Prasterone (10 μM), $n=24$, $P = 0.0977$ for DMSO vs. Prasterone 10 μM; (L) Verapamil (10 μM), $n=24$, $P = 0.116$ for DMSO vs. Verapamil 10 μM; (M) Zinc sulfide (10 μM), $n=23$, $P = 0.056$ for DMSO vs. Zinc sulfide 10 μM.

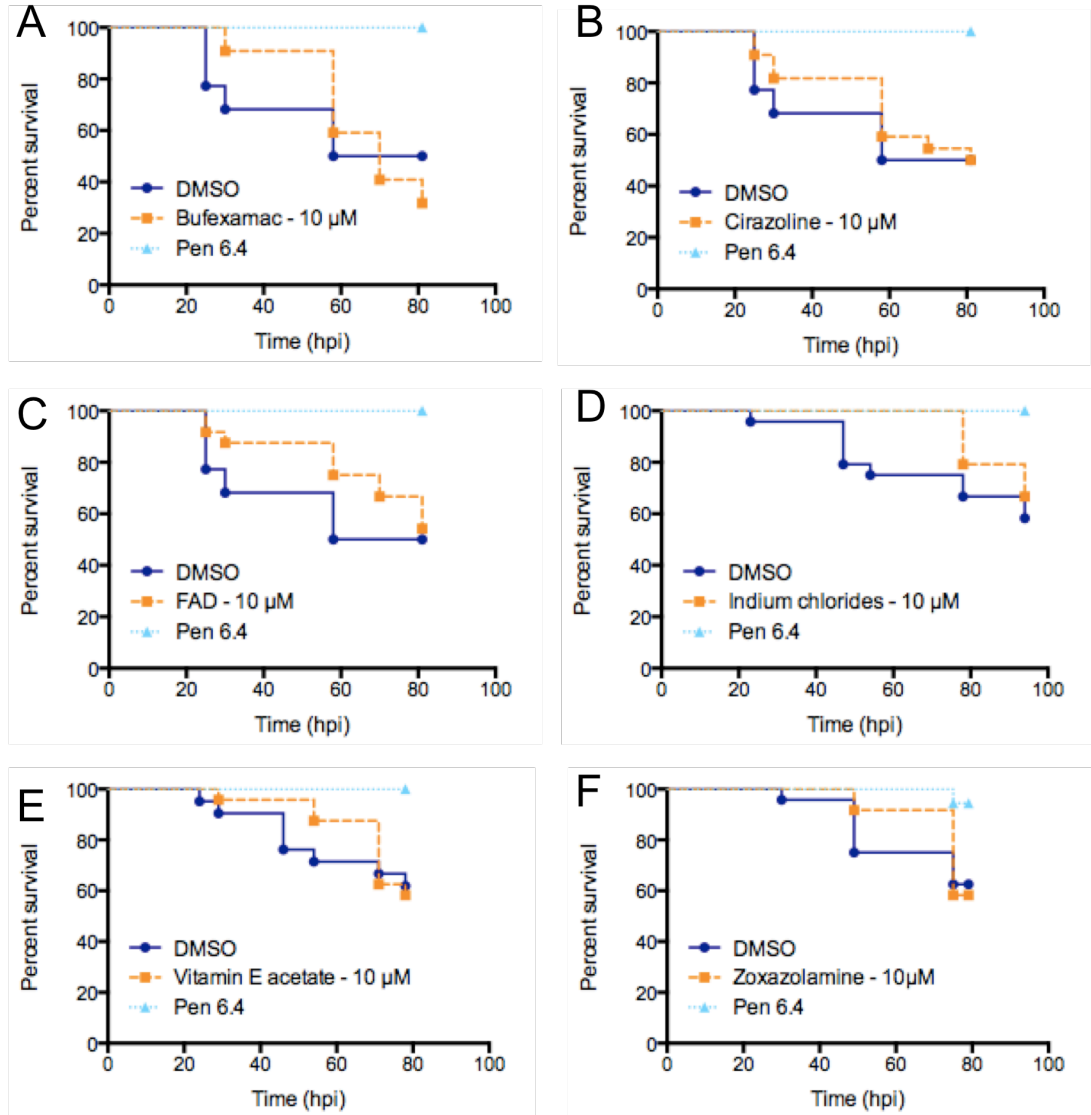


Figure 3.9. Effect of the delayed compounds on infected zebrafish embryos

LWT zebrafish embryos (30 hpf) were injected with 3700 CFU of wild-type *S. aureus* (SH1000) into their blood circulation and then were treated with DMSO, Penicillin G (6.4 mg/l) or the following compound: (A) Bufexamac (10 μ M), $n=24$, $P = 0.698$ for DMSO vs. Bufexamac 10 μ M; (B) Cirazoline (10 μ M), $n=24$, $P = 0.767$ for DMSO vs. Cirazoline 10 μ M; (C) Flavine Adenine Dinucleotide (FAD) (10 μ M), $n=24$, $P = 0.506$ for DMSO vs. FAD 10 μ M; (D) Indium chlorides (10 μ M), $n=24$, $P = 0.363$ for DMSO vs. Indium chlorides 10 μ M; (E) Vitamine E acetate (10 μ M), $n=24$, $P = 0.938$ for DMSO vs. Vitamin E acetate 10 μ M; (F) Zoxazolamine (10 μ M), $n=24$, $P = 0.949$ for DMSO vs. Zoxazolamine 10 μ M.

3.5. Detailed analysis of effects of potential hits on *S. aureus* infection

The 9 most promising compounds of the 22 potential 'hits' selected from the secondary screen were purchased from a different supplier (Sigma-Aldrich) for further investigation. The compounds promoting an increase in survival of infected embryos were tested in dose-response assays, while the compounds inducing a delayed killing pattern of the infected embryos were tested in redosing assays.

3.5.1. Dose-response assays

In dose-response assays, *S. aureus* infected zebrafish embryos were immersed in 5 concentrations of compound ranging from 0.1 μM to 100 μM .

3.5.1.1. The highly effective 'hits'

From the group of the highly effective 'hits' (Figure 3.7. A, B and C), fusidic acid was excluded from our investigations because it is already a known antibiotic. The curative effect of fusidic acid on infected larvae confirmed that anti-infective molecules could be detected through this *in vivo* screen, which supports the ability of this screen to identify new compounds to treat *S. aureus* infection. The 2 promising compounds carsalam and vitamin D2 were tested at different concentrations on *S. aureus* infected zebrafish larvae. None of the tested concentrations of carsalam (Figure 3.10.A.) or vitamin D2 (Figure 3.10.C.) seemed to have a positive effect on the survival of the infected larvae, compared to the DMSO control. For carsalam, the intermediate concentrations (1 μM , 10 μM and 30 μM) were more effective than the extreme concentrations tested (0.1 μM and 100 μM). This bell shaped dose-response curve of carsalam (Figure 3.10.B.) suggests a loss of effect or a toxicity of carsalam at higher dose. In contrast, the dose of vitamin D2 did not influence the survival of the infected zebrafish larvae (Figure 3.10.D.). Potential explanations for this finding are that the vitamin D2 purchased from Sigma-Aldrich lacks the active metabolite compared to the vitamin D2 provided in the Johns Hopkins library collection.

3.5.1.2. The intermediate effective 'hits'

The sydnone-derived compound, zinc sulfide and verapamil were selected from the group of compound with small positive effect in the secondary screen (Figure 3.8.C., M. and L.), and were also tested in dose-response assays. The infected larvae treated with the sydnone-derived compound had the same survival pattern than the DMSO treated larvae (Figure 3.11.A.). In addition, the higher the dose of sydnone-derived compound, the lower the survival of the infected larvae, suggesting some a toxicity effect of the high dose (Figure 3.11.B.).

In contrast, infected larvae treated with 10 μ M and 30 μ M of zinc sulfide showed a higher survival than the control group, while lower or higher doses did not have any effect (Figure 3.11.C.). This bell shaped dose-response curve (Figure 3.11.D.) suggests a biological variability of the target of zinc sulfide. The higher dose of zinc sulfide could have an inhibitory effect on its target.

All the infected and verapamil treated fish died more quickly than the DMSO control. It should be noted that the survival curve of the DMSO control was unusual as a dose of 3700 CFU of *S. aureus* would normally induce about 60% mortality at the end of the experiment, which was not the case here (Figure 3.11.E.). The effect on the survival of the zebrafish larvae was not influenced by the dose, as observed on the dose-response curve of verapamil (Figure 3.11.F.) This compound is further discussed in the next chapter (Chapter 4).

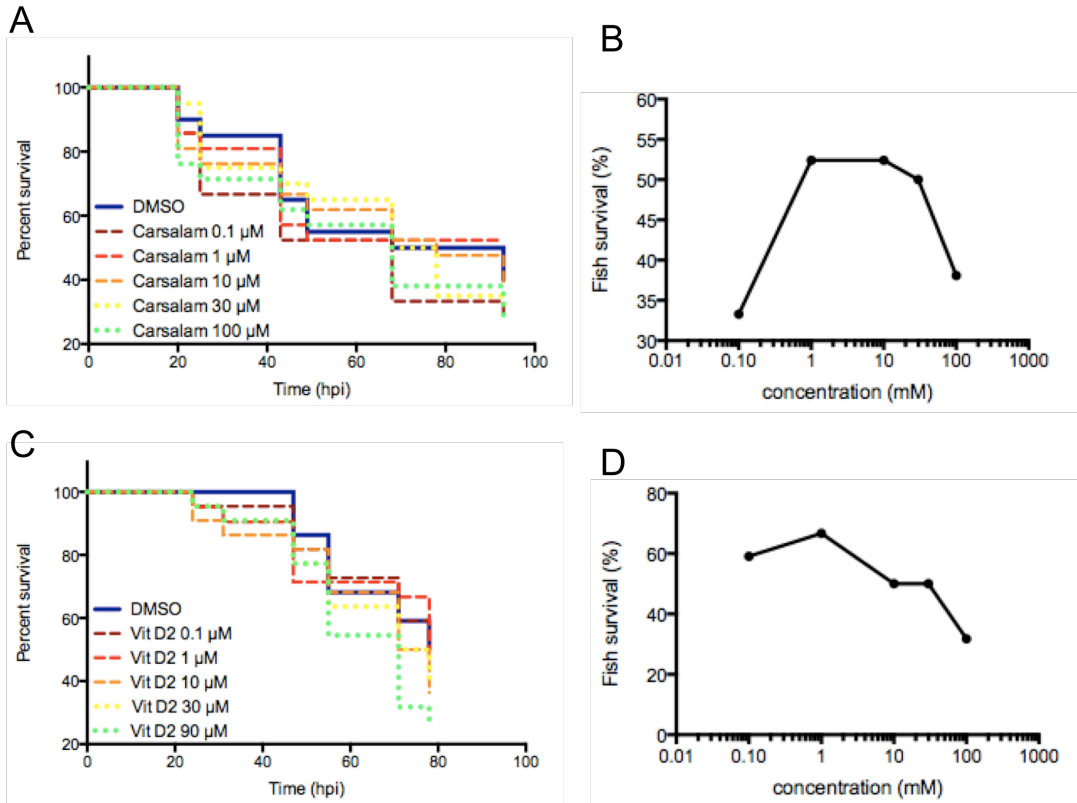


Figure 3.10. Dose-response assays of potential ‘hits’

LWT zebrafish embryos (30 hpf) were injected with 3700 CFU of wild-type *S. aureus* (SH1000) into their blood circulation and then were treated with DMSO or A) carsalam, C) vitamin D2 (vit D2) at different concentrations. Percentage of the infected zebrafish survival at 70 hpi treated with different doses of B) carsalam, D) vitamin D2
 n>21 fish per group

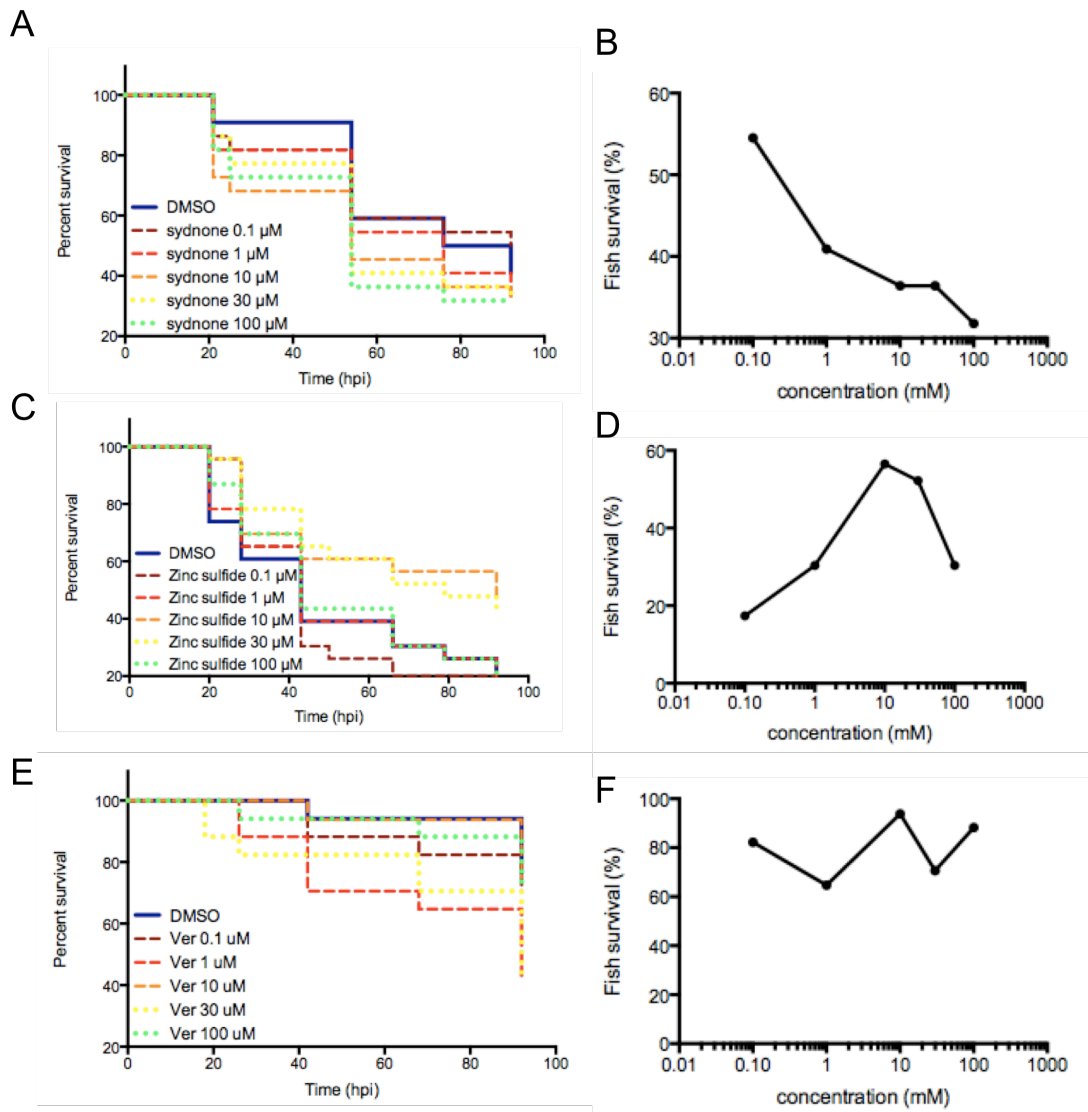


Figure 3.11. Dose-response assays of potential 'hits'

LWT zebrafish embryos (30 hpf) were injected with 3700 CFU of wild-type *S. aureus* (SH1000) into their blood circulation and then were treated with DMSO or A) sydnone derived compound, C) zinc sulfide, E) verapamil (ver) at different concentrations.

Percentage of the infected zebrafish survival at 70 hpi treated with different doses of B) sydnone derived compound, D) zinc sulfide, F) verapamil $n > 17$ fish per group

3.5.2. Redosing assays

Compounds showing delayed killing in the secondary screen (Figure 3.9.) could have lost their positive effect on survival of infected zebrafish embryos over time because of degradation of the molecules. To examine this possibility, I decided to test 4 of these 6 compounds in a redosing assay with addition of the initial compound every 24 h in the zebrafish media. The compounds tested were flavin adenine dinucleotide (FAD), indium chlorides (InCl_3), vitamin E acetate and zoxazolamine.

Infected fish treated repeatedly with FAD had a slightly lower survival rate than the infected fish treated once only (Figure 3.12.A.). However, it was not biologically significant to be pursued as lead compound for drug discovery. Similar observations were made with indium chlorides (Figure 3.12.B.), vitamin E acetate (Figure 3.12.C.) and zoxazolamine (Figure 3.12.D.). Indeed, the survival curves of infected fish treated with a new addition of the mentioned compound every day were not significantly different than the survival curves of infected fish treated once only with the compound. In addition, neither of these treated curves was significantly different than the DMSO treated group (negative control).

3.5.3. Retesting the newly purchased compounds in a survival assay

Except for zinc sulfide (discussed below in section 3.6.), the dose-response assays and redosing assays did not show significant curative effects. To ensure that the problem did not come from the preparation of the compounds purchased from Sigma-Aldrich, they were prepared and tested one more time in a secondary screen-like assay. As observed before, the infected embryos treated with carsalam, FAD, indium chlorides, sydnone derivative, vitamin D2 or zoxazolamine showed no significant difference to the control group (Figure 3.13.).

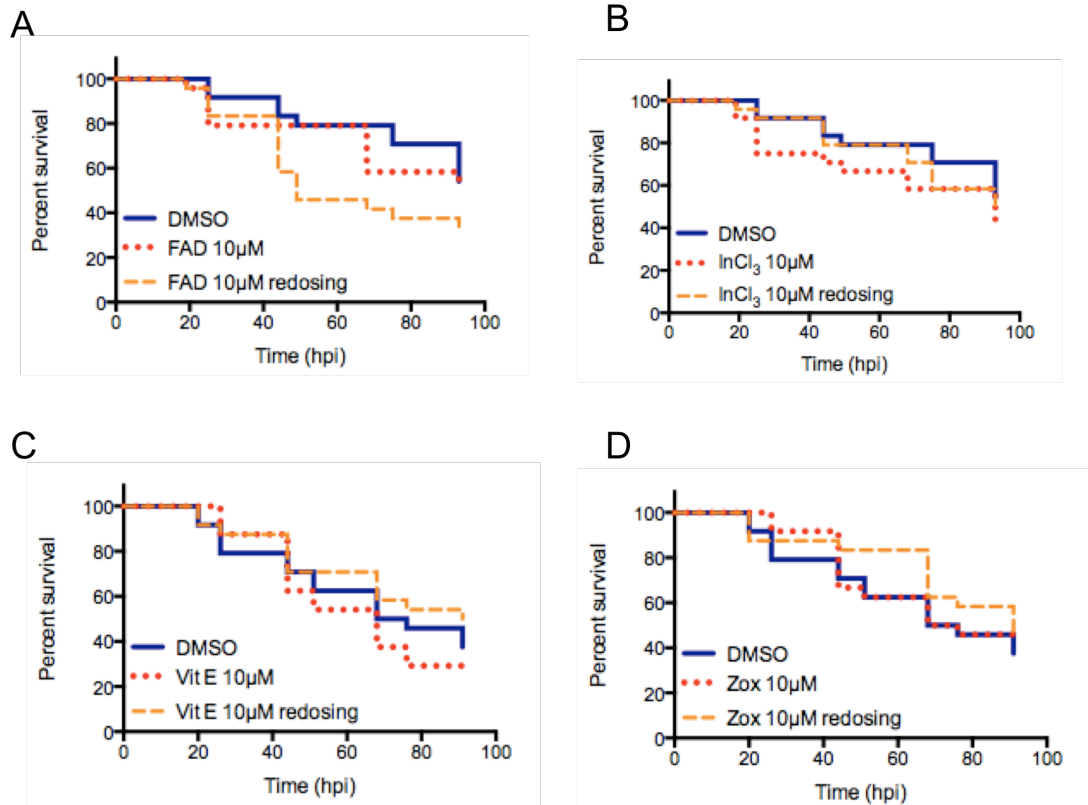


Figure 3.12. Redosing assays of the potential ‘hits’

LWT zebrafish embryos (30 hpf) were injected with 3700 CFU of wild-type *S. aureus* (SH1000) into their blood circulation and then were treated with DMSO (control) and the following compounds at either 10 μM once after the infection, or 10 μM added every 24h after the infection (redosing): A) flavin adenine dinucleotide (FAD), B) indium chlorides (InCl₃), C) vitamin E acetate (Vit E), or D) zoxazolamine (zox).

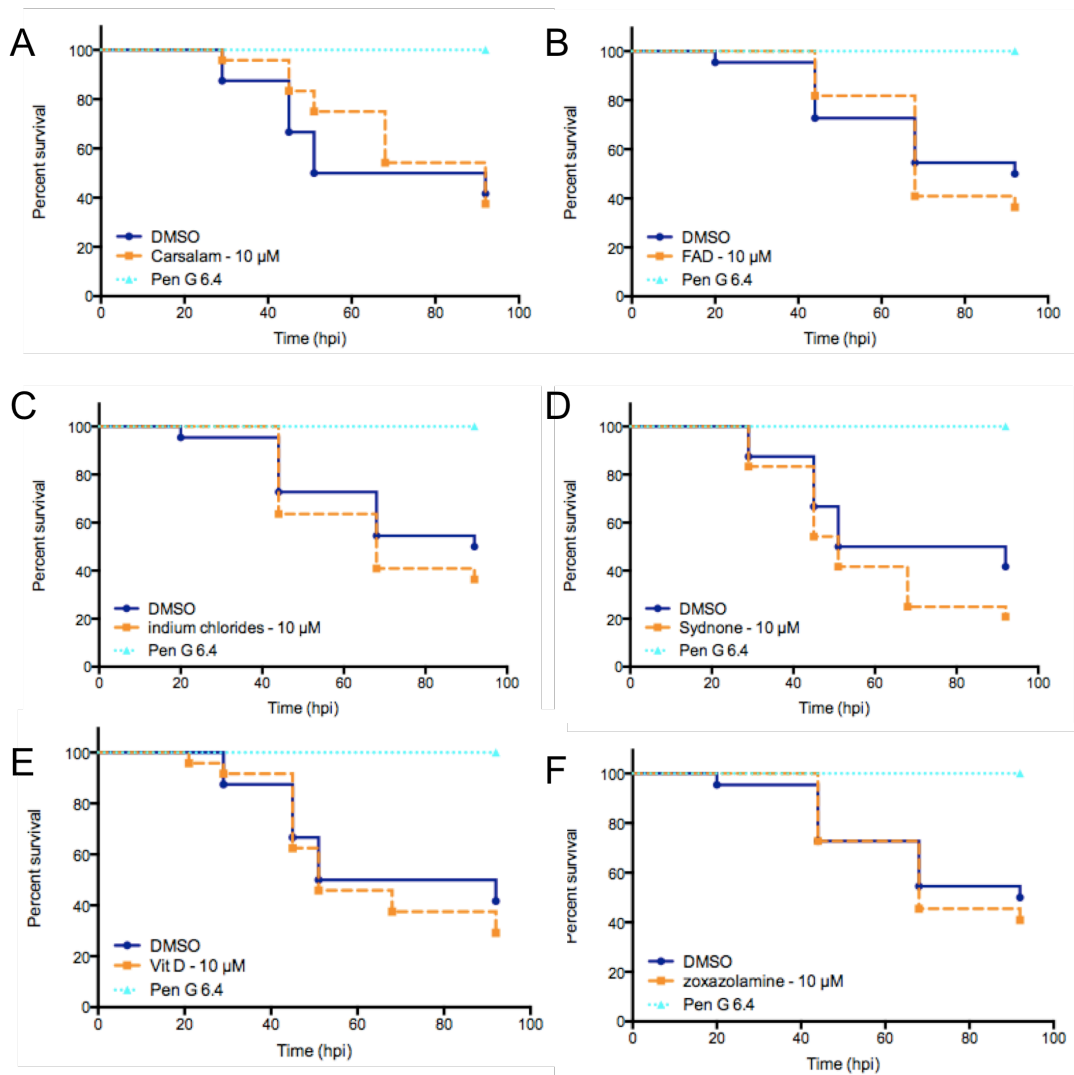


Figure 3.13. Retest of of the potential ‘hits’ in secondary screen – like assay

LWT zebrafish embryos (30 hpf) were injected with 2500 CFU of wild-type *S. aureus* (SH1000) into their blood circulation and then were treated with DMSO (negative control), Pen G (positive control) and the following compounds at 10 μM: A) carsalam, B) flavin adenine dinucleotide (FAD), C) indium chlorides (InCl_3), D) sydnone-compound, E) vitamin D, or F) zoxazolamine.

3.6. Examination of the effects of zinc sulfide on *S. aureus* infection

From the dose-response experiments and redosing assays carried out on 8 of the potential 'hits', zinc sulfide looked the more promising compound. Indeed, *S. aureus* infected zebrafish embryos treated with 10 or 30 μM of zinc sulfide showed a higher survival than the control group (Figure 3.11.C.). If zinc sulfide has an actual curative effect on *S. aureus* infected zebrafish larvae, the next question was whether zinc sulfide has an effect only in *in vivo* *S. aureus* infection or if it would affect the pathogen directly. To test this idea, 3 different concentrations of zinc sulfide were tested in *in vitro* experiments on *S. aureus* liquid culture. An expected growth rate of *S. aureus* was observed in every group containing zinc sulfide similarly to the control group, suggesting that zinc sulfide does not inhibit or kill *S. aureus* SH1000 in BHI medium (Figure 3.14.).

I then tested whether other zinc compounds could have a positive effect on *S. aureus* infected zebrafish larvae. Zinc citrate dihydrate, zinc oxide, zinc acetate, zinc iodide and zinc sulfate heptahydrate were purchased from Sigma-Aldrich and were prepared according to their solubility properties. After determination of the best solvent to dissolve the compounds, toxicity tests were performed, followed by survival assays on infected larvae. Zinc oxide is a white powder insoluble in DMSO, H_2O , ethanol, DMF or methanol, and it was therefore not possible to test it on our *in vivo* infection model. Zinc citrate dihydrate did not dissolve in any of the solvents mentioned above, and the only successful solvent was sulphuric acid. Unfortunately, even diluted 100,000 times in zebrafish water, sulphuric acid was toxic for the larvae whether zinc citrate was dissolved in it or not (Figure 3.15.A.). Zinc acetate was soluble in both water and DMSO, while zinc sulphate was only soluble in water and zinc iodide was only soluble in DMSO. A concentration of 10 μM of these 4 zinc solutions was added to the E3 water of 30 hpf zebrafish larvae for a toxicity test. All larvae remained healthy until the end of the test, 90 h later (Figure 3.15.B.). These zinc solutions were then dissolved in the water of 30 hpf *S. aureus* infected zebrafish larvae and survival recorded over time.

Compared to the corresponding control group (water or DMSO solvent used), the survival of the treated larvae was not significantly different (Figure 3.15.C and D).

3.7. Examination of the properties of potential 'anti-hits'

During the primary screen assay, compounds inducing death of all infected zebrafish larvae were designated as 'anti-hits'. The cause of complete mortality could be either toxicity of the compounds or a negative effect of the compounds on the fish, for example by modulating their ability to tackle the infection. Complete mortality could also occur if the compound had a positive action on the pathogen by increasing the bacterial virulence and leading to an enhanced mortality of the infected host.

Four of these 'anti-hits' had been previously identified as accelerators of the resolution of inflammation in an *in vivo* anti-inflammatory screening assay performed by Anne Robertson. These 'anti-hits' compounds were first retested in toxicity tests on 31 hpf uninfected fish. Naproxen and tanshinone IIA at 10 μ M did not affect the development of zebrafish larvae until the end of the experiment (Figure 3.16.A.). However, cryptotanshinone was toxic, leading to the gradual death of the larvae (Figure 3.16.A.). Zebrafish embryos treated with digitoxin at 10 μ M were visibly acquiring developmental defects including shorter length, curved tail and cardiac oedema (Figure 3.16.B.). The high mortality rate observed with infected zebrafish larvae treated with cryptotanshinone and digitoxin in the primary screen can therefore be explained by their toxicity.

The anti-inflammatory properties of naproxen are known, but no studies have shown its potential increased susceptibility to bacterial infection. To address this question, a survival experiment was performed. The infected fish treated with naproxen at 10 μ M showed no statistical difference between these groups and the DMSO control group, whether the initial dose of bacteria was 1000 CFU or 2000 CFU (Figure 3.17.).

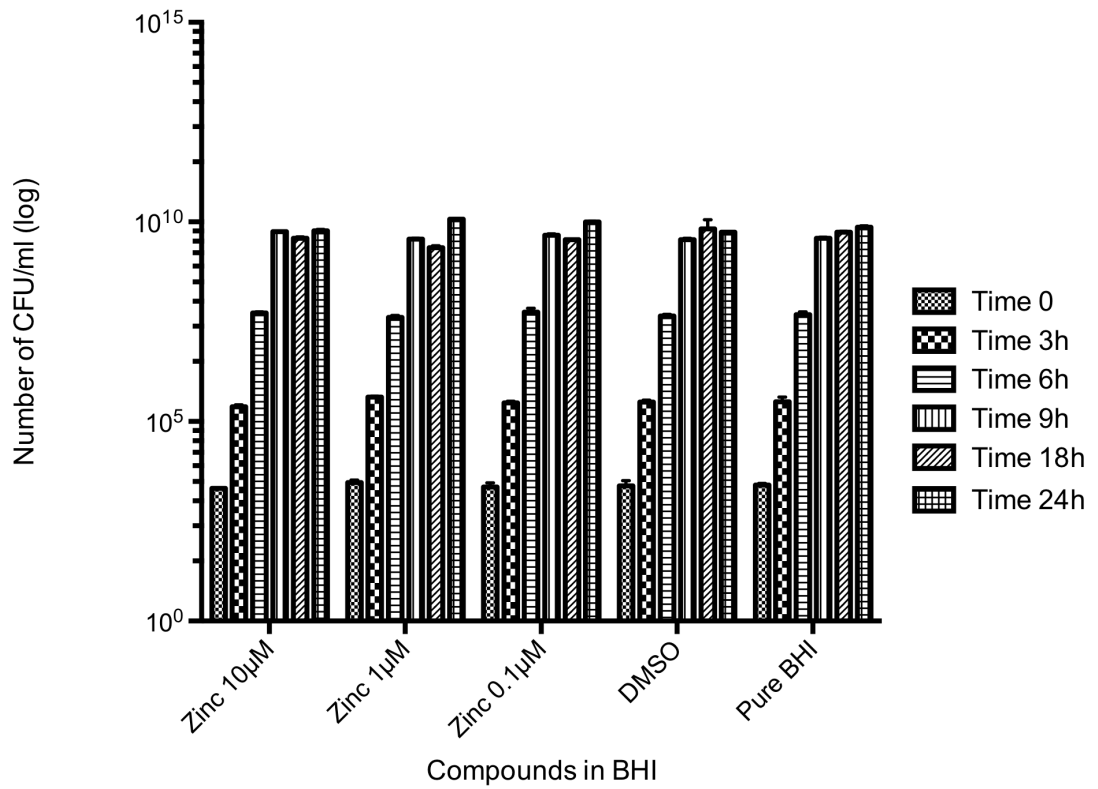


Figure 3.14. *in vitro* effect of zinc sulfide on *S. aureus* growth

Number of CFU/mL counted after *S. aureus* SH1000 incubation at 37°C during the indicated period of time in BHI with addition of zinc sulfide at 10 µM, 1 µM, 0.1 µM, DMSO or pure BHI.

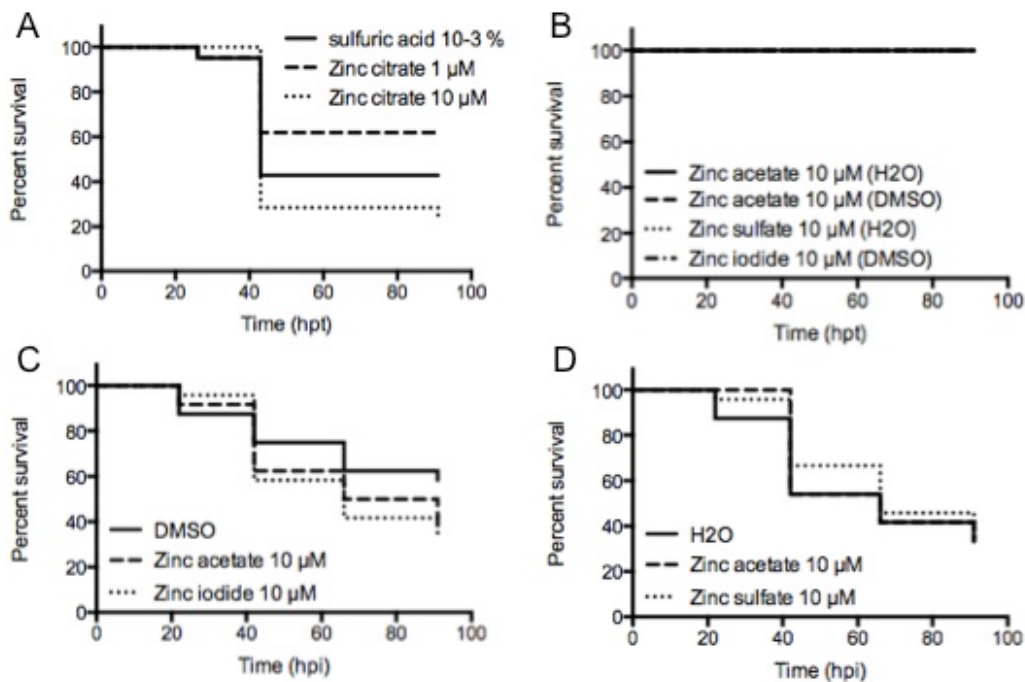


Figure 3.15. Testing other zinc derivatives compounds on *S. aureus* infected zebrafish larvae

A, B) LWT zebrafish embryos (30 hpf) were treated with A) sulfuric acid at 0.001%, or zinc citrate at 1 or 10 μ M dissolved in sulfuric acid; B) zinc acetate, zinc sulfate or zinc iodide dissolved in the solvent indicated between brackets

C, D) LWT zebrafish embryos (30 hpf) were infected with 2500 CFU of wild-type *S. aureus* (SH1000) into their blood circulation and then were treated with DMSO or H₂O (control) and the following compounds at 10 μ M: C) zinc acetate or zinc iodide, D) zinc acetate or zinc sulfate

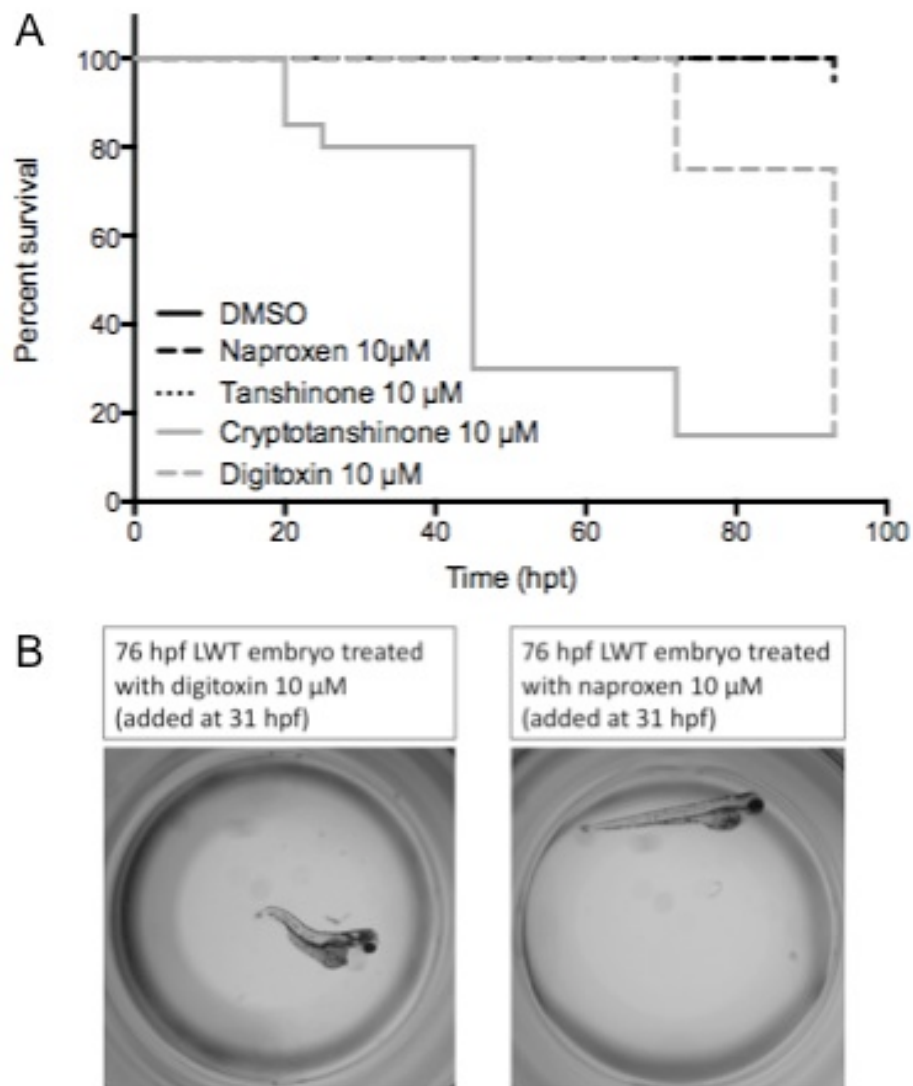


Figure 3.16. Toxicity test of some ‘antihit’ compounds

A) survival curves and B) Visualisation at 76 hpf of a toxicity test on LWT zebrafish embryos treated with 10 µM of the specified compounds at 31 hpf.

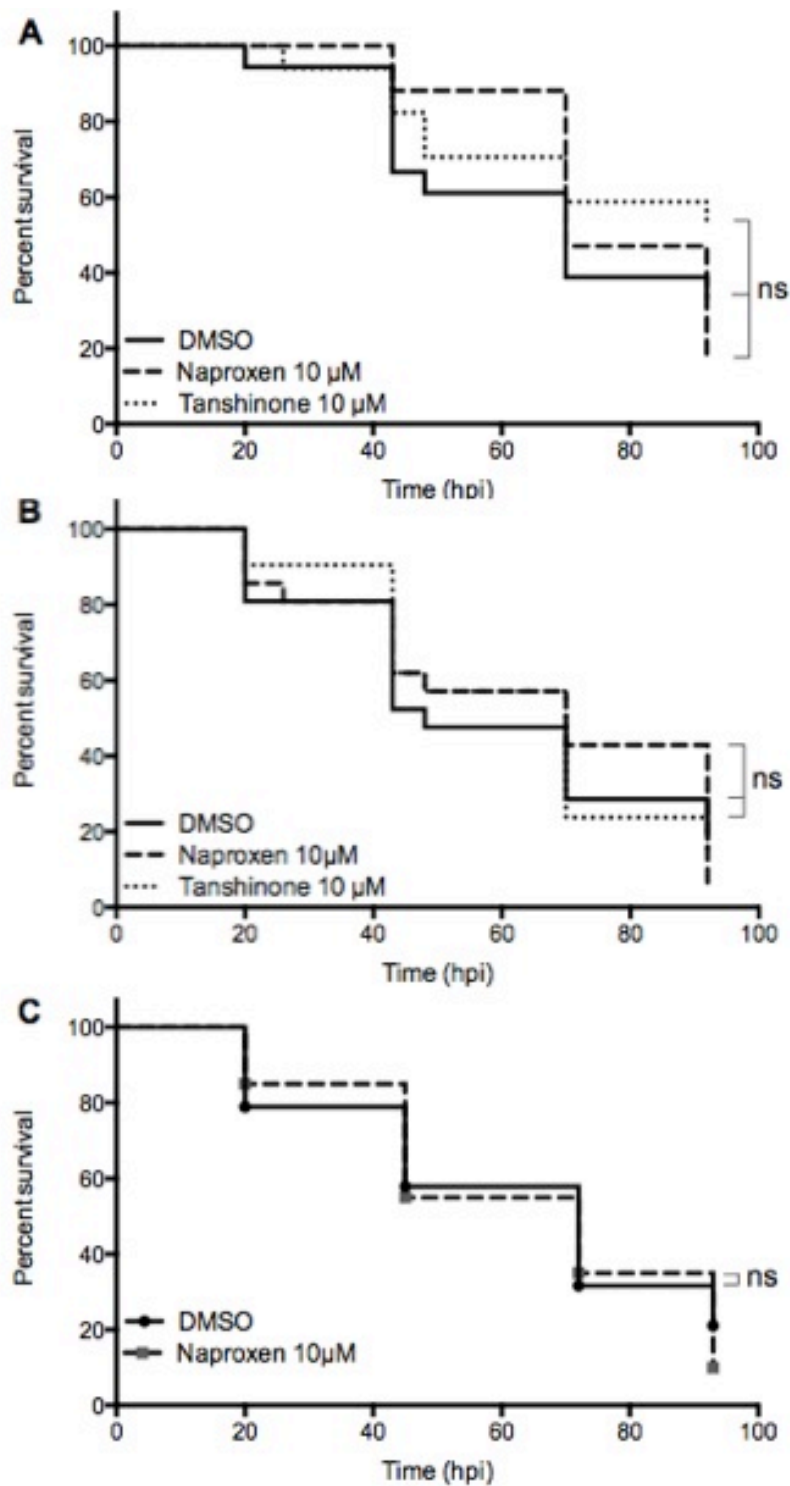


Figure 3.17. Survival tests of some ‘anti-hit’ compounds

LWT zebrafish embryos (30 hpf) were injected with either 1000 CFU (A), 2000 CFU (B) or 3000 CFU (C) of wild-type *S. aureus* (SH1000) into their blood circulation and then were treated with DMSO, naproxen (10 μM) or tanshinone IIA (10 μM). $n > 17$ fish per group. $P > 0.05$ for DMSO vs. naproxen or tanshinone IIA at 10 μM.

An *in vivo* zebrafish inflammation model has shown that tanshinone IIA induces the resolution of inflammation via the induction of both neutrophil apoptosis and neutrophils reverse migration (Robertson, Holmes et al. 2014). The effects of tanshinone IIA on the inflammatory cells of the immune system could also influence bacterial infection. To test this, a survival experiment of infected zebrafish larvae treated with tanshinone IIA at 10 μ M was performed. It failed to show any difference between the treated group and the negative control group, whether the initial dose of bacteria was 1000 CFU, 2000 CFU or 3000 CFU (Figure 3.17.).

3.8. Testing an immunomodulatory compound

Nicotinamide, also known as vitamin B3, is a competitive inhibitor of class III histone deacetylase. Alongside its effect as modulator of inflammation, nicotinamide is also described as an immunomodulator. A recently published study demonstrates the immune enhancing effect of nicotinamide on killing of *S. aureus*, either *in vivo* in a murine model, or *in vitro* in cell cultures or whole blood. Via an increase of the expression of C/EBP ϵ in myeloid cells, nicotinamide enhances the activity of the mediator of myelopoiesis by inducing antimicrobial targets, especially in neutrophils (Kyme, Thoennissen et al. 2012).

During the primary screen, nicotinamide had been tested blindly on *S. aureus* infected zebrafish larvae. The survival of the infected fish treated with nicotinamide reached the same level as the DMSO control, which means that 3 fish died out of the 5 fish tested. In case the positive effect of nicotinamide was not detected because of the conditions of the primary screen assay, we tested nicotinamide in a secondary screen-like survival assay at higher concentrations. The survival curves of the treated groups with 1 mM or 10 mM of nicotinamide were not different than the survival curve of the control group (Figure 3.18.A.). In case the action of nicotinamide was not effective because of a non-penetration of nicotinamide inside the larvae, nicotinamide was mixed with the *S. aureus* solution and injected in 30 hpf embryos into the yolk circulation valley. It has previously been shown that nicotinamide does

not have any direct anti-staphylococcal activity *in vitro* (Kyme, Thoennissen et al. 2012), and injecting less than 1 mM of nicotinamide alone into zebrafish embryos ensures more than 90% survival of the fish (Figure 3.18.B.). Injection of a mixture of *S. aureus* (300 CFU) and nicotinamide (0.1 mM or 1 mM) was performed, and the survival curves were similar between treated and untreated groups (Figure 3.18.C.).

3.9. Discussion

Antibiotic resistance of bacteria is a growing problem that prevents efficient treatment of infected people, leading to morbidity and mortality from both acute and chronic bacterial diseases. Because classical approaches to antibiotic discovery have produced only a few new compounds to the market in recent years, alternative strategies are required to discover new antimicrobial molecules. One problem with *in vitro* search for antimicrobial drugs is the lack of physiological conditions of the infection, which can be overcome by challenging the pathogen in an *in vivo* model. The zebrafish embryo is a good candidate as an *in vivo* model of infection for several pathogens, including the bacterium *S. aureus* (Prajsnar, Cunliffe et al. 2008) on which we focussed in this study. In the zebrafish *in vivo* model of infection, staphylococcal virulence factors are activated by the pathogen, while the host innate immune system plays a key host defence role. The zebrafish embryo is also a suitable platform to perform drug screens in 96-well plate formats because of its permeability to small molecules, its small size and its easy production.

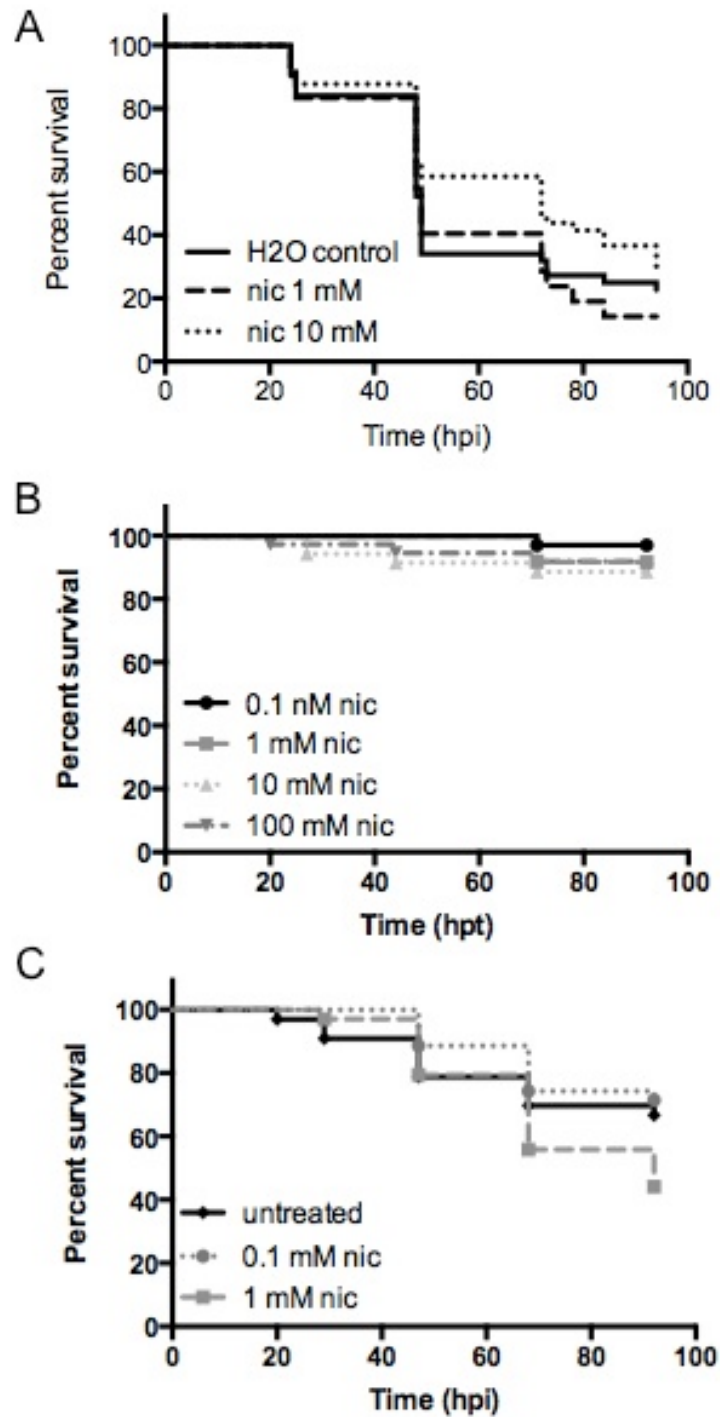


Figure 3.18. Testing the known immunomodulatory compound nicotinamide

A) LWT zebrafish embryos (30 hpf) were injected with 2000 CFU of wild-type *S. aureus* (SH1000) into their blood circulation and then were treated with water (control) or nicotinamide at 1 mM or 10 mM.

B) Toxicity test on LWT zebrafish embryos of the indicated concentrations of nicotinamide (nic) from 31 hpf.

C) LWT zebrafish embryos (30 hpf) were injected with 1 nl of a mixture of wild-type *S. aureus* SH1000 (300 CFU) and 0.1 mM or 1 mM of nicotinamide (nic) into their blood circulation.

In the infection drug screen for anti staphylococcal molecules described in this chapter, 660 compounds were tested and 22 compounds were considered as potential 'hits' after the secondary screen. Strikingly, the results of the dose-response assays or redosing assays were in contrast with the initial small positive effect of the compounds observed in the secondary screen experiments. These conflicting results are intriguing and raise several questions: Is the assay not robust enough to detect curative compounds? Were these compounds all false positive? Were the compounds purchased not exactly the same as the ones that had been tested initially in the screen, which would suggest annotation problems in the compound library, or degradation of the initial molecules?

The primary screen consisted of many experiments testing a total of 660 chemical compounds. It was important that the infection dose was consistent between experiments, as it had been shown that a difference in bacterial dose influences the mortality rate of the zebrafish larvae (Figure 3.2.). For that reason, I decided to prepare a big batch of bacterial solution that was then frozen in aliquots to be used in every experiment. The concentration of the aliquots was measured by plating dilution series of the bacteria of 1 aliquot. The size of the injection drop to be injected in the zebrafish embryos was calibrated in function of the bacterial concentration to get the desired dose of 3700 CFU. The effect of a frozen stock was tested against a freshly prepared bacterial solution in the zebrafish larvae infection model: there was no difference in the mortality rate of the infected larvae. The frozen stock was also tested one month later, and no significant difference in the mortality of the infected zebrafish embryos was observed. However, the utilisation of frozen bacterial stocks of more than 3 month-old seemed to give weird results as the usual dose of 3700 CFU would give a less lethal effect on the infected larvae. Therefore, new frozen stocks were prepared every 3 months to avoid such variability between experiments.

Some of these initial 'hits' from the secondary screen seemed very promising, especially because some antimicrobial or immune enhancing properties were reported in the literature.

Fusidic acid was identified early in the secondary screen assay. It is a known bacteriostatic antibiotic usually used externally in cream or eye drops to treat infections, or internally in combination with other antibiotics such as rifampicin to avoid emergence of resistance (Howden and Grayson 2006). As the treatment of infected larvae was performed blindly, the identification of a positive 'hit' that appeared to be an antibiotic validated the ability of the screening assay to identify protective compounds against *S. aureus* infection in the zebrafish embryo model. All the other 'hit' compounds identified during the screen were not antibiotics. In addition, no other antimicrobial molecule was present in the screened library.

Vitamin D is an essential liposoluble vitamin in bone and calcium homeostasis, but also critically important for human immunity. The vitamin D family comprises vitamin D2 (or ergocalciferol) found in plants and vitamin D3 (or cholecalciferol) found in animals. Vitamin D is usually converted by a cytochrome P450 enzyme in the liver into 25(OH)D as a storage form that can circulate freely in the serum. In many cell types, the storage form 25(OH)D of vitamin D can be converted into the active form 1,25(OH)₂D, also called calcitriol, by the CYP27B1 metabolizing enzyme. The active form of vitamin D 1,25(OH)₂D interacts through the vitamin D receptor (VDR) that is expressed in a wide variety of cell types, including almost all immune cells. The ligand activated VDR recognises specific DNA sequences called vitamin D response elements. In case of infection, 1,25(OH)₂D induces the expression of antimicrobial innate immune responses such as cathelicidin (Wang, Nestel et al. 2004; Gombart, Borregaard et al. 2005). While vitamin D2 was identified as a 'hit' in the primary screen, vitamin D3 was not. During the secondary screen using the *S. aureus*-zebrafish embryo infection model, the addition of vitamin D2 in the fish water seemed to have a protective effect on the larvae against infection. However, this result was not reproducible in the dose-response assays with newly bought vitamin D2. It should be pointed

out that we used vitamin D₂, and not directly the active form 25(OH)₂D that could have had a more potent protective effect. However, it is known that vitamin D and vitamin D metabolites such as 25-hydroxyvitamin D and 1alpha,25-dihydroxyvitamin D circulate in fish serum, and the vitamin D receptor is expressed in a variety of tissues in the developing zebrafish as well as the adult fish (Craig, Sommer et al. 2008). This suggests that vitamin D is probably converted into the active form into the zebrafish. It is also possible that the compounds library had an active metabolite with a potent effect that failed to be detected with the inactive precursor.

My data from the primary and secondary screen suggested that zinc sulfide was a good candidate to protect infected zebrafish larvae without affecting directly *S. aureus in vitro*. However, this protective action of zinc on infected zebrafish larvae was not observed with other zinc derivatives. A major difficulty was that most of the zinc compounds were not soluble in water or DMSO at concentrations around 10 mM.

Several vitamins and trace elements are important for the humoral immunity, and micronutrients deficiency leads to higher susceptibility of the host to an infection by affecting innate, T cell mediated and adaptive antibody responses. At the innate immune level, zinc increases the phagocytosis by macrophages and neutrophils, enhances the natural killer cell activity and induces the oxidative burst (Maggini, Wintergerst et al. 2007). Zebrafish embryos are only protected through their innate immunity as the adaptive immune system is still developing.

An *in vivo* infection model induces variability between experiments as many parameters are involved. I tried to be as reproducible as possible between experiments by controlling the bacterial dose injected and the developmental stage of the embryos as well as following the other optimised parameters of the protocol. However, the percent survival of the population of infected larvae showed some variations between experiments, for a similar initial bacterial dose. In the primary screen, the negative control group would usually have 2 or 3 dead fish out of the 5 tested, but sometimes 4 fish died.

Therefore a higher number of replicate (number of fish) would be useful to distinguish more accurately between real effect and 'lucky' effect of a compound during one experiment. Repeating the primary screen protocol in triplicate would most likely reduce the number of initial potential hits that need further investigation in secondary screen while increasing the likelihood of true positive identification. The rate-limiting step of the screen is the bacterial injection into the blood circulation. Therefore, automation is needed in order to increase the number of replicates. Automatic injection of bacteria into zebrafish egg yolks has been developed for *Mycobacterium marinum* (Carvalho, de Sonnevile et al. 2011), but this yolk injection system would not work with the fast growing *S. aureus*. However, a similar automatic or semi-automatic system could be developed in order to produce systemic *S. aureus* infection in zebrafish larvae.

The secondary screening assay involved survival experiments with 24 fish per group. Most of the compounds tested in this assay had a small effect with no statistical significance. It seems like the sensitivity of the screen is reduced in the survival experiments.

Small compounds of a screening library are usually dissolved in DMSO. Very low concentrations of DMSO should not affect the general health of the infected fish (Hallare, Nagel et al. 2006). However, DMSO is a penetrant carrier that can improve the efficacy of some compounds *in vivo*, in a similar way as the addition of DMSO in antiseptics increases the killing of *S. epidermidis in vitro* (Tarrand, LaSala et al. 2012). Small molecules can usually penetrate completely or partially into the zebrafish larvae through the skin, unless they are degraded into the fish or into the E3 water, or if they are unavailable because of the attraction of the compounds to the plastic of the 96-well plate or to a particular part of the zebrafish body such as the yolk. For all these reasons, the real active concentration available into the zebrafish larvae is unknown, and therefore some good compound candidates might have not been detected in the screen because their concentration was too low. To overcome this problem, injection of compounds into the zebrafish embryos circulation would be an alternative, but this would require a second

micro-injection into the embryos, which is technically challenging and could damage the fish.

Among the 22 compounds selected after the secondary screen, 3 of them share a common property as autophagy modulators. These 3 compounds are vitamin D2, verapamil and vitamin E acetate. These compounds revealed from the screen implicate autophagy as a potential pathway modulating *S. aureus* infection *in vivo*. This has biological plausibility (Schnaith, Kashkar et al. 2007; Mestre, Fader et al. 2010), and is therefore studied in detail in the following chapter.

Chapter 4: The implication of autophagy in *S. aureus* infection

4.1. Introduction: Host autophagy in pathogenesis of infectious disease

4.1.1. Autophagy

Intracellular proteins with a short-lifetime are usually degraded via the ubiquitin-proteasome pathway (reviewed in (Ciechanover 2005)). This pathway involves conjugation of ubiquitin molecules to a selected substrate, followed by degradation of the tagged protein by downstream 26S proteasome complex. In contrast, most long-lived proteins are degraded via the lysosomal machinery. The mechanism by which cytoplasmic content is delivered to lysosomes is called autophagy. Three types of autophagy have been described: macroautophagy, microautophagy and chaperone-mediated autophagy. Among them, macroautophagy is believed to be responsible for the majority of intracellular protein degradation. Macroautophagy (referred to hereafter as autophagy) is composed of several sequential steps, involving more than 30 autophagy related proteins (the ATG proteins). The first step is the formation of an isolation membrane (also called phagophore, Figure 4.1.A.). The origin of the autophagosome membranes is still controversial. A recent study showed that autophagosomes form at the endoplasmic reticulum-mitochondria contact site in mammalian cells (Hamasaki, Furuta et al. 2013). After initiation, other compartments such as Golgi, endosomes and plasma membrane contribute as membrane donors to form the autophagosome (Mari, Tooze et al. 2011). The phagophore can engulf any cytoplasmic material, selectively or non-selectively, including organelles and proteins. The complete closure of this isolation membrane forms a double membrane structure called autophagosome. In higher eukaryotic cells, a fusion with an endosome is necessary for the maturation of the autophagosome. The matured autophagosome is then called an amphisome.

In the final step, the outer membrane of the autophagosome fuses with a lysosome, forming an autolysosome (Figure 4.1.A.). The lysosomal hydrolases are then released in order to degrade the inner membrane as well as the cytoplasmic constituents. The monomeric metabolites (such as amino acids) produced through the degradation of the macromolecules can then be recycled. It is an evolutionally conserved stress-responsive process providing temporarily energy and nutrients to the cell in starvation condition. Autophagy can be upregulated in response to various extra- or intracellular stresses such as starvation, growth factor deprivation, hypoxia, oxidative stress, endoplasmic reticulum stress or pathogen infection.

The molecular mechanisms of autophagy were first discovered in the yeast *Saccharomyces cerevisiae* in the 1990s (Takeshige, Baba et al. 1992; Ohsumi 1999). Further research using mammalian cells and other animal models showed that the formation of the autophagosome is a well-conserved process from yeast to higher eukaryotes. The counterparts of the yeast autophagy proteins were identified and characterised in mammalian cells. The ATG proteins involved in non-selective macroautophagy are well conserved, stressing the importance of this process for cell survival throughout evolution (Meijer, van der Klei et al. 2007).

In mammalian cells, two main types of signalling pathways regulate autophagy: mammalian target of rapamycin (mTOR)-dependent and mTOR-independent signalling. In the classical mTOR-dependent signalling of autophagy, mTOR activity inhibits autophagy. Therefore, autophagy is activated when mTOR is inhibited, which is influenced by several signalling molecules (Akt and MAPK signalling activate mTOR while AMPK and p53 signalings are negatively regulating mTOR), by starvation conditions or by drugs such as rapamycin. The target of mTOR is the protein complex ULK1/2–Atg13–FIP200, which is an essential inducer of autophagy (Ganley, Lam du et al. 2009; Jung, Ro et al. 2010). The class III phosphatidylinositol-3-kinase (PI3K) complex, which is composed of Vps34 (vacuolar protein sorting 34) associated with a myristoylated serine/threonine kinase p150, Beclin-1 (Bcl-2-interacting protein 1) and ATG14, is also critical for the

initiation of autophagosome nucleation. Indeed, the PI3K Vps34 complex marks the membrane of the endoplasmic reticulum with an accumulation of phosphatidylinositol-3-phosphate (PI3P). The cup-shaped protrusion containing mainly PI3P lipids, named an omegasome, indicates the place where the membrane elongates to generate the isolation membrane and where the ATG proteins is recruited to continue the autophagosome biogenesis (Axe, Walker et al. 2008; Walker, Chandra et al. 2008). While the main source of PI3P during autophagy is Vps34 in mammalian cells, class II PI3Ks also contribute to PI3P generation and regulation of autophagosome formation (Devereaux, Dall'Armi et al. 2013).

In the mTOR-independent regulation pathway, low levels of free inositol and myoinositol-1,4,5-triphosphate (IP3) lead to the activation of autophagy. This can be induced by the inhibition of inositol monophosphatases (Sarkar, Floto et al. 2005). Intracellular Ca^{2+} levels and cyclic adenosine monophosphate (cAMP) also regulate the mTOR-independent pathway. Indeed, increased levels of intracellular cAMP produced by adenylyl cyclase inhibit autophagy via the activation of the guanine nucleotide exchange factor Epac. Epac activates Rap2B, which inhibits autophagy by activating phospholipase C ϵ , resulting in the production of IP3, which mediates the release of calcium (Ca^{2+}) from the endoplasmic reticulum stores. Autophagy is blocked due to increased levels of intracellular Ca^{2+} , which activates the calpains. Indeed, activated calpains mediate their effects on autophagy through Gs α , which is activated after calpain cleavage. This, in turn, increases adenylyl cyclase activity to cause an increase in cAMP levels, completing the cycle (Figure 4.1.C.) (Williams, Sarkar et al. 2008). Even though low levels of calpains can induce autophagy (and high activity of calpains inhibits autophagy) (Williams, Sarkar et al. 2008), studies with calpain-null systems generated with a knockout of calpain small 1 gene (which encodes a regulatory subunit of calpain proteases) showed impaired autophagy, highlighting the importance of calpains in the autophagic activity (Demarchi, Bertoli et al. 2006; Demarchi, Bertoli et al. 2007).

Mechanistically, the enzymes involved in the formation of the autophagosome are similar to the enzymes involved in the ubiquitination pathway. The ubiquitin-activating enzyme, also called E1 enzyme, catalyzes the first step in the ubiquitination reaction, and then passes the ubiquitin-protein to an ubiquitin-conjugating enzyme, also called E2 enzyme. Then, the E2 enzyme complexes to an ubiquitin protein ligase, also called E3 enzyme, and catalyzes the transfer of ubiquitin to the targeted protein (Figure 4.1.B.).

At the molecular level of autophagosome formation, the E1 enzyme Atg7 firstly activates Atg12 at its carboxy-terminal glycine residue, forming a thioester bond with the cysteine residue of Atg7 (Tanida, Tanida-Miyake et al. 2001) (Figure 4.1.B.). Atg12 is then transferred to the E2 enzyme Atg10 to form an Atg12-Atg10 thioester intermediate (Mizushima, Yoshimori et al. 2002). The carboxy-terminal glycine residue of the Atg12 is then covalently attached to the lysine 130 residue of Atg5 (Mizushima, Sugita et al. 1998). This Atg12-Atg5 complex is localised at the pre-autophagosomal structures and is dissociated upon formation of the autophagosome. The Atg12-Atg5 conjugate is subsequently associated to the coiled-coil protein Atg16L1L that contains multiple WD-repeats. Atg12-Atg5-Atg16L1L forms a large complex of about 800 kDa that is essential for the elongation of the isolation membranes (Mizushima, Kuma et al. 2003) (Figure 4.1.B.). The second ubiquitination-like reaction involves the conjugation of the microtubule associated protein 1 light chain 3 (LC3) to the lipid phosphatidylethanolamine (PE). LC3 is synthesized as a pro-LC3, and is immediately processed to LC3-I by a cleavage of its carboxyl-terminal tail (22 and 5 amino acids in rat and human LC3 respectively) (Kabeya, Mizushima et al. 2000) by a cysteine protease Atg4B (Tanida, Sou et al. 2004). The processed form LC3-I has an exposed glycine residue, and resides in the cytosol (Tanida, Ueno et al. 2004). LC3-I is then activated by the E1 enzyme Atg7, the same enzyme that activates Atg12 as mentioned above (Tanida, Tanida-Miyake et al. 2001), and LC3-I is transferred to the specific E2 enzyme Atg3 (Tanida, Tanida-Miyake et al. 2002). The activated complex Atg3-LC3 is recruited to the membrane by the Atg5-Atg12-Atg16L1L complex, which serves as an E3-like enzyme guiding localised LC3-PE production (Noda, Fujita et al. 2008). In

this step, the carboxyl-terminal of the LC3-I is conjugated to the head group of the PE forming the autophagosome bound lipoprotein LC3-II (Figure 4.1.B.). It is uncommon that an ubiquitin-like conjugation system is involved for protein lipidation, but this lipidation has an essential role in the membrane dynamics during autophagy (Ichimura, Kirisako et al. 2000), and LC3-II is indispensable for tethering and hemifusion of lipid membranes (Nakatogawa, Ichimura et al. 2007). In the autophagosome, LC3-II is distributed in both the exterior and the lumen of the vesicle. Once the autophagosome is formed, the Atg16L1 complex is detached. LC3 is the more commonly fluorescently marked protein to study the paralogs of yeast Atg8 protein in mammalian cells, as this protein remains associated to the autophagosome. There are 8 orthologs of Atg8 in mammals, divided in 3 subfamilies: microtubule-associated protein 1 light chain 3 (LC3), γ -aminobutyric acid receptor-associated protein (GABARAP) and Golgi-associated ATPase enhancer of 16 kDa (GATE-16) (Shpilka, Weidberg et al. 2011).

The newly formed autophagosome undergoes a maturation process, starting with the fusion with vesicles originated from early endosomes (10 min after endocytosis). Then the autophagosome fuses with multivesicular endosomes (in average at 30 min after endocytosis) (Liou, Geuze et al. 1997). This new functional intermediate structure is called amphisome and become acidic (Stromhaug and Seglen 1993), containing acid phosphatases (Tooze, Hollinshead et al. 1990) (Figure 4.1.A.). The final step is the fusion of amphisome with dense lysosome, regulated by the small GTP binding protein Rab7 in mammalian cells (Gutierrez, Munafo et al. 2004; Jager, Bucci et al. 2004). Microtubules are required as tracks and dynein as a motor in order to get the autophagosome moving in the direction of the centrosome, near the nucleus, where lysosomes are usually concentrated (Kimura, Noda et al. 2008). At this place, autophagosomes tether, dock and fuse with lysosomes, and the contents of the two vesicles are mixed (Jahreiss, Menzies et al. 2008). The combination of the autophagosome with the lysosome is called an autolysosome (Figure 4.1.A.). After fusion with the lysosome, luminal LC3-II marked with GFP is no longer detectable because of the acidic environment inside the autolysosome, as well as the digestion of

luminal LC3-II with the cargo. In contrast, lipidated LC3-II are liberated from the outer membrane due to the action of the Atg4 protease that cleaves the superficial LC3-II from PE (Tanida, Sou et al. 2004).

4.1.2. Roles of autophagy during bacterial infections

Autophagy is a recognised participant in the immune defence against microbial infection, through four different roles linked to innate and adaptive immunity: 1) it can eliminate intracellular pathogens, assisted by sequestome like-1 receptors, 2) it assists in the regulation and effector functions of pattern recognition receptors (PRRs), 3) it helps the regulation of inflammasome activation and danger signals/alarmin secretion, such as IL-1 β , and 4) it can interact with the cytoplasmic antigen processing for MHC II presentation and T cell homeostasis (Deretic 2012). As the zebrafish larvae model of infection possesses only functional innate immunity at the developmental stage of interest, this chapter focusses on the role of autophagy linked to innate immune response.

Autophagy has a broader role in the host response than just a delivery system of bacteria to lysosomes. In some cases, autophagy components contribute to immunity, while in other cases, they help the infection to expand inside the host. Depending on the type of bacterial infection, three sorts of autophagy have been reported: antibacterial, non-bacterial or pro-bacterial autophagy. Antibacterial autophagy, also called canonical autophagy, involves the elimination of some intracellular pathogens and bacterial toxins. Canonical autophagy is characterised by the formation of a double-membrane autophagosome, and involves at least 35 Atg proteins including the commonly used autophagy marker LC3. The non-bacterial autophagy coordinates cell autonomous signalling, while pro-bacterial autophagy, also called non-canonical autophagy, supports bacterial replication. Indeed, some microorganisms have developed strategies to evade or exploit autophagy degradation to remain alive intracellularly and replicate inside the host.

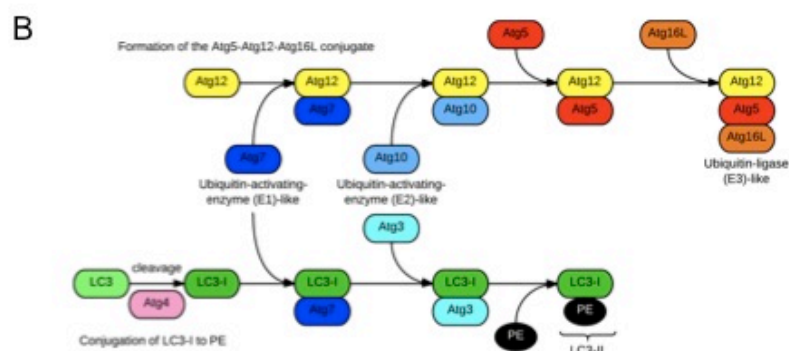
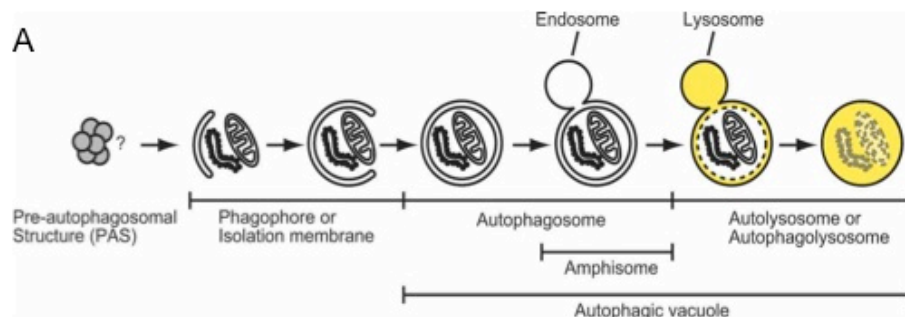


Figure 4.1. Scheme of autophagy pathway

A) The process of autophagy in mammalian cells. A portion of cytoplasm, including organelles, is enclosed by a phagophore or isolation membrane to form an autophagosome. The outer membrane of the autophagosome subsequently fuses with the endosome and then the lysosome, and the internal material is degraded.

With permission under a Creative Commons License, image and description from (Mizushima 2007).

B) Sequential participation of autophagy proteins (ATG proteins) and the 2 ubiquitin-like modification steps involved in the elongation of autophagosomes

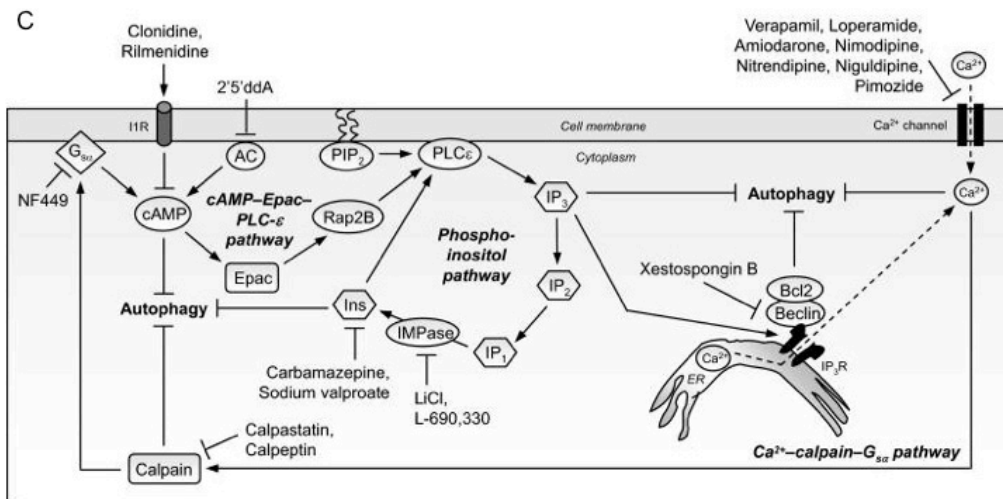


Figure 4.1. Scheme of autophagy pathway

C) Schematic representation of the cyclic mTOR-independent autophagy pathway involving cAMP, Ca²⁺, calpains and G_sα, with multiple drug targets. Intracellular cAMP levels are increased by adenylyl cyclase (AC) activity, thereby activating Epac which subsequently activates the small G-protein Rap2B, activating PLC-ε that results in the production of IP₃ and consequently Ca²⁺ release from the ER stores. Intracytosolic Ca²⁺ levels are also increased by L-type Ca²⁺ channel agonists. An increase in intracytosolic Ca²⁺ activates calpains, which cleave and activate G_sα that activates adenylyl cyclase to increase cAMP levels, thereby forming a loop. Activation of this pathway inhibits autophagy. Multiple drug targets acting at various places in this pathway trigger autophagy, such as imidazoline-1 receptors (I1R) agonists (clonidine and rilmenidine) and adenylyl cyclase inhibitor (2'5'ddA) that decrease cAMP levels; agents lowering inositol and IP₃ levels (carbamazepine and sodium valproate); IMPase inhibitors (Lithium); L-type Ca²⁺ channel antagonists (verapamil and loperamide), calpain inhibitors (calpastatin and calpeptin) and G_sα inhibitor (NF449).

With permission, image and description from (Renna, Jimenez-Sanchez et al. 2010).

At the time of its discovery, autophagy was considered as a non-selective degradation pathway activated by starvation. However, autophagy is a much more selective process than initially thought. The SLRs (sequestosomes 1/p62-like receptors) are autophagy receptors that link ubiquitination to autophagy at the molecular level. SLRs include p62 (also called sequestosome 1 (SQSTM1/p62)) (Pankiv, Clausen et al. 2007), NBR1 (neighbour or BRCA1) (Kirkin, Lamark et al. 2009), NDP52 (nuclear dot protein 52 kDa) (von Muhlinen, Thurston et al. 2010) and optineurin (OPTN) (Wild, Farhan et al. 2011). These receptors can specifically target ubiquitinated bacteria and microbicidal peptides to autophagosomes. For this purpose, SLRs can simultaneously bind intracellular ubiquitinated cargos and autophagy modifiers such as LC3 proteins via their LC3-interacting regions (LIR) motif (Birgisdottir, Lamark et al. 2013). These receptors can then mediate docking of ubiquitinated substrates to the autophagosomes to induce selective autophagic degradation of ubiquitinated proteins, organelles and intracellular bacteria.

Autophagy can target bacteria that reside in different compartments such as phagosomes, damaged vacuoles or in the cytosol. The following types of bacteria demonstrate subversion mechanisms of host antibacterial autophagy, escaping the vacuole to the cytoplasm. *Shigella flexneri* can manipulate host autophagy to its own benefit. Once in the cytosol, the surface-expressed IcsA proteins recruit N-WASP and the Arp2/3 complex to form actin tails for motility (Egile, Loisel et al. 1999). Recognition of IcsA by Atg5 triggers autophagy (Ogawa, Yoshimori et al. 2005), a process that is mediated by TECPR1, a Tectonin domain-containing protein (Ogawa, Yoshikawa et al. 2011). The type III secretion system (T3SS) effector IcsB can bind to IcsA in order to prevent the recruitment of the autophagic machinery (Ogawa, Yoshimori et al. 2005), and the binding of IcsB with cholesterol is also required (Kayath, Hussey et al. 2010). Another T3SS, VirA, counteracts autophagy by manipulating Rab1 GTPase function (Dong, Zhu et al. 2012). After its internalisation by the host cell, *Listeria monocytogenes*

can escape from the phagosome to the cytosol via the secretion of the pore-forming haemolysin listeriolysin O (LLO). Once in the cytosol, *L. monocytogenes* expresses the surface protein ActA that polymerises actin and assists in its motility, including cell-to-cell spread. As autophagy is activated by LLO and is essential for the inhibition of intracellular growth of *L. monocytogenes* by the host immune defence (Birmingham, Canadien et al. 2007; Birmingham, Higgins et al. 2008), the bacteria has evolved several evasion strategies against the autophagic machinery. The phospholipase C enzymes (PLCs), which lyse phagosomal vesicles synergistically with LLO, also negatively regulate autophagy (Birmingham, Canadien et al. 2007). In addition, the surface protein ActA can induce the recruitment of the Arp2/3 complex and Ena/VASP, contributing to a camouflage strategy to escape autophagic recognition (Yoshikawa, Ogawa et al. 2009). Independently of the ActA pathway, another surface protein named the internalin InlK is utilised by *L. monocytogenes* to mediate the decoration of its surface with the major vault protein in order to escape autophagic recognition (Dortet, Mostowy et al. 2012).

Autophagy can also restrict bacterial growth of some types of pathogen. For example, *Mycobacterium marinum* is a fish and frog pathogen, and an alternative model to study *Mycobacterium tuberculosis*. *M. marinum* survive in host macrophages by preventing phagolysosome fusion. LC3 proteins can be recruited to the *M. marinum*-containing compartment, a process that depends on ESX-1 activity. If autophagy is stimulated with a pharmacological agent such as rapamycin, the recruitment of LC3 proteins is enhanced and leads to the fusion with lysosome (Lerena and Colombo 2011). In the cytosol, *M. marinum* can follow 2 different paths: *M. marinum* can polymerise an actin tail or be ubiquitinated. Ubiquitinated *M. marinum* can be sequestered inside a double membrane vacuole that does not involve Atg5 during its formation and is not associated with LC3 proteins, but is positive for lysosomal marker LAMP-1, suggesting a non-canonical autophagy process (Collins, De Maziere et al. 2009). Phagocytosed *S. pyogenes* (Group A *Streptococcus* (GAS)) express the cholesterol-dependent pore-forming toxin streptolysin O (SLO) in order to escape from phagosomes (Yoshimori 2006). As SLO

activates autophagy, cytosolic GAS are taken up inside LC3-positive compartments called GAS-containing autophagosome-like vacuoles (GcAVs) (Nakagawa, Amano et al. 2004), which require the small GTPases Rab7, Rab9 and Rab23 (Yamaguchi, Nakagawa et al. 2009; Nozawa, Aikawa et al. 2010). GAS are degraded after the fusion of GcAVs with lysosomes, suggesting that this non-canonical autophagy pathway is essential for GAS infection control. *Salmonella enterica* serovar Typhimurium (*S. typhimurium*) is an intracellular pathogen that resides and replicates inside the Salmonella-containing vacuoles. In case of damaged Salmonella-containing vacuoles by the Salmonella pathogenicity island type-1 T3SS, autophagy targets the bacteria to maintain it inside a vacuole and therefore protecting the cytosol from bacterial colonisation (Birmingham, Smith et al. 2006). In case of a release of the bacteria into the cytosol (which happens for about 25% of them), *S. typhimurium* is targeted by ubiquitin, and subsequently targeted for autophagic degradation via the autophagy receptors p62 (Zheng, Shahnazari et al. 2009), NDP52 (Thurston, Ryzhakov et al. 2009; von Muhlinen, Thurston et al. 2010) or optineurin (Wild, Farhan et al. 2011). Cytosolic *S. typhimurium* can also be targeted for autophagic elimination via a diacylglycerol label (Shahnazari, Yen et al. 2010).

Another strategy for autophagy subversion used by some bacteria is the formation of a replicative vacuole. Intracellular bacteria can inhibit the maturation of the autophagosome, preventing its acidification in order to survive within the phagosome. After the internalisation of *Coxiella burnetii*, early phagosomes containing the pathogen fuse with other vesicles, forming large parasitophorous vacuoles in which *C. burnetii* multiply. The autophagy marker LC3 is recruited to the early stages of *C. burnetii*-containing phagosomes. It has been shown that mechanisms of autophagy accelerate the formation of the parasitophorous vacuoles, hence bacterial replication (Gutierrez, Vazquez et al. 2005; Romano, Gutierrez et al. 2007). A study using human coronary artery endothelial cells has shown that the trafficking of *Porphyromonas gingivalis* to late autophagosomes promotes the bacterial survival (Dorn, Dunn et al. 2001). Shortly after internalisation of *P. gingivalis*, the autophagic protein Atg7 is recruited, and subsequently a compartment in

which *P. gingivalis* can replicate is formed. Some evidence has shown that LC3 proteins colocalise with the bacteria at the early stages of infection (Yamatake, Maeda et al. 2007), but the bacteria hampers the late step of autophagy, preventing formation of the autolysosome. *Anaplasma phagocytophilum* remain in non-acidic vacuoles (Webster, JW et al. 1998) that have a double membrane and colocalise with LC3 proteins. Normal autophagy is subverted as fusion with the lysosome is avoided to favour proliferation of the bacteria (Niu, Yamaguchi et al. 2008). *Legionella pneumophila* exploits macrophage host autophagy to delay the maturation of its vacuole after its internalisation, and interacts with ER-like structures (Joshi and Swanson 2011). Later after the internalisation, *L. pneumophila* differentiates and multiplies in an acidic replicative niche (Sturgill-Koszycki and Swanson 2000). The bacterial effector protein RavZ interferes with autophagy by acting as an Atg4-like cysteine. RavZ irreversibly inactivates LC3 proteins by attacking the bond between LC3 proteins and the phosphatidylethanolamine of the autophagosome membrane (Choy, Dancourt et al. 2012). After the entry of *Brucella abortus* into the host cell, *Brucella*-containing vacuoles (BCV) are formed. Subsequently, *B. abortus* co-opts the autophagic machinery to utilise some autophagic components involved in the initiation of autophagy such as ULK1, Beclin 1 and ATG14. This step is required for non-canonical autophagy in order to form the autophagic BCV. These autophagic BCVs, with their late endosomal-early lysosomal features, do not degrade the bacteria, but instead seem beneficial for the spreading of the bacteria from cell to cell (Starr, Child et al. 2012). Autophagy is also involved in the formation of *Brucella*-replication niches.

4.1.3. Importance of autophagy in *S. aureus* pathogenesis

S. aureus has generally been considered to be an extracellular pathogen, but recent increasing evidence indicates that *S. aureus* can be a facultative intracellular pathogen (Garzoni and Kelley 2009). In addition, *S. aureus* utilises the autophagy system to its own advantages, benefiting from pro-bacterial autophagy to replicate.

4.1.3.1. *S. aureus* small colony variants

Certain subpopulations called small colony variants (SCV) are especially well adapted to the intracellular milieu. By definition, SCVs are macroscopically slow growing (48h to 72h on blood plate agar), are one-tenth of the 'normal' *S. aureus* size and lack pigmentation. SCVs have a reduced haemolytic activity, a reduced coagulase activity and a higher resistance to aminoglycosides (e.g. gentamicin). Most of SCVs are deficient in electron transport as a consequence of being often auxotrophic for menadione or hemin, which are components involved in the biosynthesis of electron transport chain elements. SCVs show decreased expression of exotoxins such as α -haemolysin and an increased expression of adhesins, such as clumping factor and fibronectin-binding proteins (Vaudaux, Francois et al. 2002). There is a less common subgroup of SCVs that are deficient in thymidine biosynthesis, and have emerged after long-term trimethoprim sulphamethoxazole treatment in cystic fibrosis patients. Thymidine-dependent SCVs have two colony types: 'fried egg' or pin-point white small colonies (Kahl, Belling et al. 2003).

4.1.3.2. Internalisation and persistence

A whole cytoplasmic proteomic study showed an important change in expression of several proteins between a clinically derived *S. aureus* SCV phenotype and its isogenic strain with a normal phenotype (Kriegeskorte, Konig et al. 2011). SCVs are less susceptible to antibiotics, contributing to their persistence while under antibiotic pressure *in vivo* (Brouillette, Martinez et al. 2004). The reduced secretion of α -toxin by SCVs enables the bacteria to persist intracellularly rather than lysing the host cell. Also, SCVs can survive in the lysosomal compartment, which is usually a hostile and degradative environment (Schroder, Kland et al. 2006). Recurrent infections might be due to bacterial persistence inside the environment of host cell, as it provides protection against antibodies, complement and antibiotics. Clinically, SCVs have been associated with relapsing or persistent infections, especially in osteomyelitis, cystic fibrosis and device-related infections (von Eiff, Peters et al. 2006). The switching between SCV phenotype and normal phenotype seems to be an integral part of the infection process during staphylococcal

life cycle. The wild-type phenotype is efficient at invading the host, while the SCV phenotype can persist intracellularly in non-professional phagocytes. *In vitro* and *in vivo* long-term infection studies have revealed that long-term persistence induces the upregulation of FnBP, while *hla* and *agr* are downregulated. These SCVs of *S. aureus* represent a reservoir for chronic infections, enabling the bacteria to hide inside the host. When SCVs leave the intracellular milieu, the bacteria can easily and quickly switch back to the wild-type phenotype and exert cytotoxic activity (Tuchscher, Medina et al. 2011).

While it is now clear that SCVs can persist intracellularly, evidence suggests that normal size *S. aureus* are also facultative intracellular pathogens. Through *in vitro* studies with cultured cells, it has been shown that *S. aureus* can colonise a variety of non-phagocytic mammalian cells such as mouse fibroblasts (Usui, Murai et al. 1992), mouse renal cells (Murai, Usui et al. 1992), bovine mammary epithelial cells (Almeida, Matthews et al. 1996), bovine endothelial cells (Hamill, Vann et al. 1986), chick osteoblast cells (Hudson, Ramp et al. 1995) and keratinocytes. The fate of live *S. aureus* is different after invasion of tracheal epithelial cells of cystic fibrosis (CFT-1) patients than invasion of the complemented counterpart cells (LCFSN). Indeed, *S. aureus* can replicate into CFT-1 cells but not in LCFSN cells (Jarry and Cheung 2006). This is due to phagosomal escape of the bacteria in CFT-1 cells, through the expression of α -haemolysin (Jarry, Memmi et al. 2008).

4.1.3.3. Internalisation mechanism of *S. aureus*

Adherence and invasion are prerequisite for infection of cells by *S. aureus*. Fibronectin-binding proteins (FnBPs) type A and B are a type of adhesins anchored in the bacterial cell wall and have a predominant role in the uptake of *S. aureus* (Dziewanowska, Patti et al. 1999; Sinha, Francois et al. 1999; Bingham, Rudino-Pinera et al. 2008), even though other adhesion proteins are involved in the bacterial invasion process (Brouillette, Grondin et al. 2003). Fibronectin acts as a bridging ligand between *S. aureus* binding domain and eukaryotic cells $\alpha 5 \beta 1$ integrin in non-phagocytic cells (Sinha,

Francois et al. 1999), while fibronectin is attached to $\alpha M \beta 2$ integrin in professional phagocytes (Flick, Du et al. 2004). After its attachment to the cell, *S. aureus* is internalised via the zipper mechanism (Swanson and Baer 1995; Schwarz-Linek, Werner et al. 2003). Bacteria induce rearrangements in the host cell cytoskeleton that result in its engulfment in a centripetal movement (Schroder, Schroder et al. 2006). The bacteria are therefore forcing phagocytosis by eliciting formation of pseudopod-like structures that mediate their uptake (Kahl, Goulian et al. 2000). The optimal internalisation of *S. aureus* is dependent on the expression of Src kinase (Agerer, Michel et al. 2003; Fowler, Johansson et al. 2003). The *S. aureus agr* and *sar* mutants have elevated levels of internalisation compared to the wild-type strain, probably because of a higher expression of surface proteins by the mutants, which are required for internalisation.

4.1.3.4. *S. aureus* persistence in mast cells and phagocytes

Mast cells are a double-edged sword for *S. aureus*. On one hand, mast cells can kill *S. aureus* through the release of extracellular traps and other antimicrobial granules after infection. On the other hand, mast cells can also provide a protective niche for *S. aureus*. Indeed, *S. aureus* can be internalised by mast cells and persist in the cytosol for days. Intracellular bacteria have a thicker cell wall, and alpha-haemolysin is important for their intracellular survival (Abel, Goldmann et al. 2011).

The persistence and survival of *S. aureus* inside phagocytes might constitute a route of dissemination for staphylococcal infection. After internalisation of *S. aureus* by macrophages, antiapoptotic factors are upregulated while proapoptotic factors are downregulated. These processes are responsible for extended phagocyte lifetime, and might contribute to *S. aureus* dissemination (Koziel, Maciag-Gudowska et al. 2009). However, an *in vivo* study using a *S. aureus*-zebrafish larvae infection model revealed that neutrophils are a more likely 'niche' of bacterial dissemination than macrophages (Prajnsnar, Hamilton et al. 2012). A few studies have shown that 15-50 % of phagocytosed *S. aureus* by neutrophils can survive intracellularly inside the neutrophils phagosome. These neutrophils containing viable *S. aureus* are

not effectively ingested by macrophages, and instead can undergo a programmed necrosis in a RIP-1 manner that would exacerbate staphylococcal disease (Greenlee-Wacker, Rigby et al. 2014).

4.1.3.5. *S. aureus* survival, persistence and growth

After engulfment, several parameters are required for the bacteria to survive intracellularly: 1) not killing the host cell, 2) resisting the intracellular host defences, 3) not activating the host immune system, and 4) be able to proliferate in the cytoplasm.

The intracellular persistence of *S. aureus* is a key component in chronic staphylococcal diseases as well as long-term colonisation, as it provides a protective niche against host defences and certain classes of antibiotics. Staphylococcal infections are often associated with death of tissue, and evidence suggests that intracellular bacteria can mediate apoptosis in epithelial cells (Bayles, Wesson et al. 1998), endothelial cells (Menzies and Kourteva 2000) and keratinocytes (Nuzzo, Sanges et al. 2000). Induction of cell apoptosis implicates the well-known virulence regulatory loci *agr* and *sar* (Wesson, Liou et al. 1998). Alpha toxin is important for triggering apoptosis (Menzies and Kourteva 2000), however, other virulence factors are also required (Haslinger-Loffler, Kahl et al. 2005). *S. aureus* residing within phagosomes start their intracellular replication 6-7h after their internalisation into pulmonary epithelial cells (CFT-1), with a slow replication of 3 to 5 divisions every 24 h compared to 1 division every 20 min in the extracellular milieu (Kahl, Goulian et al. 2000).

4.1.3.6. Subversion of autophagy by *S. aureus*

Some Gram-negative bacteria have similar behaviour to the Gram-positive *S. aureus* in the sense that they subvert the autophagy pathway by delaying the fusion of the autophagosome with the degradative lysosome. These bacteria are *B. abortus*, *L. pneumophila*, *P. gingivalis* and *C. burnetii* (Campoy and Colombo 2009) (see section 4.1.2. for more details).

The subversion of autophagy by *S. aureus* seems to be bacterial strain specific as well as cell type specific, as different studies present opposite

results. In human epithelial cells (HeLa), invading *S. aureus* colocalise with LC3, reaching a maximum of colocalisation at 3h post infection, suggesting that the bacteria induce autophagy in order to transit via the autophagosomes. This autophagosome is Rab7 positive, a protein present in the late endocytic vesicle, but also in autophagic vacuoles. Under normal circumstances, the autophagosome is acidified to a pH of around 5 and then fuses with a lysosome. Neither the acidification nor the fusion with lysosome happens for the *S. aureus*-containing autophagosome, which was shown by the absence of colocalisation of the bacteria with LysoTracker or LAMP-2, markers of acidic milieu and lysosome, respectively. It seems that *S. aureus* subverts the autophagy pathway at the stage of fusion with the lysosome in order to stay within the autophagosome. Therefore, the autophagosome serves as a protective niche in which intracellular *S. aureus* can survive and replicate. In presence of the autophagy inducer rapamycin, the intracellular bacterial load doubles, while it decreases with the presence of the autophagy inhibitor wortmannin (Schnaith, Kashkar et al. 2007). Similarly, the replication of *S. aureus* is impaired in Atg5-deficient mouse embryonic fibroblasts (MEF) cells, increasing the survival of the cells, indicating that *S. aureus* requires autophagy activation for its replication. After 12h of infection, *S. aureus* can escape into the cytoplasm to eventually kill the eukaryotic host cell. *S. aureus* induced cell death seems to rely on autophagic proteins, excluding the role of caspase activation to induce cell apoptosis. In contrast, invading *agr*-deficient *S. aureus* fail to induce autophagy, implicating normal maturation of the *S. aureus*-containing phagosome. Also, *agr*-deficient bacteria colocalise with LAMP-2 and LysoTracker, suggesting normal fusion of the autophagosome with lysosome and the acidification of the compartment, while both of these steps are inhibited by *agr*-expressing *S. aureus* strain. The fusion of the phagosome with the lysosome degrades *agr*-deficient *S. aureus* and cell death is avoided (Schnaith, Kashkar et al. 2007). The importance of *agr*-dependent factor(s) for *S. aureus* intracellular survival and cytotoxicity is consistent in several studies (Wesson, Liou et al. 1998; Haslinger-Loffler, Kahl et al. 2005). However, if autophagy is activated by rapamycin treatment, most of the *agr*-deficient *S. aureus* colocalise with LC3. Bacterial replication

is then activated, leading to a higher cell death rate for *agr*-mutant bacteria than wild-type bacteria.

Another cell culture infection study showed that methicillin-sensitive *S. aureus* is sequestered in localised LC3 compartments, and then degraded by autolysosomes, suggesting autophagic degradation. In Atg5 deficient MEF cells, *S. aureus* is not killed but instead could persist and multiply. However, some MRSA strains seem resistant to autophagy and can escape from the autophagosomes into the cytoplasm (Amano, Nakagawa et al. 2006). An explanation for the opposite results obtained from the Yoshimori's group study (Amano, Nakagawa et al. 2006) and the Krut's group study (Schnaith, Kashkar et al. 2007) would be the use of different *S. aureus* strains. The sensitive-*S. aureus* strain used in the Yoshimori's study that co-localise with LC3 and multiply in Atg5 *-/-* cells could be an *agr*-deficient strain, while the *S. aureus* strain resistant to autophagy would have an active *agr* locus.

One of the major toxins regulated by the *agr* system is the pore-forming toxin alpha-haemolysin (Hla). The secretion of alpha-toxin by *S. aureus* is required for the activation of autophagy during the infection of cells. This Hla-induced autophagy requires some autophagy proteins such as Atg5, and is regulated by calcium. However, Hla-induced autophagy is independent of Beclin1 and PI3K activity, suggesting a type of non-canonical autophagy. Accumulation of LC3-II proteins in infected cells and the absence of fusion with lysosomes also show that the autophagic pathway is dysfunctional. This non-canonical autophagy pathway induced by the secretion of Hla toxin allows *S. aureus* to reside and replicate inside a non-degradative and non-acidic compartment (Mestre, Fader et al. 2010). The induction of autophagy by Hla toxin secreted by *S. aureus* is mediated by a decrease in intracellular cAMP levels and the Epac-Rap2b pathway. In addition, the reduced levels of cAMP induce the opening of calcium channels, and the rise in intracellular Ca²⁺ levels inhibits the calpains, which is another way to activate autophagy by increasing the amount of key autophagy components such as Atg5 (Mestre and Colombo 2012).

A study using automated fluorescence-based high content analyses demonstrated that *S. aureus* stimulate autophagy and the bacteria are entrapped in compartments decorated with WIPI1 proteins. The effector WIPI1 is a membrane protein of both phagophores and autophagosomes that are induced by the PI3P signal, which subsequently recruits Atg12 and LC3 at the membrane. The addition of the lysosomal inhibitor bafilomycin increases the number of GFP-WIPI1 positive *S. aureus*-entrapped autophagosome-like vesicles, suggesting that the fusion with lysosome is a working defence mechanism for non-professional phagocytic cells to degrade pathogens (Mauthe, Yu et al. 2012). However, this defence mechanism is not totally efficient, and in some circumstances, a portion of bacteria is able to escape to the cytoplasm as demonstrated in previous studies (Schnaith, Kashkar et al. 2007).

4.1.3.7. Phagosomal escape of *S. aureus*

The endosomal escape of *S. aureus* followed by its replication requires the expression of *agr*-regulated proteins, which was shown in studies using bovine mammary cell line (Qazi, Counil et al. 2001) and CFT-1 cells (Jarry, Memmi et al. 2008). In other type of cells, alpha-toxin does not seem sufficient to mediate escape from phagolysosome, as shown in upper airway epithelial cells (Giese, Dittmann et al. 2009). However, *S. aureus* expressing delta-toxin can escape from phago-endosomes of human epithelial and endothelial cells. The phenol soluble modulins (PSM) delta-toxin is encoded by the *agr* effector RNAIII, and its activity and mode of action is similar as a non-ionic detergent. The phagosome membrane destruction mediated by delta-toxin is dependent on the presence of beta-toxin, which cleaves sphingomyelins to phosphorylcholine and ceramide moieties (Giese, Glowinski et al. 2010).

4.1.4. Autophagy in zebrafish

Autophagy, as a process of degradation of dysfunctional proteins, damaged organelles and cellular waste, plays a key role in cell fate decision and differentiation, including cell proliferation, sorting, migration, information transfer, differentiation and death. Autophagy has a crucial role in

maintaining neurons in a physiological state and degrading abnormal protein aggregates in nerve tissue. Excessively high or low autophagy levels can lead to pathological conditions. In case of reduced level of autophagy, accumulation of neuroproteins can cause neurodegenerative diseases such as Alzheimer disease, Huntington's disease or Parkinson's disease (Fleming and Rubinsztein 2011).

Zebrafish has only been used as an animal model to study autophagy associated to diseases in the recent years. The zebrafish model offers the advantage to study the regulation of autophagy using gene knockdown tools. In addition, signaling pathways can be temporally controlled with pharmacological inhibitors. The research area of autophagy is likely to expand in the coming years considering the new precise and targeted genome editing methods (TALENs and CRISPRs) now available to generate zebrafish mutants. Only a few studies have been performed on the function of Atg proteins in zebrafish.

During the embryonic period of the zebrafish development, autophagy is active in multiple tissues, including the heart. The majority of the *atg5* zebrafish morphants and a third of the *atg7* morphants had structural defects in their cardiac muscle (Lee, Koo et al. 2014). Autophagy transcripts of *atg5* and *atg7* are detected in 1-cell stage zebrafish embryo, suggesting a maternal contribution that lasts up to 10 hpf. *Atg5* and *atg7* mRNA are also detected at several timepoints after 10 hpf and up to 2 dpf, suggesting that they are upregulated during the early developmental program of the zebrafish embryo (Lee, Koo et al. 2014). More specifically, the amount of *atg5* mRNA reaches a maximum at 18-24 hpf and is located mainly in the encephalic region and the central nervous system, suggesting its implication in neurula formation (Hu, Zhang et al. 2011). Similarly to the mRNA transcript, Atg5 proteins are localised mainly in the region of the brain. Further investigations using knockdown and overexpression techniques in a zebrafish model showed that *atg5* is important for normal morphogenesis of brain regionalisation and body plan, as well as for expression regulation of

the neural gene markers *gli1*, *huC*, *nkx2.2*, *pink1*, *β -synuclein*, *xb51* and *zic1* (Hu, Zhang et al. 2011).

A zebrafish model of Huntington's disease was created a few years ago by expressing a green fluorescent protein tagged to a mutant form of the human huntingtin protein (HDQ71) in the photoreceptors (Williams, Sarkar et al. 2008). The clearance of huntingtin aggregates can be observed *in vivo* and are dependent on autophagy. This transgenic line has enabled to discover new regulatory mechanisms of autophagy such as the IGF-1R pathway (Renna, Bento et al. 2013).

Autophagy plays an important role in tissue differentiation and patterning. A zebrafish study has shown that autophagy is highly upregulated during the regeneration process of an amputated fin, especially at the proliferation site near the tail tip. In addition, inhibition of autophagy by knocking down *atg5* impairs the regeneration of amputated caudal fins by preventing survival and proliferation of dedifferentiating cells normally involved in the regeneration process (Varga, Sass et al. 2014).

About spatial localisation, LC3-I proteins are diffusely distributed in the cellular cytoplasm, but are linked with the membrane after their conjugation with phosphatidylethanolamine to form LC3-II during the induction of autophagy. This process can be observed *in vivo* using transgenic zebrafish lines such as *Tg(cmv:GFP-LC3)*, enabling to visualise fluorescent punctate structures (He, Bartholomew et al. 2009). The autophagic flux can be measured using these transgenic zebrafish lines in combination with a lysosomal dye (e.g. LysoTracker).

4.1.5. Aims and hypotheses

The aim of this chapter is to investigate the effects of host autophagy modulation on systemic staphylococcal infection using the *S. aureus*-zebrafish *in vivo* infection model. The hypothesis is that autophagy is subverted by *S. aureus* to promote its intracellular survival.

4.2. The *frozen* zebrafish strain and *S. aureus* infection

4.2.1. The *frozen* zebrafish strain

The zebrafish strain $\text{fro}^{\text{to27c}}/+$ was identified from a large-scale phenotypic screen of mutants initially mutagenised with ethylnitrosourea (Haffter, Granato et al. 1996). The $\text{fro}^{\text{to27c}}/+$ mutant was selected because of the locomotion defect of the early embryo of mendelian ratios of *frozen* offspring, suggesting a recessive mutation of that gene. The lack of motility is caused by problems in muscle assembly. In normal 28 hpf zebrafish embryos, somitic trunk muscles are composed of well-formed muscle fibres containing elongated multinucleated myotubes. In contrast, in the *frozen* mutant embryo, muscle fibres are disorganised and the muscle cell nuclei are round (Granato, van Eeden et al. 1996). Also, alpha-actin filaments are disorganised along the Z-lines, and therefore the myofibril assembly is dysfunctional. The mutation has been mapped to the genomic locus of autophagy gene Atg10. In addition, *frozen* fish larvae are defective in the conjugation of Atg12 to Atg5, which compromises the formation of the Atg12-Atg5 complex, leading to a loss of autophagy (Lien Chiou Lee S., poster communication).

The *frozen* mutant phenotype is visible from 20 hpf, as these embryos do not respond to any mechanical stimuli. A normal zebrafish embryo produces a 'wiggle reaction' characterised by a rapid movement from side to side and/or a big curl with the tail, while the *frozen* mutant is completely paralysed and cannot move or swim. The *frozen* mutant (-/-) phenotype is therefore easily detectable in early embryos compared to the siblings (-/+ and +/+).

4.2.2. *S. aureus* infection in *frozen* fish

Because the *frozen* zebrafish strain was thought to be defective in the autophagy pathway, and preliminary findings issued from the drug screen (see Chapter 3) implicated autophagy in *S. aureus* infection, it was decided to test the *frozen* mutant as a host organism in a *S. aureus* infection assay. *Frozen* and sibling embryos (30 hpf) were identified by phenotype and

injected with wild-type *S. aureus* SH1000, and the survival of the larvae was recorded over 4 days. Whether the zebrafish embryos were injected with a medium (2250 CFU) or high (3400 CFU) bacterial dose, there was a significant increase in zebrafish survival in the infected *frozen* group compared to the infected sibling group (Figure 4.2.). Based on the hypothesis that the *frozen* mutant lacks normal autophagy function, this experiment suggests that a lack of autophagy is detrimental for *S. aureus* proliferation, favoring the host over the pathogen.

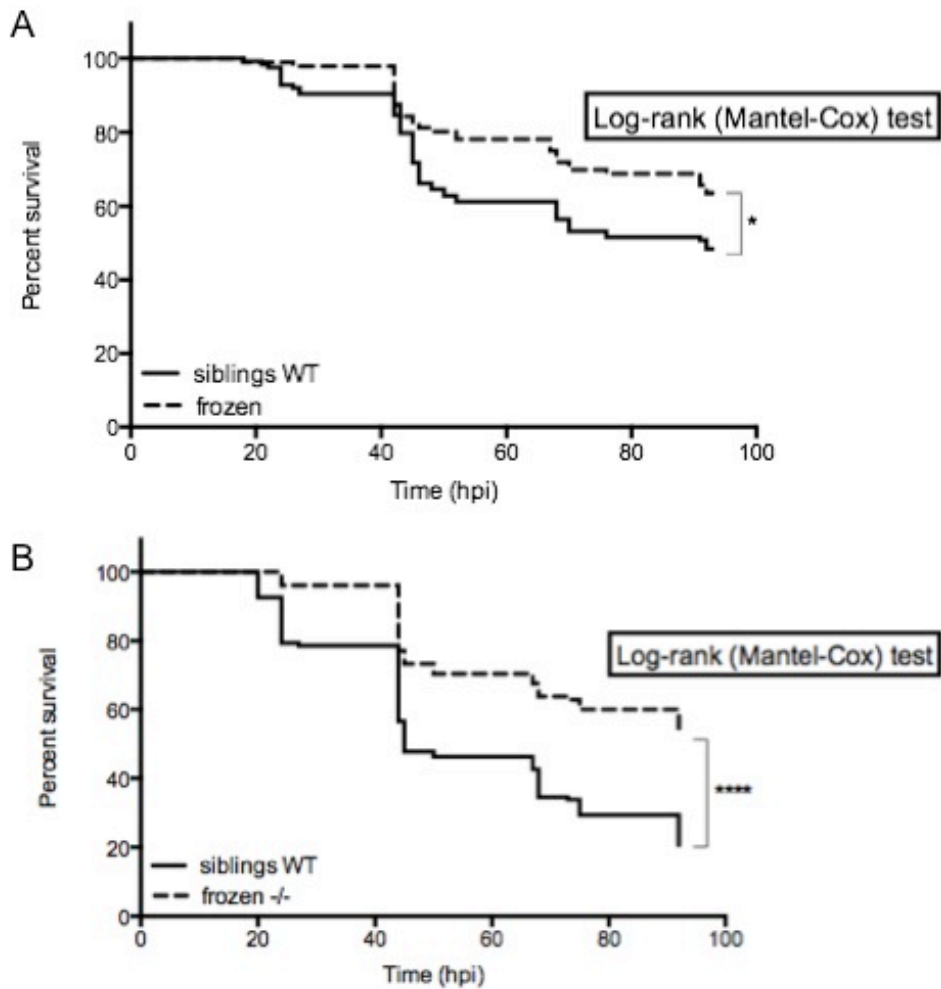


Figure 4.2. Infection of frozen mutant zebrafish larvae with *S. aureus*

Incross of $fro^{to27c/+}$ zebrafish embryos (30 hpf) divided in *frozen* (double mutant $-/-$) and siblings ($+/-$ and $+/+$) were injected with A) 2250 CFU or B) 3400 CFU of wild-type *S. aureus* (SH1000) into their blood circulation.

$n \geq 99$ fish per group (4 or 5 independent experiments).

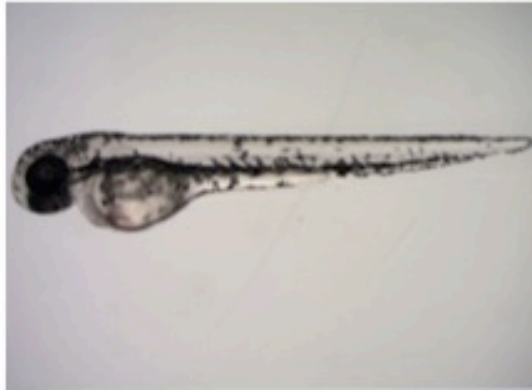
* = P-value < 0.05 ; **** = P-value < 0.0001.

Tricaine conc	30 hpf In tricaine	33 hpf In tricaine	48 hpf In tricaine	48 hpf Tricaine removed	54 hpf In E3 medium
0.33 mg/ml	- no circulation - no erythrocytes circulating	very slow to slow circulation in a few fish	- no circulation - 2/36 dead fish	- full circulation back	- normal circulation
0.5 mg/ml	- no circulation - no erythrocytes circulating		- no circulation	- no circulation	- normal circulation for 9/21 fish - yolk slightly brown
0.66 mg/ml	- no circulation - no erythrocytes circulating		- no circulation - 1/26 dead fish	- no circulation - fish alive with heart beat - small cardiac oedema - curved tail - yolk darker brown	- no circulation

Table 4.1. Observations of the state of the circulation of LWT zebrafish embryos treated with tricaine at the indicated concentration.

Treatment from 30 hpf to 48 hpf

no tricaine



0.33 mg/ml of tricaine



0.5 mg/ml of tricaine



0.66 mg/ml of tricaine

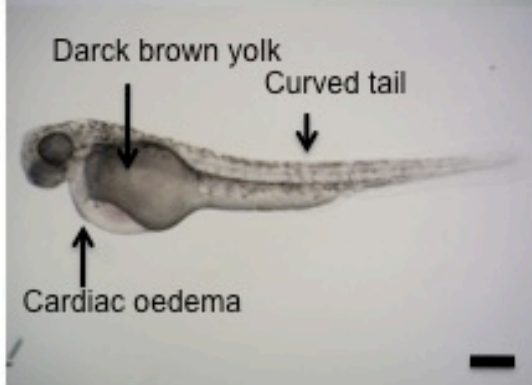


Figure 4.3. Tricaine treated zebrafish embryos

Pictures of 48hpf LWT zebrafish embryos treated with tricaine at the indicated concentration from 30 hpf to 48 hpf.

Scale bar = 80 μ m

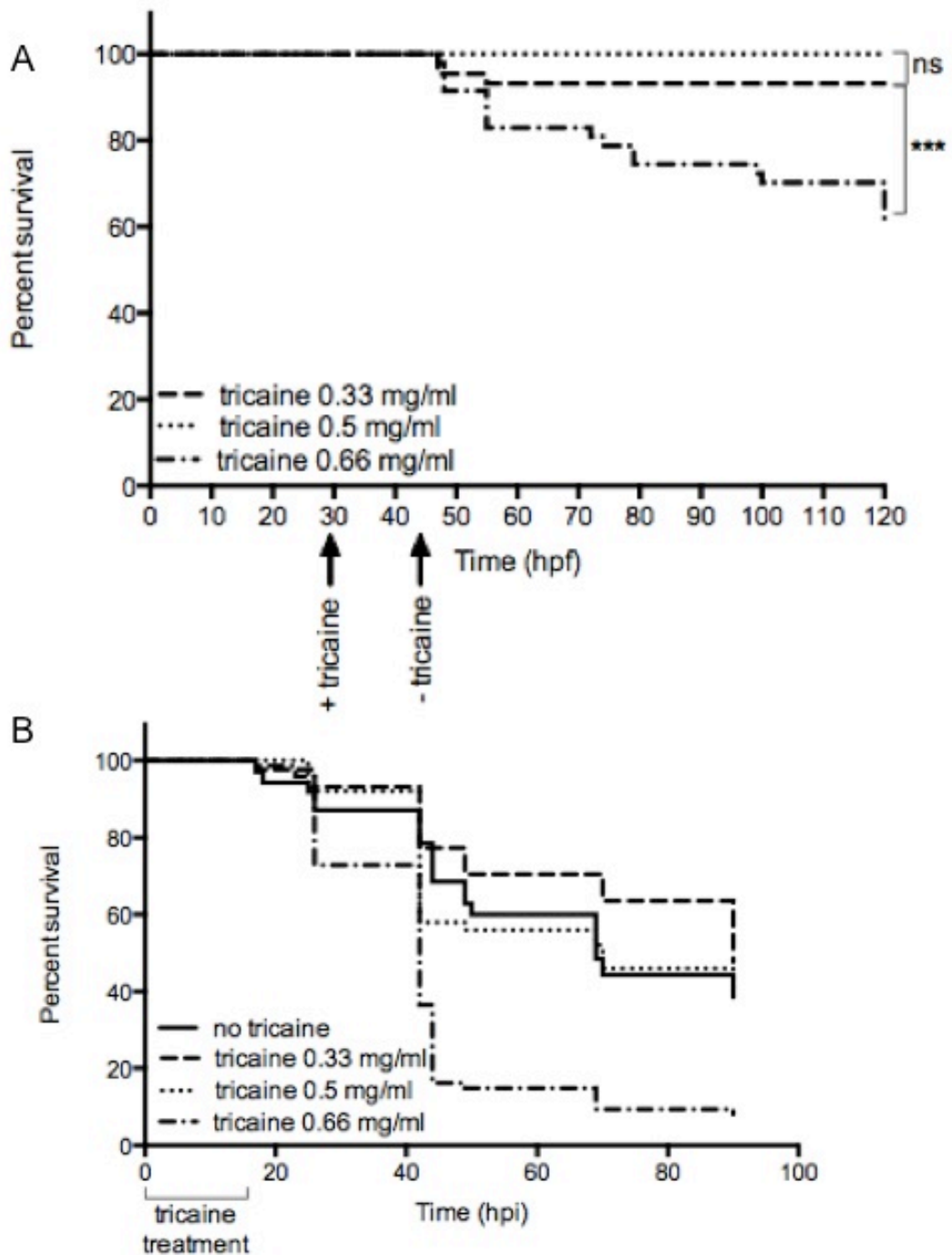
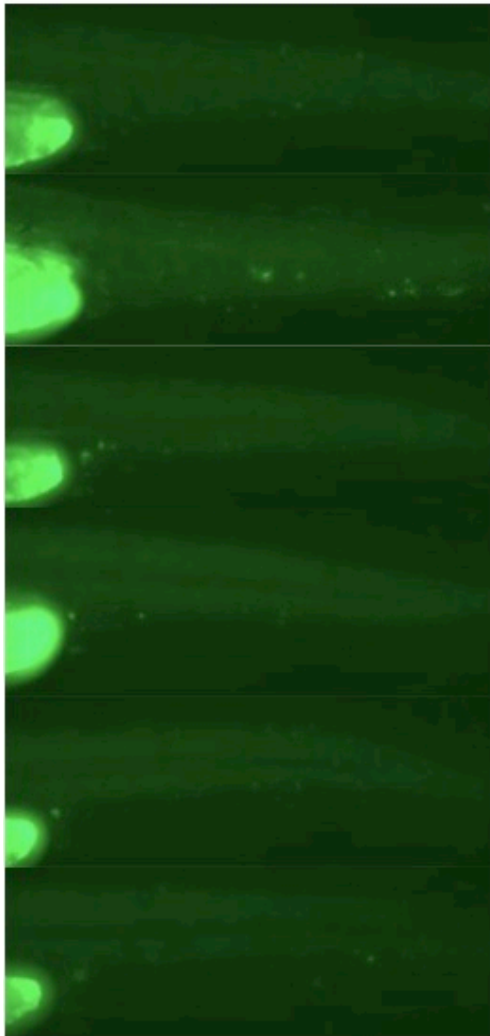


Figure 4.4. Survival curves of tricaine treated zebrafish embryos

LWT zebrafish embryos were A) treated with tricaine at the indicated concentration from 30hpf to 48hpf for a toxicity test, B) treated with tricaine and infected at 30hpf with 2200 CFU of *S. aureus* SH1000.

ns = not significant ; *** p-value < 0.001

Siblings + GFP SH1000 at 2hpi



Frozen + GFP SH1000 at 2hpi

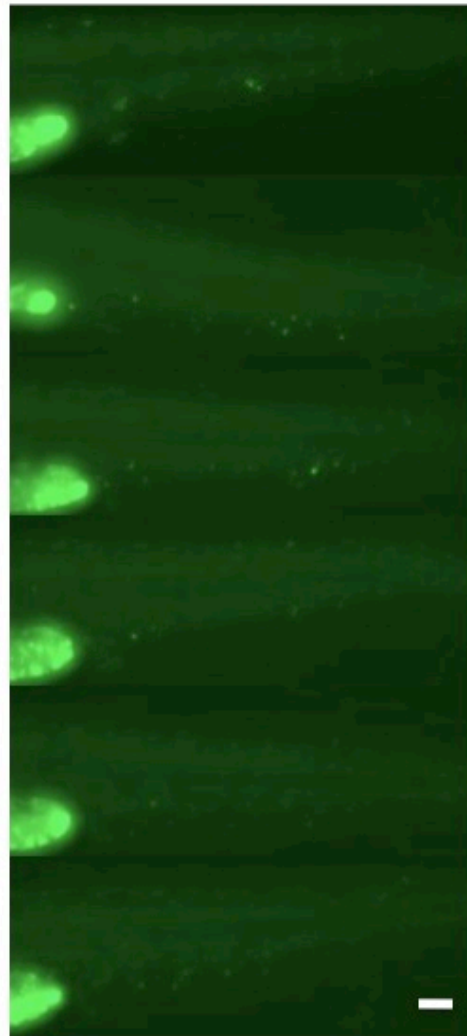


Figure 4.5.A. Tails of zebrafish larvae infected with GFP-SH1000 at 2 hpi

Incross of $fro^{to27c/+}$ zebrafish embryos divided in siblings (+/- and +/+) and *frozen* (double mutant -/-) were injected with GFP labelled wild-type *S. aureus* (GFP-SH1000⁺) into their blood circulation at 30 hpf, and the tail of these larvae were imaged at 2hpi.

Images were captured using 10x Nikon air objective NA 0.3, and consist of the extended focus of 10 slices covering 140 μ m depth.

Scale bar = 60 μ m

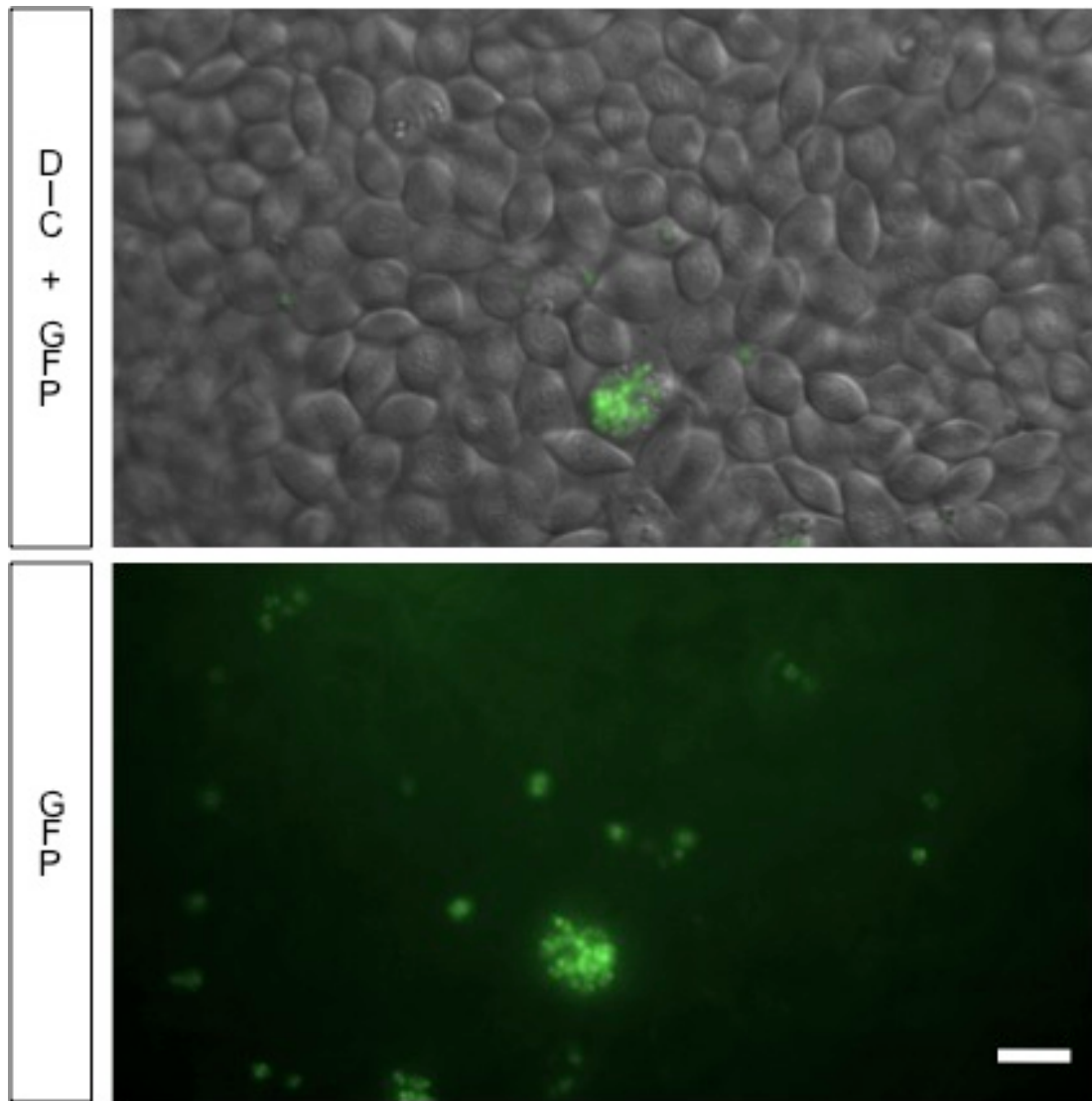


Figure 4.5.B. Phagocytosis of GFP-SH1000 in the *frozen* mutant at 2 hpi
 Incross of $fro^{to27c/+}$ zebrafish embryos selected for the *frozen* phenotype (double mutant $-/-$) were injected with GFP labelled wild-type *S. aureus* (GFP-SH1000*) into their blood circulation at 30 hpf, and the yolk sac circulation valley was imaged at 2hpi.

Images were captured using 60x Nikon oil objective NA 1.4, and consist of a single plane.

Scale bar = 11 μ m

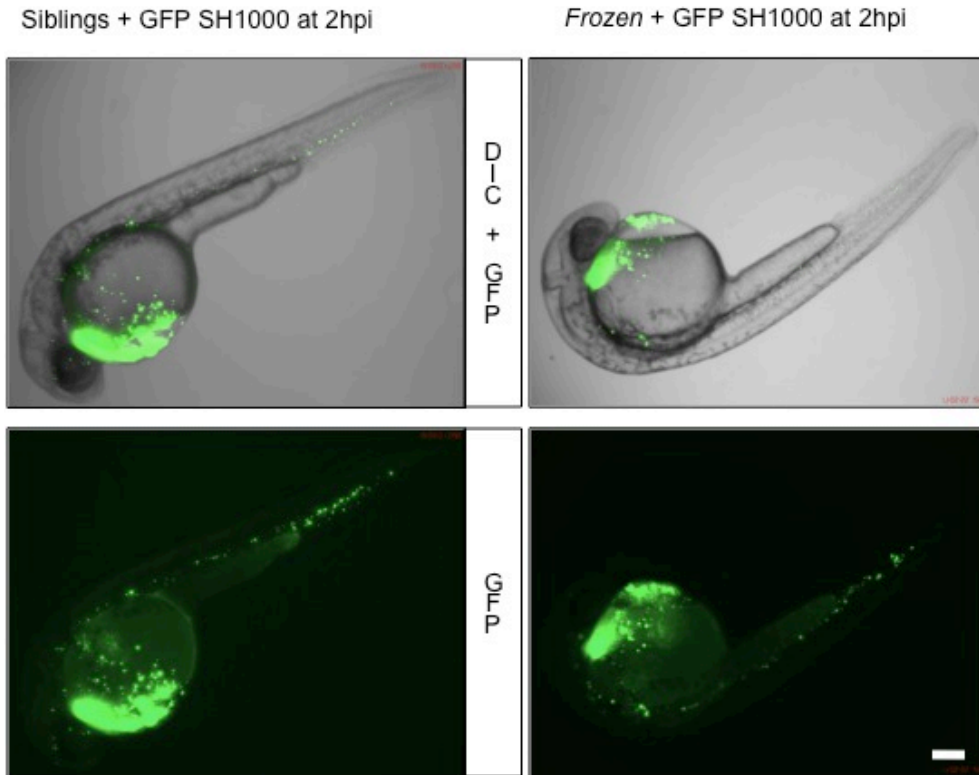


Figure 4.5.C. Whole body of zebrafish larvae infected with GFP-SH1000 at 2 hpi

Incross of $fro^{to27c/+}$ zebrafish embryos divided in siblings (+/- and +/+) and *frozen* (double mutant -/-) were injected with GFP labelled wild-type *S. aureus* (GFP-SH1000) into their blood circulation at 30 hpf, and the whole body of these larvae were imaged at 2hpi.

Images were captured using 4x Nikon air objective NA 0.13, and consist of the extended focus of 10 slices covering 400 μ m depth.

Scale bar = 160 μ m

4.2.3. Mimicking the slow circulation of the *frozen* fish with tricaine

Under a microscope, it was observed that the *frozen* zebrafish embryos have a very slow circulation at 30 hpf compared to the siblings. It is known that the *frozen* mutant has muscle assembly problems, which could also affect the cardiac muscle. A very small flow of liquid can circulate around the body of the *frozen* embryos, but most of the red blood cells are localised near the place where they are produced. However, the *frozen* larvae have a normal circulation including circulating erythrocytes after 48 hpf. To test if the defective circulation of the *frozen* strain at 1 dpf causes the increase in survival of the infected *frozen* compared to the siblings, a slower circulation in wild-type zebrafish embryos was mimicked using a high dose of tricaine, followed by infection with *S. aureus* SH1000 at 30 hpf. The effects on the zebrafish circulation of different concentrations of tricaine ranging from 0.33 mg/mL to 0.66 mg/mL from 30 hpf to 48 hpf on LWT embryos were observed. Every concentration of tricaine stopped the circulation of immersed embryos at 30 hpf. The tricaine was removed at 48 hpf, and the larvae were washed in normal E3 medium. At a concentration of 0.33 mg/mL of tricaine, the circulation was fully restored 30 min after removing the tricaine. With 0.5 mg/mL of tricaine, the circulation was partially restored in less than half of the embryos 6 h after the removal of tricaine. With 0.66 mg/mL of tricaine, the circulation could not be restored and some other phenotypic defects in the treated fish were observed, such as cardiac oedema, a darker brown yolk and a curved tail (Table 4.1. and Figure 4.3.). Most of the zebrafish embryos immersed in tricaine at concentrations of 0.33 mg/mL or 0.5 mg/mL from 30 hpf to 48 hpf stayed alive until the end of the experiment (120 hpf). However, zebrafish embryos treated from 30 hpf to 48 hpf with 0.66 mg/mL of tricaine started to die at 48 hpf and only 66% were still alive at 120 hpf (Figure 4.4.A.).

To test if the slower blood flow of the *frozen* mutant causes the resistance to *S. aureus* infection, wild-type zebrafish embryos were infected at 30 hpf and treated with tricaine from 30 hpf until 48 hpf. The survival of zebrafish embryos infected with 2200 CFU of *S. aureus* and treated with 0.33 mg/mL or 0.5 mg/mL of tricaine from 30 hpf until 48 hpf was not significantly different

to the survival of non-treated and infected zebrafish embryos (Figure 4.4.B.). However, infected zebrafish embryos treated with 0.66 mg/mL of tricaine died more quickly than the other groups, probably because of the toxic effect of that high dose of tricaine (Figure 4.4.A.). These data suggest that a slower host circulation from the time of infection (30 hpf) to 48 hpf does not affect the pathogenesis of *S. aureus* infection in zebrafish embryos.

4.2.4. Distribution of *S. aureus* in the *frozen* fish compared to the siblings

Because of the slow circulation of *frozen* zebrafish embryos at 30 hpf compared to their siblings, injected *S. aureus* bacteria into the blood circulation could be distributed at different rates in the siblings and the *frozen* fish. To test this hypothesis, GFP-*S. aureus* were injected into both zebrafish groups and the tail of the embryos imaged at 2 hpi. Green dots corresponding to the green bacteria were observed all along the tail of the siblings and the *frozen* (Figure 4.5.A.). This suggests that bacteria can distribute normally in the *frozen* larvae despite the abnormal erythrocyte circulation in the *frozen* larvae at the time of infection (30hpf). A second similar experiment was performed with a brighter GFP-SH1000 strain, confirming that bacteria distribute normally in the zebrafish body of the *frozen* mutant after the infection (Figure 4.5.C.). Phagocytosis of most of the bacteria in the *frozen* strain by 2 hpi was observed using high magnification microscopy (Figure 4.5.B.).

4.3. Modulation of autophagy using a pharmacochemical approach

It has been shown that *S. aureus* subvert autophagy for its own replication inside HeLa cells before inducing cell death (Schnaith, Kashkar et al. 2007). It is hypothesised that modulating autophagy can influence the virulence of *S. aureus*. A pharmacochemical approach was used to test the effects of enhanced or inhibited autophagy on the survival of zebrafish embryos infected with *S. aureus*. Several drugs are known to modulate autophagy,

and zebrafish embryos are sensitive to drugs dissolved in their medium. After testing their toxicity on live zebrafish embryos from 30 hpf until 120 hpf, the non-toxic compounds were tested on infected zebrafish embryos.

4.3.1. Chemical enhancers of autophagy

The autophagy inducers rapamycin at 30 μ M, rilmenidine at 50 μ M and carbamazepine at 50 μ M added to the E3 water of 30 hpf zebrafish are not toxic for the normal development of the larvae up to day 5 (Figure 4.6.A.). This suggests that experiments using these compounds can be performed on zebrafish without affecting their health. For these experiments, *S. aureus* infected zebrafish embryos at 30 hpf were treated with the indicated autophagy enhancer up to 5 dpf, recording the mortality daily.

Rapamycin is a well-known autophagy inducer acting via inhibition of the target of rapamycin (TOR) (Blommaart, Luiken et al. 1995; Noda and Ohsumi 1998). TOR is constituted of two distinct multiprotein complexes: TOR complex 1 (TORC1), which is sensitive to rapamycin, and TORC2, which is insensitive to rapamycin (Loewith, Jacinto et al. 2002). TOR can sense nutrient, growth factors and cellular stress signals, leading to the appropriate metabolic responses. TOR is an evolutionary-conserved protein kinase, which negatively regulates autophagy. So by inhibiting TOR with rapamycin, autophagy is induced. Rapamycin has been extensively used in experiments with mammalian cells to induce autophagy by mimicking starvation conditions. Rapamycin also induces autophagy in zebrafish larvae, which can be measured by the accumulation of LC3-II in response to rapamycin and lysosomal inhibitor treatment (He, Bartholomew et al. 2009). Rapamycin acts via the zTOR pathway in zebrafish (Makky, Tekiela et al. 2007).

To test the effect of the autophagy inducer rapamycin on infected zebrafish larvae, 30 hpf zebrafish were injected with 2 different doses of *S. aureus* SH1000 and the larvae treated with either 30 μ M of rapamycin or DMSO as control. The survival of the infected larvae treated with rapamycin is lower compared to the control group, whether the fish were initially injected with a

low (1000 CFU) or medium (2000 CFU) staphylococcal dose (Figure 4.7.A. and B.).

Three other autophagy enhancers were tested to treat infected zebrafish larvae. Unlike rapamycin, these compounds induce autophagy via a mTOR-independent pathway. Indeed, they appear to influence somewhere the cycle in which cAMP regulates myo-inositol-1,4,5-triphosphate (IP3) levels, influencing calpain activity, which cleaves and activates $G_s\alpha$, feeding back to regulate cAMP levels (Figure 4.1.C.). Autophagy is regulated positively or negatively at several points of this cycle (Williams, Sarkar et al. 2008).

The first compound, rilmenidine, is an imidazoline-1 receptor (I1R) agonist that induces autophagy by decreasing the cAMP levels, which interacts with the Epac-Rap2b-PLC ϵ -IP3 pathway (Williams, Sarkar et al. 2008). Rilmenidine also interacts with an $\alpha 2$ -adrenergic receptor, but with about 30-fold less affinity than I1R. The second compound, carbamazepine, similarly to lithium, decreases inositol levels (Williams, Cheng et al. 2002), which leads to a decrease of IP3 levels, which induce autophagy. This was initially shown with the induction of autophagy by lithium, which inhibits inositol monophosphatase (IMPase) and therefore decreases the levels of IP3. Autophagy is induced by lithium whether or not mTOR is activated, independently of the mTOR pathway. Carbamazepine behaves in the same way as lithium to induce autophagy (Sarkar, Floto et al. 2005). It was shown that carbamazepine has the ability to enhance the clearance of *M. marinum* in a zebrafish infection model (Schiebler, Brown et al. 2014). The third compound, verapamil, is a L-type calcium channel antagonist, and induces autophagy by abrogating calpain activation. Indeed, reduced levels of calcium decrease the activity of calpains (enzymes aiding in protein breakdown), which in turn induce autophagy in a mTOR-independent manner (Williams, Sarkar et al. 2008).

The survival curves of the *S. aureus* infected zebrafish group treated with the autophagy enhancers mTOR-independent rilmenidine (Figure 4.8.A. and B.),

carbamazepine (Figure 4.9.A.) or verapamil (Figure 4.9.B.) were not significantly different than the infected control group. These 3 compounds were tested at the recommended concentrations from preliminary or collaborators work.

4.3.2. Chemical inhibitors of autophagy

As with autophagy enhancing drugs, toxicity tests were performed on 30 hpf zebrafish larvae with several autophagy inhibitors. The following compounds were not toxic at the recommended concentration: \pm Bay K8644 at 1 μ M, LY294002 at 10 μ M, wortmannin at 100 nM and vitamin E acetate at 1 mM. However, N-acetyl cysteine (NAC) showed a serious lethal effect at concentrations from 30 μ M to 300 μ M, and only a low concentration of 10 μ M did not affect the larvae. Treatment with ammonium chloride (NH_4Cl) at 10 mM seemed possible if the incubation did not exceed 48 h, as it started to affect the fish after 48 hours post treatment (hpt) and was lethal for all of them by 72 hpt. Nocodazole at 10 μ M was very damaging for the larvae if incubated longer than a few hours, but a treatment of only 30 min kept the fish alive (Figure 4.6.B.).

Phosphatidylinositol-3-kinases (PI3Ks) are composed of 3 main classes: I, II and III, which have different functions. Three PI3Ks inhibitors are known to modulate autophagy: LY294002, wortmannin and 3-methyladenine. LY294002 (2-(4-morpholinyl)-8-phenylchromone) is a morpholine derived from quercetin, and a potent but reversible class I PI3K inhibitor (Vlahos, Matter et al. 1994). However, LY294002 also inhibits the catalytic domain of mTOR at similar concentrations used to inhibit PI3K (Brunn, Williams et al. 1996). The steroid fungal metabolite wortmannin is a potent and selective PI3Ks inhibitor. Wortmannin interacts with the ATP binding site of the PI3K enzyme, leading to an electrophilic attack on the lysine residue required for the phosphotransferase reaction. This modifies the enzyme irreversibly (Wymann, Bulgarelli-Leva et al. 1996). At low concentrations (1-10 nM), wortmannin inhibits class III PI3K and class I PI3K (Fruman, Meyers et al. 1998). Wortmannin inhibits the autokinase activity of mTOR with the same mechanism as for PI3K, but the mTOR inhibition is about 100 fold less

sensitive, the IC_{50} being about 200 nM (Brunn, Williams et al. 1996). Similarly, high concentrations of wortmannin can also affect other PI3Ks (class II) as well as other PI3K-related enzymes such as DNA-PK, some phosphatidylinositol 4-kinases, myosin light chain kinase and mitogen-activated protein kinase (Fruman, Meyers et al. 1998). It has also been reported that by inhibiting PI3K activity, wortmannin suppresses autophagic sequestration and degradation in rat hepatocytes. Similarly, the 2 other PI3K inhibitors LY294002 and 3-methyladenine also inhibit autophagy (Blommaert, Krause et al. 1997). While class I PI3K products seem to inhibit autophagy, class III PI3K triggers autophagy (Petiot, Ogier-Denis et al. 2000). Indeed, class III PI3K plays a critical role in the early stages of autophagosome formation through formation of an essential complex with Beclin 1 (Tassa, Roux et al. 2003). In particular, class III PI3K Vps34 is important in the induction of autophagy. Vps34 is inhibited by wortmannin and 3-methyladenine, preventing the formation of new autophagosomes. However, these 2 compounds seem to also act via other pathways independently of Vps34 to suppress autophagy (Jaber, Dou et al. 2012).

Using these compounds, the survival curves of the infected zebrafish larvae treated with wortmannin (Figure 4.10.A) or LY294002 (Figure 4.10.B.) were significantly lower compared to the control group. Indeed, the mortality of the infected fish treated with wortmannin or LY294002 was higher than the non-treated fish. This suggests that autophagy and/or PI3K products are important for host defence against *S. aureus* infection *in vivo*.

The drug \pm Bay K8644 is a L-type Ca^{2+} channel agonist and an inhibitor of mTOR-independent autophagy. This drug has the same molecular target as verapamil, but the opposite effect (Williams, Sarkar et al. 2008). Indeed, \pm Bay K8644 promotes the entry of Ca^{2+} into the cells, activating calpains, which cleave and activate $G_s \alpha$ that activates adenylyl cyclase to increase cAMP levels. These high levels of cAMP have an inhibitory effect on autophagy. Infecting zebrafish embryos with a dose of 1000 CFU or 2000 CFU of *S. aureus* SH1000 and then treating them with 1 μ M of \pm Bay K8644 did not induce a significant effect on the survival of the larvae (Figure 4.11.).

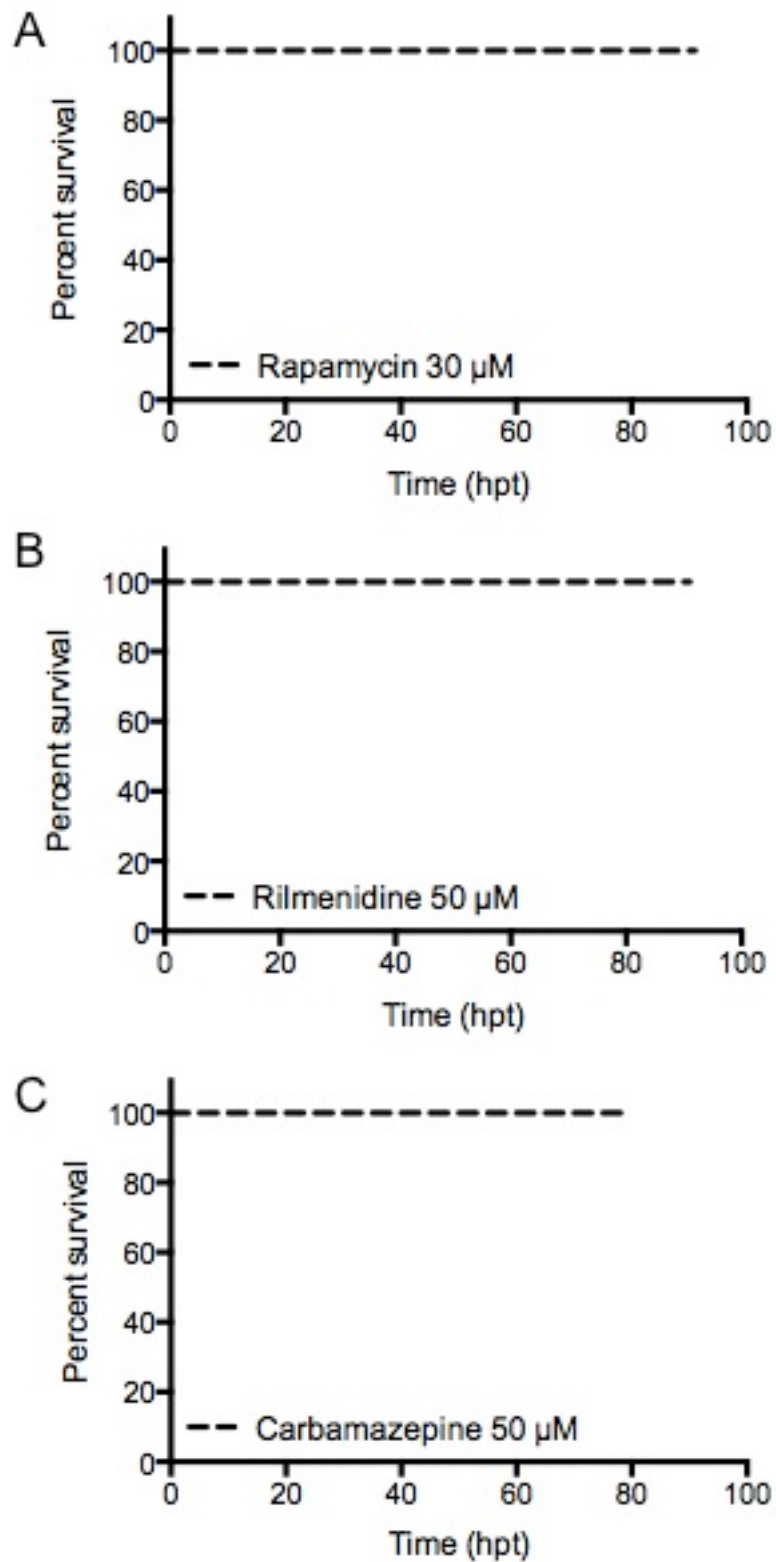


Figure 4.6. Toxicity test of autophagy enhancing and inhibiting drugs

LWT zebrafish embryos were incubated with the mentioned autophagy enhancer (A-C) or autophagy inhibitor (D-J) from 30hpf till 120 hpf, and the survival was recorded over time.

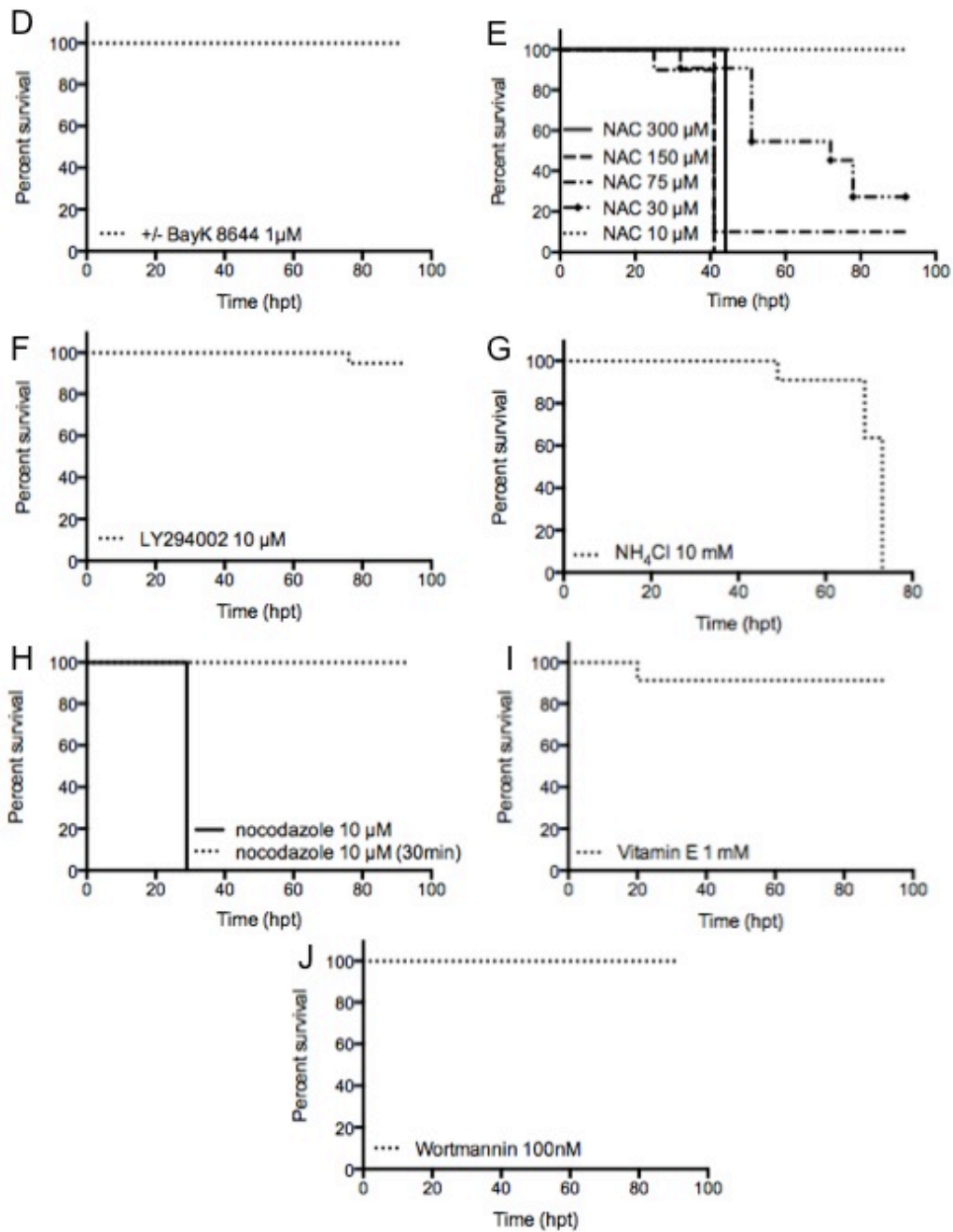


Figure 4.6. Toxicity test of autophagy enhancing and inhibiting drugs

LWT zebrafish embryos were incubated with the mentioned autophagy enhancer (A-C) or autophagy inhibitor (D-J) from 30hpf till 120 hpf, and the survival was recorded over time.

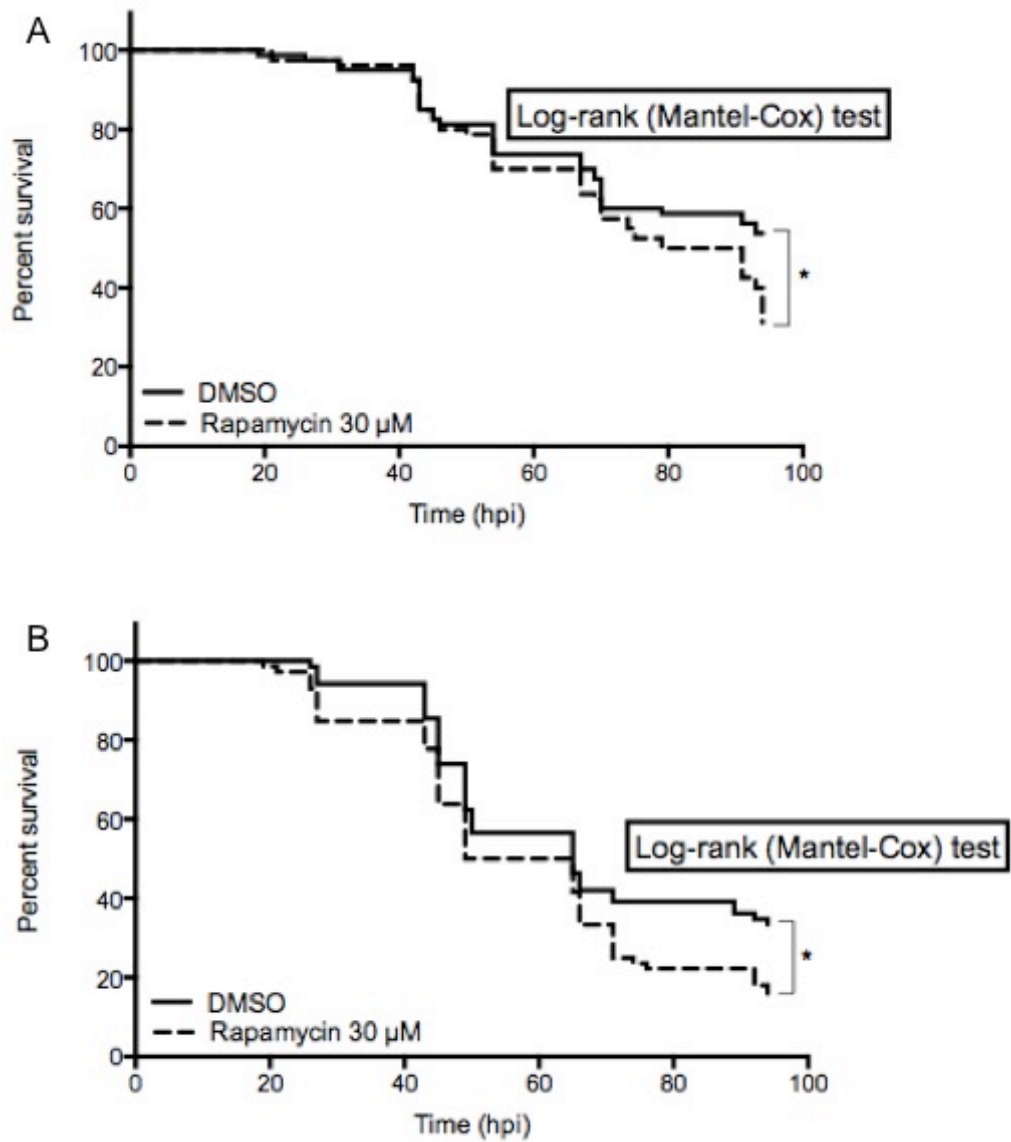


Figure 4.7. Effect of the autophagy enhancer rapamycin on zebrafish embryos infected with *S. aureus*

LWT zebrafish embryos were infected with A) 1000 CFU or B) 2600 CFU of *S. aureus* SH1000 and treated with 30 μ M of rapamycin at 30 hpf.

A) 4 or B) 3 independent experiments, $n > 70$ fish per group

* = P-value < 0.05

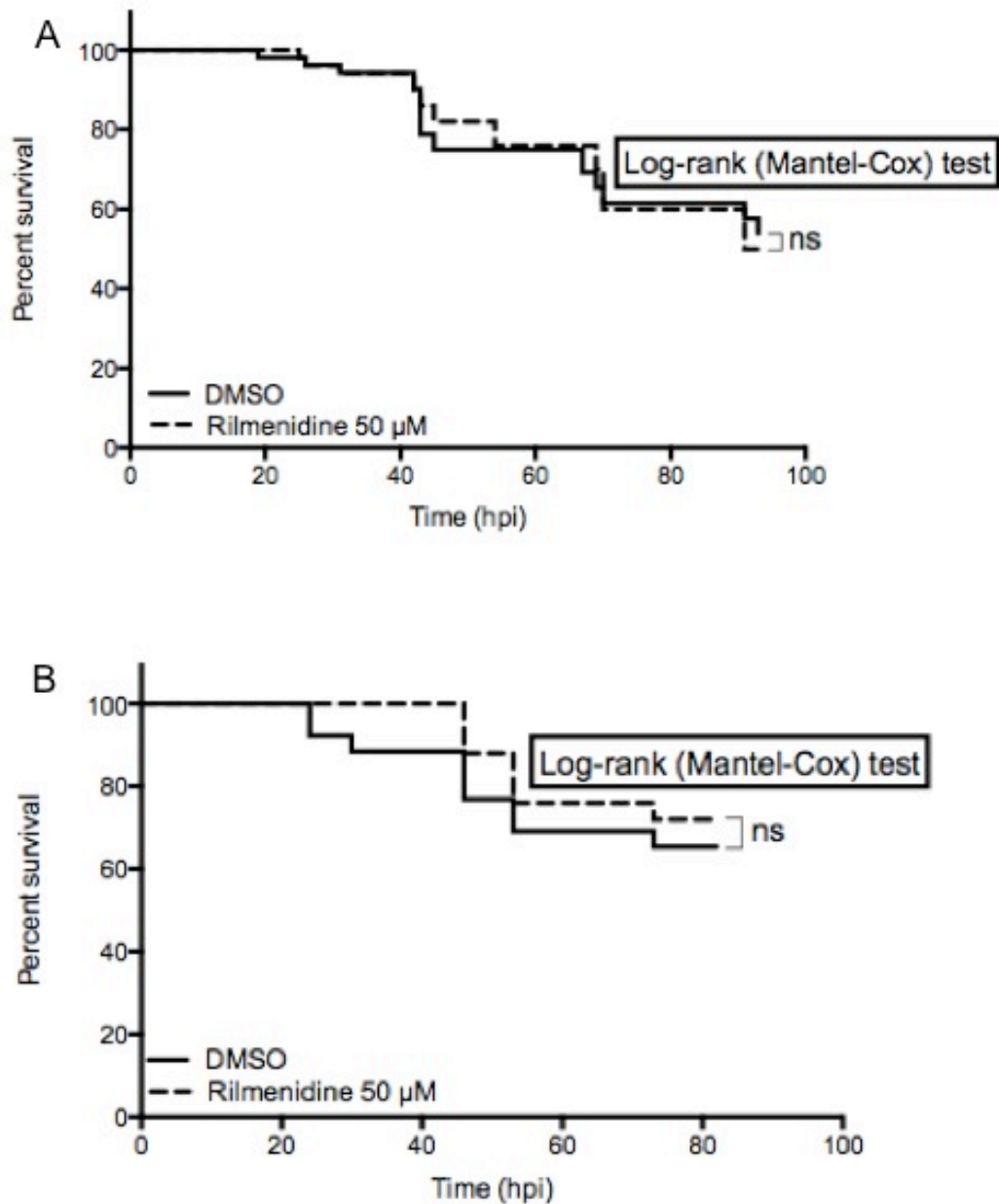


Figure 4.8. Effect of the autophagy enhancer rilmenidine on zebrafish embryos infected with *S. aureus*

LWT zebrafish embryos were infected with A) 1000 CFU or B) 2300 CFU of *S. aureus* SH1000 and treated with 50 µM of rilmenidine at 30 hpf.

A) 3 independent experiments, n=50 fish per group; B) 1 experiment, n=25 fish per group.

ns = not significant

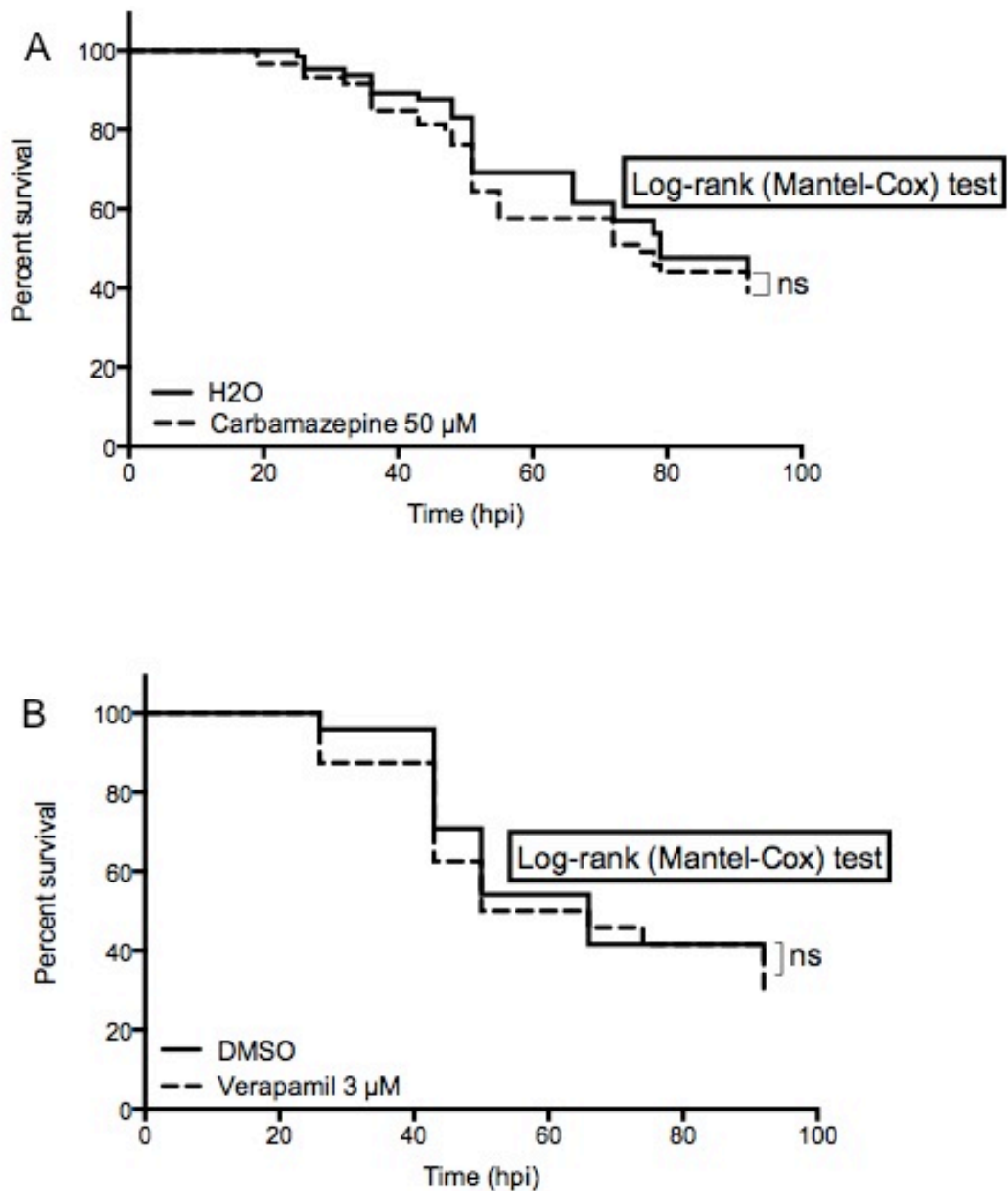


Figure 4.9. Effect of the autophagy enhancer carbamazepine or verapamil on zebrafish embryos infected with *S. aureus*

A) LWT zebrafish embryos were infected with 2000 CFU of *S. aureus* SH1000 and treated with 50 μM of carbamazepine at 30 hpf. 3 independent experiments, n=60 fish per group. ns = not significant

B) LWT zebrafish embryos were infected with 2800 CFU of *S. aureus* SH1000 and treated with 3 μM of verapamil at 30 hpf. 1 experiment, n=24 fish per group. ns = not significant

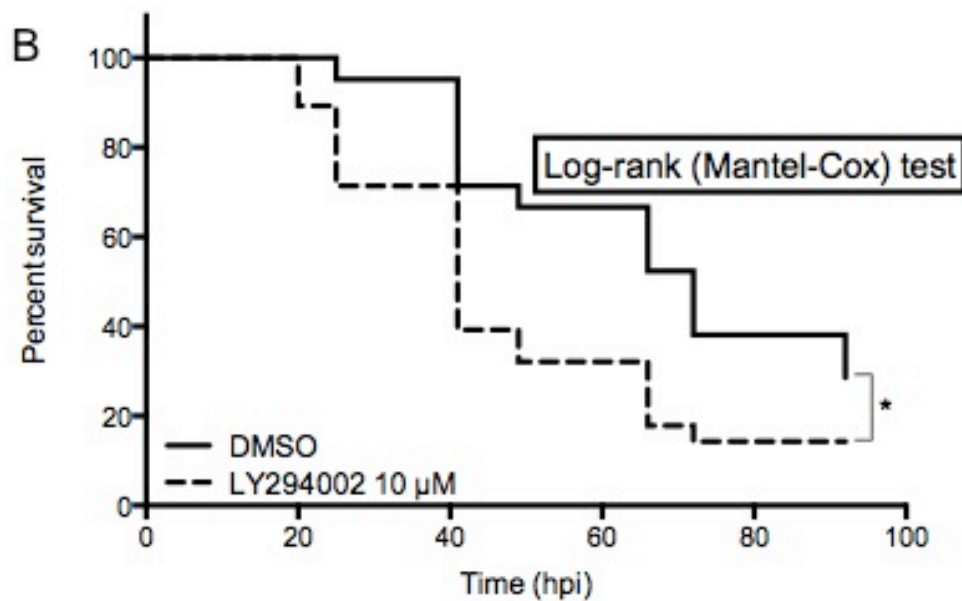
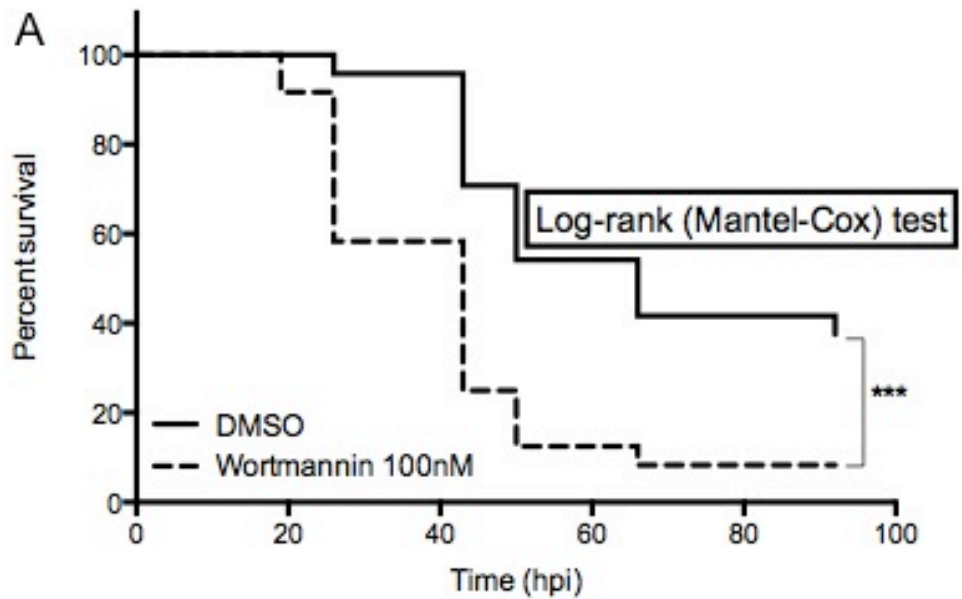


Figure 4.10. Effect of the PI3K inhibitors wortmannin or LY294001 on zebrafish embryos infected with *S. aureus*

A) LWT zebrafish embryos were infected with 2800 CFU of *S. aureus* SH1000 and treated with 100 nM of wortmannin at 30 hpf. n=24 fish per group. *** = P-value < 0.001

B) LWT zebrafish embryos were infected with 2100 CFU of *S. aureus* SH1000 and treated with 10 μM of LY294002 at 30 hpf. n=24 fish per group. * = P-value < 0.05

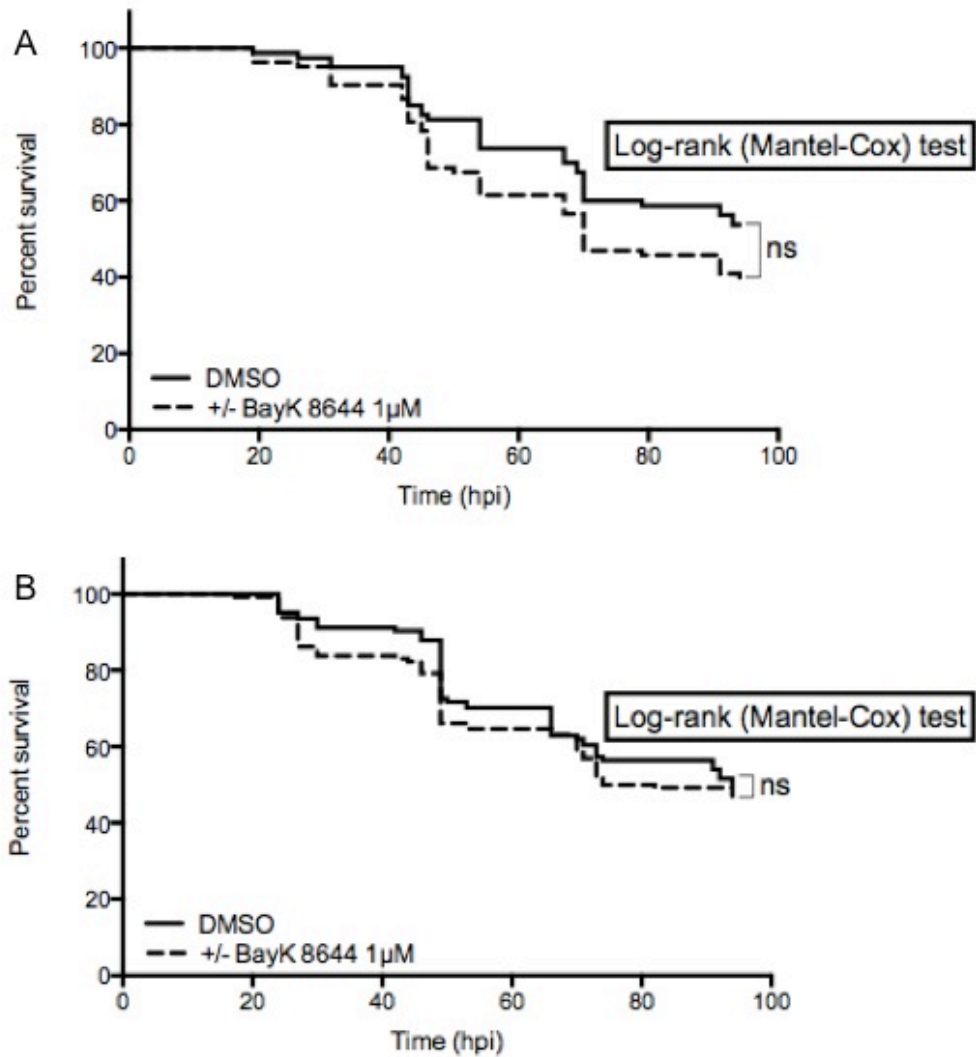


Figure 4.11. Effect of the autophagy inhibitor +/- Bay K8644 on *S. aureus* infected zebrafish embryos

LWT zebrafish embryos were infected with A) 1000 CFU or B) 2000 CFU of *S. aureus* SH1000 and treated with 1 µM of +/- BayK 8644 at 30 hpf. A) 4 independent experiments, n=80 fish per group; B) 5 independent experiments, n=130 fish per group.

ns = not significant

The two other mTOR-independent autophagy inhibitors tested were N-acetyl-L-cysteine (NAC) and vitamin E acetate. NAC is a general antioxidant and catalase, which specifically decomposes H_2O_2 , while vitamin E acetate (or DL-alpha-tocopherol) is a non-thiol antioxidant. Both NAC and vitamin E can inhibit basal and inducible autophagy by preventing autophagosome synthesis. Vitamin E enhances mTOR, which normally inhibits autophagy. However, NAC surprisingly inhibits mTOR, but also decreases the phosphorylation of c-Jun N-terminal protein kinase 1 and Bcl-2 (Underwood, Imarisio et al. 2010), which inhibit autophagy by causing the dissociation of Bcl-2 from Beclin1 (Wei, Pattingre et al. 2008). In the *S. aureus* infection experiment using zebrafish embryos, treatment with NAC (Figure 4.12.A.) or vitamin E acetate (Figure 4.12.B.) did not change the survival of the larvae infected with a dose of 2000 CFU of *S. aureus* SH1000 compared to the untreated group.

Ammonium chloride (NH_4Cl) and nocodazole inhibit the last step of autophagy by blocking the autophagosome/lysosome fusion. Ammonium chloride prevents phagosome-lysosome fusion, favouring the induction of phagosome-endosome fusion, as shown by a study using cultured macrophages infected by *Mycobacterium microti* or *Saccharomyces cerevisiae* (Hart and Young 1991). Consistent with these findings, treatment of zebrafish embryos with NH_4Cl induces a significant increase in LC3-II levels due to an accumulation of autophagosomes that cannot fuse with lysosomes (Underwood, Imarisio et al. 2010). Nocodazole is an inhibitor of microtubule polymerisation, and therefore prevents the fusion of autophagosome to lysosome (Kochl, Hu et al. 2006).

Wild-type zebrafish (30 hpf) were infected with 3 different doses of *S. aureus* SH1000 and then treated with 10 mM of NH_4Cl . Only the larvae treated and infected with the intermediate bacterial dose of 2250 CFU showed a significant lower survival compared to the control (Figure 4.13.B.). The survival curves of treated and infected fish with the lower dose (1650 CFU) and higher dose (3700 CFU) were similar to the control (Figure 4.13.A. and

C.). These experiments were performed only once for each dose, and would need to be repeated to confirm if there is a dose-dependent effect of NH₄Cl on *S. aureus* infected zebrafish larvae, or if it is due to an experimental artefact. The treatment with 10 μM of nocodazole during 30 min on 30 hpf zebrafish larvae infected with 1000 CFU of *S. aureus* SH1000 induced a highly significant lower survival curve compared to the control group (Figure 4.14.). This suggests that the microtubule system is important for the host to fight the infection, whether it is autophagy related or not.

4.4. Modulation of autophagy by interfering at the transcription level

Morpholino oligonucleotides (MO) are synthetic molecules commonly used as anti-sense “knockdown” tools to study the function of certain proteins. MOs are short chains of 25 morpholinos subunits, each one is composed of a nucleic acid base, a morpholine ring and a non-ionic phosphorodiamidate intersubunit linkage (Figure 4.17.A.). MOs bind to the target RNA sequence by standard nucleic acid base-pairing and operate via a steric blocking mechanism RNase H-independent. Therefore, MOs prevent the translation of RNA into protein (Summerton and Weller 1997; Summerton 1999) or modify the normal splicing of the pre-mRNA *in vivo* (Draper, Morcos et al. 2001) (Figure 4.17.B.). MOs have shown efficacy in animals, plants, bacteria, protists and cell cultures. In zebrafish, MOs are traditionally injected into the yolk of 1-to-8-cell-staged embryos. The hydrophilic MOs diffuse rapidly into the cells, resulting in ubiquitous delivery. Effects of MOs decrease over time, as they become more diluted into the cells after each division. MOs are effective and specific translational inhibitors in zebrafish (Nasevicius and Ekker 2000).

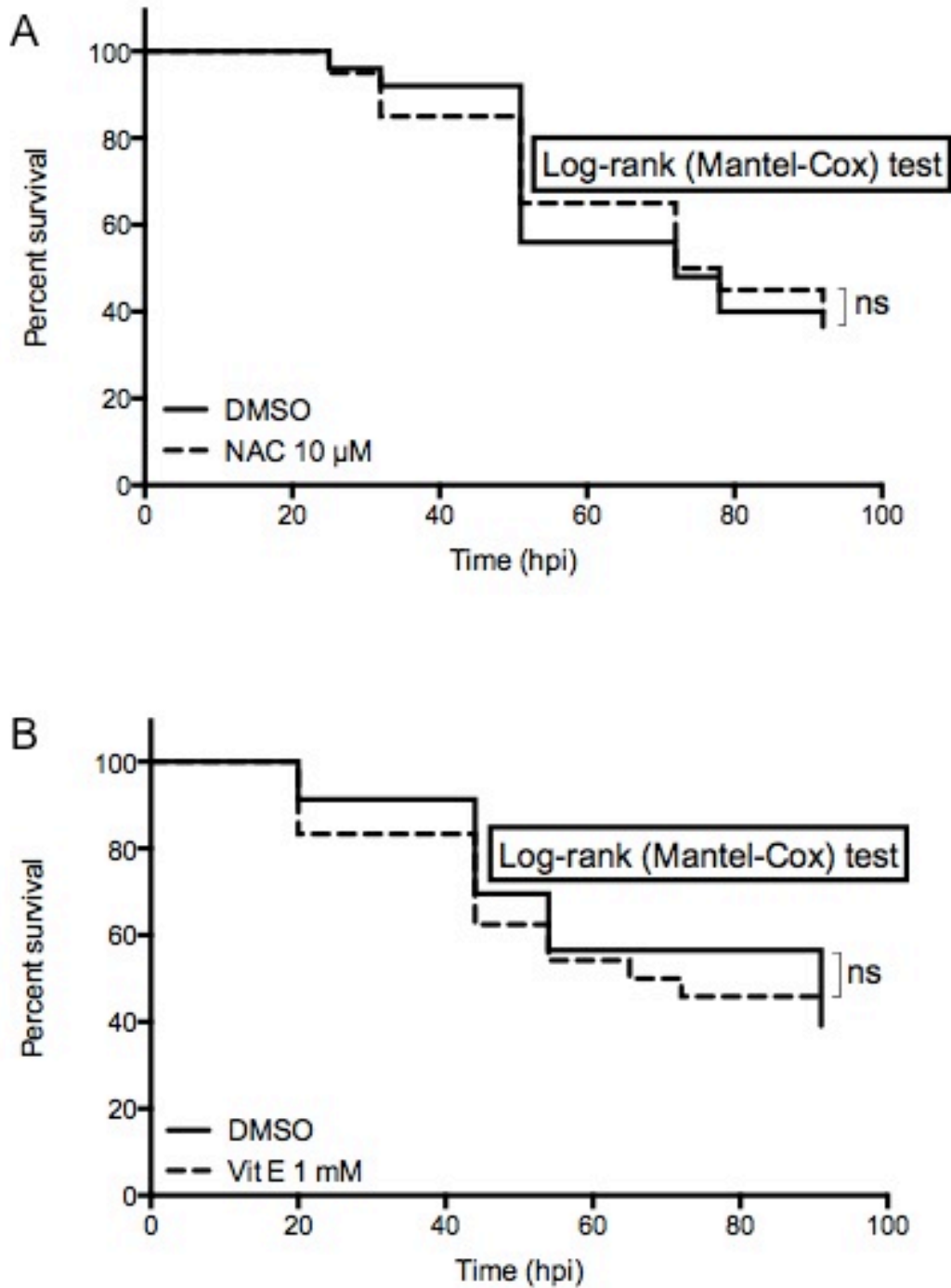


Figure 4.12. Effect of the autophagy inhibitor NAC or vitamin E acetate on *S. aureus* infected zebrafish embryos

A) LWT zebrafish embryos were infected with 2000 CFU of *S. aureus* SH1000 and treated with 10 μM of N-acetyl cysteine (NAC) at 30 hpf. n=20 fish per group.

B) LWT zebrafish embryos were infected with 2100 CFU of *S. aureus* SH1000 and treated with 1 mM of vitamin E acetate at 30 hpf. n=24 fish per group.

ns = not significant

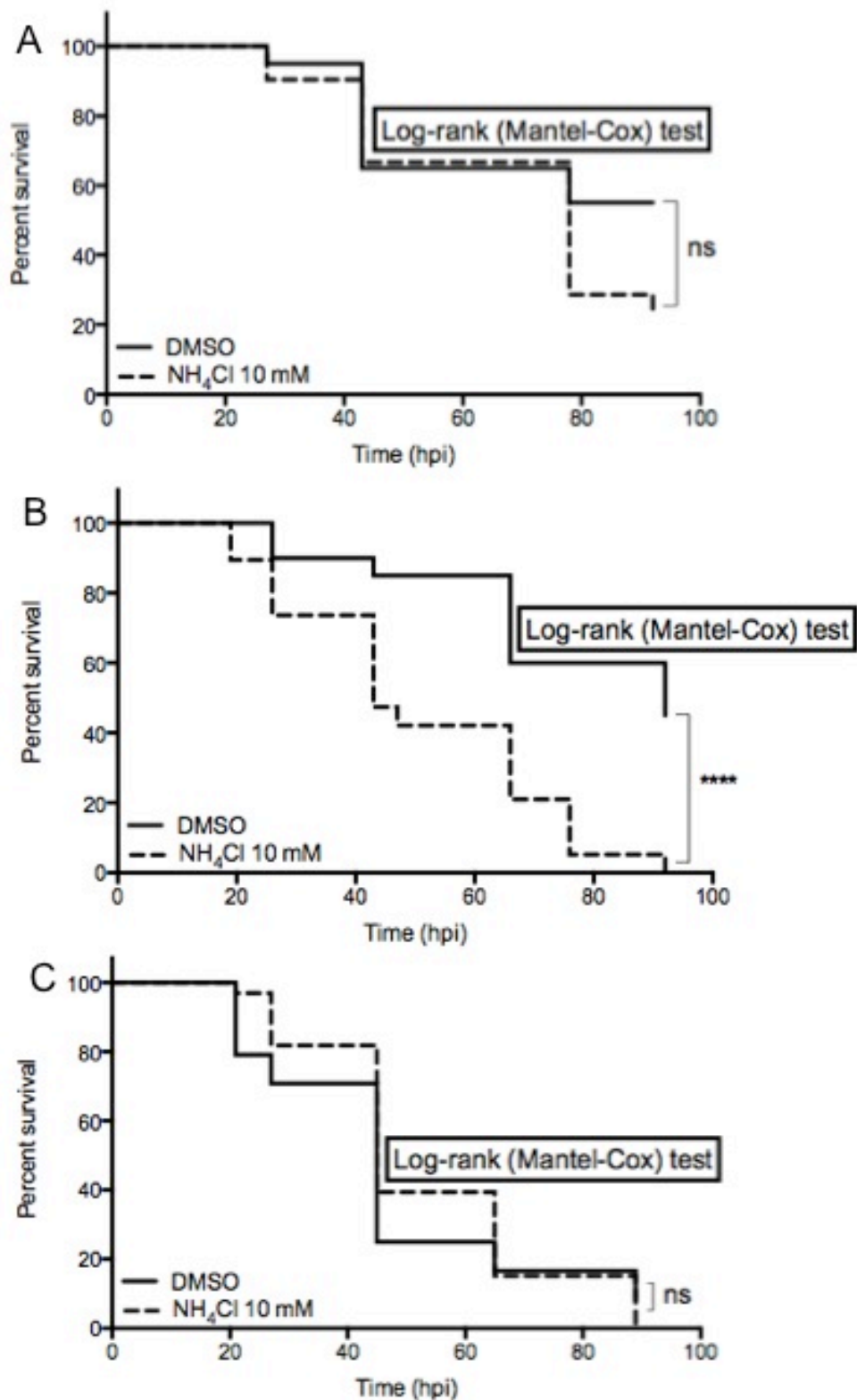


Figure 4.13. Effect of the autophagy inhibitor NH₄Cl on *S. aureus* infected zebrafish embryos

LWT zebrafish embryos were infected with A) 1650 CFU, B) 2250 CFU or C) 3700 CFU of *S. aureus* SH1000 and treated with 10 mM of NH₄Cl at 30 hpf. n > 20 fish per group. ns = not significant, **** = P-value < 0.0001

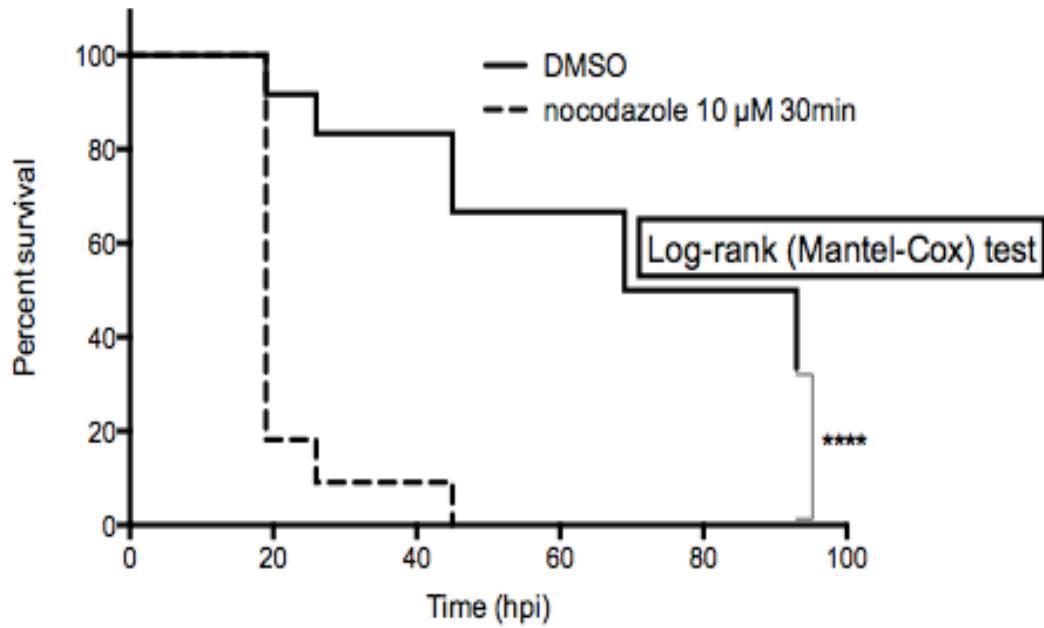


Figure 4.14. Effect of the microtubule inhibitor nocodazole on *S. aureus* infected zebrafish embryos

LWT zebrafish embryos were infected with 1000 CFU of *S. aureus* SH1000 and treated with 10 μM of nocodazole at 30 hpf for 30 min. n=11 fish per group, **** = P-value < 0.0001

The formation of an autophagosome is based on the participation of several autophagy related proteins (atg) (Figure 4.1.B.), so knocking down one of the important host atg proteins should block the formation of autophagosomes. Zebrafish Atg proteins are orthologous to human Atg proteins, as they share about 73% identity and about 80% similarity. More specifically, the Atg5 protein shares 81% identity (Appendix 1.A.), the Atg7 protein shares 74% identity (Appendix 1.B.), the Atg10 protein shares 50% identity (Appendix 1.C.) and the Atg16L1 protein shares 64% identity (Appendix 1.D.). For each of these human genes, there is only one corresponding zebrafish gene. A little note should be mentioned about the fact that the *atg16* yeast gene has 2 orthologous genes in both zebrafish and human, called *atg16L1* and *atg16L2*. However, little is known about the function of Atg16L2 protein. Even though Atg16L2 can form an Atg5-12-16L2 complex, it is not essential and cannot compensate for Atg16L1 in the formation of the autophagosome in case of Atg16L1 knockout/knockdown (Ishibashi, Fujita et al. 2011).

The zebrafish larvae infection model was used to test whether knocking down host autophagy would influence *S. aureus* infection. For this purpose, start or splice MO were injected into zebrafish eggs to block the normal transcript of the targeted atg protein. These morphants were then infected with *S. aureus* SH1000 at 30 hpf, and the survival was recorded over time.

The formation of the Atg12-Atg5-Atg16L1L complex is essential for the elongation of the isolation membrane to form the autophagosome (Mizushima, Yamamoto et al. 2001; Mizushima, Kuma et al. 2003). To determine whether the elongation of autophagosome plays a role in *S. aureus* infection management, MOs targeting *atg5* and *atg16l1* were used. The two other essential atg proteins that are catalysing the formation of this Atg12-Atg5-Atg16L1L complex are Atg7 and Atg10. To test the importance of Atg7 and Atg10 proteins in *S. aureus* infection, experiments using MOs targeting *atg7* and *atg10* were also performed.

Experiments with 3 different MOs for Atg5 were carried out, acting either by blocking the start codon (*atg5-1*), blocking the 5'UTR (*atg5-2*) or modifying the normal splicing of exon 2 (*atg5 splice*). The survival curves of zebrafish larvae morphants injected with 0.8 ng of *atg5-1* MO or 5.3 ng of *atg5-2* MO and then infected with 2350 CFU of *S. aureus* SH1000 were similar to the control group of embryos injected with the corresponding *atg5* mismatch MO and infected with the same bacterial dose (Figure 4.15.A. and 4.15.B.). Similarly, the survival curve of the infected zebrafish larvae injected with 6 ng of *atg5 splice* MO was not significantly different than the infected zebrafish larvae injected with the control MO, with a bacterial dose of 2000 CFU (Figure 4.16.D.).

One advantage of using splice MO is that their activity can be tested by RT-PCR. Depending on the target of the splice MO, it will either include an intron during the splicing step of the pre-mRNA, or exclude a full exon, which is the more common mechanism (Figure 4.18.A.). In both cases, it leads to the formation of a non-functional transcript, therefore preventing the formation of a functional protein. The *atg5 splice* MO is designed to overlap on exon 3 and intron 3-4. Therefore exon 3 is cut out during the splicing step of the pre-mRNA. The efficacy of the *atg5 splice* MO can be tested by RT-PCR, using primers binding on exon 2 (forward) and exon 4 (reverse). The normal product size amplified by these primers using a cDNA template is 257 bp, while the shorter product size that has excluded exon 3 is 129 bp long. In practice, the RNA of 2 dpf morphants injected with 2 ng or 8 ng of *atg5 splice* MO was extracted, then the corresponding cDNA was synthesised. This cDNA was used as a template to amplify the sequence comprised between the 2 primers described earlier, flanking the region of the MO. After running the samples on an agarose gel, the bands revealed the sizes of the DNA fragments amplified by PCR. In the uninjected control group, the wild-type band was visible at 257 bp. The 2 ng injected morphants had both the wild-type band and the splice band, while the 8 ng injected morphants displayed only the splice band (Figure 4.18.C.). This suggests that a medium dose of MO (2 ng) only partially inhibits Atg5 transcription, while a higher dose of MO (8 ng) inhibits completely *atg5* transcription in 2 dpf zebrafish larvae.

Experiments knocking down *atg7* were performed with a splice MO. The survival curve of the zebrafish morphants injected with 6 ng of *atg7* splice MO and then infected with 2000 CFU of *S. aureus* SH1000 was similar to the survival curve of the infected zebrafish larvae injected with the control MO (Figure 4.16.C.). The *atg7* splice MO used in this experiment binds to the overlap of intron 2-3 and exon 3, suggesting that exon 3 is cut out during the splicing step of the pre-mRNA. PCR primers have been designed to bind on exon 1 (forward) and exon 4-5 (reverse), amplifying a product of 306 bp in wild-type conditions, and a product of 189 bp when the exon 3 is spliced out due to the MO. On the gel of the RT-PCR, only the wild-type band was amplified in the uninjected control group. However, in 2 dpf morphants, there was an increase in the intensity of the splice band visible on the gel when the dose of MO increases. In the sample injected with 8 ng of MO, the splice band was stronger than the wild-type band, while it was the opposite in the sample injected with 2 ng or 4 ng of MO (Figure 4.18.B.). This suggests a partial knockdown of *atg7* in all samples, with a greater knockdown efficacy for the high dose of MO.

Two different MOs were tested to knockdown *atg16l1*, targeting either the start codon (*atg16l1-1*) or the 5'UTR region (*atg16l1-2*). Two different control groups were performed: either normal uninjected LWT or the corresponding mismatch MO (mM control) injected fish. When infecting these *atg16l1* morphants or corresponding controls with a staphylococcal dose of 2350 CFU, some differences were observed. Strikingly, the 2 types of control had different survival curves when infected with *S. aureus*: the uninjected LWT control had a lower survival rate than the mismatch MO fish. This was intriguing as the mismatch MO is a control that should not affect the fish, but in this case it seemed to affect it positively, as being more resistant to the infection. Compared to the mismatch MO control, the infected morphants had a significant lower survival curve in both the start codon (Figure 4.15.C.) and the 5'UTR targeted knockdown group (Figure 4.15.D.). However, the survival curves of the infected *atg16l1* morphants (knockdown with the start codon

MO or 5'UTR MO) were similar to the uninjected LWT control (Figure 4.15.C. and D.).

As shown previously (see section 4.2.), the *frozen* mutant has a lack of motility phenotype, and the mutation is mapped to the genomic locus of *atg10*. Therefore, experiments using 2 different MO targeting this gene were performed: an *atg10* start MO and an *atg10* splice MO. Phenotypically, the morphants generated using either 1 ng of *atg10* start MO or 1 ng of *atg10* splice MO did not present any phenotype corresponding to the *frozen* mutant, as all larvae were moving normally in the water. One infection experiment with 3300 CFU of *S. aureus* SH1000 was performed with these morphants, but no difference in the survival curves was observed between the infected morphants and the infected standard control MO injected larvae (Figure 4.16.A. and B.).

The *atg10* splice MO is localised on intron 4-5 and exon 5, suggesting that exon 5 is spliced out. Using primers binding on exon 4 (forward) and exon 6 (reverse) and cDNA as template, the wild-type product size amplified is 260 bp long, while the exon 5 spliced out product size would be 162 bp long. However, the RT-PCR using samples injected with *atg10* splice MO was unsuccessful, as a very faint wild-type band was visible in all samples, but no splice band. This PCR was not optimised, as no *frozen* phenotype was visible, suggesting that this *atg10* MO does not induce the same effect as the *frozen* mutant. Therefore this suggests that injecting 1 ng of *atg10* start or splice MO in zebrafish does not mimic the *frozen* phenotype. Without a clear phenotype to compare to, the efficacy of these *atg10* morpholinos at 1 ng cannot be tested.

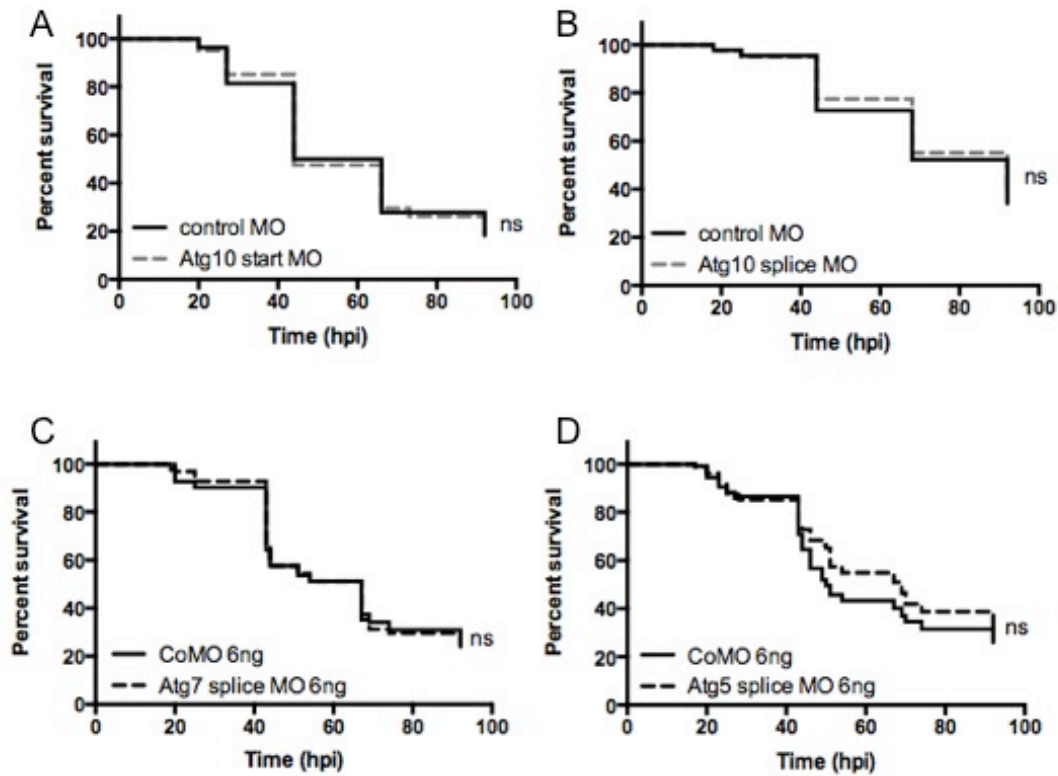


Figure 4.16. Infection of autophagy knockdown zebrafish embryos

A) *atg10* start MO (1 ng) or control MO injected zebrafish embryos were infected with 3300 CFU of *S. aureus* SH1000, 1 experiment, n > 55 fish per group

B) *atg10* splice MO (1 ng) or control MO injected zebrafish embryos were infected with 3300 CFU of *S. aureus* SH1000, 1 experiment, n > 40 fish per group

C) *atg7* splice MO (6ng) or control MO injected zebrafish embryos were infected with 2000 CFU of *S. aureus* SH1000, 3 independent experiments, n = 125 fish per group

D) *atg5* splice MO (6ng) or control MO injected zebrafish embryos were infected with 2000 CFU of *S. aureus* SH1000, 4 independent experiments, n > 125 fish per group

ns = not significant

Figure 4.17. Structure and mechanism of morpholinos

- A) Structure of morpholino oligonucleotide
- B) Mechanism of action of morpholino target

Images issued from www.gene-tools.com

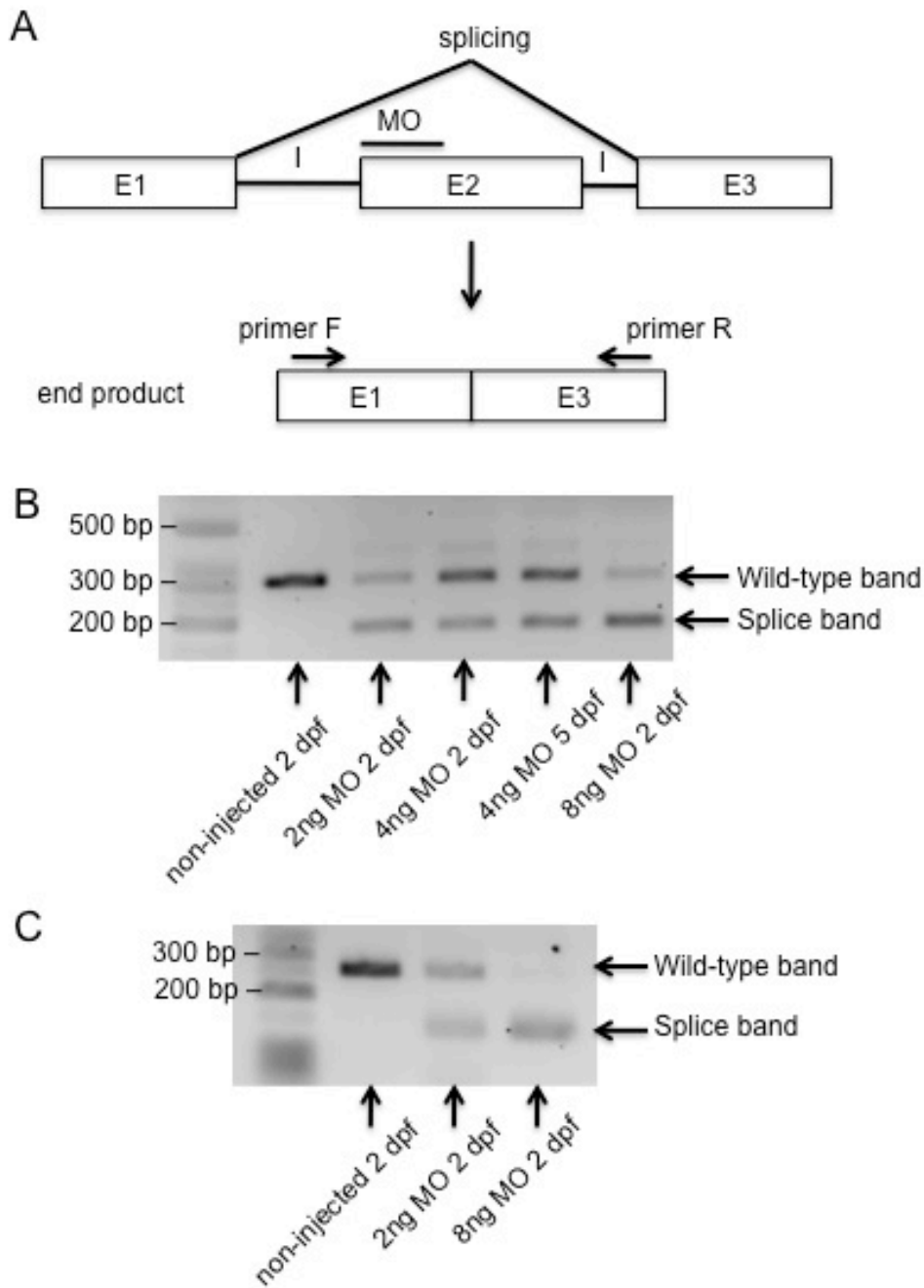


Figure 4.18. Efficacy of splice morpholinos *atg7* and *atg5*

A) Principle of splice morpholinos

B) RT-PCR of *atg7* splice MO injected zebrafish at the indicated doses and the indicated time (dpf)

C) RT-PCR of *atg5* splice MO injected zebrafish at the indicated doses and the indicated time (dpf)

4.5. Utilisation of a transgenic zebrafish line to visualise autophagy

4.5.1. Transgenic zebrafish lines

Several tools have been developed to visualise the formation of autophagosomes by microscopy. A common strategy is to label some specific marker proteins of autophagy with fluorescent proteins. For example, the Atg5-Atg12 conjugate behaves as a single molecule after their posttranslational covalently attachment. This conjugate localises on the isolation membrane throughout the elongation process and dissociates when the autophagosome is fully formed (Mizushima, Yamamoto et al. 2001; Mizushima, Kuma et al. 2003). Atg5 proteins tagged with GFP can be used as a marker for autophagosome precursor. WIPI-1 and WIPI-2 are proteins evolved from the yeast homolog Atg18. They specifically bind PI3P and are linked to autophagy. Indeed, WIPI-1 and WIPI-2 localise at initial autophagosomal inner and outer membranes that are also positive for other autophagy marker such as LC3. This suggests that WIPI-1 and WIPI-2 are reliable autophagosome markers, especially to track the origin of the membranes (coming from endoplasmic reticulum, plasma membrane and golgi area) (Proikas-Cezanne, Ruckerbauer et al. 2007; Proikas-Cezanne and Robenek 2011).

However, the most commonly used marker of autophagy is the microtubule-associated protein 1 (MAP1) light chain 3 (LC3), which is the Atg8 yeast orthologue protein. During the autophagy process, the conjugated form of LC3 to phosphatidylethanolamine (called LC3-II proteins) is anchored to the inner and outer membranes of autophagosome. LC3-II proteins are bound on the membranes of the isolation membrane, contributing to its elongation up to its closure forming the spherical shaped autophagosome (Kabeya, Mizushima et al. 2000). Upon formation of the autophagosome, LC3-II proteins localised on the outer membrane are removed by the cysteine protease Atg4B and recycled (Tanida, Sou et al. 2004), while LC3-II proteins bound to the inner membrane remain attached until their degradation by the

lysosomal enzymes with the enveloped cytosolic contents (Tanida, Minematsu-Ikeguchi et al. 2005). This specific localisation pattern of LC3 make it an excellent tool for monitoring the formation of autophagosome as well as the amount of degradable cargo that is transported from the autophagosome to the lysosomal compartment (i.e. autophagic flux). By using cell lines expressing LC3 protein fused with a green fluorescent protein (GFP), autophagosomes can be identified under fluorescent microscopy as ring-shaped structures (Mizushima, Kuma et al. 2003) or as little dots if they are smaller than 1 μm (Kabeya, Mizushima et al. 2000). Autophagosomes usually measure between 0.5 and 1.5 μm (Seglen and Bohley 1992). The fluorescent labelling of LC3 has been successfully used in many organisms including *S. cerevisiae* (Klionsky, Cuervo et al. 2007), *A. thaliana* (Yoshimoto, Hanaoka et al. 2004), *D. melanogaster* (Rusten, Lindmo et al. 2004), mice (Mizushima, Yamamoto et al. 2004), zebrafish (He, Bartholomew et al. 2009), as well as live cells (Bampton, Goemans et al. 2005).

LC3 proteins can also be detected on autolysosomes, but at a much less minor extent. By using a GFP-tagged LC3 system, only the autophagosomes can be visualised. Indeed, the GFP fluorescence is lost after the autophagosome-lysosome fusion due to the acidic and degradative conditions. However, red-fluorescent protein (RFP) is insensitive to the acidic environment due to its lower pKa, so its fluorescence is visible both before and after fusion with lysosome. Therefore, tagging LC3 proteins with RFP enables to visualise both autophagosomes and autolysosomes. Taking these 2 facts into account, a tandem fluorescent tagged system LC3-RFP-GFP was designed (Kimura, Noda et al. 2007). During the formation of autophagosome, both GFP and RFP are detectable, while only RFP is visible after the fusion with lysosome. Therefore, the maturation of autophagosome and its fusion with lysosome can be recorded with this method. A HeLa cell line constitutively expressing LC3 tagged with both RFP and GFP has been used to differentiate autophagosomes from autolysosomes. Autophagosomes are surrounded with both red and green dots, or as yellow dots if the pictures are merged, while autolysosomes are sprinkled with red dots that are not green (Underwood, Imarisio et al. 2010).

In zebrafish research, the two-component gene expression system Gal4/UAS is used to study the expression of genes and their functions. Two transgenic lines have to be generated, carrying either the activator construct (Gal4) or the effector (also called reporter) construct (UAS). In the activator line, the yeast transcription factor Gal4 is under the control of a given promoter; while in the effector line, the gene of interest is fused to the upstream activator sequence (UAS) to which Gal4 specifically binds to activate gene transcription. Crosses of animals from the activator and effector lines generate a progeny in which the transgene of interest linked to the UAS is expressed within the spatial pattern specified by the chosen promoter linked to Gal4. In practice, the Gal4 gene expression is driven by a known promoter that will drive the expression of a pattern of interest, which could be a certain population of cells or a specific tissue. To induce the expression of certain genes in some particular cell lines such as neutrophils or macrophages, the specific promoters *mpx* or *mpeg1* respectively can be chosen. Indeed, the myeloid-specific peroxidase (*mpx*) is a marker for neutrophil granulocytes in zebrafish (Bennett, Kanki et al. 2001; Lieschke, Oates et al. 2001), while the *mpeg1* promoter drives transgene expression in zebrafish macrophages (Ellett, Pase et al. 2011).

To visualise the formation of autophagosome *in vivo*, the effector zebrafish transgenic line UAS:RFP-GFP-LC3 was generated. In parallel, two activator zebrafish transgenic lines were used, driving the expression in neutrophils (*mpx:Gal4*) or macrophages (*mpeg1:Gal4*). By crossing these transgenic lines, fluorescent LC3 proteins can be expressed specifically in neutrophils or in macrophages. The LC3 proteins are coloured in red and green in autophagosomes, while only the red colour of the LC3 proteins is visible in autolysosomes (Figure 4.19.).

4.5.2. Selection of the transgenic zebrafish lines

Transgenic zebrafish lines are generated by microinjection of plasmid DNA into 1-cell stage embryo. Stable integration of plasmid DNA allows efficient

expression of introduced genes. However, plasmid DNA integration is usually partial, producing mosaic individuals. The transmission of the transgene to the progeny is possible only if it is integrated in the germline. Therefore, the fish effectively carrying the transgenes need to be selected. One method is by injecting a construct containing both the transgene of interest and a second transgene that will be 'easily visible'. One of these 'easily visible' transgenes is one driving the expression of a green heart (*cm1c2:GFP*). The green heart is easily detectable under a dissecting scope in early embryos. The transgenic zebrafish line carrying the UAS:RFP-GFP-LC3 transgene was generated by injecting a construct containing both the UAS:RFP-GFP-LC3 and a green heart marker. Therefore, zebrafish embryos expressing a green heart are most likely to have integrated the other part of the construct in their genome. At 3 dpf, injected zebrafish embryos were screened for the green heart marker and subsequently grown up to adulthood (Figure 4.20.).

The transgenic lines that carry the *mpx:Gal4* or *mpeg1:Gal4* construct can be screened in 2 different manners. The first option is to cross the adult fish with a zebrafish line carrying a known UAS construct that is easily detectable. For example, crossing a *mpx:Gal4* fish to a UAS:kaede transgenic fish produces a progeny that express the kaede protein in all neutrophils, which is easily detectable under a dissecting scope. Similarly for a *mpeg1:Gal4* fish crossed to a UAS:kaede fish, the progeny expresses the kaede protein in all macrophages. If the progeny does not express any kaede, it means that the parent fish corresponding does not carry the promoter:Gal4 construct. The second option to screen the promoter:Gal4 zebrafish line is to do a PCR test on the adult fish. In practice, a small part of the fin of an anaesthetised adult fish is cut, the genomic DNA is extracted from the fin clip and subsequently used as a template for a PCR. Specific primers amplifying a small portion of the Gal4 sequence have been designed. The primers used in this study amplify a sequence of 60 bp if the adult fish carries the promoter:Gal4 construct (Figure 4.20.B.).

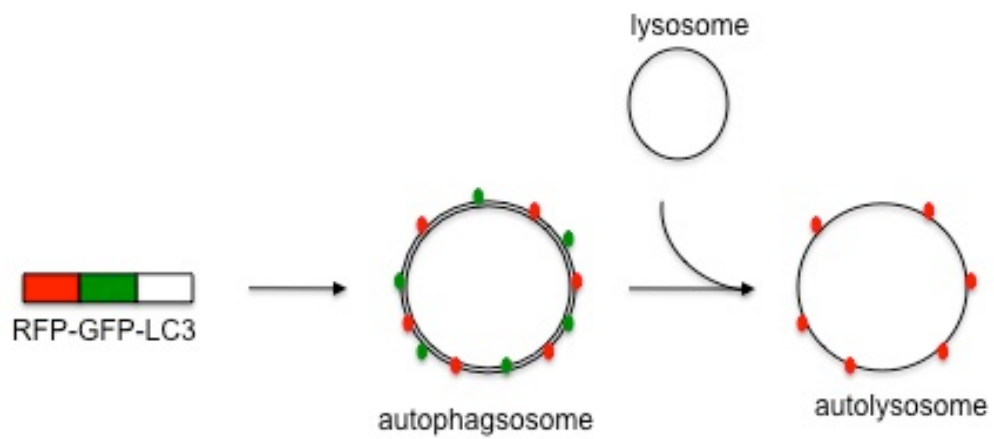
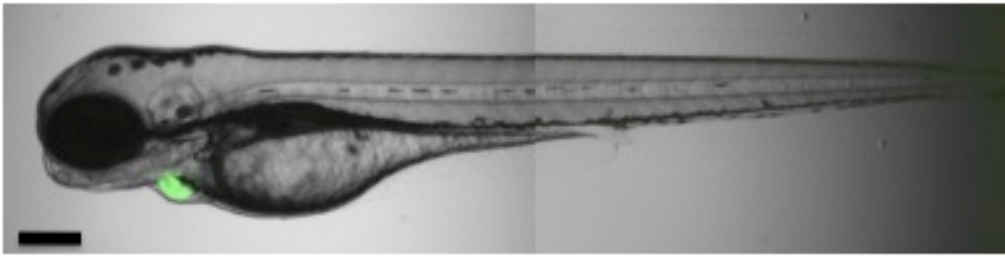


Figure 4.19. Schematic representation of the RFP-GFP-LC3 tandem fluorescent system

With zebrafish expressing the RFP-GFP-LC3 construct, the autophagosomes are decorated with green and red LC3 proteins, while autolysosomes are only decorated with red LC3 proteins

A



B

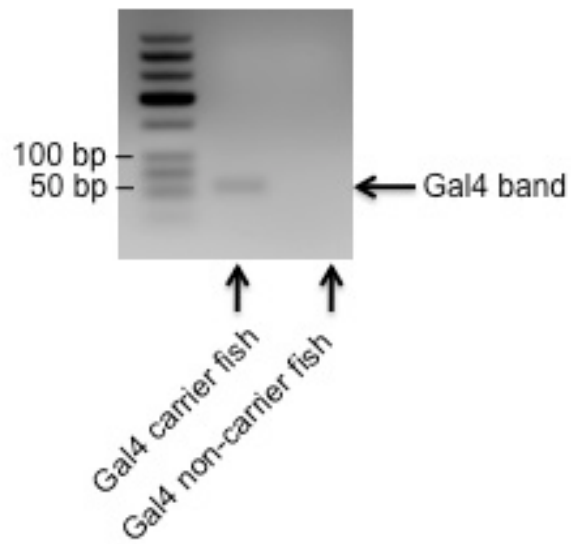


Figure 4.20. Screening transgenic fish

A. A 3 dpf UAS-RFP-GFP-LC3 carrier fish with its green heart.

B. Gel showing the 60 bp DNA band of a portion of Gal4 amplified by PCR.

Scale bar = 200 μ m

4.5.3. Expression of LC3 proteins exclusively in zebrafish macrophages

The expression of autophagy proteins LC3 can be driven in macrophages by crossing the UAS:RFP-GFP-LC3 zebrafish line to a *mpeg1:Gal4* zebrafish line. As a result, a high proportion of the progeny successfully express the RFP-GFP-LC3 construct in macrophages.

The expression of the RFP-GFP-LC3 transgene in macrophages was tested by incubating 29 hpf zebrafish larvae in 30 μ M of the autophagy inducer rapamycin for 3 h. The yolk circulation valley area was then observed under a spinning disk confocal microscope. It was expected to see some red and green colours expressed by LC3 proteins. The intensity of the colours is expected to vary in function of the stage of the autophagosome formation (both red and green) or autolysosome (only red). Experimentally, these 2 colours were effectively detectable, even though the expression was quite weak. However, by using a medium exposure time of the sample and by enhancing the gain, the red and green colours were sufficiently visible and distinctive from the background. Some round shapes coloured both red and green inside some macrophages were observed. At the position where the colours were expressed, the differential interference contrast (DIC) picture showed a more round structure inside the macrophages (Figure 4.21.A. and B.). These structures expressing LC3 proteins (red and green) were occupying a large part of the space inside the cell.

It has been shown that the autophagic machinery is recruited after *S. aureus* internalisation in HeLa cells (Schnaith, Kashkar et al. 2007). To visualise the formation of autophagosome *in vivo* following *S. aureus* infection, 30 hpf zebrafish embryos issued from a cross between the UAS:GFP-RFP-LC3 and *mpeg1:Gal4* zebrafish lines were infected with *S. aureus* labelled with a blue-tag (CFP-SH1000). At 2 hpi, pictures of infected macrophages were taken with the spinning disk confocal microscope. Figure 4.22. shows a situation in which a high number of bacteria were engulfed by a macrophage, as represented by the number of blue dots inside the cell. The whole cell is also

coloured in both green and red, suggesting the expression of LC3 proteins. In contrast with the high number of bacterial cells from Figure 4.22., Figure 4.23. shows 2 different situations in which a macrophage contained less than 5 *S. aureus* colonies. These bacteria seemed to be localised in a restricted compartment, perhaps a vacuole. A few dots of green and red were also visible inside this compartment, suggesting the presence of LC3 proteins. An intermediate situation to the one with a lot of bacteria spread in the cell (Figure 4.22.) and the other one with only a few bacteria confined in a compartment (Figure 4.23.) is visible in Figure 4.24.. Some bacteria seemed to be localised in one or two small compartments, while some other bacteria seemed to be in the cytosol. The compartment and area surrounding the bacteria were coloured in red and green (Figure 4.24.A. and B.).

Pictures of infected macrophages inside living zebrafish embryos were also captured at 6 hpi. Some similar situations to the earlier time were observed. The first picture represents a macrophage infected by 3 or 4 bacteria (Figure 4.25.). Three bacterial cells were located on the left side of the cell, and the fourth bacterium was at the edge at the right top side. The whole cell was expressing green and red colours. The second picture shows a macrophage infected with some bacteria. At the bottom of the cell, there is an area coloured with red and green puncta, as well some blue bacteria (Figure 4.26.). The third picture is an example of colocalisation of colours inside a macrophage. Indeed, there were 3 spots of blue bacteria inside the cell. At the same location, red and green coloured were visible. Therefore, the colocalisation of the blue (bacteria) with the red and green (LC3 proteins) was clearly distinctive (Figure 4.27.).

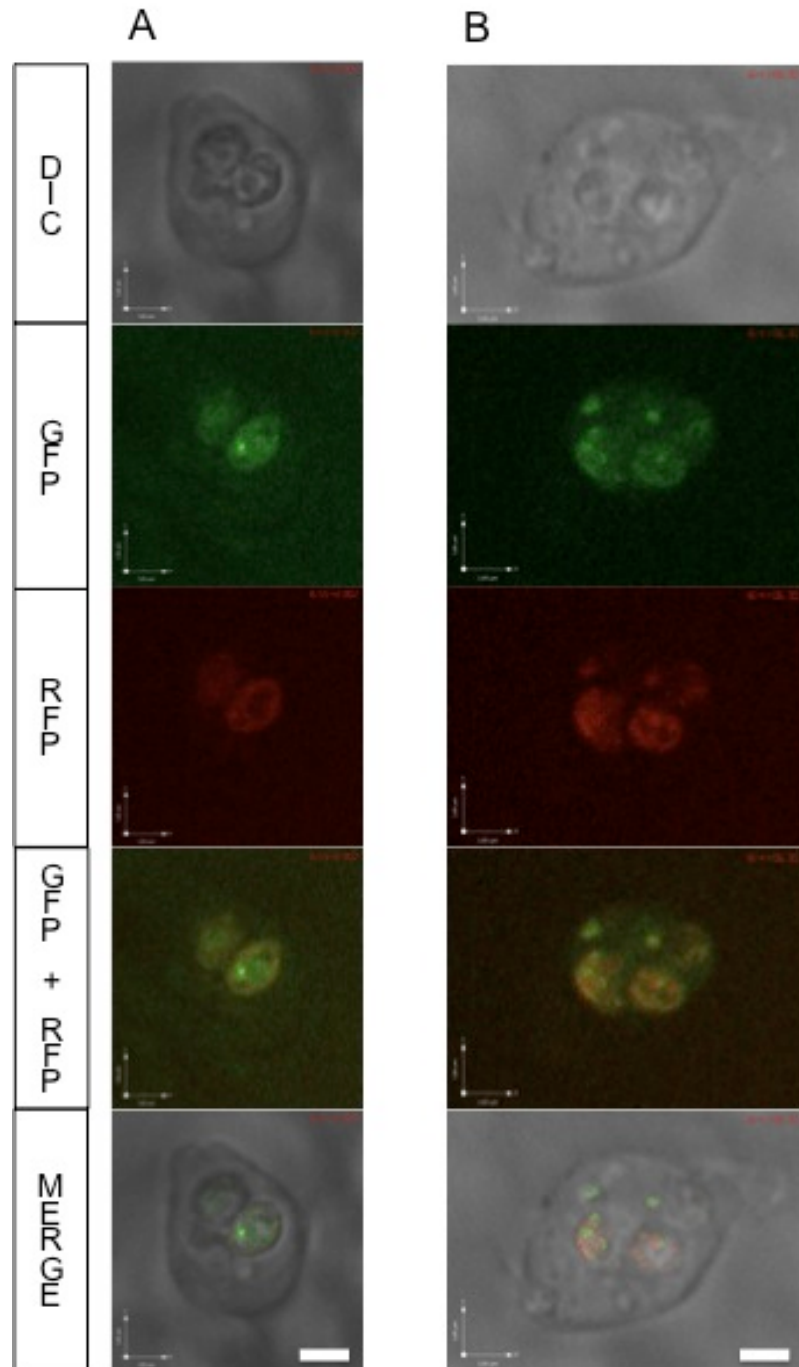


Figure 4.21. Rapamycin induces the expression of autophagy LC3 proteins in zebrafish macrophages

In vivo images of the yolk circulation valley area of 32 hpf *mpeg1:Gal4 x UAS:RFP-GFP-LC3* zebrafish larvae treated with 30 μ M of rapamycin for 3h.

A and B are both single focal planes from a different macrophage situation. Scale bars in A and B = 3.8 μ m

Images were captured using a spinning disk confocal microscope and a 60x oil objective.

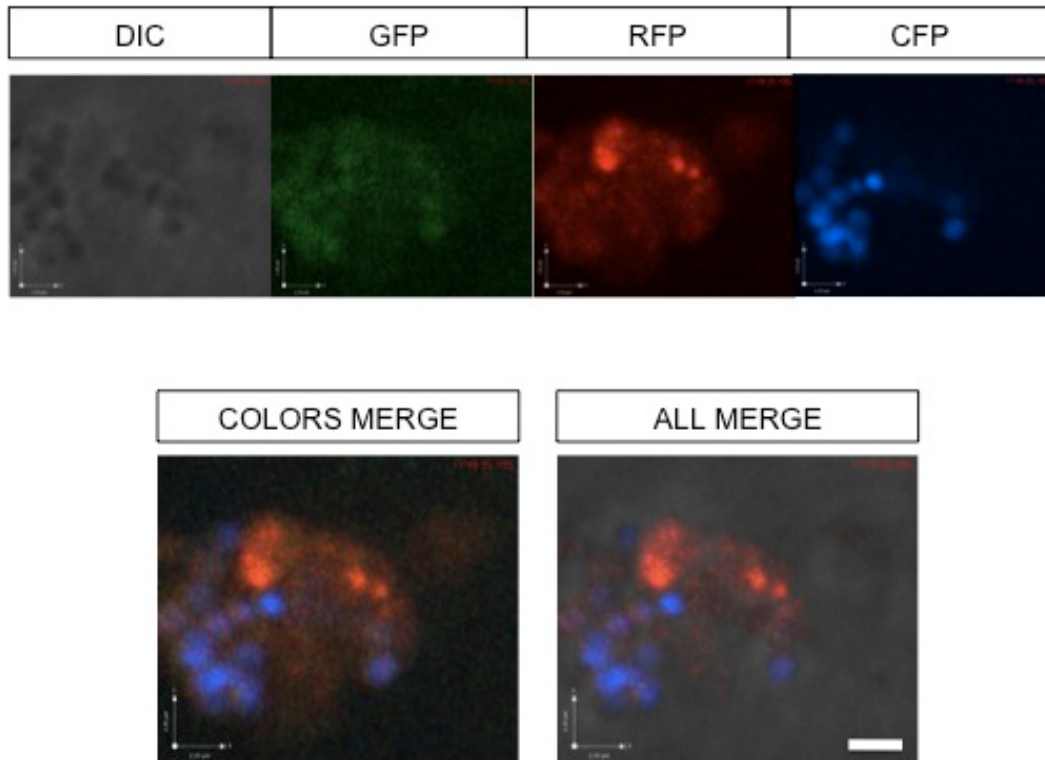


Figure 4.22. A zebrafish infected macrophage containing a high number of *S. aureus* expresses autophagy LC3 proteins

In vivo images of the yolk circulation valley area of 2 hpi *mpeg1:Gal4* x *UAS:RFP-GFP-LC3* zebrafish larvae infected with *S. aureus* CFP-SH1000 strain at 30 hpf.

1 single focal plane.

Scale bar = 2.3 μ m.

Images were captured using a spinning disk confocal microscope and a 60x oil objective.

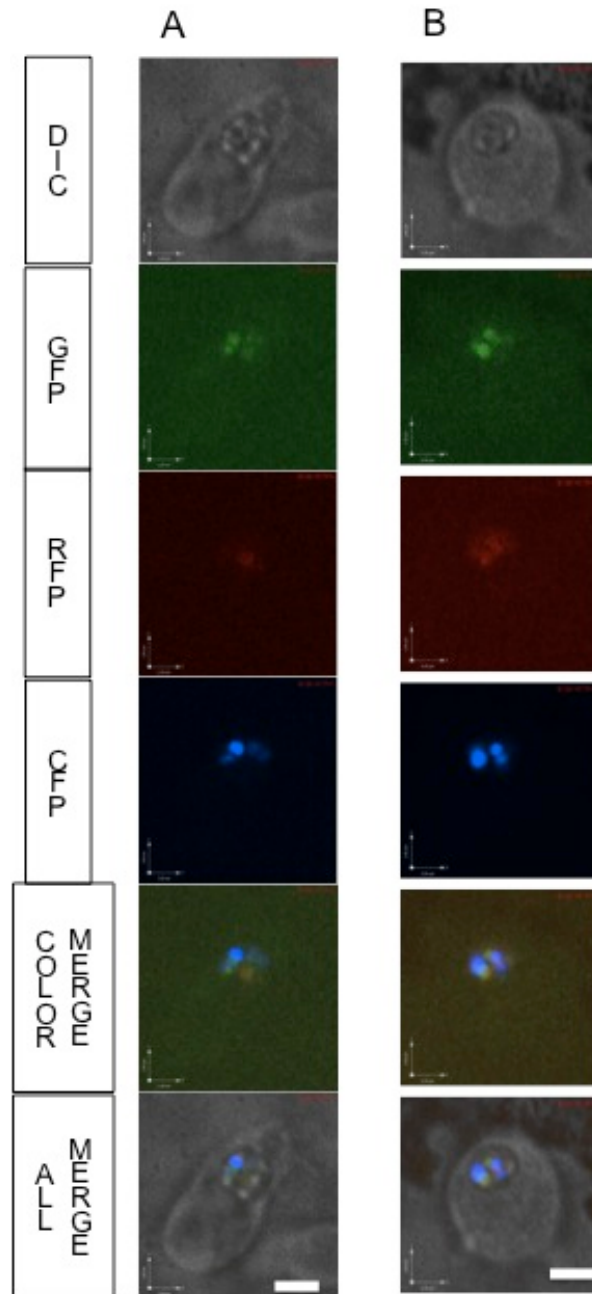


Figure 4.23. *S. aureus* bacteria are localised in a LC3 proteins positive vacuole inside a zebrafish macrophage

In vivo images of the yolk circulation valley area of 2 hpi *mpeg1:Gal4* x *UAS:RFP-GFP-LC3* zebrafish larvae infected with *S. aureus* CFP-SH1000 strain at 30 hpf.

A and B are both single focal planes of a different macrophage situation in the same larvae.

Scale bars in A and B = 2.9 μ m

Images were captured using a spinning disk confocal microscope and a 60x oil objective.

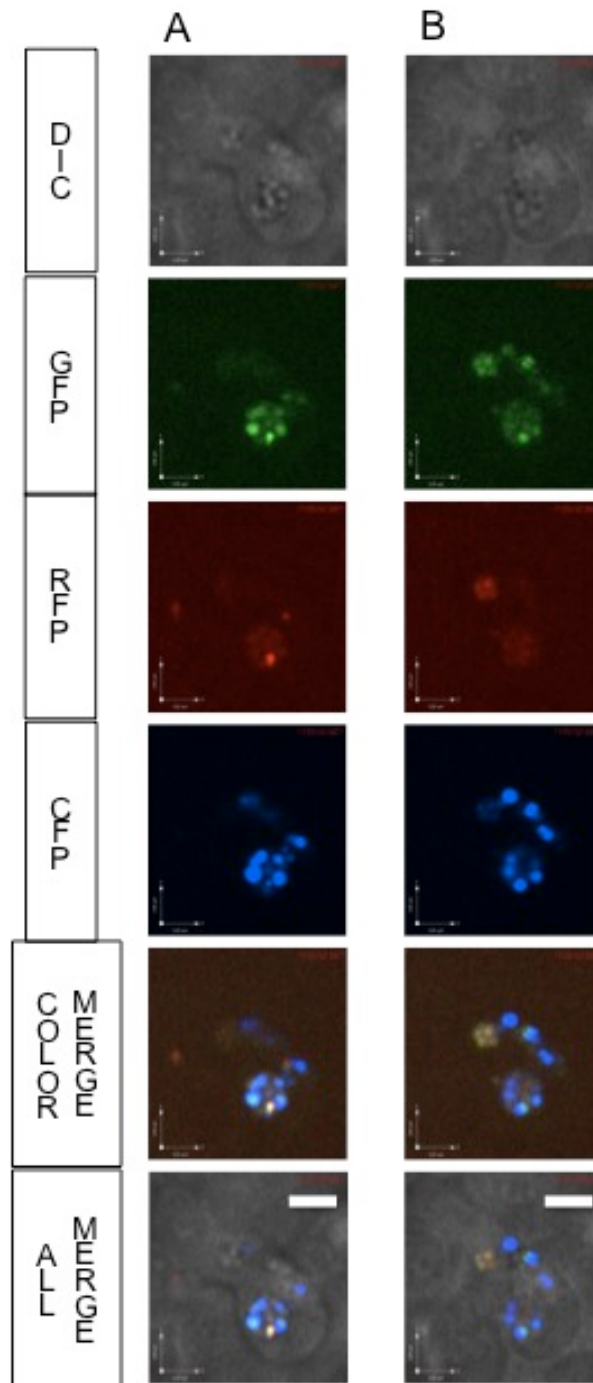


Figure 4.24. Several *S. aureus* bacteria phagocytosed in a zebrafish macrophage are also colocalised with autophagy LC3 proteins

In vivo images of the yolk circulation valley area of 2 hpi *mpeg1:Gal4* x *UAS:RFP-GFP-LC3* zebrafish larvae infected with *S. aureus* CFP-SH1000 strain at 30 hpf.

A and B: 2 different focal planes covering the same field.

Scale bars in A and B = 3.8 μ m

Images were captured using a spinning disk confocal microscope and a 60x oil objective.

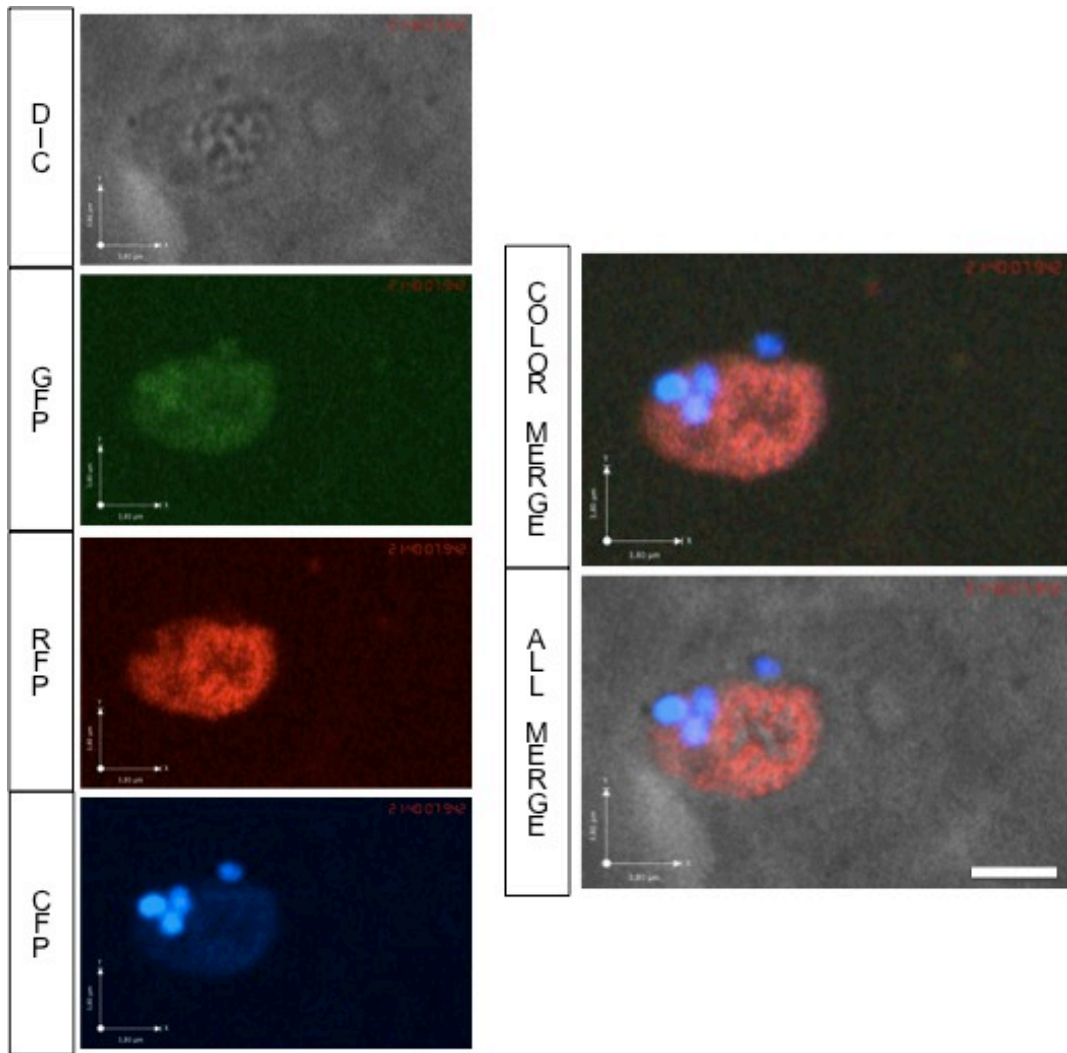


Figure 4.25. A large vacuole containing a few *S. aureus* bacteria expresses the autophagy LC3 proteins in an infected zebrafish macrophage at 6 h after infection

In vivo images of the yolk circulation valley area of 6 hpi *mpeg1:Gal4* x *UAS:RFP-GFP-LC3* zebrafish larvae infected with *S. aureus* CFP-SH1000 strain at 30 hpf.

1 single focal plane.

Scale bar = 3.8 μ m

Images were captured using a spinning disk confocal microscope and a 60x oil objective.

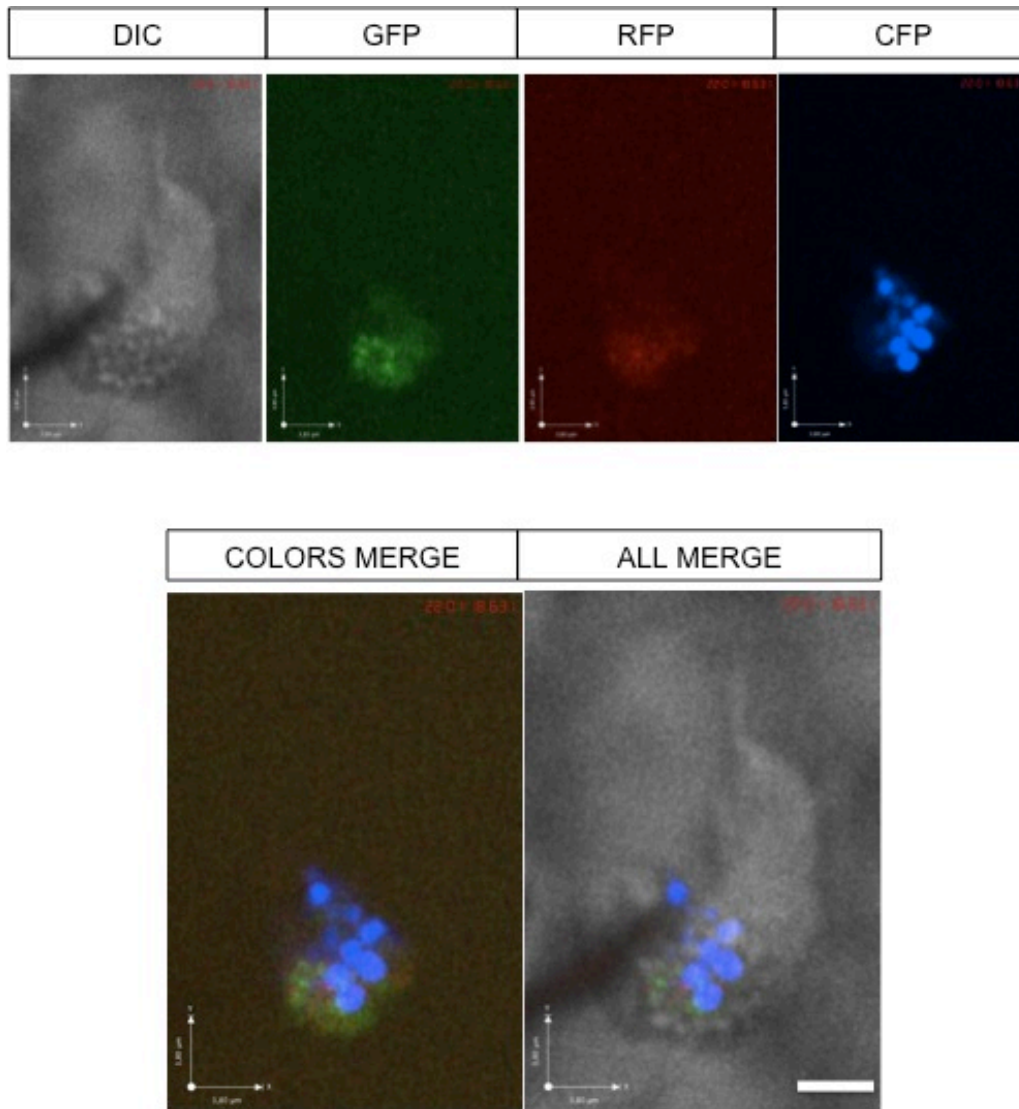


Figure 4.26. Colocalisation of autophagy LC3 proteins and a high number of *S. aureus* bacteria in an infected zebrafish macrophage at 6 h after infection

In vivo images of the yolk circulation valley area of 6 hpi *mpeg1:Gal4* x *UAS:RFP-GFP-LC3* zebrafish larvae infected with *S. aureus* CFP-SH1000 strain at 30 hpf.

1 single focal plane.

Scale bar = 3.8 μ m

Images were captured using a spinning disk confocal microscope and a 60x oil objective.

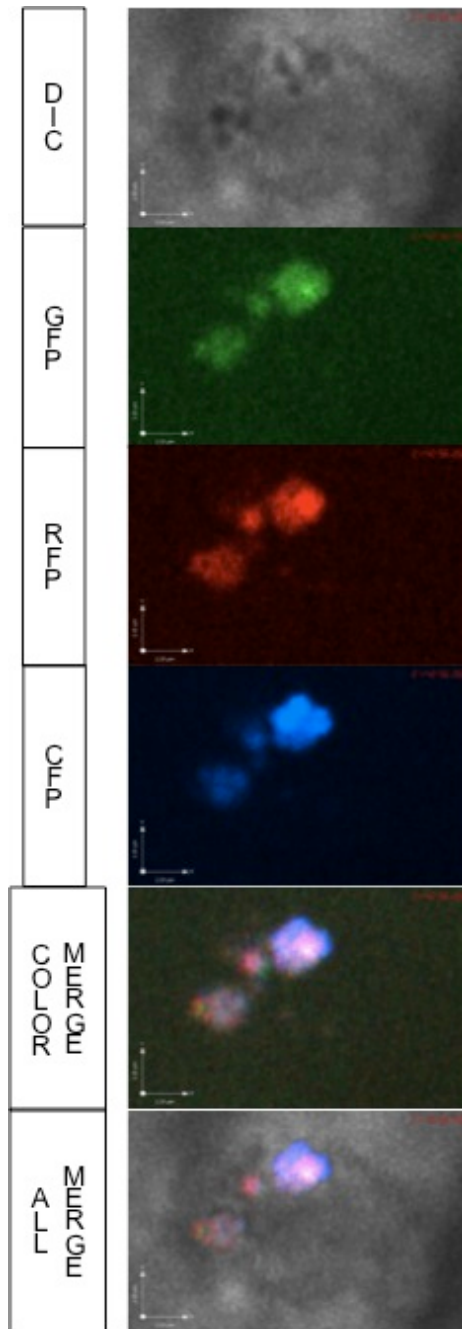


Figure 4.27. Colocalisation of autophagy LC3 proteins and *S. aureus* bacteria in a zebrafish macrophages 6 h after infection

In vivo images of the yolk circulation valley area of 6 hpi *mpeg1:Gal4* x *UAS:RFP-GFP-LC3* zebrafish larvae infected with *S. aureus* CFP-SH1000 strain at 30 hpf.

1 single focal plane.

Scale bar = 2.3 μ m

Images were captured using a spinning disk confocal microscope and a 60x oil objective.

4.5.4. Expression of LC3 proteins exclusively in zebrafish neutrophils

As of macrophages, the expression of autophagy proteins LC3 can be driven in neutrophils by crossing a UAS:RFP-GFP-LC3 carrier adult fish to a *mpx:Gal4* carrier adult fish. A high proportion of the progeny obtained express the RFP-GFP-LC3 construct in neutrophils.

The first experiment was designed to test the LC3 expression by incubating 29 hpf zebrafish progeny of *mpx:Gal4* x UAS:RFP-GFP-LC3 in 30 μ M of the autophagy inducer rapamycin for 3h. The yolk circulation valley area was then observed under a spinning disk confocal microscope for the expression of red and green colours in neutrophils. Indeed, green and red colours should be detectable where LC3 proteins are expressed. As the expression of these colours was quite weak, the gain was enhanced in order to distinguish the coloured puncta from the background. In Figure 4.28., the whole cell was weakly coloured with both green and red, and some very bright red spots were also visible. The colocalisation of green and red colours was also observed. In Figure 4.29., there were 1 or 2 small colocalised areas of red and green inside a vacuole inside the neutrophils, suggesting the formation of small autophagosomes.

The same zebrafish cross *mpx:Gal4* x UAS:RFP-GFP-LC3 was infected with blue tagged *S. aureus* (CFP-SH1000) at 30 hpf, and the yolk circulation valley area was imaged at 2 hpi with a spinning disk confocal microscope. Figure 4.30. represents two infected neutrophils next to each other. The right neutrophil showed a few blue bacteria in an area also expressing the red and green colours. This suggests the presence of LC3 proteins at the same localisation than the phagocytosed *S. aureus* bacteria inside the neutrophil. In Figure 4.31., a few blue bacteria were clearly engulfed in a closed compartment such as a vacuole. This vacuole was also expressing the green and red colours. This suggests that the vacuole containing *S. aureus* bacteria was decorated with LC3 proteins. In Figure 4.32., the blue bacteria were localised at the top end of the neutrophil, and this area was also spotted with green and red colours, suggesting the presence of LC3 proteins. At 6 hpi, the

colocalisation of blue (bacteria), red and green (LC3 proteins) in neutrophils was also clearly observable (Figure 4.33.).

4.5.5. Autophagosome formation in the *frozen* mutant

As it was initially thought that the zebrafish *frozen* mutant was an Atg10 mutant (see section 4.2.), it would be assumed that the *frozen* mutant is an autophagy mutant. Therefore, it was hypothesised that the *frozen* mutant was defective for the formation of autophagosome. To address this question, the UAS:RFP-GFP-LC3 line, the *mpeg1:Gal4* line and the *mpx:Gal4* line were crossed to the *frozen* mutant and grown. After selection of the adult zebrafish carrying both a *frozen* allele and the other desired UAS or Gal4 transgene (see section 4.5.3. for the selection process), these adult fish were crossed to get a progeny of siblings and *frozen* mutant expressing coloured LC3 proteins in either macrophages or neutrophils. After infection with CFP-*S. aureus* strain, frozen zebrafish embryos were imaged with a spinning disk confocal microscope. Figure 4.34. shows two macrophages of the *frozen* mutant containing some blue bacteria on the outskirts of the cells. These macrophages also expressed large red areas that were not colocalising with the blue bacteria, and very little green was expressed. In *S. aureus* infected neutrophils of the *frozen* mutant, the colocalisation of blue-tagged bacteria with the green and red colours corresponding to the LC3 proteins was observed very clearly (Figures 4.35. and 4.36.).

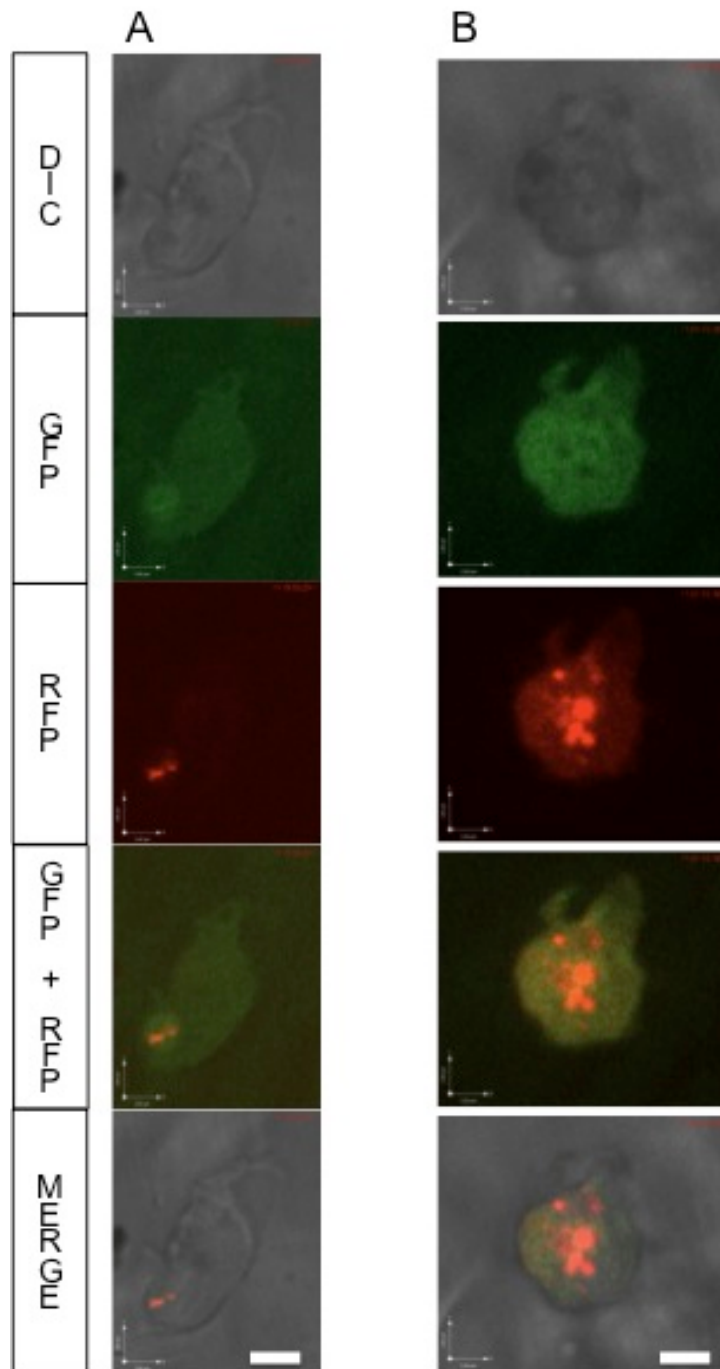


Figure 4.28. Rapamycin induces the expression of autophagy LC3 proteins in zebrafish neutrophils

In vivo images of the yolk circulation valley area of 32 hpf *mpx:Gal4* x *UAS:RFP-GFP-LC3* zebrafish larvae treated with 30 μ M of rapamycin for 3h. A and B are both single focal planes from a different neutrophil situation. Scale bar in A = 3.8 μ m, scale bar in B = 2.9 μ m

Images were captured using a spinning disk confocal microscope and a 60x oil objective.

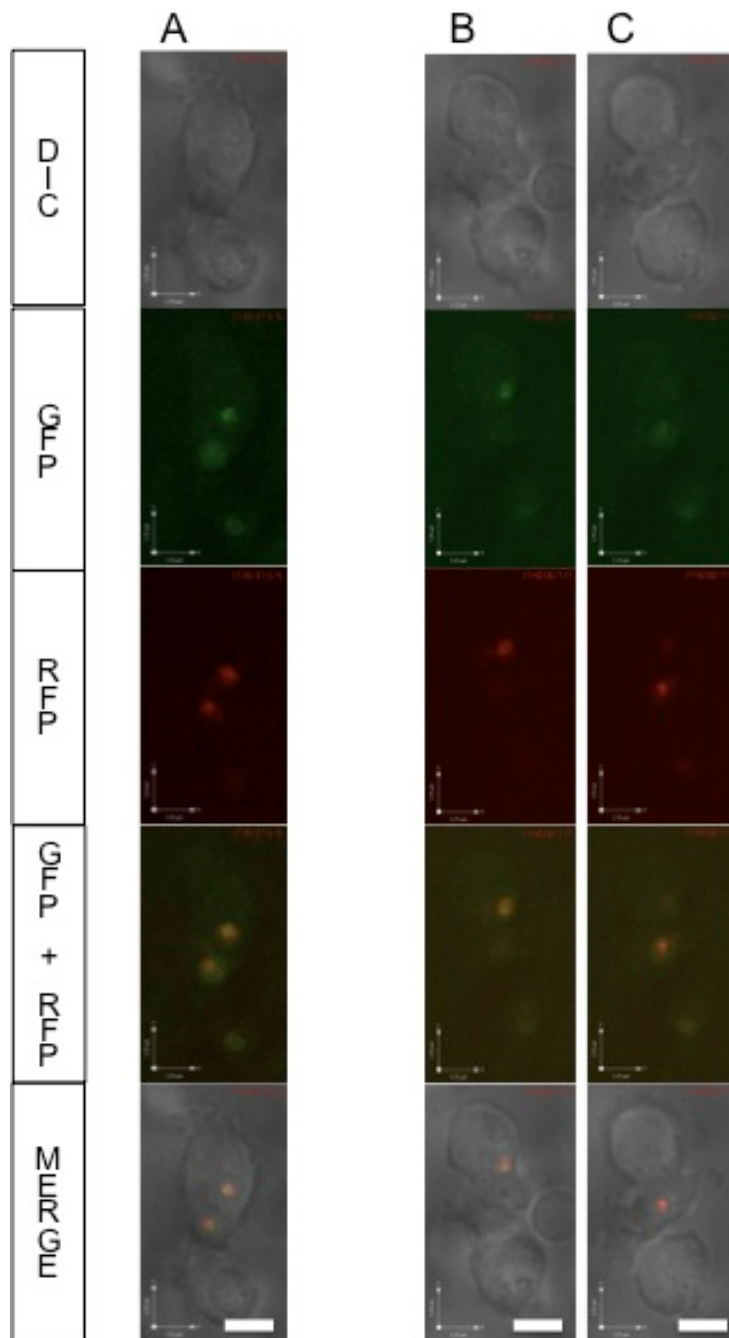


Figure 4.29. Rapamycin induces the expression of autophagy LC3 proteins in zebrafish neutrophils

In vivo images of the yolk circulation valley area of 32 hpf *mpx:Gal4* x *UAS:RFP-GFP-LC3* zebrafish larvae treated with 30 μ M of rapamycin for 3h. A: 1 single focal plane; B and C: 2 different focal planes covering the same field

Scale bard in A, B and C = 5.7 μ m

Images were captured using a spinning disk confocal microscope and a 60x oil objective.

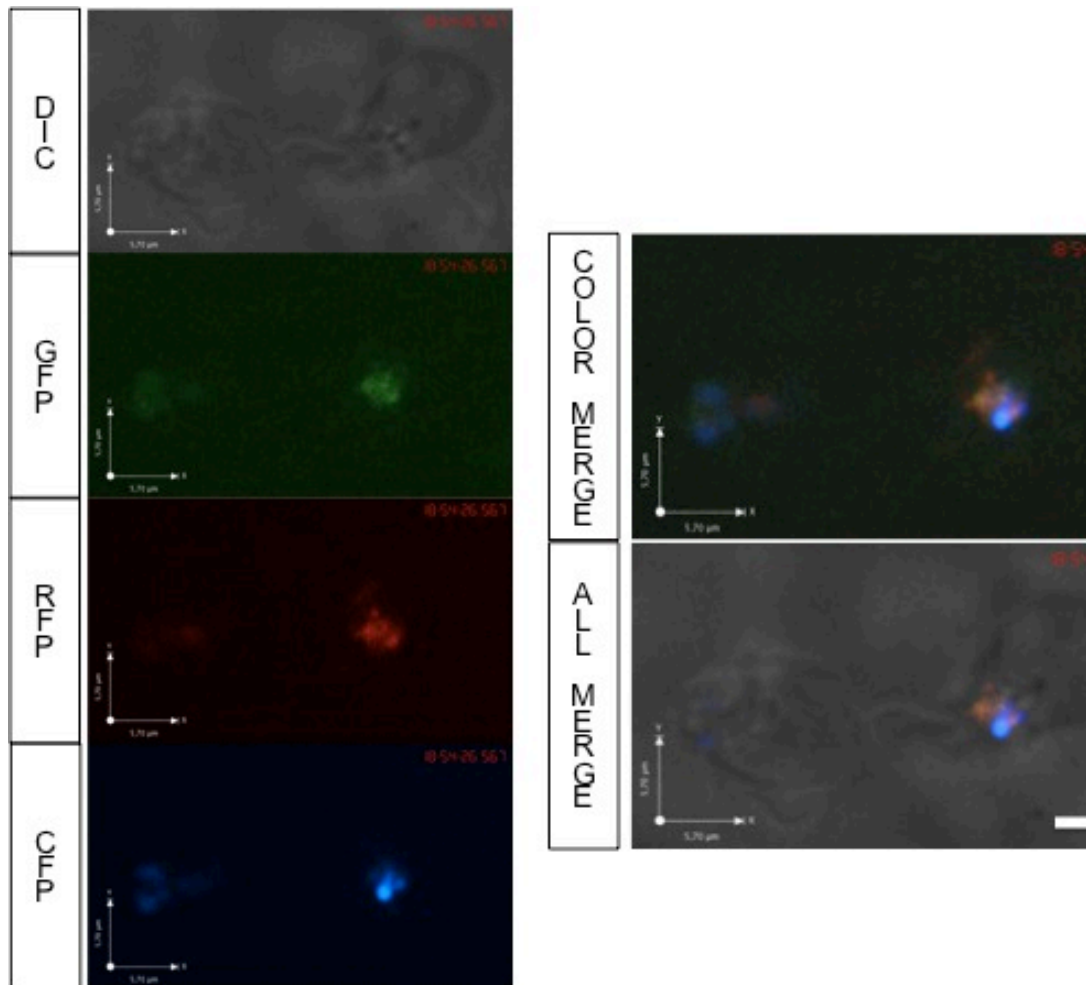


Figure 4.30. Colocalisation of autophagy LC3 proteins and *S. aureus* bacteria inside a zebrafish neutrophil

In vivo images of the yolk circulation valley area of 2 hpi *mpx:Gal4* x *UAS:RFP-GFP-LC3* zebrafish larvae infected with *S. aureus* CFP-SH1000 strain at 30 hpf.

1 single focal plane.

Scale bar = 5.7 µm

Images were captured using a spinning disk confocal microscope and a 60x oil objective.

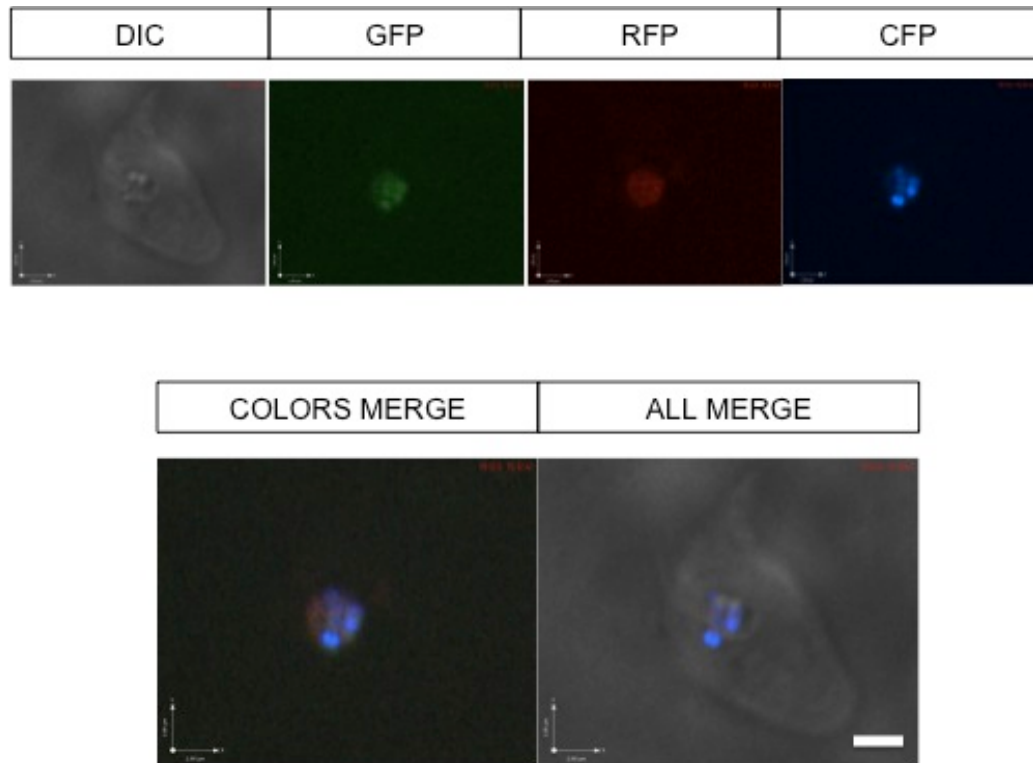


Figure 4.31. *S. aureus* bacteria are localised in a LC3 proteins-decorated autophagosome inside a zebrafish neutrophil

In vivo images of the yolk circulation valley area of 2 hpi *mpx:Gal4* x *UAS:RFP-GFP-LC3* zebrafish larvae infected with *S. aureus* CFP-SH1000 strain at 30 hpf.

1 single focal plane.

Scale bar = 2.9 μ m

Images were captured using a spinning disk confocal microscope and a 60x oil objective.

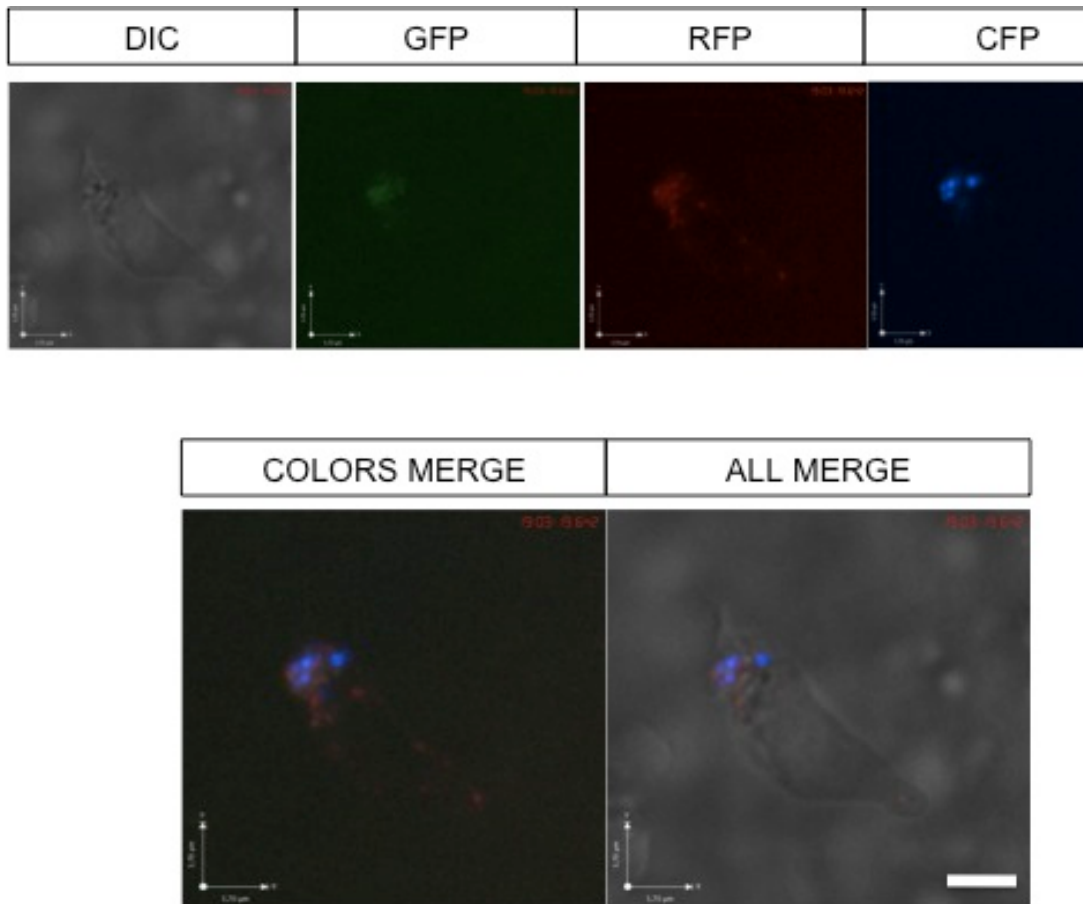


Figure 4.32. Colocalisation of autophagy LC3 proteins and *S. aureus* bacteria in an infected zebrafish neutrophil

In vivo images of the yolk circulation valley area of 2 hpi *mpx:Gal4* x *UAS:RFP-GFP-LC3* zebrafish larvae infected with *S. aureus* CFP-SH1000 strain at 30 hpf.

1 single focal plane.

Scale bar = 5.7 μ m

Images were captured using a spinning disk confocal microscope and a 60x oil objective.

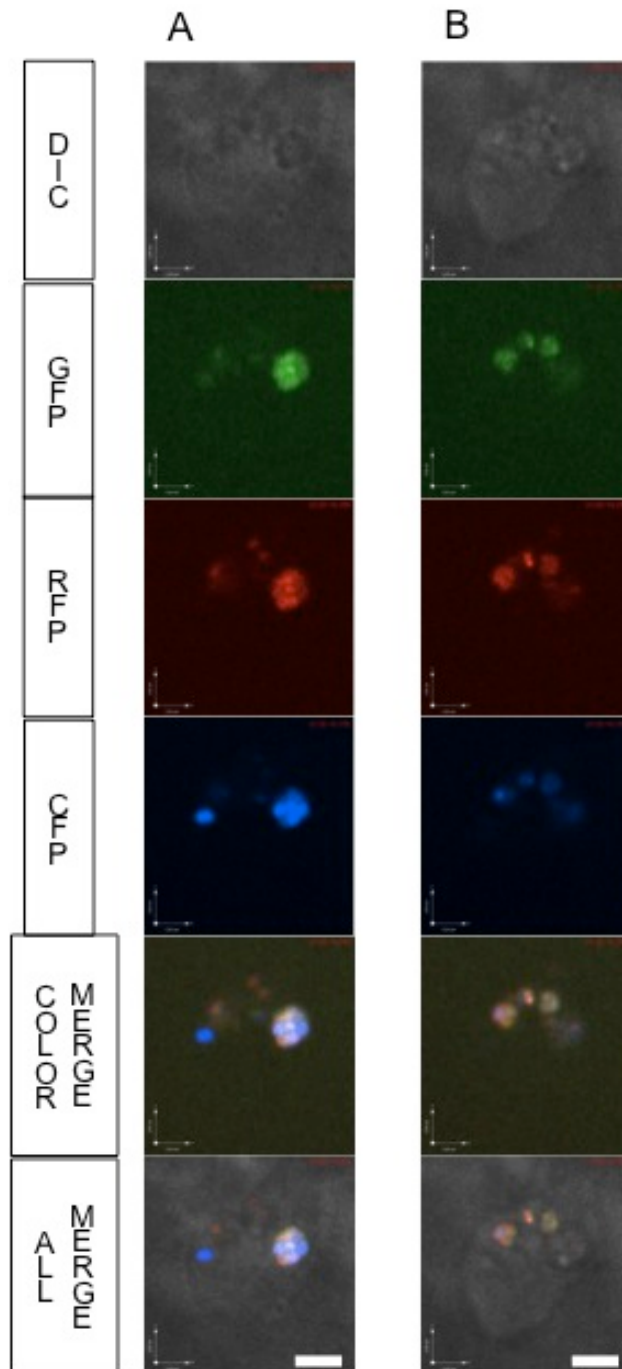


Figure 4.33. Colocalisation of autophagy LC3 proteins and *S. aureus* bacteria in a zebrafish neutrophil 6 h after infection

In vivo images of the yolk circulation valley area of 6 hpi *mpx:Gal4* x *UAS:RFP-GFP-LC3* zebrafish larvae infected with *S. aureus* CFP-SH1000 strain at 30 hpf.

1 single focal plane.

Scale bar = 2.9 μ m

Images were captured using a spinning disk confocal microscope and a 60x oil objective.

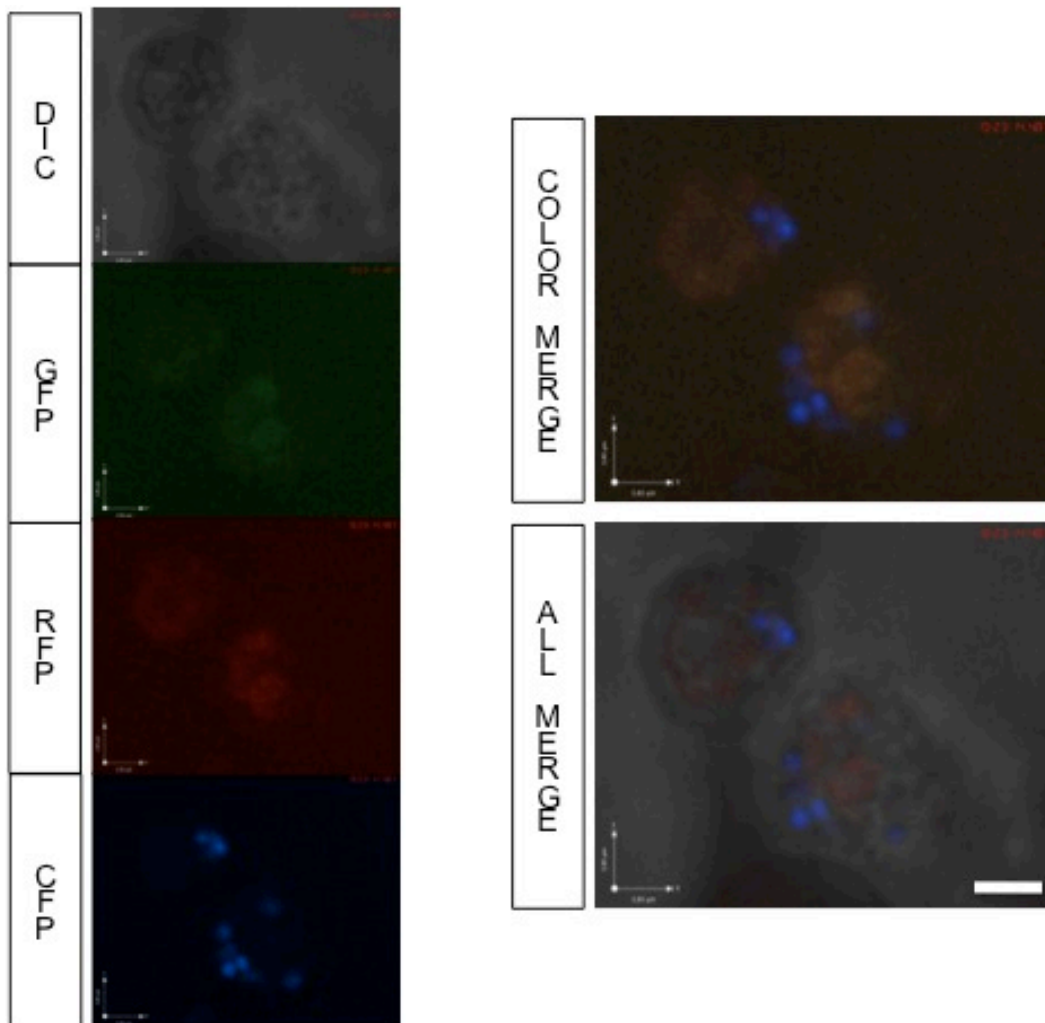


Figure 4.34. Colocalisation of autophagy LC3 proteins and *S. aureus* bacteria in an infected macrophage of the zebrafish *frozen* mutant

In vivo images of the yolk circulation valley area of 2 hpi *frozen* x *mpeg1:Gal4* x *UAS:RFP-GFP-LC3* zebrafish larvae infected with *S. aureus* CFP-SH1000 strain at 30 hpf.

1 single focal plane in the circulation valley area

Scale bar = 3.8 μ m

Images were captured using a spinning disk confocal microscope and a 60x oil objective.

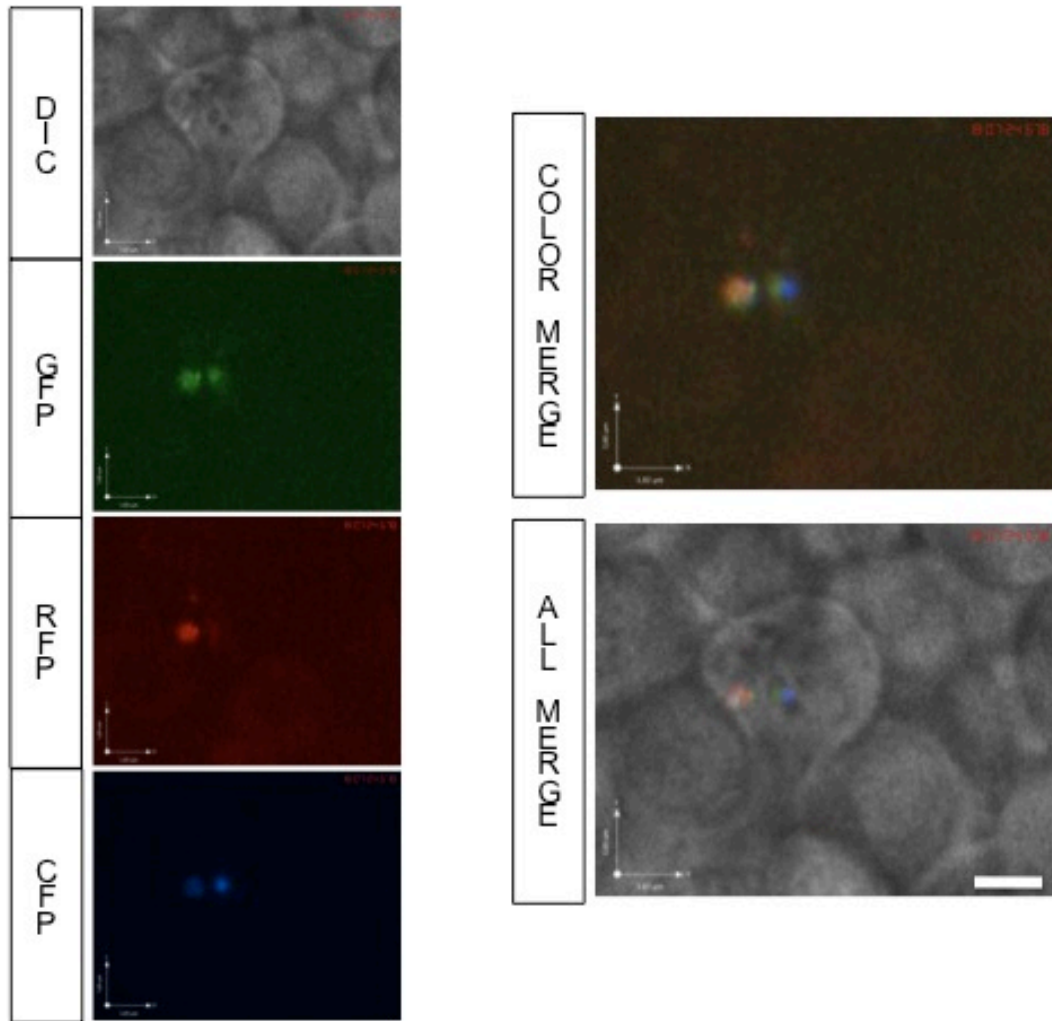


Figure 4.35. Colocalisation of autophagy LC3 proteins and 2 *S. aureus* bacteria in an infected neutrophil of the zebrafish *frozen* mutant

In vivo images of the yolk circulation valley area of 2 hpi *frozen* x *mpx:Gal4* x *UAS:RFP-GFP-LC3* zebrafish larvae infected with *S. aureus* CFP-SH1000 strain at 30 hpf.

1 single focal plane in the circulation valley area

Scale bar = 3.8 μ m

Images were captured using a spinning disk confocal microscope and a 60x oil objective.

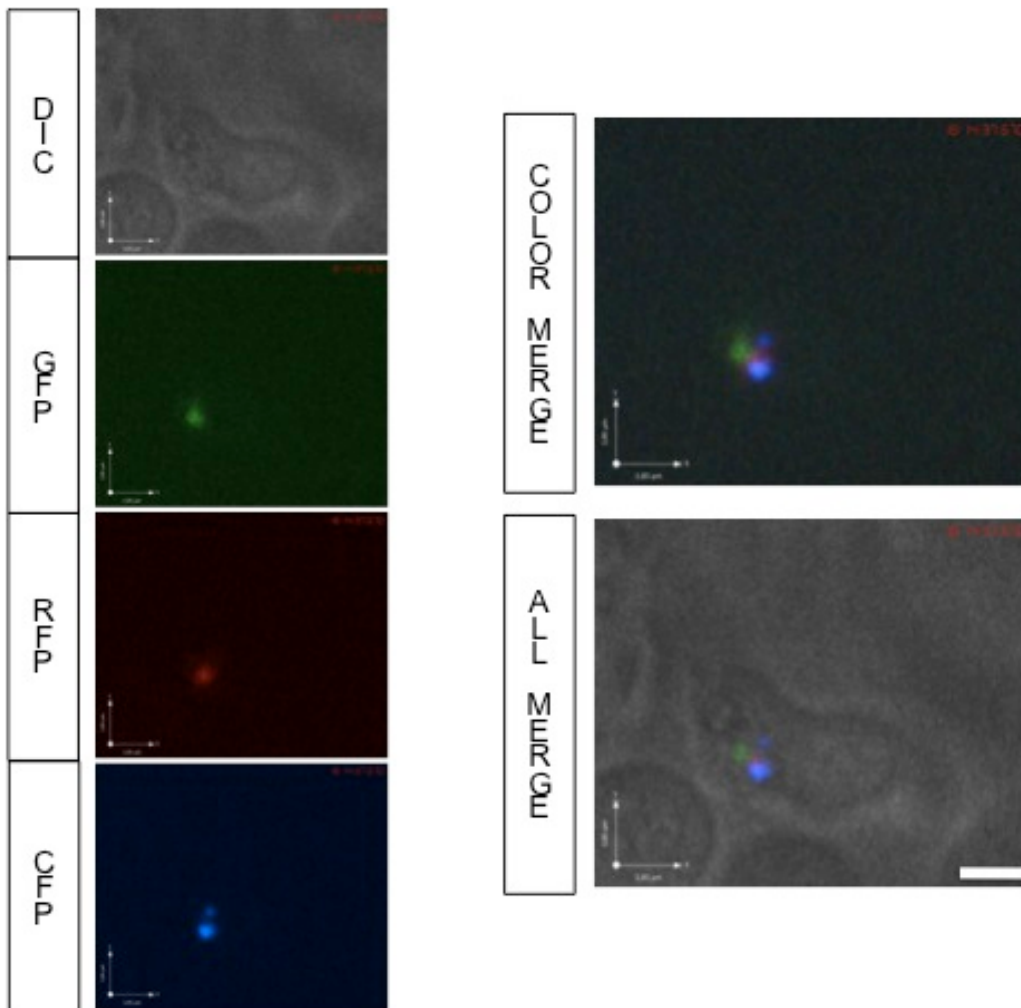


Figure 4.36. Colocalisation of autophagy LC3 proteins and 2 *S. aureus* bacteria in an infected neutrophil of the zebrafish *frozen* mutant

In vivo images of the yolk circulation valley area of 2 hpi *frozen* x *mpx:Gal4* x UAS:RFP-GFP-LC3 zebrafish larvae infected with *S. aureus* CFP-SH1000 strain at 30 hpf.

1 single focal plane in the circulation valley area

Scale bar = 3.8 μ m

Images were captured using a spinning disk confocal microscope and a 60x oil objective.

4.6. Discussion

In this chapter, I have described several methods used to explore the role of autophagy in *S. aureus* infection in the zebrafish embryo infection model: the utilisation of the *frozen* mutant, a pharmacological approach with enhancing and inhibiting drugs of autophagy, a genetic approach by knocking down some important autophagy proteins and finally a microscopy approach to visualise the formation of autophagosomes during *S. aureus* infection *in vivo* in the zebrafish embryo.

4.6.1. *Frozen* mutant

The infection of zebrafish mutant strain fro^{to27c}/+ called *frozen* with *S. aureus* lead to a higher survival of the infected *frozen* larvae than the survival of the infected siblings (Figure 4.2.).

At the start of the project, the fro^{to27c}/+ zebrafish line was thought to be an Atg10 mutant, as the mutation had been mapped to the genetic locus of this gene. However, some recent evidence has raised a doubt about this *frozen* mutant being an Atg10 knockout mutant. First, the injection of 2 different sets of Atg10 morpholinos in zebrafish embryos did not produce any *frozen* phenotype, and the survival of these infected morphants were not different than the control group (Figure 4.16.A and B). In addition, LC3 proteins, which are the most common autophagosome markers, were expressed normally in the visualisation experiments using the *frozen* mutant (Figures 4.34., 4.35. and 4.36.). Finally, a member of the department has generated an Atg10 knockout zebrafish line with the TALEN technique, and the double mutant did not show any *frozen* phenotype. More details about the TALEN technique as a method to generate targeted mutations is exposed in Chapter 5. Even if the *frozen* mutation is not an Atg10 knockout strain, it could still be related to the Atg10 gene, but at a different level as initially expected. Full genome sequencing has been performed and analysis is in progress with the intention to understand the mutation that affects the fro^{to27c}/+ zebrafish line. Even if the fro^{to27c}/+ is not an Atg10 mutation, it would be interesting to know what is the

genetic defect of the *frozen* mutant that confers a significant survival advantage when infected with *S. aureus*. Even if the *frozen* mutant cannot physically move, the bacteria can disseminate rapidly in the host body, which was visualised by microscopy using GFP-tagged bacteria (Figure 4.5.A. and 4.5.C.).

4.6.2. Pharmacological approach

In order to test the implication of host autophagy in *S. aureus* infection, a pharmacological approach was carried out using known inducers and inhibitors of autophagy. Even though these drugs are reported to influence the formation of autophagosome in the literature, these drugs could also interact with off-target molecules, leading to undesirable side effects that are not autophagy-related.

4.6.2.1. Autophagy enhancing drugs

The experiments of infected zebrafish larvae treated with autophagy enhancers showed two trends. The only autophagy inducer that had a significant effect on the survival of infected fish was rapamycin. The rapamycin treated group died more quickly than the control group (Figure 4.7.). In contrast, the survival curves of the infected fish remained unchanged when treated with rilmenidine, carbamazepine or verapamil compared to the untreated group (Figures 4.8. and 4.9.). The mode of action to induce autophagy is different between rapamycin and the 3 other autophagy enhancers tested. Indeed, rapamycin induces autophagy via mTOR, while rilmenidine, carbamazepine and verapamil are autophagy inducers mTOR-independent.

Knowing that rapamycin induces autophagy by inhibiting the mTOR pathway, the lower survival rate of the infected larvae treated with rapamycin could be explained by the induction of autophagy. As hypothesised, based on the *frozen* mutant results, autophagy would favour *S. aureus* infection over the host survival. However, the higher death rate of infected zebrafish larvae treated with rapamycin could also be due to side effects of this drug. Even though rapamycin did not influence the survival of healthy embryos in the

toxicity test (Figure 4.6.A.), rapamycin could interfere with some unknown functions that are independent of autophagy but important to fight *S. aureus* infection. It has been reported that rapamycin has immunosuppressant properties, however the scientific literature usually implicates this adverse effect on alterations in proliferation of B and T cells (Kay, Kromwel et al. 1991). However, this is not relevant in the zebrafish larvae infection model, as B and T cells are part of the adaptive immunity, which is not fully functional at this developmental stage. Another possibility is that the inhibition of mTOR affects other important innate immune functions. A potential mTOR dependent neutrophil function is an increased rate of neutrophil extracellular traps (NETs) release following neutrophil stimulation with the bacteria-derived peptide formyl-Met-Leu-Phe (fMLP) after inhibition of mTOR. The release of NETs is called NETosis and is an active form of cell death distinct from apoptosis and necrosis. NETosis allows neutrophils to achieve their antimicrobial function beyond their lifespan. Indeed, NETs are defined as decondensed chromatin fibres loaded with antimicrobial granular cargos to trap and kill pathogens. mTOR-mediated NETs require both autophagy and reactive oxygen species (ROS) production (Remijnsen, Kuijpers et al. 2011; Itakura and McCarty 2013). If this NETosis process helps the infected zebrafish larvae to fight the infection in its early time, it seems that the larvae treated with rapamycin become more importantly overwhelmed with *S. aureus* after 70 hpi till the end of the experiment at 90 hpi (Figure 4.7.). In another study, the induction of NETs induced *S. aureus* to generate a deoxyadenosine product from these NETs, which triggers the caspase-3 mediated death of immune cells. The nuclease and adenosine synthase enzymes secreted by *S. aureus* necessary to produce the deoxyadenosine product also have a cytotoxic activity on the surrounding macrophages, therefore excluding them from staphylococcal abscesses (Thammavongsa, Missiakas et al. 2013).

It is known from cell infection studies that *S. aureus* induces autophagy by influencing cAMP levels (Mestre and Colombo 2012). However, the 3 autophagy mTOR-independent compounds tested here (rilmenidine, carbamazepine and verapamil) also induce autophagy via the cAMP pathway.

As the survival of the infected larvae treated with these compounds was not significantly different than the control group (Figures 4.8. and 4.9.), one explanation could be that the addition of an autophagy enhancer acting on the cAMP levels does not influence the fate of *S. aureus* infection because the bacteria has potentially already induced autophagy via cAMP during the early times of the infection. In this case, the action of autophagy drugs acting via the cAMP pathway does not seem synergistic with the induction of autophagy mediated by *S. aureus*.

Another explanation would be that influencing autophagy only via a mTOR-independent pathway is not sufficient for a distinctive effect on the survival of infected zebrafish larvae. Using a combination of autophagy enhancing compounds from different categories that are acting on different molecular pathways (mTOR dependent and mTOR independent) could have a greater effect on the infection model in case of a synergy. To test this, two compounds such as rapamycin (mTOR inhibition) and lithium (inhibition of IMPase) could be used as their synergistic effect has been shown previously (Sarkar, Krishna et al. 2008). A single compound acting on both pathways would also be useful.

While the pro-autophagy effects of rilmenidine, carbamazepine and verapamil were demonstrated via the increase of LC3-II levels in cell culture, their capacity to induce autophagy in zebrafish was shown through their capacity to rescue Huntington's disease phenotypes in zebrafish (Williams, Sarkar et al. 2008). The pro-autophagic effect of carbamazepine in the muscles of zebrafish larvae using the UAS:RFP-GFP-LC3 x actin:Gal4 transgenic line has also been demonstrated. In this zebrafish line, the muscles expressed the LC3 proteins in both green and red (in case of an autophagosome) or only red (in case of an autolysosome) (Katherine Henry, personal communication).

Verapamil was used as an autophagy inducer based on a study presenting the inhibitory effect of verapamil on the intracellular currents of calcium via the L-type calcium channel, which reduces the activity of calpains, which

subsequently induces autophagy (Williams, Sarkar et al. 2008). However, verapamil did not show any effect on the survival of *S. aureus* infected zebrafish larvae (Figure 4.9.B.). Some studies contradict the verapamil effect on autophagy. Even though verapamil increases the number of LC3-GFP⁺ vesicles, it might not be a very powerful autophagy inducer, as it does not induce a change in the amount of FYVE-RFP⁺ levels in an image-based assay with mammalian cell culture. The authors believe that compounds that truly increase autophagy should also increase PI3P levels, which is measured by using FYVE levels as a marker (Zhang, Yu et al. 2007).

Two other pharmacological agents acting on calcium flux via other calcium channels could have a more potent pro-autophagic activity than verapamil, and could be tested for their autophagy effect: ionomyin, which raises the intracellular Ca²⁺ levels via their release from intracellular stores, and thapsigargin, which is a sarco-endoplasmic reticulum Ca²⁺/Mg²⁺-ATPase inhibitor (Gordon, Holen et al. 1993).

In a study using HeLa cells expressing the tandem fluorescent-tagged RFP-wasabi-LC3 reporter system, it was shown that even though rapamycin promotes the formation of autophagosomes, a high dose of rapamycin (30 µM) impairs autophagic flux by reducing the autophagosome/lysosome fusion, while a low dose of rapamycin (500 nM) has the opposite effect (Zhou, Zhong et al. 2012). While 30 µM of rapamycin is the dose used in the zebrafish experiments, it does not imply necessarily that it is the active dose that has penetrated the larvae to induce autophagy. A proper control would be useful to determine if the autophagic flux is impaired. In any case, it seems that the dosage of chemical autophagy inducers has to be considered as it can influence autophagy flux in cells, and possibly in zebrafish larvae.

4.6.2.2. Autophagy inhibiting drugs

The utilisation of autophagy inhibitors in the *S. aureus*-zebrafish infection model also revealed several interesting results. The treatment of infected zebrafish larvae has been demonstrated with either wortmannin or LY294002 and in both cases increased the mortality of the fish (Figures 4.10.A. and B.). These compounds have been widely used (especially wortmannin) as

autophagy inhibitors in numerous studies. However, these compounds also inhibit PI3K. Therefore, these results could be due to the inhibition of autophagy or due to the PI3K inhibition. A study using endothelial cells showed that the PI3K-Akt-mTOR pathway is important for *S. aureus* internalisation (Oviedo-Boyso, Cortes-Vieyra et al. 2011). In addition to its role in phagocytosis, PI3K has a vital role in the chemotaxis of leukocytes (Stephens, Ellson et al. 2002), which is important in resolving infections. If the phagocytosis of *S. aureus* and/or the chemotaxis of leukocytes were impaired in the zebrafish infection model, it could explain the lower survival rate of the infected larvae treated with wortmannin or LY294002 compared to the control (Figures 4.10. A. and B.). An experiment to test these two options would be to perform a phagocytosis visualisation assay using fluorescently-labelled bacteria to check their internalisation by microscopy, in both infected treated group and infected untreated group of fish. The chemotaxis could be tested via a tracking experiment of fluorescently marked leukocytes.

In the *S. aureus*-infected zebrafish larvae experiments, no difference in the survival curves was observed when treated with +/-BayK 8644 (Figure 4.11.), NAC (Figure 4.12.A.) or vitamin E acetate (Figure 4.12.B.). Calpains control basal autophagy via the cleavage of Atg5 (Xia, Zhang et al. 2010). During *S. aureus* infection, the α -hemolysin toxin released by the bacteria induces autophagy, via inhibition of calpains (Mestre and Colombo 2012). However, the +/-BayK 8644 compound inhibits autophagy via a positive effect on L-type calcium channels to increase the calcium flux, which activates the calpains and subsequently inhibit autophagy. The mode of action of *S. aureus* α -toxin and the +/-BayK 8644 drug seem to be contradictory, which could explain the same survival curves obtained in the experiments comparing the infected zebrafish larvae treated with +/-BayK 8644 to the DMSO-treated control group. Indeed, the inhibitory effect on calpains induced by *S. aureus* could be winning against the activation effect on calpains induced by +/-BayK 8644 due to the opening of calcium channels, resulting in an overall inhibition of calpains. The treatment of the infected zebrafish larvae with 10 μ M of NAC did not have any effect on the survival

curve compared to the control group (Figure 4.12.A.), probably because of the too low concentration of drug used. The concentration of 300 μ M was recommended to be effective on zebrafish (Underwood, Imarisio et al. 2010), however, that concentration was toxic after 1 day of incubation when using 30 hpf embryos. The lower concentration of NAC that was not toxic for the larvae was 10 μ M (Figure 4.6.E.). Vitamin E acetate was one of the 22 compounds issued from the secondary screen, and previously tested at 10 μ M, unsuccessfully (see Chapter 3). At the higher concentration of 1 mM, vitamin E acetate should have an inhibitory effect on autophagy by enhancing the mTOR activity (Underwood, Imarisio et al. 2010), but did not influence the survival of infected zebrafish larvae (Figure 4.12.B.).

The last two autophagy inhibitors tested on the *S. aureus*-zebrafish infection model were ammonium chloride (NH_4Cl) and nocodazole. These two compounds are autophagy inhibitors that prevent the fusion of the autophagosome with the lysosome. Interestingly, the survival curve of the larvae infected with 2250 CFU of *S. aureus* and treated with NH_4Cl was highly significantly lower than the control group (Figure 4.13.B.). However, this was only a one-time experiment, which was not confirmed in two others experiments using a staphylococcal dose of 1650 CFU (Figure 4.13.A.) or 3700 CFU (Figure 4.13.C.). NH_4Cl blocks autophagosome/lysosome fusion, which allows to investigating autophagy flux, especially if used in combination with other pro- or anti-autophagic compounds (Underwood, Imarisio et al. 2010). The dose (10 μ M) and time of exposure (30 min) of nocodazole used to treat infected embryos in the experiments follow the same experimental procedure of a previous study using nocodazole on zebrafish larvae in an *in vivo* inflammation study. The disruption of microtubules induced by the treatment of zebrafish embryos with nocodazole impaired the recruitment of macrophages to the wound. This recruitment problem is due to the activation of the small GTPase Rho, as the concomittent treatment of nocodazole and the Rho kinase inhibitor Y-27632 restores the recruitment of macrophages (Redd, Kelly et al. 2006). The activation of the small GTPase Rho by the microtubule disassembly was also shown in human neutrophils, which interferes with the polarity of these

cells (Niggli 2003). If the recruitment of leukocytes is impaired by the depolymerisation of microtubules, is it more likely that the normal phagocytosis of bacteria by neutrophils and macrophages is impaired as well. This process would explain the low survival curve of the treated group compared to the DMSO group (Figure 4.14.), which is unrelated to autophagy, but more important for a good control of *S. aureus* infection.

Because of unknown off-target of chemical compounds used, another approach modulating the autophagy pathway was required. Important proteins involved in the formation of autophagosome are known – the ATG proteins. Therefore, a genetic approach to modulate autophagy was tested.

4.6.3. Morpholino approaches

The morpholino (MO) technique was used to transiently knockdown specific core genes of the autophagy pathway and the survival of *S. aureus* infected morphants was compared to the control group. In this study, the injection of different sets of MOs targeting *atg5*, *atg7* and *atg10* did not influence the survival curve of the infected fish compared to the control group (Figures 4.15. and 4.16.). The results of the experiments using *atg16l1* MO were more questionable. There was a decrease of the survival curve between the infected control group injected with the mismatch control MO compared to the infected group injected with the Atg16L1 MO. However, the fish injected with mismatch control MO did not all look healthy, having most likely off-target effects. Therefore an infected, but MO uninjected group of fish was carried out alongside. The survival curve of this last group (infected and no MO) was comparable to the infected Atg16L1 MO group (Figures 4.15.C. and D.). The experiment with Atg16L1 MOs was only carried out once with Atg16L1-1 MO and once with Atg16L1-2 MO, so replicates would be necessary to make a firm conclusion. However, the comparison of the MO to the uninjected control appeared to be more reliable than the mismatch control. The initial trend observed with these one-time experiment suggests that the Atg16L1 knockdown confers a survival advantage to the *S. aureus* infected zebrafish embryos.

One question that arises when using MO is their actual efficacy, related to the dose of MO initially injected. While the embryo grows, the efficacy decreases as the MO becomes more diluted in the cells. The doses chosen in some experiments were following the recommendations of some collaborators who provided the MO (*atg5-1*, *atg5-2*, *atg16l1-1*, *atg16l1-2*, *atg10* start, *atg10* splice). The evaluation of the effective knockdown of start MO is more difficult than splice MO. As there was no clear phenotype generated by the above-mentioned MOs, their efficacy could be assessed using antibodies of the proteins of interest if they are available and work well *in vivo* (Hutchinson and Eisen 2006), otherwise the utilisation of western-blotting can be performed (Nasevicius and Ekker 2000). The efficacy of the MO received from collaborators could have been lost over time. Even though MOs are usually stable with some examples of MOs with a shelf life of more than 7 years, some other MOs in aqueous solution can lose efficacy after a few weeks. Effective knockdown of splice MO can be assessed by RT-PCR, which was performed with *atg5* splice MO and *atg7* splice MO. The efficacy was partial at 2 dpf with the dose used in the experiments (6 ng), which could explain the not significant change in the survival curves, especially as 50% knockdown of RNA does not implicate 50% reduction in protein levels.

Next to the question of its efficacy, the second major problem with the use of MO is the off-target effects, meaning that the MO can inhibit the function of an irrelevant gene instead of, or as well as, the desired gene. Comparing the phenotype obtained with the MO to an existing mutant is advisable (Eisen and Smith 2008).

Following the hypothesis that *S. aureus* growth is favoured when host autophagy is active, and based on the MOs experiments that did not show any difference at the level of the survival of infected zebrafish larvae, either the MOs were not effective enough, or the autophagy protein knockdown were not as important for autophagosome formation as expected. It has been reported that in certain stress conditions different to starvation, autophagy can also occur in an alternative Atg7/Atg5-independent pathway, which leads

to the bulk degradation of cellular proteins, similar to conventional autophagy (Nishida, Arakawa et al. 2009). In alternative pathways of autophagy, LC3 proteins are not involved, but the GTPase Rab9 is required for the formation of autophagic vacuoles (Shimizu, Arakawa et al. 2010). Therefore, Rab9 is a potential marker of alternative pathway of autophagy that could be used to test the formation of autophagosome in an unconventional way.

4.6.4. Autophagy visualisation

In the *in vivo* visualisation experiments using the Tg(UAS:RFP, GFP) transgenic zebrafish lines that were specifically expressing the LC3 proteins in neutrophils (*mpx:Gal4*) or macrophages (*mpeg1:Gal4*), different situations have been observed.

LC3 proteins are autophagy markers decorating autophagosomes. Green and red colours should be expressed in presence of an autophagosome, while only red colour should be expressed in presence of autolysosome. Some cells were completely coloured and had some brighter spots of one colour, as seen in infected macrophages (Figure 4.22.) and rapamycin-treated neutrophils (Figure 4.28.). Dominant colours could be revealing some specific stage of autophagosome formation: a dominance of red colour could be a sign of autolysosome (Figure 4.25.).

In some *S. aureus* infection experiments using CFP-tagged bacteria, colocalisation of blue bacteria with the red and green colours of LC3 proteins was obvious (Figures 4.27. and 4.33.). In other cases it can be assumed there was a colocalisation even though the 3 colours (green, red and blue) appeared next to each other on the image (Figure 4.36.). Indeed, the capture of each set of pictures was performed with 4 different channels opening one after another for each focal plane. The succession of these channels was DIC, GFP, RFP and CFP, which is consistent with the order of colours seen in some 'almost colocalisation' images. In fact, these images were performed in living zebrafish larvae, meaning that any cells, in particular circulating neutrophils and macrophages, can move during the capture of the images. Using fixed samples could be a solution for better colocalisation images, but

that could affect the advantages of the dynamic aspect of live imaging that the zebrafish model offers.

In both macrophage and neutrophil pictures, a situation arose in which *S. aureus* bacteria were contained in a small compartment such as a vacuole that was also decorated with red and green dots corresponding to LC3 proteins (Figures 4.23. and 4.31.). These *S. aureus* containing LC3 decorated vacuoles could be autophagosomes, therefore linking *S. aureus* infection to host autophagy.

In the experiments performed with *S. aureus* infected *frozen* mutant zebrafish expressing LC3 proteins in neutrophils, three cases of 'almost colocalisation' of colours were observed (Figure 4.35. and 4.36.). This suggests that vacuoles decorated with LC3 proteins can be formed in the mutant zebrafish line. This would theoretically be impossible in the traditional pathway of autophagy formation if the mutation was impairing Atg10, an important E2 enzyme required for the formation of the Atg12-Atg5 complex. Therefore, these pictures of LC3 expressing cells reinforce the new hypothesis that the *frozen* mutant is not a knockout *atg10* mutant.

Some conclusions can be drawn from this autophagy visualisation data. During the first few hours following the infection of *S. aureus* in zebrafish embryos and at least up to 6 hpi, macrophages or neutrophils having internalised bacteria can express LC3 proteins, suggesting the formation of autophagosomes in these immune cells, or the recruitment of autophagy proteins to the *S. aureus* containing compartment. This is coherent with published data in which *S. aureus* colocalise with LC3 proteins in infected HeLa cells, with a maximum at 3 hpi (Schnaith, Kashkar et al. 2007). Secondly, the bacteria and LC3 proteins can be localised together in a closed small compartment inside the cell, even though this is not always the case. Finally, the *frozen* mutant zebrafish line is able to express coloured LC3 proteins in macrophages and neutrophils, similar to their siblings.

Even if LC3 proteins are commonly known as autophagosome markers,

these proteins can also be recruited to other membranes including single-membrane phagosomes. This process is called LC3-associated phagocytosis (LAP), involving the recruitment of LC3 by phagosomes containing bacteria, dead cells or even latex beads (Sanjuan, Dillon et al. 2007; Gong, Cullinane et al. 2011; Martinez, Almendinger et al. 2011). Therefore, a LC3-positive compartment does not necessarily imply that this compartment is an autophagosome. The main difference is the double or single membrane(s), indicating an autophagosome or a LAP respectively. The single or double membrane(s) can be detected with powerful microscopy such as electron microscopy. The formation of LAP was demonstrated for *Burkholderia pseudomallei* (Gong, Cullinane et al. 2011) and *Mycobacterium marinum* (Lerena and Colombo 2011) in macrophage RAW264.7 cell line. In the case of *Listeria monocytogenes*, this structure is called spacious *Listeria*-containing phagosome, which is an intracellular niche of slow-growing *Listeria* associated with persistent infections (Lam, Cemina et al. 2013). These examples illustrate that some autophagy components, in particular LC3 proteins, can be associated with a different pathway than canonical autophagy. Therefore, these experiments show that *S. aureus*-containing vacuoles can be decorated with LC3 proteins, but further investigation is needed in order to determine the type of autophagy or other LC3-associated process, for example with electron microscopy.

4.6.5. Conclusions

Much of the work presented in this chapter has focused on modulating or visualising autophagy in the context of *in vivo* infection of *S. aureus* in zebrafish larvae. Based on experiments with the *frozen* mutant zebrafish line and published cell infection studies, the working hypothesis was that autophagy confers a survival advantage for *S. aureus* over the infected host. Most of the experiments using chemical modulation of autophagy and knockdown of autophagy with the morpholinos technique did not produce clear evidence that the hypothesis is true or false. Off-target effects of these approaches are most likely, and other experimental conditions modulating autophagy in a more reliable way are required, such as the utilisation of

autophagy mutant zebrafish line. The *in vivo* visualisation experiments showed that most of *S. aureus* contained macrophages and neutrophils were also decorated with LC3 proteins, an important autophagosome marker. This suggests that at least some of the autophagy machinery is required in host management of *S. aureus* infection.

Because of the off-target effects of the techniques used in this chapter, a more reliable approach tackling the question of the importance of autophagosome formation in *S. aureus* infection is required. Knocking out an important gene of a molecular process is a scientific method to test its biological usefulness. Therefore, an essential autophagy gene deletion approach is described in the next chapter.

Chapter 5: Generation of zebrafish *apg3l* mutants by genome editing with TALENs.

5.1. Introduction

Cell-based studies have shown that *S. aureus* can subvert the host autophagy pathway to survive and replicate in autophagosome-like vacuoles, before killing host cells (Schnaith, Kashkar et al. 2007). The impact of autophagy on *S. aureus* infection can be further studied using strategies involving the modulation of host autophagy. A better understanding of the role of autophagy in *S. aureus* infection is required in order to develop novel treatment strategies to treat staphylococcal infections. Zebrafish is a suitable model organism that can easily be genetically modified, and the *S. aureus*-zebrafish embryo is a well-characterised infection model system (Prajsnar, Cunliffe et al. 2008; Prajsnar, Hamilton et al. 2012). To avoid the side effects that occur with pharmacological compounds for autophagy modulation or gene knockdown with the morpholino technique (see chapter 4), a knockout strategy of an essential autophagy gene was used. The first part of this chapter presents the generation of a knockout zebrafish mutant of the *apg3l* gene, using the TALEN technology. The second part examines the effect of a systemic staphylococcal infection into 3 different knockout zebrafish lines for 3 different autophagy genes: *apg3l*, *atg5* and *atg10*, illustrating the outcome of reduced host autophagy on *S. aureus* infection into zebrafish larvae.

5.1.1. Genome editing with TALENs

Site-directed mutagenesis is a molecular biology tool that introduces a specific and intentional change in the DNA sequence of a gene. The targeted gene inactivation is a powerful strategy to study how the genotype influences the phenotype by investigating the structure or the loss of biological function of the gene, RNA or protein derived from the inactivated gene. Early mutagenesis tools introduced random and non-specific mutations by using

chemical mutagens or radiation. Since then, scientists have developed other methods to facilitate the creation of mutations at a specific gene location. In the past decade, a genome-editing technology approach has been developed, enabling manipulation of virtually any gene in any cell type or organisms. The engineered-endonucleases (EENs) are efficient genome-editing techniques generating specific genomic mutations. EENs are composed of a sequence-specific DNA-binding domain fused to a non-specific DNA cleavage module. Transcription activator-like effector nucleases (TALENs) are part of the EENs family, as are zinc-finger nucleases (ZFN) and clustered regularly interspaced short palindromic repeats CRISPR-associated (Cas) system (Gaj, Gersbach et al. 2013).

TALENs consist of specific DNA-recognition components called TALEs domains and DNA-cleavage components called FokI domains. Transcription activator-like (TAL) effectors are key virulence factors naturally produced by phytopathogenic bacteria in the genus *Xanthomonas*. TAL effectors naturally bind to plant host DNA to induce the transcription of effector-specific host genes leading to changes in the plant development contributing to disease symptoms. TAL effectors are typically composed of 1.5 to 28.5 almost identical repeats. These repeats have a length of 34 amino acids including a polymorphic pair of adjacent residues at positions 12 and 13 that are called a 'repeat-variable di-residue' (RVD). The specificity of the target depends on these RVDs, one RVD recognising one base pair of the DNA (Boch, Scholze et al. 2009; Moscou and Bogdanove 2009). TALENs are the fusion of TAL effectors to FokI nuclease. The TAL effectors bind specifically to a genomic region of interest and the catalytic domain of FokI induces targeted DNA double-strand breaks (DSBs). TALENs work in pair, binding opposite targets across a spacer region over which the 2 FokI domains join together to create the DNA break (Cermak, Doyle et al. 2011). DSBs are then repaired by the well-conserved error-prone non-homologous end-joining (NHEJ) system or by homology directed repair (HDR). The NHEJ repair system often creates small insertions or deletions, resulting in a knockout of gene function via frameshift mutations. In the presence of a donor plasmid with extended homology arms, HDR can lead to the introduction of single or multiple

transgenes to replace or correct the existing genes (Wyman and Kanaar 2006; Shrivastav, De Haro et al. 2008).

TAL effectors have been successfully customised to create targeted transcription factors. They have a wide range of flexibility in target site, which enables the design and construction of artificial effectors with specificities to any region of a gene of interest, including the methionine translation start site. The TALEN technique induces successful mutations in plants (Li, Liu et al. 2012; Shan, Wang et al. 2013; Zhang, Zhang et al. 2013), human pluripotent cells (Hockemeyer, Wang et al. 2011; Ding, Lee et al. 2013; Frank, Skryabin et al. 2013), yeast (Li, Huang et al. 2011), drosophila (Katsuyama, Akmammedov et al. 2013), *Xenopus* (Lei, Guo et al. 2012; Lei, Guo et al. 2013), sea urchin (Hosoi, Sakuma et al. 2014), zebrafish (Cade, Reyon et al. 2012; Moore, Reyon et al. 2012; Zu, Tong et al. 2013), mouse (Qiu, Liu et al. 2013; Sung, Baek et al. 2013; Wefers, Panda et al. 2013) and rats (Ponce de Leon, Merillat et al. 2014). Compared to ZFN-induced mutations *in vivo*, TALENs are 10-fold more efficient to generate targeted DNA mutations in developing zebrafish, in both somatic and germline tissues. The indel mutations introduced by the TALENs can have a wide diversity of lengths (Moore, Reyon et al. 2012; Chen, Oikonomou et al. 2013). Deleting large chromosomal sequences is also possible by using 2 pairs of TALENs instead of 1. In this case, one pair would target an early exon and another would target a late exon of the coding sequence. When the FokI nucleases cut at both targeted sites, the whole chromosomal region located between the 2 target sites of the TALENs can be lost (Ma, Lee et al. 2013; Xiao, Wang et al. 2013).

The construction of the TALENs is based on Golden Gate cloning to assemble multiple DNA fragments in an ordered fashion, in a single reaction. The Golden Gate method uses Type IIS restriction endonucleases, which cleave outside their recognition site, creating unique 4 bp overhangs. Digestion and ligation happen in the same reaction mixture, which increases the speed of the cloning. The assembly of a custom TALEN can be

performed in 5 days involving 2 steps explained in detail in the paper written by Voytas's group (Cermak, Doyle et al. 2011).

5.1.2. The importance of ATG3 in the autophagy pathway

ATG3 is an autophagy-like protein that takes part in the sequestration of cytoplasmic constituents leading to the formation of autophagosomes. At the molecular level, ATG3 acts as the E2 enzyme required for the LC3 lipidation process (Ichimura, Kirisako et al. 2000). The high-energy ATG3-LC3 intermediate is activated by ATG7, and then recruited to the membrane via the interaction between ATG3 and ATG12 (Tanida, Tanida-Miyake et al. 2002). ATG3 catalyses the lipidation reaction between LC3 and phosphatidylethanolamine (PE) at a membrane location specified by the ATG16L complex that performs an E3-like role (Fujita, Itoh et al. 2008). Therefore, ATG3 is a crucial enzyme for autophagocytosis.

The homologous gene to the human autophagy-related protein *ATG3* in the zebrafish is called *APG3* autophagy 3-like and symbolised by *apg3l*. The *apg3l* gene is conserved in human, chimpanzee, Rhesus monkey, dog, cow, mouse, rat, chicken, fruit fly, mosquito, *C. elegans*, *S. pombe*, *A. thaliana*, and rice. The zebrafish *apg3l* gene has only 1 transcript (1 splice variant) with 12 coding exons. The zebrafish *Apg3l* protein is 317 amino acids long, while the human *ATG3* protein is 314 amino acids long. A BLAST (Basic Local Alignment Search Tool) shows that the 2 protein sequences share 84% identity (Figure 5.1.).

5.1.3. Aims and hypotheses

The first aim of this chapter is to generate a zebrafish mutant for the *apg3l* gene using the TALEN technology. The second aim of this chapter is to explore the *in vivo* effects of host autophagy knockout on *S. aureus* infection in the zebrafish embryo model. It is hypothesised that a *S. aureus* infection experiment using a mutant zebrafish line for an important *Atg* protein should be disadvantageous for the bacteria, and therefore promote host survival.

5.2. Generation of an *apg3l* mutant zebrafish line

5.2.1. Construction of the TALENs targeting exon 4 of the *apg3l* gene

In the *Danio rerio* Tuebingen strain genomic sequence information, *apg3l* gene is located on chromosome 6 and has 12 coding exons. Using the <https://tale-nt.cac.cornell.edu/node/add/talen-old> online program, a suitable pair of TALENs located on exon 4 was designed. The parameters chosen were a length of TALEs from 15 to 21 RVDs and a spacer of 15 to 18 bp with a T preceding each TAL binding site. These parameters match the parameters usually found in natural TALENs, from which general guidelines for the design of TALENs have been written (Cermak, Doyle et al. 2011). A pair of PCR primers amplifying a DNA segment that included both TALENs and the spacer region was designed. In addition, the restriction enzyme MwoI was chosen because it recognises a wide restriction site that appeared exclusively inside the spacer region. The customised TALENs designed against the exon 4 of the zebrafish *apg3l* gene are represented in Figure 5.2.

The left and right TALEN subunits were each initially constructed in two halves that were afterwards joined together along with the last RVD. The first 4 reactions assembled the Left part A, the Left part B, the Right part A and the Right part B. The parts A and B of each TALEN were then ligated together, as well as the last RVD and the destination vector. Part A was assembled into plasmid pFusA with the first 10 RVD plasmids, while part B was assembled into the pFusB plasmid appropriate for the TALEN length remembering that the last RVD was not added to the pFusB. The Left TALEN of *apg3l* gene had 17 RVDs and therefore pFusB6 was used for this part B; while the Right TALEN of *apg3l* gene had 16 RVDs and therefore pFusB5 was used for this part B. The RVD plasmids of parts A and B of each TALEN were assembled together into the correct pFusB plasmid using a Golden Gate reaction. The plasmids were then transformed into NEB10Beta competent cells and plated on spectinomycin/Xgal LB plates. Minipreps were performed on an overnight culture grown from single white colonies of the 4 different transformed cells. The extracted DNA plasmids were checked on a

gel following a NheI + XbaI digest. There were 3 visible bands for each part located at 266 bp, 2132 bp and between 500 bp and 1100 bp depending on the number of RVDs, being 10 RVDs for the parts A, 6 RVDs for the Left part B and 5 RVDs for the Right part B (Figure 5.3.A.). The parts A and B were then ligated together, along with the last RVD, an NG, and inserted into the destination vector, using a second Golden Gate reaction. The Left and Right TALEN plasmids were transformed and plated on carbenicillin/Xgal LB plates. The plasmids were extracted using midipreps nucleobond kit, and were then checked on a gel after a BamHI + XbaI digest. The Left TALEN generated 2 bands with a size of 2411 bp and 5322 bp (Figure 5.3.B.), and similarly, the Right TALEN generated 2 bands with a size of 2309 bp and 5322 bp. The two TALEN were mixed together and linearized using the NotI restriction enzyme, generating a thick band corresponding to the 7733 bp and 7631 bp bands expected from the Left and Right TALENs (Figure 5.3.D.). The correct sequences of the linearised L and R TALENs were confirmed by sequencing. Finally, RNA corresponding to the TALENs was synthesised using the Epicenter T7 MessageMax ARCA kit and run on a gel for a test (Figure 5.3.E.).

5.2.2. Testing the efficiency of the TALENs targeting exon 4 of the *apg3l* gene

Purified TALEN RNA synthesised *in vitro* was mixed with some phenol red and injected into 1-cell stage LWT zebrafish eggs at 0.5 nl, 1 nl or 1.5 nl. The efficiency of the TALEN to generate a mutation was tested on 3-day old zebrafish larvae. Genomic DNA was extracted from 5 individual uninjected larvae and 6 injected larvae for each dose. After PCR amplification and a MwoI digest on the 342 bp PCR products (Figure 5.4.A.), mutation analysis was performed. For uninjected samples, expected bands at 162 bp and 180 bp were visible (Figure 5.4.B.). There was also an extra third shorter band around 140 bp, as well as a fourth very short band around 40 bp. These 2 shorter bands were created by an unexpected polymorphism in the genome of LWT fish that we used (for more explanations, see section 5.3.3.). In samples injected with 3 different doses of TALEN RNA, 2 (or 3) cut bands

were visible, but an uncut band around 340 bp was also visible in at least 4 out of the 6 larvae tested. This uncut band indicated that a mutation had been created in the *MwoI* restriction site, preventing the enzyme cutting there as it normally would. This genetic sequence modification was due to the action of the TALENs that had cut in the spacer region, and an 'indel' (insertion or deletion) mutation had been generated following the NHEJ repair mechanism. The remaining larvae injected with 1 nl of the RNA TALEN were grown to adulthood in the aquarium.

5.2.3. Effects of genomic polymorphism in *apg3l* locus

A polymorphism of 2 bp was discovered in the intronic region between exon 3 and exon 4 of the *apg3l* gene, creating an additional *MwoI* restriction site in the PCR product generated using the *Atg3Tal1For* and *Atg3Tal1Rev* primers. In the absence of this polymorphism, according to the zebrafish genomic sequences obtained from the ZFIN data, the 342 bp PCR product should be cut once by the *MwoI* enzyme, generating 2 fragments of 162 bp and 180 bp. However, in the intronic region located about 50 bp earlier than the expected and known *MwoI* restriction site, there was a region with multiple thymine nucleotides. By sequencing the PCR product using the *Atg3Tal1For* primer, the chromatogram showed that this T region finished with GC. In addition, in some sequences, the peaks of the last 2 T included 2 smaller peaks that could be read as GC (Figure 5.5.A.). As the sequencing machine could have made a mistake in the reading of the sequence because of the repeating Ts, the presence of the 2 bp polymorphism was tested with another method. The gDNA of uninjected LWT embryos was used for this test - these uninjected fish being the same batch of fish used to initially inject the TALEN mRNA that were grown up. A PCR on the gDNA of the uninjected embryos was performed, and a *MwoI* digest was subsequently carried out. Both the PCR product and the *MwoI* digested products were run on an agarose gel. In the undigested lane, only the 342 bp PCR product was observed. In the *MwoI* digested lane, 3 bands were observed: the 2 expected bands at 162 bp and 180 bp, as well as a smaller one around 140 bp, which would match to the polymorphism hypothesis (Figure 5.5.B.). Both the sequencing and the gel

show that a real 2 bp polymorphism exists in some alleles of the *apg3l* gene in the LWT zebrafish strain. This polymorphism is a new pair of GC, which creates a new MwoI restriction site. Indeed, MwoI enzyme recognises a GCNNNNNNNGC sequence, meaning a sequence containing 2 pairs of GC separated by 7 random nucleotides. With the 2 bp polymorphism, the distance between the previous GC and the new GC generated by the polymorphism is reduced to 7 nucleotides, which is the length recognised by the MwoI enzyme. It is sufficient to create a new site recognised by the restriction enzyme (Figure 5.5.C.). This explains why the normal PCR product cut with MwoI generated 2 fragments of 162 bp and 180 bp, while the PCR product that includes the polymorphism cut with MwoI generated 3 fragments of 48 bp, 132 bp and 162 bp (Figure 5.5.D.).

5.2.4. Screening potential founder fish for a defective mutation in exon 4 of the *apg3l* gene

Adult fish injected with the TALEN were screened for founders that carry a mutation in at least some of their germ cells. Indeed, a germline mutation is detectable and heritable to the progeny. Each TALEN injected adult fish was outcrossed to a wild-type fish (LWT) of the opposite sex, and the progeny was tested for mutation using a PCR and restriction enzyme test. At 72 hpf, 8 pools of 3 larvae of every pairs of fish were put in wells of a 96-well plate and their gDNA was extracted. After the PCR with the Atg3Tal1 primers, a MwoI digestion was carried out and the products were run on an agarose gel. If the gel shows 3, 4 or 5 uncut bands out of the 8 lanes issued from the same progeny, the parent fish was considered as a founder (Figure 5.6.), and the progeny were further grown. Forty-two adult fish were screened, and 4 founders were selected.

```

1  MQNVINSVKGKTALGVAEFLTPVLKESKFKETGVITPEEFVAAGDHLVHHCPTWKWASGEE 60 zebrafish_apg31
1  MQNVINTVKGKALEVAEYLTPVLKESKFKETGVITPEEFVAAGDHLVHHCPTQWATGEE 60 human_atg3
*****:***, ** ***:*****:*****:***:***

61  AKVKPYLPNDKQFLLRNVPFCYKRCKQMEYSDELEAIIEDDGGWVDTPHNSGVTGVT 120 zebrafish_apg31
61  LKVKAYLPTGKQFLVTKNVPCYKRCKQMEYSDELEAIIEDDGGWVDTYHNTGITGIT 120 human_atg3
*** ***, ***:***:*****:*****:***:***:***

121  EAVREISLDNKNMNMNVKTGACNSGDDDDDEEGEAADMEEYEEESGLETTDDATLDTSK 180 zebrafish_apg31
121  EAVKEITLENKDNIRLQDCSALCEE---EEDEDEGEAADMEEYEEESGLETTDEATLDRK 177 human_atg3
***:***:***:***:***:***:***:***:***:***:***:***:***:***

181  MADLSKTKAEAGGEDAILQTRTYDLYITYDKYYQTPRLWLFQYDEDRQPLTVDQMYEDIS 240 zebrafish_apg31
178  IVEACKAKTDAGGEDAILQTRTYDLYITYDKYYQTPRLWLFQYDEQRQPLTVEHMYEDIS 237 human_atg3
!.: .*:***:*****:*****:*****:*****:*****:*****

241  QDHVKKTVTIENHPNLPPPAMCSVHPCRHAEMVKKIIETVAEGGGELGVHMYLLIFLKFV 300 zebrafish_apg31
238  QDHVKKTVTIENHPNLPPPAMCSVHPCRHAEMVKKIIETVAEGGGELGVHMYLLIFLKFV 297 human_atg3
*****:*****:*****:*****:*****:*****:*****

301  QAVIPTIEYDYTRHFTM 317 zebrafish_apg31
298  QAVIPTIEYDYTRHFTM 314 human_atg3
*****

```

Figure 5.1. BLAST alignment of zebrafish Apg3l protein sequence and human Atg3 protein sequence

The grey colour identifies the similar residues between the 2 orthologous protein sequences.

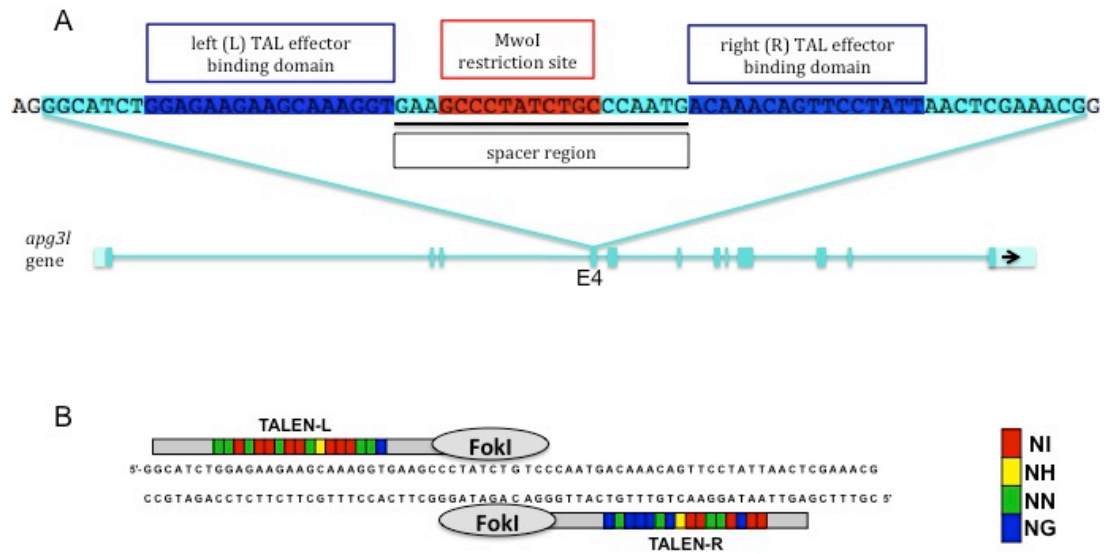


Figure 5.2. Design of the TALENs targeting the exon 4 of the zebrafish *apg3l* gene

A) Among the 12 exons of the *apg3l* gene, the sequence of the exon 4 is highlighted in light blue, the left and right TAL effector binding domains are highlighted in blue, the spacer region is underlined in black, and the MwoI restriction site is highlighted in red.

B) The left and right TALENs are composed of the RVDs corresponding to the targeted DNA sequences (see the coloured legend), and associated to the FokI nucleases creating a dimer that will cut somewhere in the spacer region.

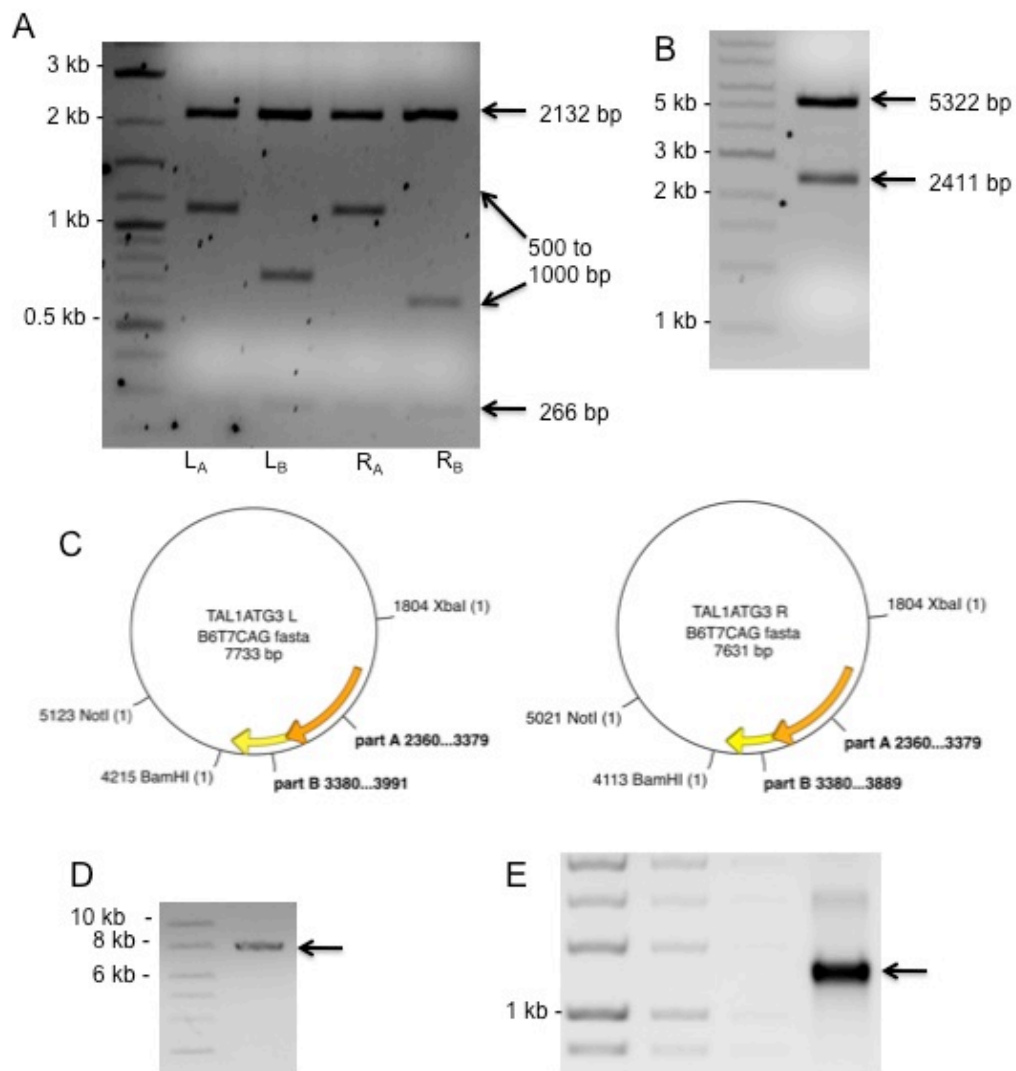


Figure 5.3. TALEN plasmid construction and the mRNA synthesis

A) NheI + XbaI digest of the DNA plasmid containing the subunits A and B of the left and right TALENs. There are 3 bands: 266 bp, 2132 bp and 500 bp-1100 bp depending on RVD number

B) BamHI + XbaI digest of the DNA plasmid containing the Left TALEN. There are 2 bands: 2411 bp and 5322 bp

C) Left and Right TALEN plasmids map

D) NotI digest linearising the TALENs plasmids, with a size of 7631 bp and 7733 bp

E) 0.5 μ l of mRNA synthesised *in vitro* using the 2 TALENs plasmids as templates.

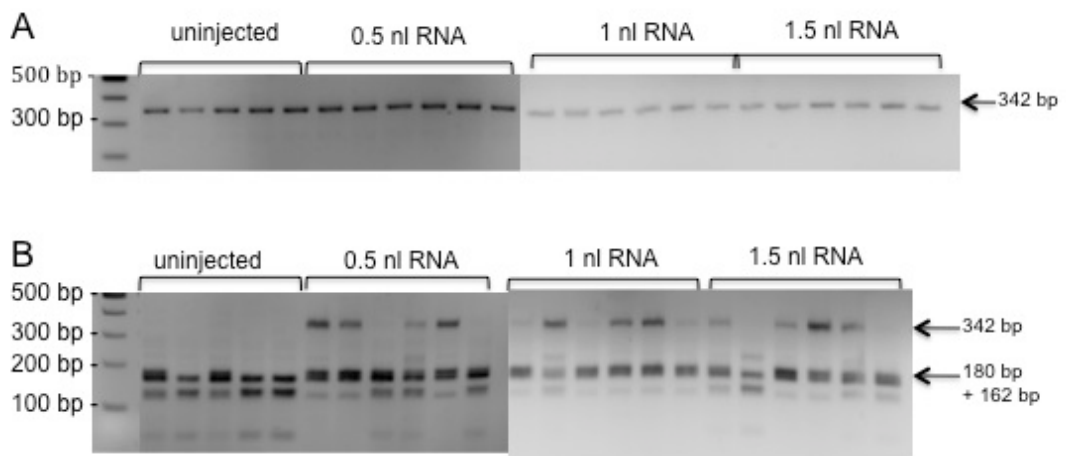


Figure 5.4. Testing the efficacy of apg3l TALEN after mRNA injection into 1-cell stage zebrafish egg

A) PCR on gDNA extracted from 3 dpf zebrafish injected at 1-cell stage with 3 doses of TAL ATG3 RNA. PCR product = 342 bp

B) MwoI digest realised on the PCR product from A. Cut bands = 162 bp + 180 bp

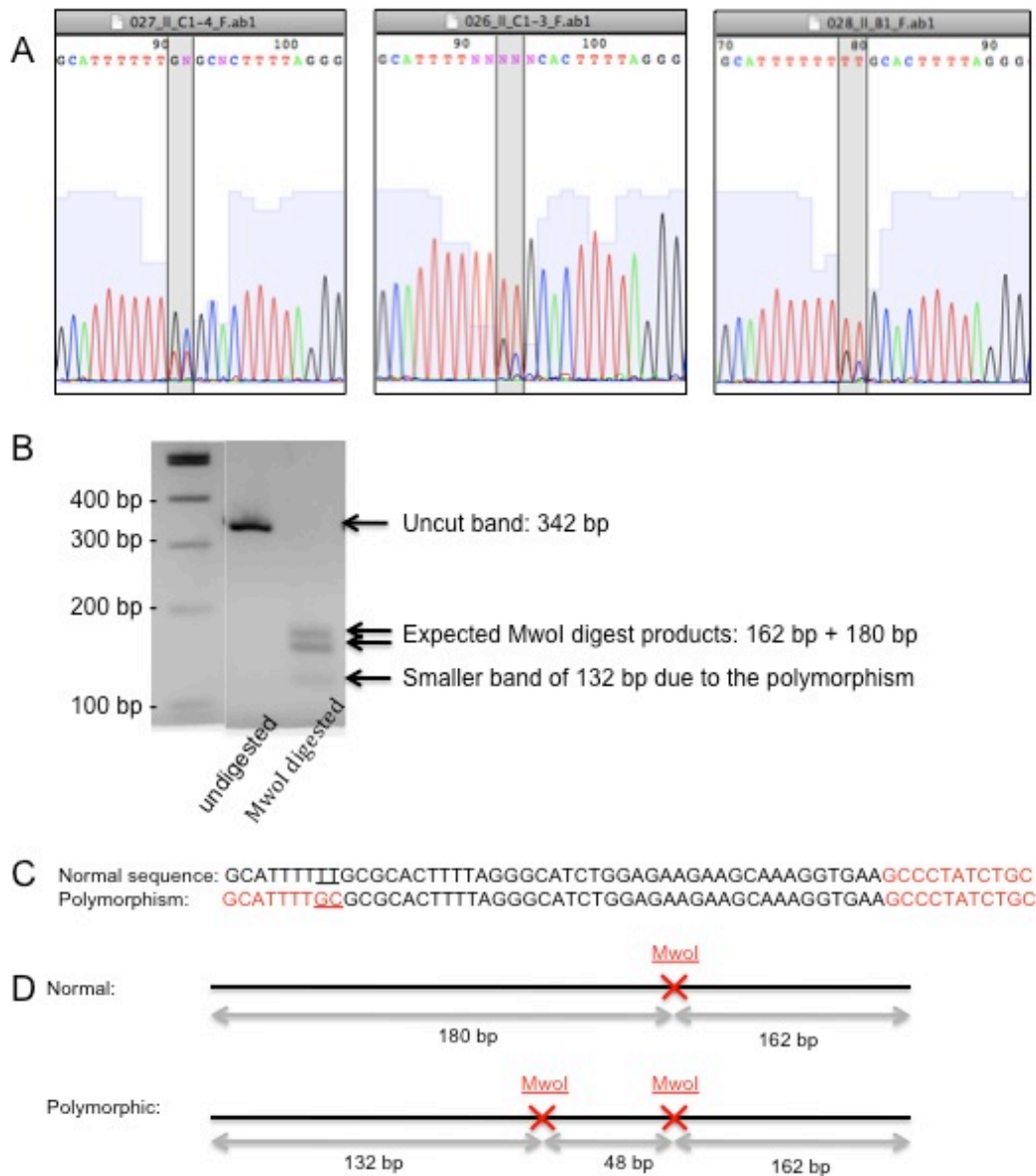


Figure 5.5. Effects of genomic polymorphism in *apg3l* locus

A) Portion of the sequencing of 3 different fish, highlighting the 2 bp polymorphism

B) PCR product of an uninjected LWT fish, before and after the MwoI digest

C) The changed sequence with the polymorphism of 2 bp underlined, and the MwoI restriction site highlighted in red

D) PCR product and MwoI restriction sites with and without polymorphism

5.2.5. Analysis of the *apg3l* mutation carried by the founder fish

Mutation of founder fish was determined by sequencing. An Atg3Tal1 PCR amplification was performed using one of the gDNA samples issued from the screen for the founders, in which an uncut band was observed on the gel (section 5.3.4.). The gDNA of the 4th lane was used as template for founder 1, the gDNA of the 8th lane was used as template for founder 2, the 4th lane was used as template for founder 3 and the 5th lane was used a template for founder 4. The PCR was cleaned with an Exol SAP treatment and sent for sequencing with the corresponding forward and reverse primers.

The results of the sequencing are represented on chromatograms, on which coloured peaks represent nucleotides. Starting somewhere in the spacer region, small peaks are visible in addition to the normal high peaks. This is the place where a mutation has been inserted. By reading the sequence of nucleotides generated by the small peaks alongside the high peaks, it is possible to determine the mutated sequence, and therefore working out what mutation has been introduced in the gene by the TALEN (Figures 5.7.A. and B, 5.8.A. and B., 5.9.A. and B., 5.10.A. and B.).

It was determined that founder 1 carries a 5 bp deletion (Figure 5.7.C.), founder 2 carries a 2 bp addition (Figure 5.8.C.), founder 3 carries a 10 bp deletion (Figure 5.9.C.) and founder 4 carries a 7 bp deletion (Figure 5.10.C.). All of these mutations introduce a frameshift in the 3-nucleotide codon sequence. The proteins translated from the mutated sequences should be shorter than the wild-type Apg3l protein and therefore be dysfunctional, due to the presence of an earlier stop codon generated by the mutation. The Expasy translation tool was used to obtain the hypothetical translated protein sequence generated from the mutated genomic sequence (Gasteiger, Gattiker et al. 2003). The comparison of the wild-type protein sequence of Apg3l to the predicted mutated protein sequence using a BLAST alignment shows that the protein sequence is similar up to the mutation point, after which several stop codons have been introduced in the mutated protein

sequence. The first stop codon is located a few residues after the site of mutation. Therefore, Apg3l mutated protein produced by the defective *apg3l* gene of founder 1 (called *apg3l*^{ΔCTATC}) should have only 67 amino acids (Figure 5.11.), Apg3l mutated protein produced by the defective *apg3l* gene of founder 2 (called *apg3l*^{+AT}) should have only 75 amino acids (Figure 5.12.), Apg3l mutated protein produced by the defective *apg3l* gene of founder 3 (called *apg3l*^{ΔCTATCTGCC}) should have only 71 amino acids (Figure 5.13.) and Apg3l mutated protein produced by the defective *apg3l* gene of founder 4 (called *apg3l*^{ΔCCCAATG}) should have only 72 amino acids (Figure 5.14.). These predicted mutated proteins are a lot shorter than the 317 amino acids of the wild-type Apg3l protein, and it is most likely that they are non-functional.

5.2.6. Generation of heterozygous fish carrying a defective mutation in exon 4 of the *apg3l* gene

Each founder fish was crossed to a wild-type fish of the opposite sex in order to produce a progeny carrying the mutation on one of the allele in every cell of the fish. Indeed, the founder fish does not carry the mutation in every cell of its germline, as highlighted by the screening step (section 5.3.4. and Figure 5.6.). Therefore, a first generation of progeny (F1) from the founders was generated. The progeny were grown up, and after 2-3 months, they were fin clipped and screened by PCR and restriction digestion. The fish that were effectively carrying the genetic mutation in the fin clip tissue were selected. A tank of heterozygous mutant zebrafish was created, with adult fish carrying a mutation in the *apg3l* gene on one of the 2 alleles of their genome, in every cell.

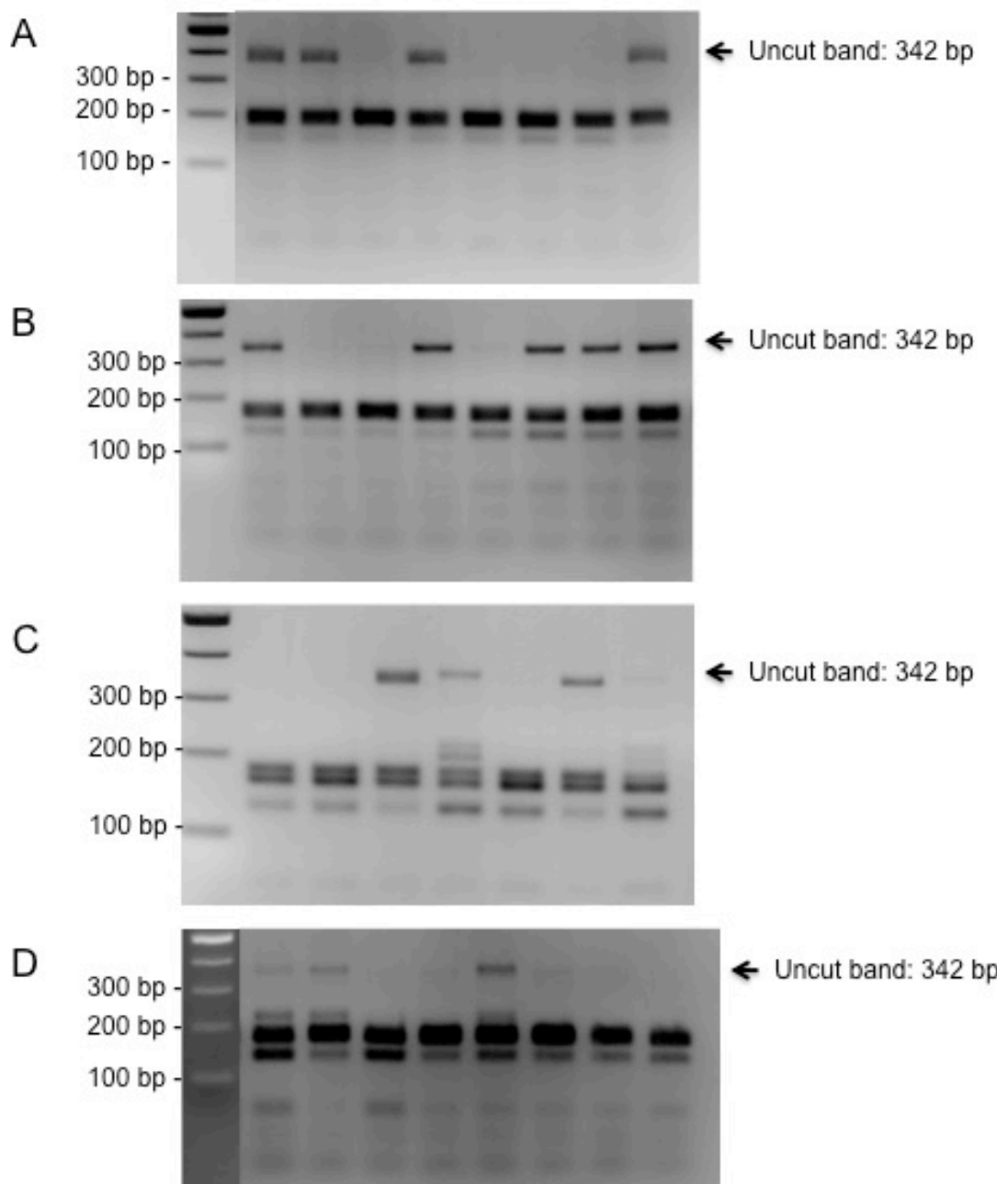


Figure 5.6. Screening the progeny of founder fish carrying an *Atg3* mutation

Gel of the *MwoI* digest of the *Atg3*Tal1 PCR product carried out on 8 pools of 3 embryos coming from an outcross between potential founder fish and LWT fish. The arrow highlights the 342 bp uncut band created due to a mutation. Screening test of the progeny from A) founder fish 1, B) founder fish 2, C) founder fish 3, D) founder fish 4

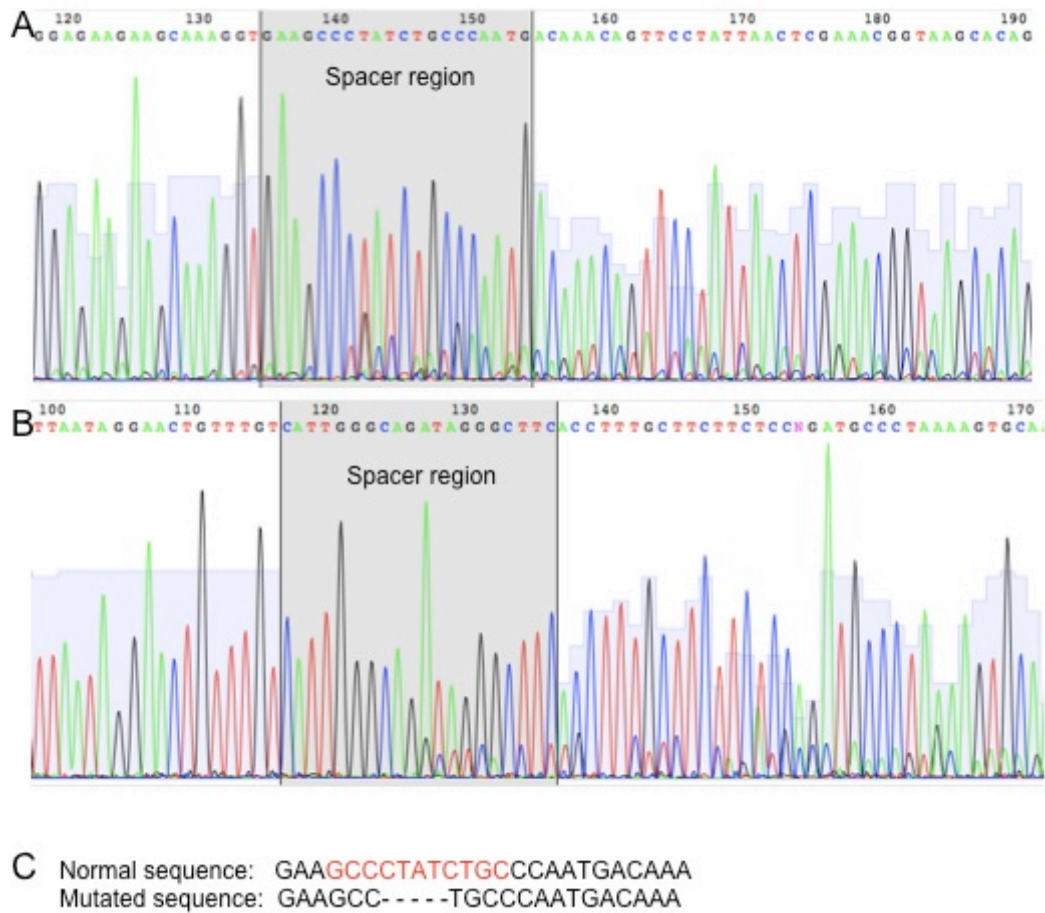


Figure 5.7. Sequencing result of founder 1 around the TALEN spacer region

Somewhere in the spacer region, a mutation has been generated, which is illustrated with the small double peaks in the chromatogram of the sequencing results A) using Atg3Tal1For primer, B) using Atg3Tal1Rev primer.

C) The normal sequence compared to the mutated sequence that has 5 bp deletion. The residues in red identify the MwoI restriction site in the normal sequence.

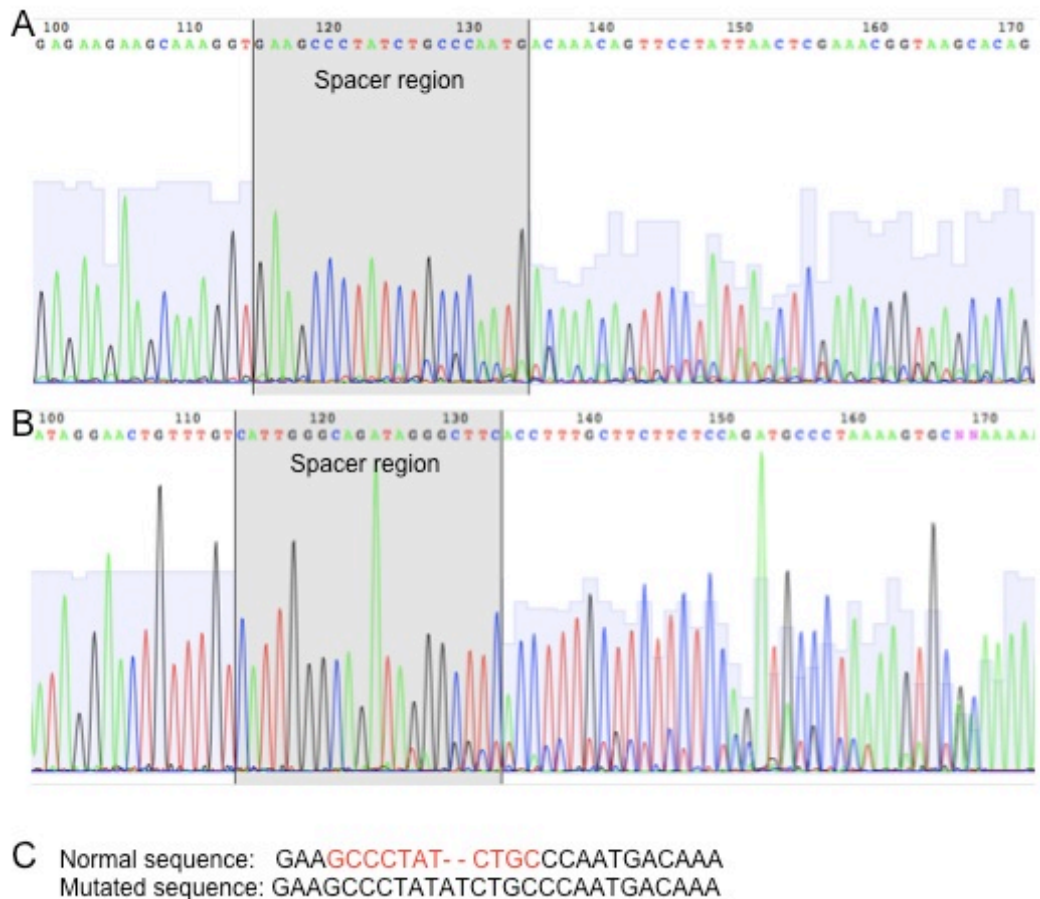
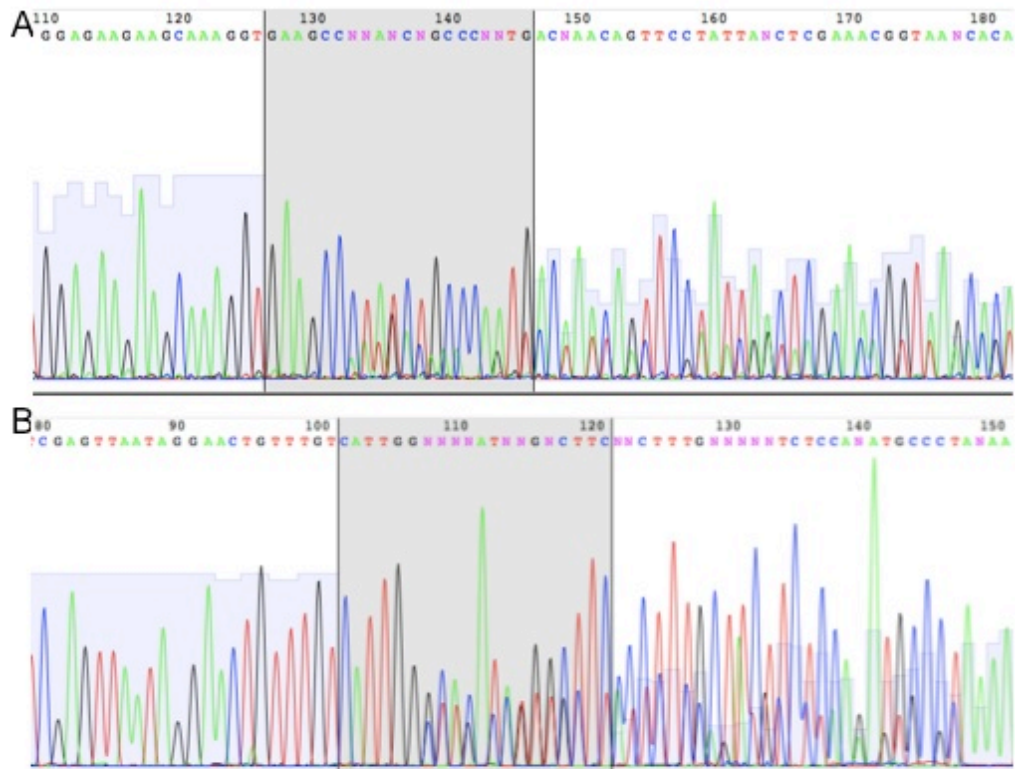


Figure 5.8. Sequencing result of founder 2 around the TALEN spacer region

Somewhere in the spacer region, a mutation has been generated, which is illustrated with the small double peaks in the chromatogram of the sequencing results A) using Atg3Ta1For primer, B) using Atg3Ta1Rev primer.

C) The normal sequence compared to the mutated sequence that has 2 bp addition. The residues in red identify the MwoI restriction site in the normal sequence.



C Normal sequence: GAAGCCCTATCTGCCCAATGACAAA
 Mutated sequence: GAAGCC-----AATGACAAA

Figure 5.9. Sequencing result of founder 3 around the TALEN spacer region

Somewhere in the spacer region, a mutation has been generated, which is illustrated with the small double peaks in the chromatogram of the sequencing results A) using Atg3Tal1For primer, B) using Atg3Tal1Rev primer.

C) The normal sequence compared to the mutated sequence that has 10 bp deletion. The residues in red identify the MwoI restriction site in the normal sequence.

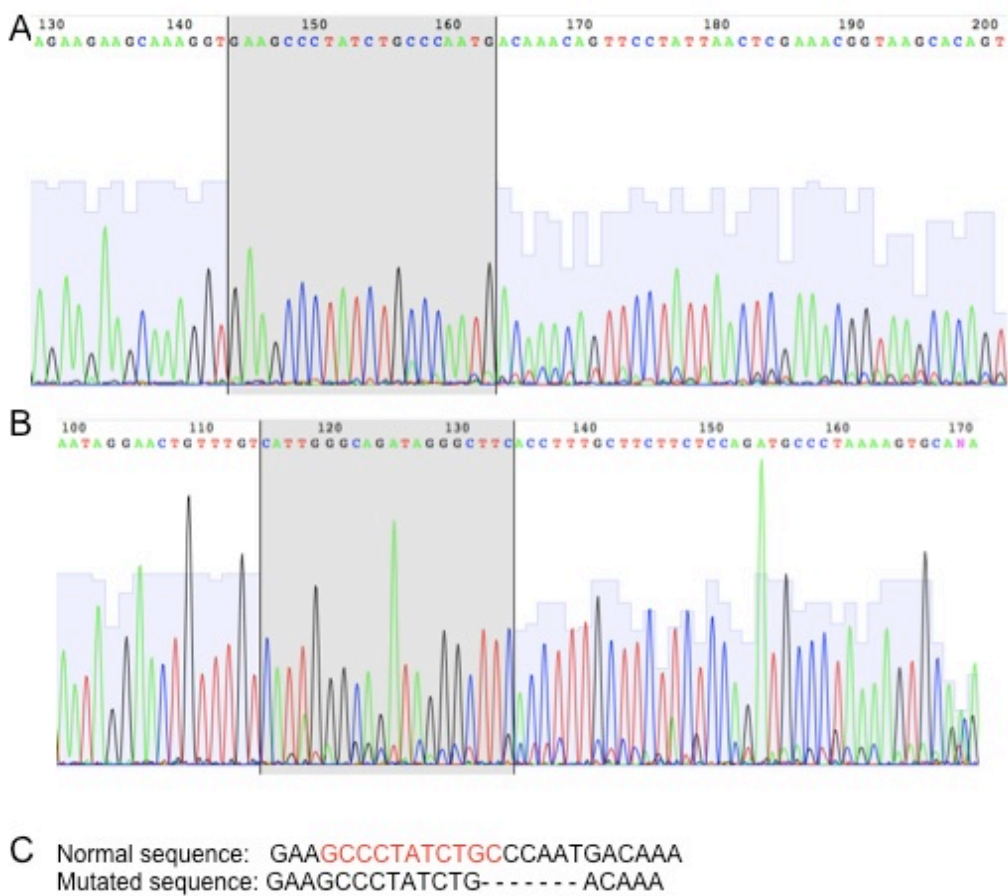


Figure 5.10. Sequencing result of founder 4 around the TALEN spacer region

Somewhere in the spacer region, a mutation has been generated, which is illustrated with the small double peaks in the chromatogram of the sequencing results A) using Atg3Ta1For primer, B) using Atg3Ta1Rev primer.

C) The normal sequence compared to the mutated sequence that has 7 bp deletion. The residues in red identify the MwoI restriction site in the normal sequence.

CLUSTAL O(1.2.0) multiple sequence alignment

```

wild-type      MQNVINSVKGTALGVAEFLTPVLKESKFKETGVITPEEFVAAGDHLVHHCPTWKWASGEE
founder1      MQNVINSVKGTALGVAEFLTPVLKESKFKETGVITPEEFVAAGDHLVHHCPTWKWASGEE
*****

wild-type      AKVKPYLPNDKQFLLTRNVPCYKRCKQMEYSDELEAII EEDDGGDGGVDTFHNSGVTGVT
founder1      AKVKPAQ*QTVPINSKRSML*A-----L*TDGVLR*AGGHHRRGRWRWRMGG--HLS*L
*****
          ↑
          STOP

wild-type      EAVREISLDNKDNMNMNVKTGACGNSGDDDDDEEGEADMEEYE-ESGLLETDDATLDTS
founder1      GCYR-----GD*SCS--GN---LIG**G*-YEYECEDGCLWK-----*W
. *
          : * . * :
          * . * * * .

wild-type      KMADLSKTKAEAGGEDAILQTRTYDLYITYDKYYQTPRLWLFGYDEDROPLTVDQMYE--
founder1      R---*R***RRRGRH-----GRI*RKWTFGNR*CHS*HK*NG*FK*N
:
          . * * .
          : * * * * : . . : :

wild-type      -----DISQDHVKKTVTI
founder1      *GRSWRGRCHSTDKNL*PVYHI*QILDPKTMAVWI**GQTASNCGSDV*RHQPGSC*KN
          * : : . .

wild-type      ENHPN-LPPPAMCSVHPCRHAEMVKKIIETVAEGGELGVHMYLLIFLKFVQAVIPTIEY
founder1      RHH*ESP*SPSTCYVLR*TSMQTR*GDE-KDYRDCGRRR*TR-----GPYVSSDFPEICA
..* :
          * : * *
          . : : **
          : * . : * *

wild-type      DY-----TRHFTM-
founder1      SCHSNNRVRLHKAFHHV
.
          : *
  
```

Figure 5.11. BLAST alignment between Apg3l zebrafish protein sequence and the hypothesised protein sequence due to the TALEN mutation

The mutated gene *apg3l*^{ACTATC} of founder 1 would produce a protein that has only 67 amino acids, because of the introduction of a stop codon due to the mutation.

* in the mutated sequence represent STOP codons

CLUSTAL O(1.2.0) multiple sequence alignment

```

wild-type      MQNVINSVKGTALGVAEFLTPVLKESKFKETGVITPEEFVAAGDHLVHHCPTWKWASGEE
founder2      MQNVINSVKG...
*****

wild-type      AKVKPYLPNDKQFLLTR---NV--PCYKRCKQMEYSDELEAII EDDGGGWVDTFHN...
founder2      AKVKPYICPM...
*****: .:  ↑ .:  : ..**.: . : :*  ** . : .
              STOP
wild-type      VTGVTEA-----VREISLDNKD-----NMNMNVKTGACGNSGDDDDDEEGEADME
founder2      LQG*LKLF...
: * :      : * * :      : * * : * .

wild-type      EYESGLET-----DDATLDTSKMADLSKTKAEAGGEDAIL
founder2      FWKQMP...
: :  * *      : * * : * : : : : : : : : : * : :

wild-type      QTRTYDLYITYDKYYQTPRLWLFGYDEDR-----QPLTV...
founder2      RTDS-----L*...
: * :      ** : . .      . ** : :

wild-type      NHPNLPPAMCSVHPCRHA...
founder2      ----SLHLLC--...
: * * * * : : : . .      . * : : . : : * . *

wild-type      --VQAVIPTIEYDYTRHFTM
founder2      TITQGISPC-----
. * . : *

```

Figure 5.12. BLAST alignment between Apg3l zebrafish protein sequence and the hypothesised protein sequence due to the TALEN mutation

The mutated gene *apg3l*^{AT} of founder 2 would produce a protein that has only 75 amino acids, because of the introduction of a stop codon due to the mutation.

* in the mutated sequence represent STOP codons

CLUSTAL O(1.1.0) multiple sequence alignment

```

wild-type      MQNVINSVKG TALGVAEFLTPVLKESKFKETGVITPEEFVAAGDHLVHHCP TWK WASGEE
founder3(2)   MQNVINSVKG TALGVAEFLTPVLKESKFKETGVITPEEFVAAGDHLVHHCP TWK WASGEE
*****

wild-type      AKVKPYLPNDKQFLLTRNVPCY-KRCKQMEYSDELEAIIEDDDGGGWVDTFHNSGVTVG
founder3(2)   AKVKPMTNSSY*LETFHVISAVNRWSTQMSWRPS*KRTMEMA---DGWTFPI TR-VLQG*
***** .. : : : . : ..**.: . : :*      ** . : . : *

wild-type      TEA-----VREISLDNKD-----NMNMNVKTGACGNSGDDDDDEEGEAADMEEYEE
founder3(2)   LKLF GKSHWIIRII*I*M-RRVPVEIVEMTMMMKKERRQ-----TWKNMKKVD FWKQ
:           :* * :           :*. * :*.           : .: : :

wild-type      SGLLETDDA-----TLDTSKMADLSKTKA EAGGEDAILQTRTY
founder3(2)   M PLLTQVKWLI*VKLRPKLE GKMPFYRQELMTCISHMTNITR--PQDYGCLDMMR TDS-
* * :           *: * : : : : : : : * * : : : * :

wild-type      DLYITYDKYYQTPRLWLFYGEDR-----QPLTV DQMYEDISQDHVKKTVTIENHPNL
founder3(2)   -----L* LWIRCMKTSARIMLK KPSPLRITLI-----
           ** : . . . ** : :

wild-type      PPPAMCSVHPCRHA EVM-----KKI IETVAEGGELGVHMYLLIF--LKF-----VQA
founder3(2)   SLHLLC--APYIHADTLR**KRLSRLWRKEEVNSGSICIF*FS*NLCKLSFPQQ-STITQG
: * * ** : : . : : . . . * : : : : : * * * * . * .

wild-type      VIPTIEYDYTRHFTM
founder3(2)   ISPC-----
: *

```

Figure 5.13. BLAST alignment between Apg3l zebrafish protein sequence and the hypothesised protein sequence due to the TALEN mutation

The mutated gene *apg3l*^{ΔCTATCTGCC} of founder 3 would produce a protein that has only 71 amino acids, because of the introduction of a stop codon due to the mutation.

* in the mutated sequence represent STOP codons

CLUSTAL O(1.2.0) multiple sequence alignment

```

wild-type      MQNVINSVKGTALGVAEFLTPVLKESKFKETGVITPEEFVAAGDHLVHHCPTWKWASGEE
founder4      MQNVINSVKGTALGVAEFLTPVLKESKFKETGVITPEEFVAAGDHLVHHCPTWKWASGEE
*****

wild-type      AKVKPYLPNDKQFLLRNVPC--YKRCKQMEYSDELEAIEEDDGGGVDTFHNSGVTG
founder4      AKVKPYLTNSSY*LETFHVISAVNRWSTQMSWRPS*KRTMEMA---DGWTPFITR-VLQG
***** *..      ↑
                STOP
wild-type      VTEA-----VREISLDNKD-----NMNMNVKTGACGNSGDDDDDEEGEADMEEYE
founder4      *LKLFGKSHWIIIRII*I*M*RRVPVEIVEMTMMMKKERQ-----TWKNMKKVDFWK
:              : * * :              : * * : * . :              : . : :

wild-type      ESGLLETDDA-----TLDTSKMADLSKTKAEAGGEDAILQTRT
founder4      QMPLLTQVKWLI*VKLRPKLEGKMPFYRQELMTCISHMTNITR--PQDYGCLDMMRTDS
:   * * :              * : * : : : : :   :   *   : : * :

wild-type      YDLYITYDKYYQTPRLWLFYDEDR-----QPLTVDQMYEDISQDHVKKTVTIENHPN
founder4      -----L*WIRCMKTSARIMLKKSPLRITLI-----
                ** :   . .   . ** :

wild-type      LPPPAMCSVHPCRHAEVM-----KKIIEIVAEGGELGVHMYLLIF--LKF-----VQ
founder4      -SLHLLC--APYIHADTLR**KRLSRLWRKEEVNSGSICIF*FS*NLKLSFQQ*STITQ
: *   *   * * : :   . : :   . .   . * : : : :   : * *   . *

wild-type      AVIPTIEYDYTRHFTM
founder4      GISPC*-----
. : *
    
```

Figure 5.14. BLAST alignment between Apg3I zebrafish protein sequence and the hypothesised protein sequence due to the TALEN mutation

The mutated gene *apg3*^{ACCCAATG} of founder 4 would produce a protein that has only 72 amino acids, because of the introduction of a stop codon due to the mutation.

* in the mutated sequence represent STOP codons

The fin clip screen was carried out on the F1 generation fish from founder 1 and founder 3. In the progeny of founder 1, 42 fish were fin clipped and screened, and 3 females were carrying the 5 bp deletion mutation *apg3*^{ΔCTATC}. This corresponds to a mutation transmission of 7%. In the progeny of founder 3, 58 fish were fin clipped and screened, and only 8 fish were carrying the 10 bp deletion mutation *apg3*^{ΔCTATCTGCCC}. This corresponds to a mutation transmission of 14%. Among the fish carrying the *apg3*^{ΔCTATCTGCCC} mutated gene, 2 types of gel patterns were distinguishable. Indeed, 3 fish (2 males and 1 female) showed the expected band around 350 bp, corresponding to an uncut PCR product, indicating the presence of the mutation in the TALEN spacer region (Figure 5.15.B. Type B. row b.). These fish were designed type B of the 10 bp deletion mutation type. However, the genotyping of 5 other fish (1 male and 4 females) were not showing the expected uncut band around 350 bp. They were still of interest, as they had a band around 210 bp, which is distinguishable to the expected normal cut bands at 180 bp and 162 bp. The 180 bp band was not actually seen, and instead there was a lower band around 130 bp. Therefore, these fish were called type A of the 10 bp deletion mutation type (Figure 5.15.B. Type A. row b.). The presence of the 10 bp deletion mutation was confirmed by sequencing, for both the fish carrying the type A and type B of the mutation.

5.3. Screening *atg5* mutant zebrafish line

An *atg5* mutant zebrafish line generated with the zinc-finger nuclease technique by Phil Ingham's group in Singapore was sent to Sheffield. The mutation is a 23 bp deletion in exon 3 of the *atg5* gene. Zebrafish *atg5* gene is located on chromosome 16 and has 7 exons.

The adult zebrafish were screened by fin clip. The genomic DNA was extracted from the fin clip, and was used as a template for a PCR with the first set of *Atg5* primers, amplifying a 644 bp product. The sequencing results of the PCR product with the *Atg5SeqRev* primer highlighted which fish were

carrying the mutation. Out of 40 fish screened, 25 fish were carrying the mutation on one of their alleles (Figure 5.16.).

Since screening fish by sequencing is not convenient for experiments, a new screening method was outlined. A new pair of primers was designed, surrounding closely the mutation place, in order to amplify a fragment of 104 bp in a normal sequence, and 81 bp in case of the 23 bp mutation (Figure 5.17.A.). These 2 fragments can be separated and distinguishable on an agarose gel (Figure 5.17.B.). Another screening possibility for the 23 bp mutation in the *atg5* gene is by PCR and a restriction enzyme test. Indeed, the PCR product amplified with the Atg5 primers can be digested with the restriction enzyme BslI. The PCR product contains only one BslI restriction site, located inside the 23 bp mutation region. Therefore, the BslI enzyme cannot cut the PCR fragment if there is a mutation, resulting with a single band at 644 bp, while the 23 bp mutation will generate 2 bands with a size of 165 bp and 480 bp.

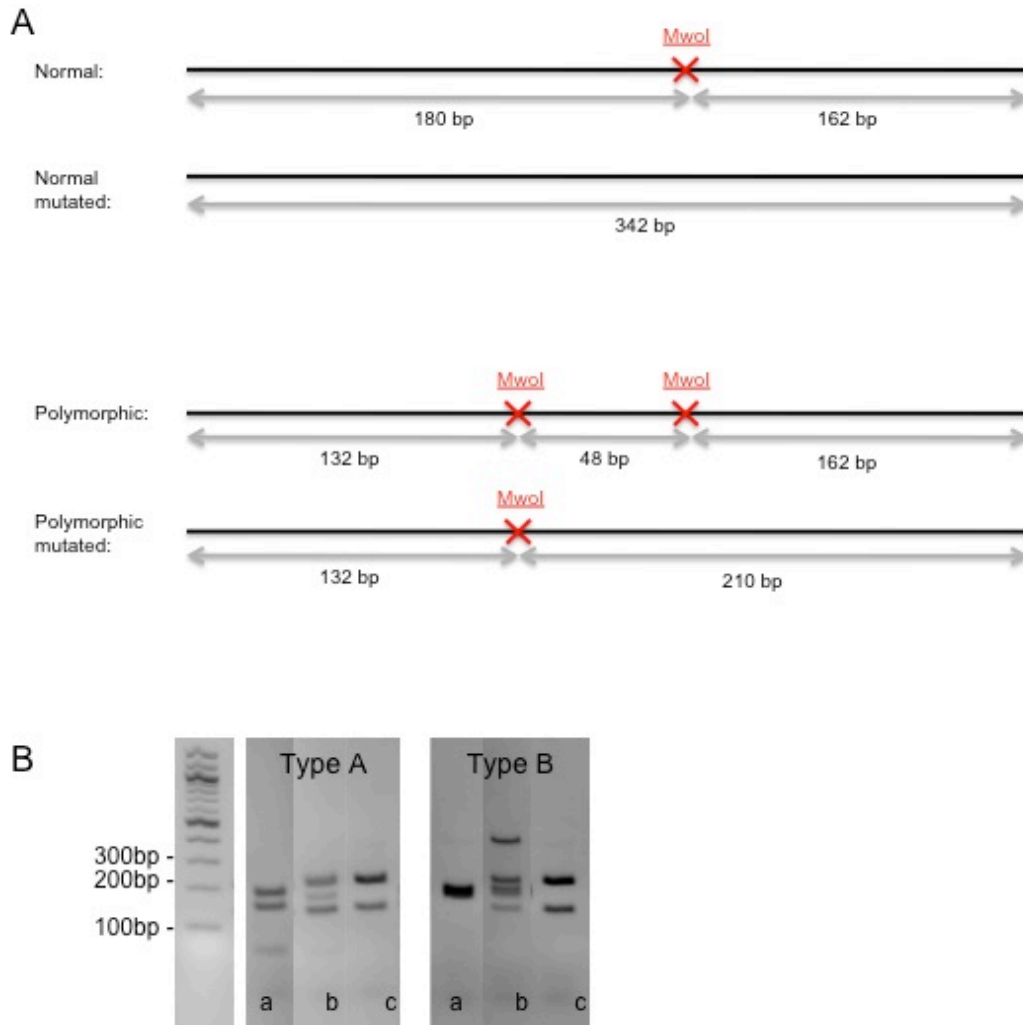


Figure 5.15. Genotyping of the *apg3l* mutants

A. *MwoI* digestions of the *Atg3Tal1* PCR products, leading to bands patterns in case of normal or polymorphic sequence, with and without the TALEN mutation.

B. Pattern of the PCR followed by *MwoI* digest on a 2.5% gel to genotype fish carrying *apg3l*^{ACTATCTGCC} mutation (10 bp deletion) type A or B.

a) wild-type +/+, b) hets -/+, c) homs -/-

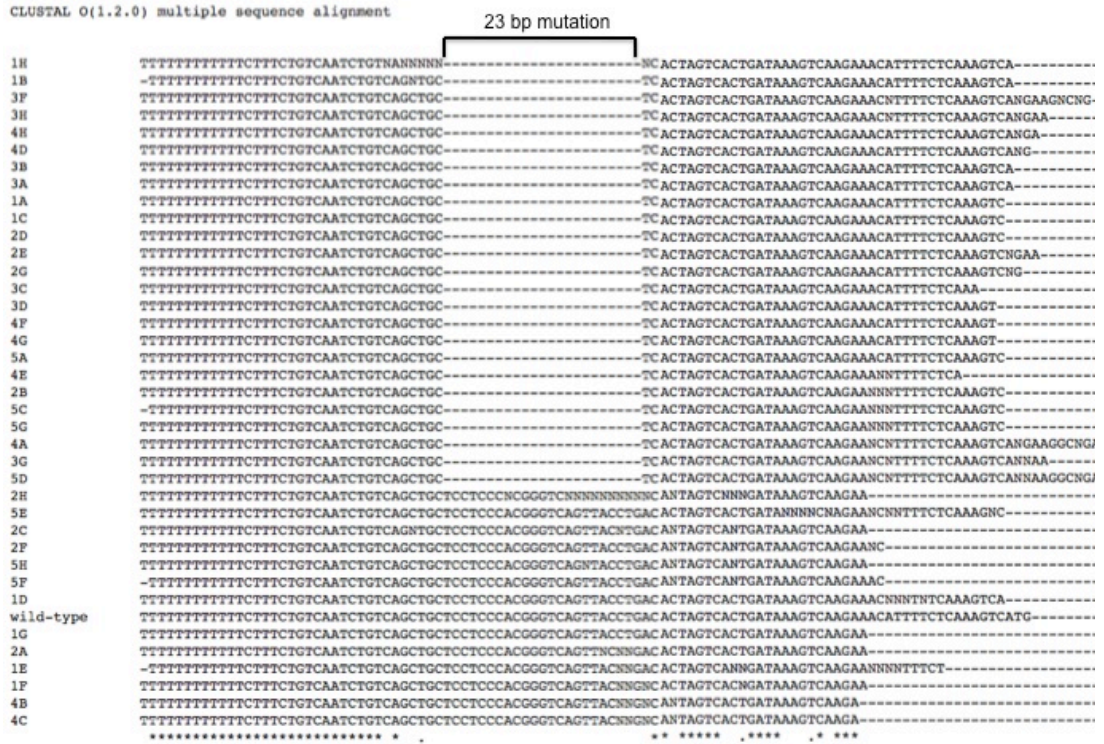


Figure 5.16. The 23 bp mutation in exon 3 of the *atg5* gene

Screening and sequencing of 40 fish, highlighting the 25 heterozygous mutant fish compared to the wild-type fish and non mutant carriers fish.

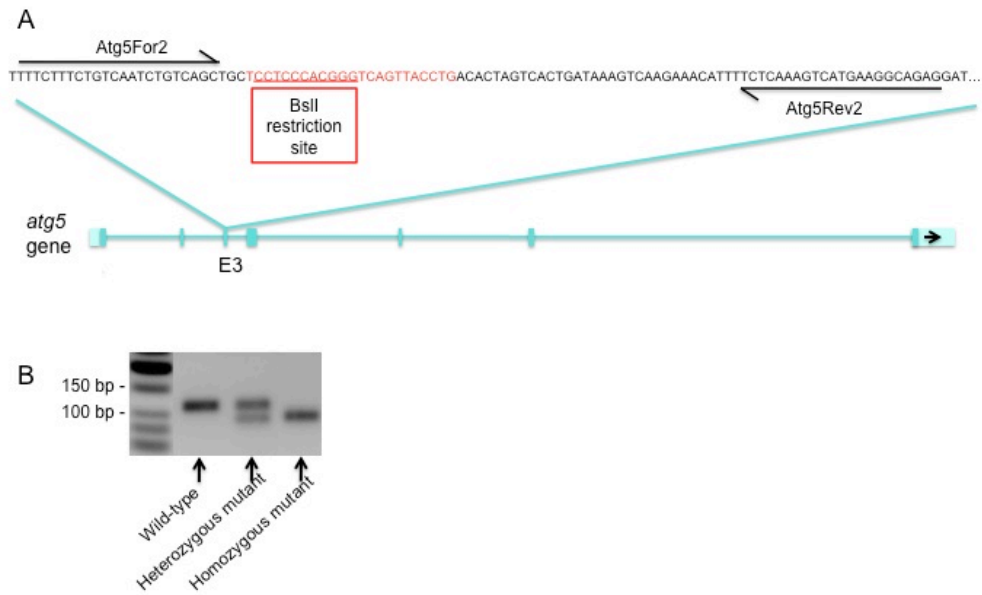


Figure 5.17. The 23 bp mutation in exon 3 of the *atg5* gene

A. The 23 bp mutation sequence is highlighted in red, the BsalI restriction site is underlined and the Atg5For2 and Atg5Rev2 primers are represented.

B. Genotyping pattern on a 2.5% agarose gel, using the Atg5For2 and Atg5Rev2 primers

5.4. The *atg10* mutant zebrafish line

The *atg10* mutant zebrafish line was generated with the TALEN technology by Stone Elworthy in the University of Sheffield (UK). The *atg10* mutant zebrafish line contains a 2 bp deletion at the beginning of the exon 3 of the *atg10* gene. The mutant line is called *atg10*^{A2}. The zebrafish *atg10* gene is located on chromosome 10 and has 7 exons. There are 2 splice variants of the gene, leading to skipping the exon 4 in some cases.

The *atg10*^{A2} mutant larvae were screened with a PCR and restriction enzyme test. The gDNA of the larvae was extracted, then the Atg10For and Atg10Rev primers were used to amplify a fragment of 262 bp by PCR, followed by a digestion with the BanII restriction enzyme. In case of a wild-type chromosome, BanII enzyme produced 2 fragments of 108 bp and 154 bp (Figure 5.18.A.). If the *atg10* gene was mutated at the beginning of exon 3, then BanII could cut the PCR product. The digestion pattern of the wild-type, heterozygous mutant and homozygous mutant could be observed on a 2.5% agarose gel (Figure 5.18.B.). Due to a polymorphism, an additional uncut band around 270 bp could be detected on the gel in some cases, corresponding to the heterozygous mutant (Figure 5.18.B.).

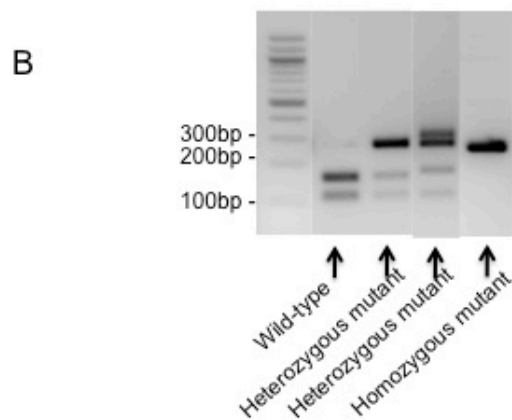
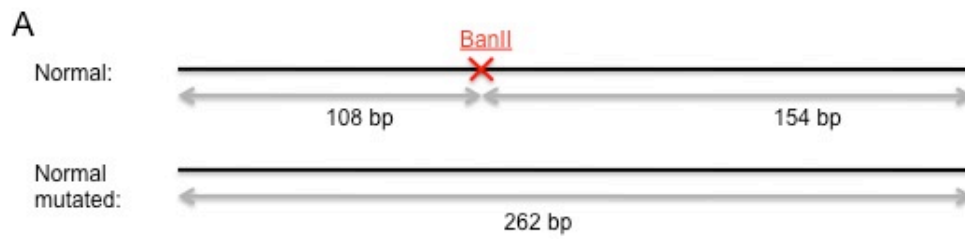


Figure 5.18. Genotyping of the *atg10^{A2}* mutants

A. *Ban*II digestions of the *Atg10* PCR products, leading to bands patterns in case of normal or polymorphic sequence, with and without the TALEN mutation.

B. Pattern of the PCR followed by *Ban*II digest on a 2.5% gel to genotype fish carrying *atg10^{A2}* (2 bp deletion).

5.5. *S. aureus* infection into zebrafish mutant lines

5.5.1. Abscess formation precedes the death of *S. aureus* infected zebrafish embryos

Survival experiments using the *S. aureus*-zebrafish infection model are a tool to evaluate the effects of chemical compounds, knockdown or knockout of bacterial or host genes on the progression of the infection. In these experiments, time of death of each zebrafish larvae is recorded until the last timepoint of the experiment. Dead larvae can decompose quite quickly, leaving very little tissue for future analysis. This can be unpractical in some cases such as the genotyping of mutant zebrafish larvae. Indeed, the mutation of the zebrafish larvae issued from the mutant *apg3l*, *atg5* or *atg10* zebrafish lines needs to be determined with a PCR and restriction enzyme test. A good amount of high quality DNA is required to effectively genotype the mutation carried by these zebrafish larvae. To perform survival experiments with these zebrafish mutant lines, another method to detect the late stage of staphylococcal infection before host death was required.

Following *S. aureus* injection into zebrafish embryos, one or more bacteria can form foci of infection in several parts of the zebrafish body, which can lead to the formation of abscesses. At this point, the zebrafish larvae immune system is overwhelmed, and the abscesses keep growing until the death of the host (Prajsnar, Hamilton et al. 2012). In most cases, abscesses developed in the zebrafish larvae heart, near to the site of injection (Figure 5.19.A.), or in the yolk area (Figure 5.19.B.). These abscesses could appear as soon as 18 hpi, and throughout the experiment. In some rare cases, staphylococcal particles colonised the whole vasculature, leading to host death (Figure 5.19.C.). It was hypothesised that the apparition of abscesses were indicators of late stage of infection, closely preceding the death of the host. To test this, LWT zebrafish larvae were infected at 30 hpf with fluorescently labelled *S. aureus* (GFP-SH1000 strain), and both the appearance of bacterial abscesses and the death of the zebrafish larvae were recorded over time. The percentages of no abscesses and survival

were reported on a graph (Figure 5.19.D.). It showed that the percentage of all the live fish was slightly higher than the percentage of healthy fish that did not have visible abscesses, but the 2 curves were not significantly different. The appearance of bacterial abscesses preceded the death of the larvae by maximum 12 h. Therefore, recording the number of fish bearing bacterial abscesses is a reliable approach to record the progression of a *S. aureus* infection in the zebrafish infection model.

5.5.2. Bacterial virulence in *apg3l* mutant zebrafish line

To test the susceptibility of zebrafish larvae carrying the *apg3l* mutation to *S. aureus* infection, an infection experiment was performed and the survival pattern of the zebrafish larvae recorded. For these experiments, the progeny of an incross between 2 *apg3l*^{ACTATCTGCC} adult heterozygous mutants was used. The incross of heterozygous mutants produced a mix of homozygous mutants, heterozygous mutants and wild-type. At 30 hpf, the progeny was infected with GFP labelled *S. aureus* into their circulation. After the detection of important abscesses in the zebrafish larvae, or at the last timepoint of the experiment for the remaining alive zebrafish (at 90 hpi), the larvae were genotyped to identify the genetic mutation status of the *apg3l* gene that they were carrying. The genomic DNA was extracted from the larvae, followed by an Atg3Tal1 PCR and a MwoI restriction enzyme test. The digestion products were then run on an agarose gel. According to the pattern of the bands on the gel, the mutation status (homozygous mutant, heterozygous mutant or wild-type) of the larvae was determined. A representative pattern of the bands corresponding to the mutation status is shown in Figure 5.15.B.. The types A and B of the mutation produced slightly different patterns on a gel, depending on the presence or absence of the 2 bp polymorphism in the sequence (see section 5.2.3.).

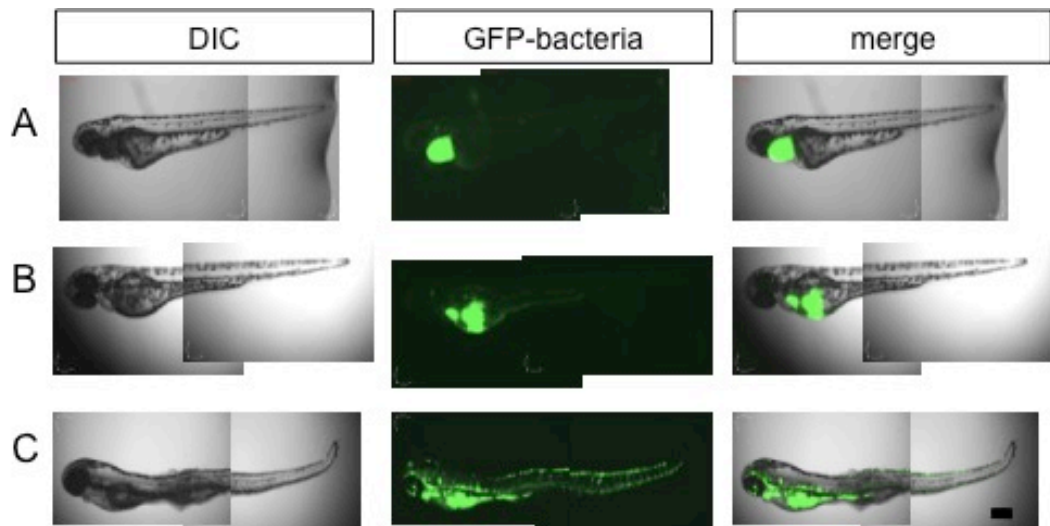


Figure 5.19. Late stage of staphylococcal infection can be recorded via mortality or abscesses formation

A) Abscesses in the heart of 28 hpi zebrafish larvae infected with GFP-labelled *S. aureus*.

B) Abscesses in the yolk sac circulation valley area of 28 hpi zebrafish larvae infected with GFP-labelled *S. aureus*.

C) Bacterial colonisation of the vasculature of 42 hpi zebrafish larvae infected with GFP-labelled *S. aureus*.

Scale bar = 180 μ m

All images were captured using 10x Nikon air objective NA 0.3, and consist and consist of the extended focus of 10 slices covering 600 μ m depth. DIC and GFP-channels.

D) LWT zebrafish embryos were infected with 2000 CFU of *S. aureus* GFP-SH1000 at 30 hpf. 1 experiment, n=35 fish. ns = not significant.

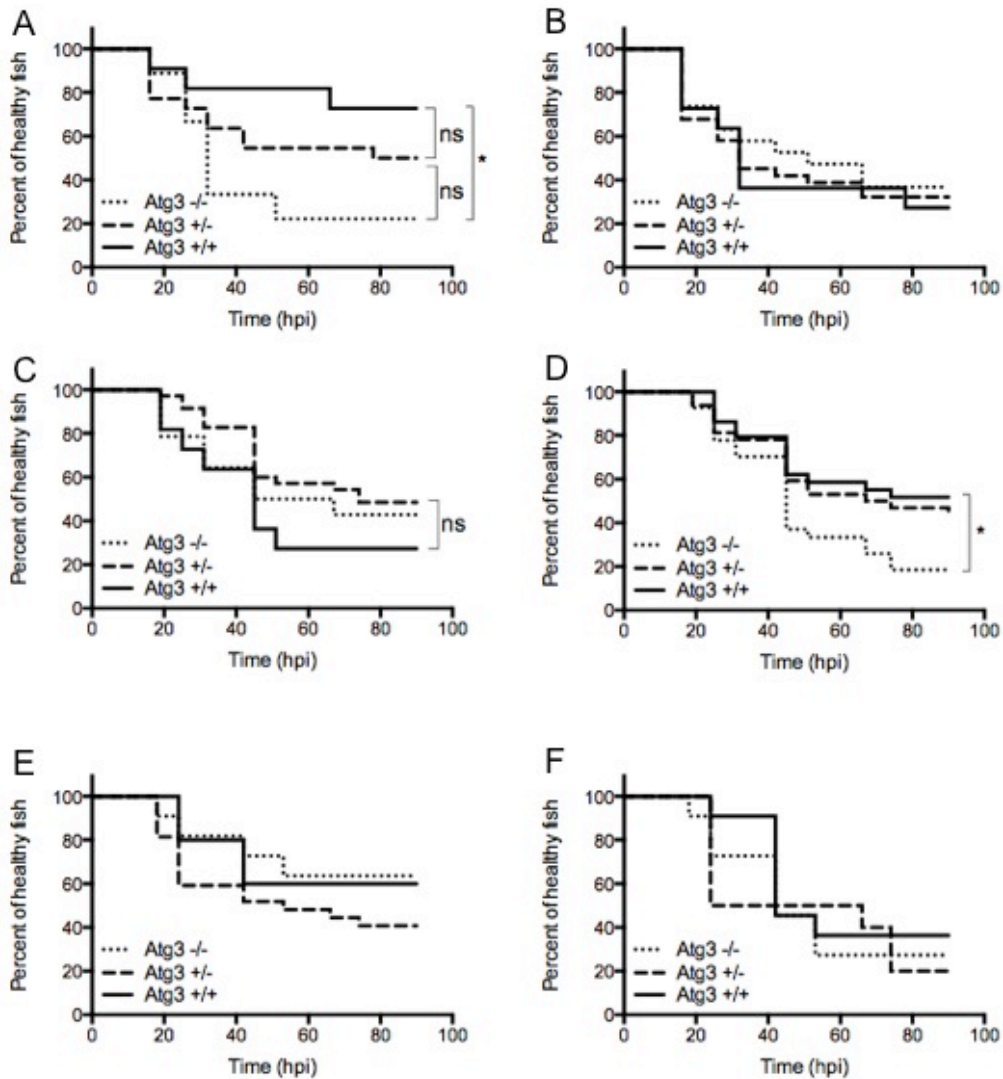


Figure 5.20. *S. aureus* infection of the *apg3l*^{ΔCTATCTGCCC} mutant zebrafish line

Infection with *S. aureus* GFP-SH1000

A) 1454 CFU, 9<n fish<22; B) 1752 CFU, 11<n fish<34; C) 1413 CFU, 11<n fish<35; D) 1586 CFU, 27<n fish<32; E) 1962 CFU, 5<n fish<27; F) 1833 CFU, n fish=10-11

ns = not significant, * = p<0.05

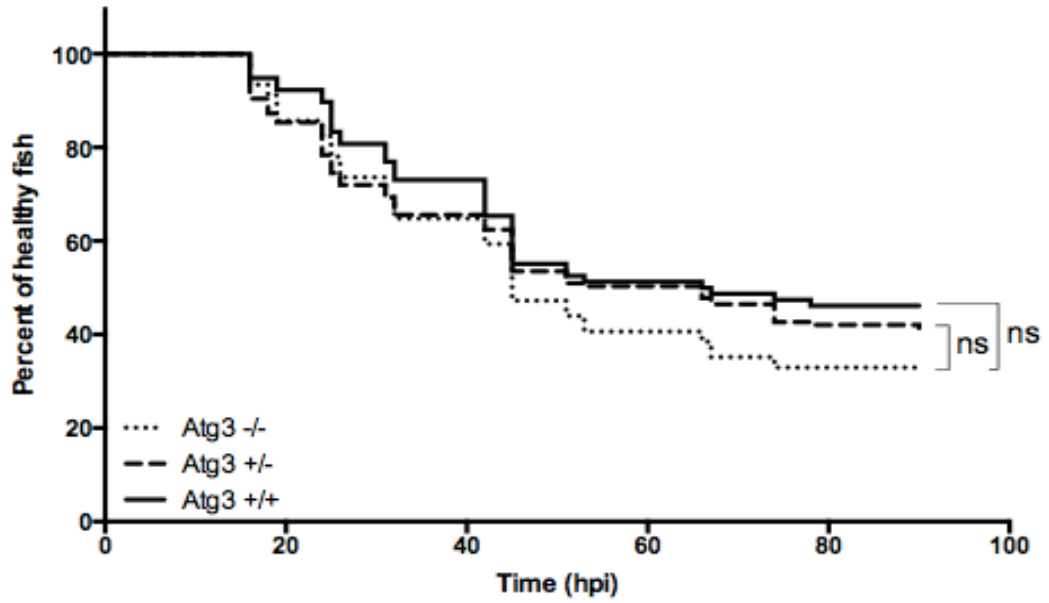


Figure 5.21. *S. aureus* infection of the *apg3l*^{ΔCTATCTGCCC} mutant zebrafish line

Infection with a dose of 1650 CFU of *S. aureus* GFP-SH1000
 6 independent experiments, n=91 fish for mutants -/-, n=157 fish for hets +/-, n=78 fish for wild-type
 ns= not significant

Six independent experiments were performed, generating a variety of results, sometimes opposite (Figure 5.20.). In 2 single experiments, a significant decrease in the survival of the infected homozygous mutant compared to the infected wild-type group was observed (Figure 5.20.A. and 5.20.D.). However, by combining the data of the 6 experiments together, there was no significant difference between the survival curves of larvae infected with 1650 CFU of *S. aureus* and carrying a homozygous *apg3l*^{ΔCTATCTGCCC} mutation compared to the infected wild-type group (Figure 5.21.).

5.5.3. Bacterial virulence in *atg5* mutant zebrafish line

A staphylococcal infection experiment was performed with the *atg5* mutant zebrafish line, using GFP labelled *S. aureus* to infect the progeny of an incross between *atg5*^{Δ23} heterozygous mutants. The first observation was that all the larvae derived from the *atg5*^{Δ23} mutant zebrafish line were very sensitive to the staphylococcal infection, as they died very quickly and decomposed completely in the wells of the 96-well plate. Therefore, 2 different doses of fluorescent bacteria were tested for the experiments: 1170 CFU (Figure 5.22.A.) and 2340 CFU (Figure 5.22.B.), and the genotyping of the mutation was carried out on larvae showing a staphylococcal abscess. The survival curves of infected healthy fish carrying a homozygous mutation, a heterozygous mutation or no mutation were similar.

5.5.4. Bacterial virulence in *atg10* mutant zebrafish line

The *atg10*^{Δ2} zebrafish line carrying a 2 bp deletion in the *atg10* gene was used in a staphylococcal infection experiment. The progeny of an incross between heterozygous mutants carrying the *atg10*^{Δ2} mutation was used and infected with GFP labelled *S. aureus*. The results of 2 independent infection experiments (Figure 5.23.A. and B.) were combined together (Figure 5.24.), suggesting that an infection of 1650 CFU of *S. aureus* did not influence the survival curves of the larvae, whether they carry a homozygous, heterozygous or no deletion of 2 bp in the exon 3 of *atg10* gene.

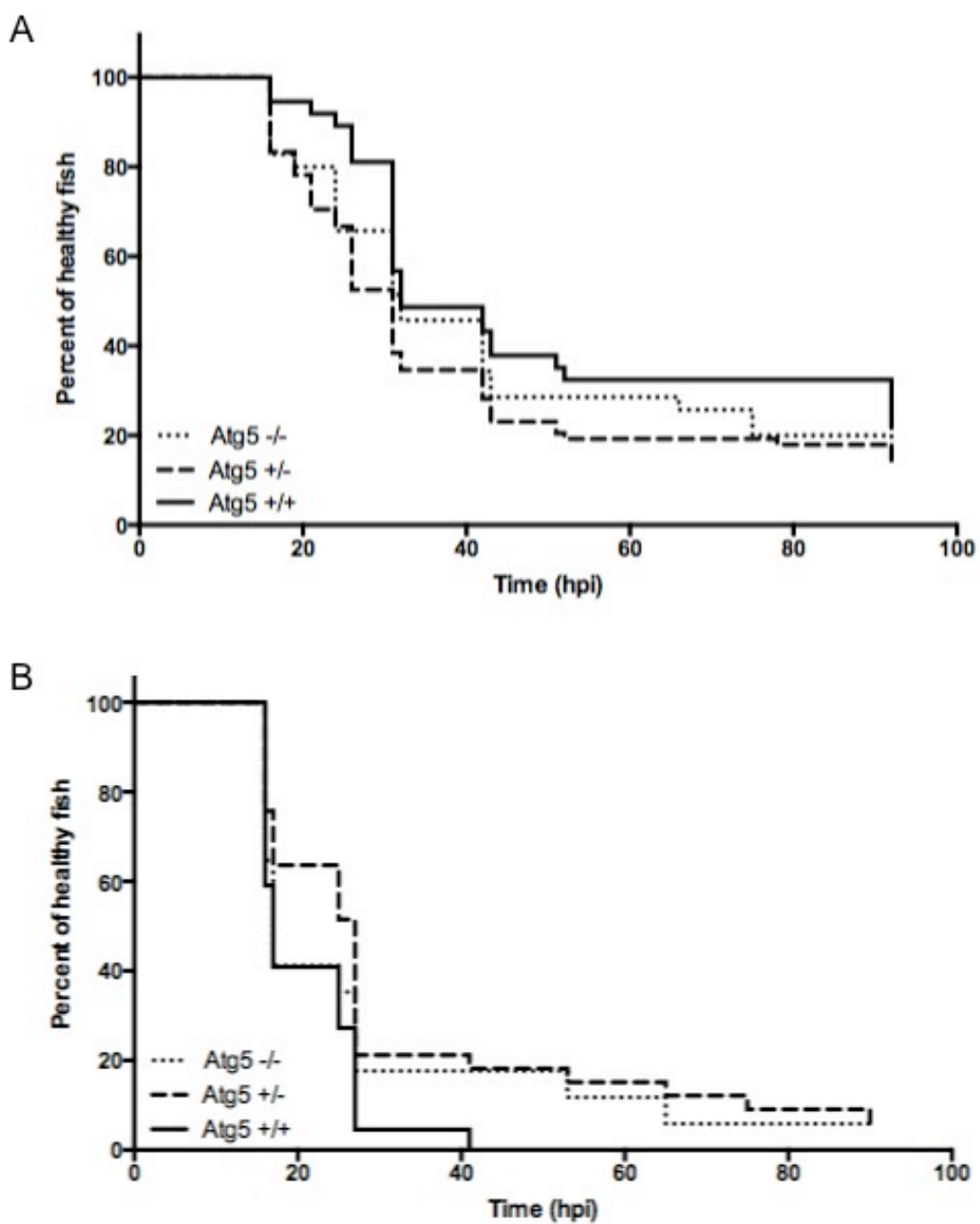


Figure 5.22. *S. aureus* infection of the *atg5*^{Δ23} mutant zebrafish line

Infection with *S. aureus* GFP-SH1000

A) 3 independent experiments, 1170 CFU, 35<n fish<78

B) 2 independent experiments, 2340 CFU, 17<n fish<33

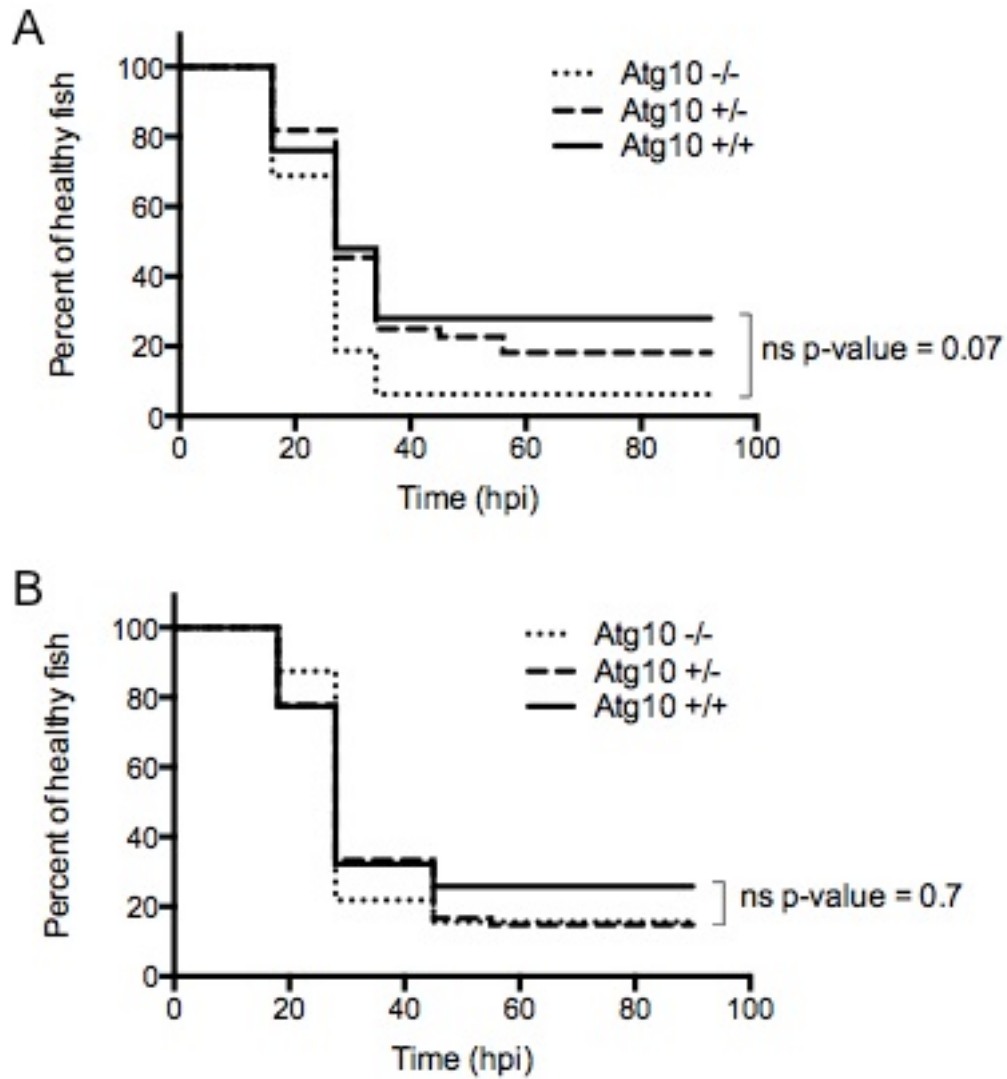


Figure 5.23. *S. aureus* infection of the *atg10^{A2}* mutant zebrafish line

Infection with *S. aureus* GFP-SH1000

A) 1555 CFU, 16 < n fish < 44; B) 1750 CFU, 31 < n fish < 54

ns = not significant

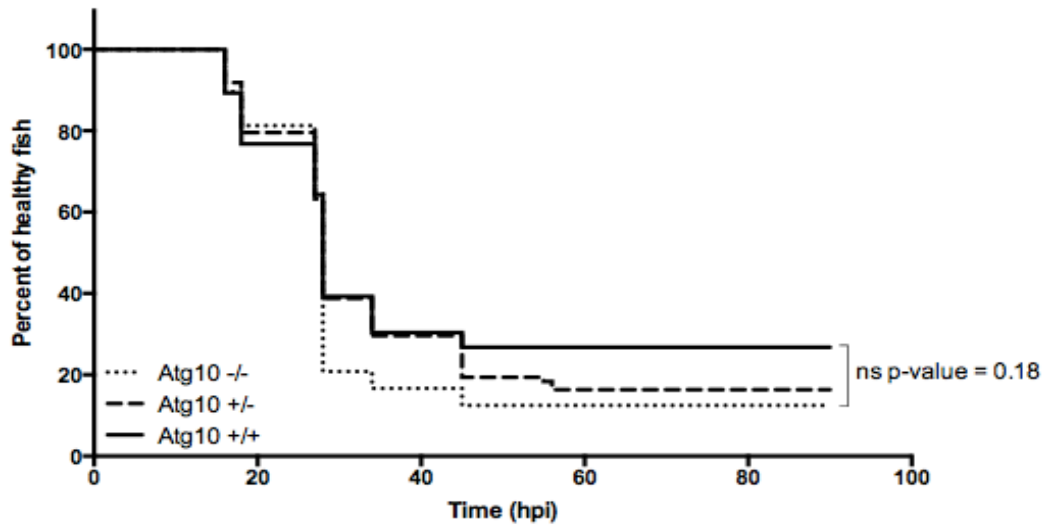


Figure 5.24. *S. aureus* infection of the *atg10*^{Δ2} mutant zebrafish line

Infection with a dose of 1650 CFU of *S. aureus* GFP-SH1000

2 independent experiments, n=48 fish for mutants -/-, n=98 fish for hets +/-, n=56 fish for wild-type

ns = not significant

5.6. Discussion

In this chapter, a zebrafish autophagy mutant for the *apg3l* gene has been generated using the TALEN technology. This *apg3l* mutant, as well as an *atg5* and an *atg10* mutant zebrafish line have been used in an infection experiment with GFP-labelled *S. aureus*. The number of abscesses was recorded over time, and the survival curves of the infected mutants were similar to the survival curves of the control group.

TALEN technology is a powerful tool for targeted mutagenesis that has generated an *apg3l* defective zebrafish mutant in the exon 4 of its gene. Both the restriction enzyme test and sequencing have confirmed the inserted or deleted genetic mutation. By translating the mutated genetic sequence, the putative protein formed would be only 67, 75, 71 or 72 amino acids long, for the 5 bp deletion mutant (*apg3l*^{ΔCTATC}), the 2 bp addition mutant (*apg3l*^{+AT}), the 10 bp deletion mutant (*apg3l*^{ΔCTATCTGCC}) or the 7 bp deletion mutant (*apg3l*^{ΔCCCAATG}) respectively. The mutations have introduced a premature stop codon in the sequence, predicting to generate shorter mutant proteins compared to the 317 amino acids of the wild-type protein. The structure of *S. cerevisiae* Atg3 protein has been elucidated by X-ray diffraction (Yamada, Suzuki et al. 2007). As Atg3 is a quite conserved protein, the important residues and regions are similar with other organism Atg3 homologs. In particular, the catalytic cysteine is highly conserved between organisms, and therefore residue 267 is recognised as the catalytic cysteine of the zebrafish Apg3l protein, by similarity. Due to the premature position of the stop codon in the mutated gene sequence and consequently the short translated mutated Apg3l protein, the catalytic cysteine of the zebrafish Apg3l protein located at position 267 within a HPC motif should lack in the mutant protein. In addition, both the handle region and the flexible region, 2 regions that mediate the binding to Atg8 (LC3) and Atg7 respectively (Yamada, Suzuki et al. 2007), should also be absent in the mutant proteins. The N-terminal region of *S. cerevisiae* Atg3 is required for the transfer of Atg8 to PE, as a mutation in the last 7 residues at the N-terminal of Atg3 produces a defective protein for the conjugation reaction (Hanada, Satomi et al. 2009). Atg3 also interacts with Atg12, facilitating the Atg12-Atg5 conjugation (Tanida, Tanida-

Miyake et al. 2002). The 4 critical residues for the binding to Atg12 are located in the flexible region of the Atg3 protein (Metlagel, Otomo et al. 2013), which should be lacking in the zebrafish *apg3l* mutants. Compared to the structures and functional analyses of Apg3l protein homologs, it is most likely that the Apg3l mutant protein generated in the *apg3l* mutant zebrafish line is non-functional. However, experimental studies to show functional knockout of Apg3l proteins in the zebrafish mutant are required.

In a study, Atg3-deficient mice have been generated by disruption of exon 10, which codes for the active site cysteine, and was replaced by a neo-resistant gene cassette. The Atg3-mutant mice did not survive longer than 1 day after birth, as autophagy is important to provide amino acids to the newborn (Sou, Waguri et al. 2008). Homozygous *apg3l*^{ACTATCTGCC} zebrafish mutant did not present any apparent developmental or behavioural defect, at least up to 5 dpf. No adult zebrafish carriers of the *apg3l* mutation have been genotyped yet, so the survival of the mutants after 5 dpf has not been determined. The loss of Atg3 in mouse embryonic fibroblasts (MEFs) was associated with defective autophagosome formation, including a dysregulated elongation of the isolation membrane, no complete closure of the autophagosome-like structures, and no localisation of LC3 to the membrane (Sou, Waguri et al. 2008). To confirm that *apg3l* zebrafish mutants actually have a defect in Apg3l protein, further experimental tests are required. First of all, the presence of *apg3l* mRNA could be tested by northern blot and similarly, the presence of Apg3l proteins could be tested by western blot. As the recruitment of LC3 proteins to the membrane is impaired in Atg3^{-/-} MEFs (Sou, Waguri et al. 2008), the *apg3l* zebrafish mutants should present the same feature. By crossing *apg3l* zebrafish mutants to a transgenic zebrafish line expressing fluorescently labelled LC3 proteins, the correct or defective recruitment of LC3 proteins to autophagosomes could be observed under microscopy, taking advantage of the transparency feature of the zebrafish larvae. Another way to measure the recruitment of LC3 proteins would be to quantify the conversion of LC3-I to LC3-II form by western blot, which should be impaired in the mutant.

An *apg3l* zebrafish mutant la015987Tg was generated by viral transgenic insertion of Tg(nLacZ-GTvirus) by the Burgess and Lin lab, and is available at the Zebrafish International Resource Center (ZIRC, <http://zebrafish.org>) (Varshney, Lu et al. ; Wang, Jao et al. 2007; Burgess and Lin 2012). As no further research has been investigated and published with that zebrafish mutant, it would be interesting to compare the phenotypic features of the 2 *apg3l* zebrafish mutant lines generated with 2 different techniques.

Even though Atg3 is considered essential for autophagy, some evidence has shown an Atg7 and Atg3 independent autophagy pathway that eases size reduction programmes of the cells of the midgut of the intestine during intestine cell death (Chang, Shrivage et al. 2013). This study highlights the fact that different autophagy programmes can be used by different cell types in a whole organism.

Atg5 is an important autophagy protein that conjugates to Atg12 protein, and subsequently form the Atg5-Atg12-Atg16L1L complex. By similarity to the catalytic lysine 130 of the human Atg5 sequence and the catalytic lysine 149 of the *S. cerevisiae* Apg5 sequence, the zebrafish catalytic lysine residue would be located in position 130. Due to the 23 bp deletion mutation, the mutant *atg5*^{A23} zebrafish line should code for a shorter unfunctional protein of only 43 amino acids. A study using morpholino oligo knockdown and mRNA overexpression of the zebrafish *atg5* gene demonstrated the importance of the *atg5* gene in the development of the embryonic nervous system and the regulation of the expression of several neural gene markers such as *gli1*, *huC*, *nkx2.2*, *pink1*, *β-synuclein*, *xb51* and *zic1*. Atg5 can regulate itself by a feedback inhibition loop, while its conjugate Atg12 seemed to be expressed at similar level all the time, like a housekeeping gene. *atg5* is also implicated in normal morphogenesis of brain regionalisation and body plan (Hu, Zhang et al. 2011).

Atg5-deficient mice develop normally inside the mother, but die 1 or 2 days after birth. It was shown that autophagy is highly increased at 3 to 12h after birth, and goes back to a basal level after 1-2 days. It is also known that post

natal mice undergo hypoglycaemia and hypolipidaemia, suggesting that the amino acids degraded from the proteins are the major energy metabolism, until the nutrient supply coming from the mother's milk are steady. Atg5-deficient mice, lacking autophagy, do not survive the starvation period between the time of birth and the steady supply of nutrients through milk (Kuma, Hatano et al. 2004). As zebrafish develop externally, the necessary nutrients at the larval stage are supplied by the yolk sac, and after 5 dpf, the larvae are able to eat their food from the environment via their mouth. The *atg5* mutant zebrafish could therefore survive at the adulthood. So far, 1 homozygous *atg5* mutant adult zebrafish has been screened by fin clip (Josie Gibson, personal communication), suggesting that the mutation is not lethal.

A point mutation *atg5* zebrafish line sa22749 has been generated by treating adult males with ENU. It involves a change of nucleotide from a C to a T in the exon 5 of the gene, affecting the 154th amino acid during the translation (Busch-Nentwich, Kettleborough et al. 2013). No functional studies have been published on this *atg5* mutant zebrafish line. It would be interesting to compare the 2 *atg5* mutant zebrafish lines, generated by 2 different techniques.

By similarity of protein sequence with *S. cerevisiae* and *Homo sapiens* ATG10, the catalytic site of the zebrafish Atg10 corresponds to the cysteine residue 174 of the 224 amino acids sequence. The Atg10 protein formed by the 2 bp deletion *atg10* mutant should be shorter and lacking the important residue that interacts with Atg7 and is responsible to catalyse the formation of the Atg5-Atg12 complex. It was thought that the *frozen* mutant was an *atg10* mutant. However, the cross between the *atg10* mutant line and the *frozen* line was possible, and the progeny carrying both a *frozen* allele and an *atg10* mutant allele could survive without presenting any sign of *frozen* phenotype.

As with the *apg3l* mutant zebrafish line, the effective defect of the *atg5* and *atg10* mutant zebrafish line could be checked by northern blot or western blot for the corresponding mRNA and protein. Besides, impaired autophagy could

be checked by western blot for LC3-I and LC3-II, or with a fluorescent LC3 marker.

By using GFP-labelled *S. aureus*, it was shown that recording the presence of abscesses in alive larvae was similar to recording the mortality of the fish (Figure 5.19.A.), and that in most cases, the abscesses appeared in the heart and the yolk area (Figures 5.19.B. and C.). A rational explanation to this abscesses localisation is that the injection of *S. aureus* was performed into the yolk circulation valley. The injected bacteria were immediately in the circulation, and could reach easily and quickly the heart.

The survival curves of GFP-labelled *S. aureus* infecting *apg3l*, *atg5* and *atg10* zebrafish mutant progeny were similar for the homozygous mutants, heterozygous mutants and wild-type (Figures 5.20. to 5.24.). Due to their genetic mutation, these 3 zebrafish mutant lines should produce non-functional autophagic proteins. Assuming that these zebrafish mutant lines have an effective defect in autophagy, the infections experiments would show that the canonical autophagic pathway involving Apg3l, Atg5 or Atg10 is not required for *S. aureus* to form fatal abscesses in the zebrafish larvae. This would suggest that autophagy is not the most important process for staphylococcal survival and development, and that *S. aureus* has alternative strategies to invade and replicate inside host cells.

The functional defect of autophagy in the *apg3l*, *atg5* and *atg10* zebrafish mutant line has not been experimentally demonstrated yet. The survival experiments have been carried out with zebrafish larvae aged from 30 hpf to 5.2 dpf. Some studies have shown that the first few hours of zebrafish development until the zygotic genome is activated – a timepoint called the midblastula transition – rely on maternal factors that are stored in the egg during oogenesis (Abrams and Mullins 2009; Lindeman and Pelegri 2010). Therefore, maternally derived RNAs and proteins could partially mask the effects of zygotic mutations. The mother fish used in the experiments was a heterozygous mutant for *apg3l*, *atg5* and *atg10*, meaning that it had a copy of the corresponding functional gene. If these Atg proteins are critical for early

zebrafish development, it is most likely that they have been provided by the maternal factors. It is possible that an effect of the Atg mutation would be visible if the survival experiments were extended to a later timepoint.

A difference in the survival rate between the 3 autophagy mutant lines was observed. The background of the *apg3l* mutant is LWT, while the background for the *atg5* mutant fish is a Singapore local strain and *atg10* mutant has been generated in a mix of LWT and nacre background. It is possible that the initial background of the fish influences the sensitivity to infection. Comparing the survival of these different zebrafish lines between each other is therefore problematic. However, within one strain of fish the survival of the different groups (homozygous mutant, heterozygous mutant and wild-type) can be compared.

To summarise, this chapter has demonstrated that:

- the TALEN technology is a powerful tool to introduce targeted mutation in a specific zebrafish gene
- in the systemic model of *S. aureus* infection, bacterial abscesses are formed in most cases into the heart or yolk area of the zebrafish larvae; however, some cases of bacterial colonisation of the whole vasculature is possible
- the survival of infected zebrafish larvae mutated for 3 different autophagy genes (*apg3l*, *atg5* and *atg10*) was not different than the survival of infected control larvae

Chapter 6: Conclusion and perspectives

S. aureus is an important human pathogen causing several diseases. Infected patients are currently treated with antibiotic drugs aiming to kill colonising live bacteria. However, *S. aureus* has evolved several mechanisms to acquire resistance to newly developed antibiotics. Due to bacterial genome plasticity, resistance genes can easily spread among the bacterial community, especially in conditions of heavy antibiotics use.

Increasing evidence has shown that *S. aureus* can survive intracellularly in both professional and non-professional phagocytes, which would explain chronic staphylococcal infections, even following antibiotic treatment. More understanding of the intracellular survival mechanisms of *S. aureus* would be helpful to design new treatment targeting intracellular bacteria.

6.1. The potential of an *in vivo* drug screen for the discovery of antistaphylococcal compounds

Using a *S. aureus*-zebrafish infection model, I designed a screening assay aiming to identify compounds that could cure staphylococcal infection *in vivo*. It is a novel approach of antistaphylococcal drug discovery never described before that has great potential. It was designed to identify compounds able to promote the survival of *S. aureus* infected zebrafish larvae. Therefore, even compounds with a different mechanism of action than current antibiotics could be detected, e.g. drugs enhancing the host innate immune system or inhibiting the *in vivo* bacterial virulence factors. A main advantage of an *in vivo* approach is the combination of small molecule screening and animal testing in a single step. In addition, an *in vivo* environment provides natural conditions for *S. aureus* that can express all their virulence factors according to their stage of infection in the host.

This screening assay was effective to detect compounds inducing large differences of survival. However, from the 660 compounds screened in this study, it became apparent that compounds inducing a small effect were not easily distinguished as the limit between false positive and 'hit' compounds was closer. The difficulty to identify compounds may be explained by inappropriate dosage of the drug, absorption deficiency, toxicity or lack of function in zebrafish. In addition, most putative 'hit' compounds identified in the primary and secondary assays failed to reproduce the survival increase of the infected larvae. The *in vivo* drug screening assay for antistaphylococcal drug discovery is promising but needs some automation and further optimisation.

6.2. The *frozen* zebrafish mutant is resistant to *S. aureus* pathogenesis

The *frozen* zebrafish mutant injected with intravenous *S. aureus* SH1000 was less sensitive to the infection compared to infected control group. The initial hypothesis suggested that the mutation was related to the *atg10* gene. However, experiments using morpholinos targeting the *atg10* transcript or using a zebrafish mutant at exon 3 of the *atg10* gene generated with the TALEN technique failed to reproduce the characteristic *frozen* phenotype. In addition, neither the *atg10* knockdown morphant nor the *atg10* knockout zebrafish were more resistant to *S. aureus* infection.

The utilisation of transgenic zebrafish lines showed that the *frozen* mutant could express LC3 proteins in both macrophages and neutrophils. As LC3 proteins are markers of autophagosome formation, these microscopy pictures suggest that the *frozen* mutant is not an autophagy mutant zebrafish line.

The full sequencing of the *frozen* genome is awaited to understand the mutation carried by this mutant fish and study its advantageous resistance mechanism to systemic staphylococcal infection. Much work is required to

determine the molecular mechanism underlying the survival advantage of frozen zebrafish to *S. aureus* infection.

6.3. Autophagy

Recent evidence has shown that *S. aureus* can hijack autophagy to survive intracellularly. These studies were all performed in cell culture *in vitro*. The zebrafish model is a convenient tool to study this phenomenon *in vivo*, which has never been done before. In this study, the autophagy pathway was modulated using pharmacological, knockdown and knockout techniques. Most of these approaches failed to produce clear evidence of a possible advantage of autophagy for *S. aureus* infection. However, a transgenic zebrafish line enabled to visualise the colocalisation of bacteria with LC3 proteins, suggesting that *S. aureus* is in some cases contained in an autophagosome vacuole inside neutrophils and macrophages.

6.4. Generation of targeted mutation in zebrafish

The TALEN technology has proven to be a quick, easy and powerful tool to generate targeted mutation in zebrafish. At the genomic level, the targeted gene can be easily tested with a PCR and restriction enzyme test. The targeted gene was disrupted with an insertion or deletion of base pairs, generating a translation shift. However, the efficiency at the protein level remains to be tested, and functional analysis determining the dysfunction of autophagy and autophagosome formation is also required.

6.5. Concluding remarks

In this thesis, I have described the design, optimisation and implementation of an *in vivo* antistaphylococcal drug screening assay performed in zebrafish embryos. I aimed to screen a range of FDA-approved compounds with the hypothesis that some drugs able to cure systemic *S. aureus* infection would be identified. A common property of a few of the 'hit' compounds was their effect on the autophagy pathway, which led to the new working hypothesis that autophagy plays a role in *S. aureus* infection. I used several approaches

(pharmacological, knockdown, knockout and microscopy) to address this research question.

There are some limitations to the *S. aureus*-zebrafish infection model. As zebrafish embryos lack the acquired immune response, studies in this model dissect specifically the interaction between the innate immune system and *S. aureus* infection. It is an advantage at the time of laboratory experiments, but translation of the findings discovered in this model to general immunity mechanisms should be done carefully. Additional experiments should be tested in other mammalian models to understand the larger effect.

Most experiments using the *S. aureus*-zebrafish infection model in this study were survival tests comparing the mortality of infected zebrafish larvae in different conditions. The survival of the zebrafish larvae was the main readout to tell if an experimental condition was influencing the infection or not. Even though no change in zebrafish survival was observed, some other more subtle parameters of the infection could be influenced by the experimental conditions. This could be the formation of abscesses, the distribution of staphylococcal population inside the host or a modification in the immune response cells. Therefore, other measurements of staphylococcal infection stage and progression would be useful to dissect the host and bacterial mechanisms underlying.

Further investigation is required to understand the molecular mechanisms of intracellular *S. aureus* infection and the role of autophagy *in vivo*. Expanding our knowledge in this area of research will enable to design of more effective treatment for chronic staphylococcal infections.

References

- Abel, J., O. Goldmann, et al. (2011). "Staphylococcus aureus evades the extracellular antimicrobial activity of mast cells by promoting its own uptake." J Innate Immun **3**(5): 495-507.
- Abraham, E. P., E. Chain, et al. (1941). "FURTHER OBSERVATIONS ON PENICILLIN." The Lancet **238**(6155): 177-189.
- Abrams, E. W. and M. C. Mullins (2009). "Early zebrafish development: it's in the maternal genes." Current Opinion in Genetics and Development **19**(4): 396-403.
- Agerer, F., A. Michel, et al. (2003). "Integrin-mediated invasion of Staphylococcus aureus into human cells requires Src family protein-tyrosine kinases." Journal of Biological Chemistry **278**(43): 42524-31.
- Almeida, R. A., K. R. Matthews, et al. (1996). "Staphylococcus aureus invasion of bovine mammary epithelial cells." Journal of Dairy Science **79**(6): 1021-6.
- Amano, A., I. Nakagawa, et al. (2006). "Autophagy in innate immunity against intracellular bacteria." J Biochem **140**(2): 161-6.
- Anderson, A. S., A. A. Miller, et al. (2012). "Development of a multicomponent Staphylococcus aureus vaccine designed to counter multiple bacterial virulence factors." Hum Vaccin Immunother **8**(11): 1585-94.
- Arman, M., K. Krauel, et al. (2014). "Amplification of bacteria-induced platelet activation is triggered by FcγRIIA, integrin αIIbβ3, and platelet factor 4." Blood **123**(20): 3166-74.
- Arthur, M. and P. Courvalin (1993). "Genetics and mechanisms of glycopeptide resistance in enterococci." Antimicrobial Agents and Chemotherapy **37**(8): 1563-71.
- Axe, E. L., S. A. Walker, et al. (2008). "Autophagosome formation from membrane compartments enriched in phosphatidylinositol 3-phosphate and dynamically connected to the endoplasmic reticulum." Journal of Cell Biology **182**(4): 685-701.
- Bae, T., A. K. Banger, et al. (2004). "Staphylococcus aureus virulence genes identified by bursa aurealis mutagenesis and nematode killing." Proceedings of the National Academy of Sciences of the United States of America **101**(33): 12312-7.
- Bampton, E. T., C. G. Goemans, et al. (2005). "The dynamics of autophagy visualized in live cells: from autophagosome formation to fusion with endo/lysosomes." Autophagy **1**(1): 23-36.
- Bandmann, O. and E. A. Burton (2010). "Genetic zebrafish models of neurodegenerative diseases." Neurobiology of Disease **40**(1): 58-65.
- Barbazuk, W. B., I. Korf, et al. (2000). "The syntenic relationship of the zebrafish and human genomes." Genome Research **10**(9): 1351-8.
- Barber, M. and M. Rozwadowska-Dowzenko (1948). "Infection by penicillin-resistant staphylococci." Lancet **2**(6530): 641-4.

- Baxendale, S., C. J. Holdsworth, et al. (2013). "Identification of compounds with anti-convulsant properties in a zebrafish model of epileptic seizures." Dis Model Mech **5**(6): 773-84.
- Bayles, K. W., C. A. Wesson, et al. (1998). "Intracellular Staphylococcus aureus escapes the endosome and induces apoptosis in epithelial cells." Infection and Immunity **66**(1): 336-42.
- Begun, J., C. D. Sifri, et al. (2005). "Staphylococcus aureus virulence factors identified by using a high-throughput Caenorhabditis elegans-killing model." Infection and Immunity **73**(2): 872-7.
- Benard, E. L., A. M. van der Sar, et al. (2012). "Infection of zebrafish embryos with intracellular bacterial pathogens." J Vis Exp(61).
- Benjamin, D. K., R. Schelonka, et al. (2006). "A blinded, randomized, multicenter study of an intravenous Staphylococcus aureus immune globulin." Journal of Perinatology **26**(5): 290-5.
- Bennett, C. M., J. P. Kanki, et al. (2001). "Myelopoiesis in the zebrafish, Danio rerio." Blood **98**(3): 643-51.
- Bera, A., S. Herbert, et al. (2005). "Why are pathogenic staphylococci so lysozyme resistant? The peptidoglycan O-acetyltransferase OatA is the major determinant for lysozyme resistance of Staphylococcus aureus." Molecular Microbiology **55**(3): 778-87.
- Bertrand, J. Y., N. C. Chi, et al. (2010). "Haematopoietic stem cells derive directly from aortic endothelium during development." Nature **464**(7285): 108-11.
- Bertrand, J. Y., A. D. Kim, et al. (2008). "CD41+ cmyb+ precursors colonize the zebrafish pronephros by a novel migration route to initiate adult hematopoiesis." Development **135**(10): 1853-62.
- Bertrand, J. Y., A. D. Kim, et al. (2007). "Definitive hematopoiesis initiates through a committed erythromyeloid progenitor in the zebrafish embryo." Development **134**(23): 4147-56.
- Bienfait, C. C. (2005). "Nabi Biopharmaceuticals Announces Results of StaphVAX(R) Confirmatory Phase III Clinical Trial." Retrieved November 1, 2005, from <http://phx.corporate-ir.net/phoenix.zhtml?c=100445&P=irol-newsArticle&ID=776196&highlight=>.
- Bingham, R. J., E. Rudino-Pinera, et al. (2008). "Crystal structures of fibronectin-binding sites from Staphylococcus aureus FnBPA in complex with fibronectin domains." Proceedings of the National Academy of Sciences of the United States of America **105**(34): 12254-8.
- Birgisdottir, A. B., T. Lamark, et al. (2013). "The LIR motif - crucial for selective autophagy." Journal of Cell Science **126**(Pt 15): 3237-47.
- Birmingham, C. L., V. Canadien, et al. (2007). "Listeria monocytogenes evades killing by autophagy during colonization of host cells." Autophagy **3**(5): 442-51.
- Birmingham, C. L., D. E. Higgins, et al. (2008). "Avoiding death by autophagy: interactions of Listeria monocytogenes with the macrophage autophagy system." Autophagy **4**(3): 368-71.
- Birmingham, C. L., A. C. Smith, et al. (2006). "Autophagy controls Salmonella infection in response to damage to the Salmonella-containing vacuole." Journal of Biological Chemistry **281**(16): 11374-83.

- Bischoff, M., J. M. Entenza, et al. (2001). "Influence of a functional sigB operon on the global regulators sar and agr in *Staphylococcus aureus*." Journal of Bacteriology **183**(17): 5171-9.
- Blommaart, E. F., U. Krause, et al. (1997). "The phosphatidylinositol 3-kinase inhibitors wortmannin and LY294002 inhibit autophagy in isolated rat hepatocytes." European Journal of Biochemistry **243**(1-2): 240-6.
- Blommaart, E. F., J. J. Luiken, et al. (1995). "Phosphorylation of ribosomal protein S6 is inhibitory for autophagy in isolated rat hepatocytes." Journal of Biological Chemistry **270**(5): 2320-6.
- Boch, J., H. Scholze, et al. (2009). "Breaking the code of DNA binding specificity of TAL-type III effectors." Science **326**(5959): 1509-12.
- Bremell, T., S. Lange, et al. (1991). "Experimental *Staphylococcus aureus* arthritis in mice." Infection and Immunity **59**(8): 2615-23.
- Bronner, S., H. Monteil, et al. (2004). "Regulation of virulence determinants in *Staphylococcus aureus*: complexity and applications." FEMS Microbiology Reviews **28**(2): 183-200.
- Brothers, K. M., Z. R. Newman, et al. (2011). "Live imaging of disseminated candidiasis in zebrafish reveals role of phagocyte oxidase in limiting filamentous growth." Eukaryot Cell **10**(7): 932-44.
- Brouillette, E., G. Grondin, et al. (2003). "In vivo and in vitro demonstration that *Staphylococcus aureus* is an intracellular pathogen in the presence or absence of fibronectin-binding proteins." Microbial Pathogenesis **35**(4): 159-68.
- Brouillette, E., A. Martinez, et al. (2004). "Persistence of a *Staphylococcus aureus* small-colony variant under antibiotic pressure in vivo." FEMS Immunology and Medical Microbiology **41**(1): 35-41.
- Brunn, G. J., J. Williams, et al. (1996). "Direct inhibition of the signaling functions of the mammalian target of rapamycin by the phosphoinositide 3-kinase inhibitors, wortmannin and LY294002." EMBO Journal **15**(19): 5256-67.
- Bubeck Wardenburg, J., W. A. Williams, et al. (2006). "Host defenses against *Staphylococcus aureus* infection require recognition of bacterial lipoproteins." Proceedings of the National Academy of Sciences of the United States of America **103**(37): 13831-6.
- Buck, L. M., M. J. Winter, et al. (2012). "Ototoxin-induced cellular damage in neuromasts disrupts lateral line function in larval zebrafish." Hearing Research **284**(1-2): 67-81.
- Buehlmann, M., R. Frei, et al. (2008). "Highly effective regimen for decolonization of methicillin-resistant *Staphylococcus aureus* carriers." Infection Control and Hospital Epidemiology **29**(6): 510-6.
- Bunce, C., L. Wheeler, et al. (1992). "Murine model of cutaneous infection with gram-positive cocci." Infection and Immunity **60**(7): 2636-40.
- Burgess, S. M. and S. Lin. (2012). "Viral Insertion Mutants Overwrite Data. ZFIN Direct Data Submission (<http://zfin.org>)."
- Burgos, J. S., J. Ripoll-Gomez, et al. (2008). "Zebrafish as a new model for herpes simplex virus type 1 infection." Zebrafish **5**(4): 323-33.
- Busch-Nentwich, E., R. Kettleborough, et al. (2013). "Sanger Institute Zebrafish Mutation Project mutant data submission."

- Cade, L., D. Reyon, et al. (2012). "Highly efficient generation of heritable zebrafish gene mutations using homo- and heterodimeric TALENs." Nucleic Acids Res **40**(16): 8001-10.
- Campoy, E. and M. I. Colombo (2009). "Autophagy in intracellular bacterial infection." Biochimica et Biophysica Acta **1793**(9): 1465-77.
- Cao, Y., N. Semanchik, et al. (2009). "Chemical modifier screen identifies HDAC inhibitors as suppressors of PKD models." Proceedings of the National Academy of Sciences of the United States of America **106**(51): 21819-24.
- Carvalho, R., J. de Sonnevile, et al. (2011). "A high-throughput screen for tuberculosis progression." PLoS One **6**(2): e16779.
- Ceri, H., M. E. Olson, et al. (1999). "The Calgary Biofilm Device: new technology for rapid determination of antibiotic susceptibilities of bacterial biofilms." Journal of Clinical Microbiology **37**(6): 1771-6.
- Cermak, T., E. L. Doyle, et al. (2011). "Efficient design and assembly of custom TALEN and other TAL effector-based constructs for DNA targeting." Nucleic Acids Res **39**(12): e82.
- Chain, E., H. W. Florey, et al. (1940). "PENICILLIN AS A CHEMOTHERAPEUTIC AGENT." The Lancet **236**(6104): 226-228.
- Chambers, H. F. (1997). "Methicillin resistance in staphylococci: molecular and biochemical basis and clinical implications." Clinical Microbiology Reviews **10**(4): 781-91.
- Chan, P. F., S. J. Foster, et al. (1998). "The Staphylococcus aureus alternative sigma factor sigmaB controls the environmental stress response but not starvation survival or pathogenicity in a mouse abscess model." Journal of Bacteriology **180**(23): 6082-9.
- Chang, T. K., B. V. Shrivage, et al. (2013). "Uba1 functions in Atg7- and Atg3-independent autophagy." Nat Cell Biol **15**(9): 1067-78.
- Chao, C.-C., P.-C. Hsu, et al. (2010). "Zebrafish as a Model Host for Candida albicans Infection." Infection and Immunity **78**(6): 2512-2521.
- Chen, S., G. Oikonomou, et al. (2013). "A large-scale in vivo analysis reveals that TALENs are significantly more mutagenic than ZFNs generated using context-dependent assembly." Nucleic Acids Res **41**(4): 2769-78.
- Chen, Y. Y., C. C. Chao, et al. (2013). "Dynamic transcript profiling of Candida albicans infection in zebrafish: a pathogen-host interaction study." PLoS One **8**(9): e72483.
- Cheung, A. L., A. S. Bayer, et al. (2004). "Regulation of virulence determinants in vitro and in vivo in Staphylococcus aureus." FEMS Immunology and Medical Microbiology **40**(1): 1-9.
- Cheung, A. L., K. A. Nishina, et al. (2008). "The SarA protein family of Staphylococcus aureus." International Journal of Biochemistry and Cell Biology **40**(3): 355-61.
- Chico, T. J., P. W. Ingham, et al. (2008). "Modeling cardiovascular disease in the zebrafish." Trends in Cardiovascular Medicine **18**(4): 150-5.
- Choy, A., J. Dancourt, et al. (2012). "The Legionella effector RavZ inhibits host autophagy through irreversible Atg8 deconjugation." Science **338**(6110): 1072-6.
- Ciechanover, A. (2005). "Proteolysis: from the lysosome to ubiquitin and the proteasome." Nat Rev Mol Cell Biol **6**(1): 79-87.

- Clarke, S. R., P. G. Dalglish, et al. (1952). "HOSPITAL CROSS-INFECTIONS WITH STAPHYLOCOCCI RESISTANT TO SEVERAL ANTIBIOTICS." The Lancet **259**(6719): 1132-1135.
- Clatworthy, A. E., J. S. Lee, et al. (2009). "Pseudomonas aeruginosa infection of zebrafish involves both host and pathogen determinants." Infection and Immunity **77**(4): 1293-303.
- Coates, A. R., G. Halls, et al. (2011). "Novel classes of antibiotics or more of the same?" British Journal of Pharmacology **163**(1): 184-94.
- Coia, J. E., G. J. Duckworth, et al. (2006). "Guidelines for the control and prevention of methicillin-resistant Staphylococcus aureus (MRSA) in healthcare facilities." Journal of Hospital Infection **63 Suppl 1**: S1-44.
- Collins, C. A., A. De Maziere, et al. (2009). "Atg5-independent sequestration of ubiquitinated mycobacteria." PLoS Pathog **5**(5): e1000430.
- Collins, L. V., S. A. Kristian, et al. (2002). "Staphylococcus aureus strains lacking D-alanine modifications of teichoic acids are highly susceptible to human neutrophil killing and are virulence attenuated in mice." Journal of Infectious Diseases **186**(2): 214-9.
- Collins, L. V. and A. Tarkowski (2000). Animal models of experimental *Staphylococcus aureus* infection. Gram-Positive Pathogens. F. V. A. e. al. Washington, ASM Press.
- Colucci-Guyon, E., J. Y. Tinevez, et al. (2011). "Strategies of professional phagocytes in vivo: unlike macrophages, neutrophils engulf only surface-associated microbes." Journal of Cell Science **124**(Pt 18): 3053-9.
- Corey, G. R. (2009). "Staphylococcus aureus bloodstream infections: definitions and treatment." Clinical Infectious Diseases **48 Suppl 4**: S254-9.
- Craig, T. A., S. Sommer, et al. (2008). "Expression and regulation of the vitamin D receptor in the zebrafish, Danio rerio." Journal of Bone and Mineral Research **23**(9): 1486-96.
- D'Costa, V. M., C. E. King, et al. (2011). "Antibiotic resistance is ancient." Nature **477**(7365): 457-61.
- Da'as, S., E. M. Teh, et al. (2011). "Zebrafish mast cells possess an FcγR1-like receptor and participate in innate and adaptive immune responses." Developmental and Comparative Immunology **35**(1): 125-34.
- Davis, J. M., H. Clay, et al. (2002). "Real-time visualization of mycobacterium-macrophage interactions leading to initiation of granuloma formation in zebrafish embryos." Immunity **17**(6): 693-702.
- DeJonge, M., D. Burchfield, et al. (2007). "Clinical trial of safety and efficacy of INH-A21 for the prevention of nosocomial staphylococcal bloodstream infection in premature infants." Journal of Pediatrics **151**(3): 260-5, 265 e1.
- Demarchi, F., C. Bertoli, et al. (2007). "Calpain as a novel regulator of autophagosome formation." Autophagy **3**(3): 235-7.
- Demarchi, F., C. Bertoli, et al. (2006). "Calpain is required for macroautophagy in mammalian cells." Journal of Cell Biology **175**(4): 595-605.

- Deng, Q., E. A. Harvie, et al. (2012). "Distinct signalling mechanisms mediate neutrophil attraction to bacterial infection and tissue injury." Cell Microbiol **14**(4): 517-28.
- Deora, R. and T. K. Misra (1996). "Characterization of the primary sigma factor of *Staphylococcus aureus*." Journal of Biological Chemistry **271**(36): 21828-34.
- Deretic, V. (2012). "Autophagy: an emerging immunological paradigm." Journal of Immunology **189**(1): 15-20.
- Devereaux, K., C. Dall'Armi, et al. (2013). "Regulation of mammalian autophagy by class II and III PI 3-kinases through PI3P synthesis." PLoS One **8**(10): e76405.
- Ding, C. B., J. P. Zhang, et al. (2011). "Zebrafish as a potential model organism for drug test against hepatitis C virus." PLoS One **6**(8): e22921.
- Ding, Q., Y. K. Lee, et al. (2013). "A TALEN genome-editing system for generating human stem cell-based disease models." Cell Stem Cell **12**(2): 238-51.
- Dixon, J. and C. J. Duncan (2014). "Importance of antimicrobial stewardship to the English National Health Service." Infect Drug Resist **7**: 145-52.
- Dobson, J. T., J. Seibert, et al. (2008). "Carboxypeptidase A5 identifies a novel mast cell lineage in the zebrafish providing new insight into mast cell fate determination." Blood **112**(7): 2969-72.
- Dong, N., Y. Zhu, et al. (2012). "Structurally distinct bacterial TBC-like GAPs link Arf GTPase to Rab1 inactivation to counteract host defenses." Cell **150**(5): 1029-41.
- Dorn, B. R., W. A. Dunn, Jr., et al. (2001). "Porphyromonas gingivalis traffics to autophagosomes in human coronary artery endothelial cells." Infection and Immunity **69**(9): 5698-708.
- Dortet, L., S. Mostowy, et al. (2012). "Listeria and autophagy escape: involvement of InlK, an internalin-like protein." Autophagy **8**(1): 132-4.
- Draper, B. W., P. A. Morcos, et al. (2001). "Inhibition of zebrafish fgf8 pre-mRNA splicing with morpholino oligos: a quantifiable method for gene knockdown." Genesis **30**(3): 154-6.
- Dziewanowska, K., J. M. Patti, et al. (1999). "Fibronectin binding protein and host cell tyrosine kinase are required for internalization of *Staphylococcus aureus* by epithelial cells." Infection and Immunity **67**(9): 4673-8.
- Egile, C., T. P. Loisel, et al. (1999). "Activation of the CDC42 effector N-WASP by the *Shigella flexneri* IcsA protein promotes actin nucleation by Arp2/3 complex and bacterial actin-based motility." Journal of Cell Biology **146**(6): 1319-32.
- Eisen, J. S. and J. C. Smith (2008). "Controlling morpholino experiments: don't stop making antisense." Development **135**(10): 1735-43.
- Eisen, M. B., P. T. Spellman, et al. (1998). "Cluster analysis and display of genome-wide expression patterns." Proceedings of the National Academy of Sciences of the United States of America **95**(25): 14863-8.
- Ellett, F., L. Pase, et al. (2011). "mpeg1 promoter transgenes direct macrophage-lineage expression in zebrafish." Blood **117**(4): e49-56.

- Fattom, A. I., G. Horwith, et al. (2004). "Development of StaphVAX, a polysaccharide conjugate vaccine against *S. aureus* infection: from the lab bench to phase III clinical trials." Vaccine **22**(7): 880-7.
- Fleming, A. and D. C. Rubinsztein (2011). "Zebrafish as a model to understand autophagy and its role in neurological disease." Biochimica et Biophysica Acta **1812**(4): 520-6.
- Flick, M. J., X. Du, et al. (2004). "Fibrin(ogen)-alpha M beta 2 interactions regulate leukocyte function and innate immunity in vivo." Exp Biol Med (Maywood) **229**(11): 1105-10.
- Foster, T. (1996). Medical Microbiology, Chapter 12 Staphylococcus. Texas, Samuel Baron editor.
- Foster, T. J. (2005). "Immune evasion by staphylococci." Nat Rev Microbiol **3**(12): 948-58.
- Fournier, B. and D. J. Philpott (2005). "Recognition of *Staphylococcus aureus* by the innate immune system." Clinical Microbiology Reviews **18**(3): 521-40.
- Fowler, T., S. Johansson, et al. (2003). "Src kinase has a central role in in vitro cellular internalization of *Staphylococcus aureus*." Cell Microbiol **5**(6): 417-26.
- Fowler, V. G., K. B. Allen, et al. (2013). "Effect of an investigational vaccine for preventing *Staphylococcus aureus* infections after cardiothoracic surgery: a randomized trial." JAMA **309**(13): 1368-78.
- Frank, D. N., L. M. Feazel, et al. (2010). "The human nasal microbiota and *Staphylococcus aureus* carriage." PLoS One **5**(5): e10598.
- Frank, S., B. V. Skryabin, et al. (2013). "A modified TALEN-based system for robust generation of knock-out human pluripotent stem cell lines and disease models." BMC Genomics **14**: 773.
- Fridkin, S. K., J. C. Hageman, et al. (2005). "Methicillin-resistant *Staphylococcus aureus* disease in three communities." New England Journal of Medicine **352**(14): 1436-44.
- Fruman, D. A., R. E. Meyers, et al. (1998). "Phosphoinositide kinases." Annual Review of Biochemistry **67**: 481-507.
- Fujita, N., T. Itoh, et al. (2008). "The Atg16L complex specifies the site of LC3 lipidation for membrane biogenesis in autophagy." Molecular Biology of the Cell **19**(5): 2092-100.
- Fujiyuki, T., K. Imamura, et al. (2010). "Evaluation of therapeutic effects and pharmacokinetics of antibacterial chromogenic agents in a silkworm model of *Staphylococcus aureus* infection." Drug Discov Ther **4**(5): 349-54.
- Gaj, T., C. A. Gersbach, et al. (2013). "ZFN, TALEN, and CRISPR/Cas-based methods for genome engineering." Trends in Biotechnology **31**(7): 397-405.
- Ganley, I. G., H. Lam du, et al. (2009). "ULK1.ATG13.FIP200 complex mediates mTOR signaling and is essential for autophagy." Journal of Biological Chemistry **284**(18): 12297-305.
- Garcia-Lara, J., A. J. Needham, et al. (2005). "Invertebrates as animal models for *Staphylococcus aureus* pathogenesis: a window into host-pathogen interaction." FEMS Immunology and Medical Microbiology **43**(3): 311-23.

- Garzoni, C. and W. L. Kelley (2009). "Staphylococcus aureus: new evidence for intracellular persistence." Trends in Microbiology **17**(2): 59-65.
- Gasteiger, E., A. Gattiker, et al. (2003). "ExPASy: The proteomics server for in-depth protein knowledge and analysis." Nucleic Acids Res **31**(13): 3784-8.
- Ghebremedhin, B., F. Layer, et al. (2008). "Genetic classification and distinguishing of Staphylococcus species based on different partial gap, 16S rRNA, hsp60, rpoB, sodA, and tuf gene sequences." Journal of Clinical Microbiology **46**(3): 1019-25.
- Gibbs, E. M., E. J. Horstick, et al. (2013). "Swimming into prominence: the zebrafish as a valuable tool for studying human myopathies and muscular dystrophies." FEBS J **280**(17): 4187-97.
- Gibson, G. W., S. C. Kreuser, et al. (2007). "Development of a mouse model of induced Staphylococcus aureus infective endocarditis." Comp Med **57**(6): 563-9.
- Giese, B., S. Dittmann, et al. (2009). "Staphylococcal alpha-toxin is not sufficient to mediate escape from phagolysosomes in upper-airway epithelial cells." Infection and Immunity **77**(9): 3611-25.
- Giese, B., F. Glowinski, et al. (2010). "Expression of delta-toxin by Staphylococcus aureus mediates escape from phago-endosomes of human epithelial and endothelial cells in the presence of beta-toxin." Cell Microbiol **13**(2): 316-29.
- Gombart, A. F., N. Borregaard, et al. (2005). "Human cathelicidin antimicrobial peptide (CAMP) gene is a direct target of the vitamin D receptor and is strongly up-regulated in myeloid cells by 1,25-dihydroxyvitamin D3." FASEB Journal **19**(9): 1067-77.
- Gong, L., M. Cullinane, et al. (2011). "The Burkholderia pseudomallei type III secretion system and BopA are required for evasion of LC3-associated phagocytosis." PLoS One **6**(3): e17852.
- Goodyear, C. S. and G. J. Silverman (2004). "Staphylococcal toxin induced preferential and prolonged in vivo deletion of innate-like B lymphocytes." Proceedings of the National Academy of Sciences of the United States of America **101**(31): 11392-7.
- Gordon, P. B., I. Holen, et al. (1993). "Dependence of hepatocytic autophagy on intracellularly sequestered calcium." Journal of Biological Chemistry **268**(35): 26107-12.
- Granato, M., F. J. van Eeden, et al. (1996). "Genes controlling and mediating locomotion behavior of the zebrafish embryo and larva." Development **123**: 399-413.
- Gray, C., C. A. Loynes, et al. (2011). "Simultaneous intravital imaging of macrophage and neutrophil behaviour during inflammation using a novel transgenic zebrafish." Thrombosis and Haemostasis **105**(5): 811-9.
- Greenlee-Wacker, M. C., K. M. Rigby, et al. (2014). "Phagocytosis of Staphylococcus aureus by human neutrophils prevents macrophage efferocytosis and induces programmed necrosis." Journal of Immunology **192**(10): 4709-17.
- Gresham, H. D., J. H. Lowrance, et al. (2000). "Survival of Staphylococcus aureus inside neutrophils contributes to infection." Journal of Immunology **164**(7): 3713-22.

- Grunwald, D. J. and J. S. Eisen (2002). "Headwaters of the zebrafish -- emergence of a new model vertebrate." Nat Rev Genet **3**(9): 717-24.
- Gutierrez, M. G., D. B. Munafo, et al. (2004). "Rab7 is required for the normal progression of the autophagic pathway in mammalian cells." Journal of Cell Science **117**(Pt 13): 2687-97.
- Gutierrez, M. G., C. L. Vazquez, et al. (2005). "Autophagy induction favours the generation and maturation of the Coxiella-replicative vacuoles." Cell Microbiol **7**(7): 981-93.
- Haffter, P., M. Granato, et al. (1996). "The identification of genes with unique and essential functions in the development of the zebrafish, *Danio rerio*." Development **123**: 1-36.
- Hall, C., M. V. Flores, et al. (2007). "The zebrafish lysozyme C promoter drives myeloid-specific expression in transgenic fish." BMC Dev Biol **7**: 42.
- Hallare, A., K. Nagel, et al. (2006). "Comparative embryotoxicity and proteotoxicity of three carrier solvents to zebrafish (*Danio rerio*) embryos." Ecotoxicology and Environmental Safety **63**(3): 378-88.
- Hamasaki, M., N. Furuta, et al. (2013). "Autophagosomes form at ER-mitochondria contact sites." Nature **495**(7441): 389-93.
- Hamill, R. J., J. M. Vann, et al. (1986). "Phagocytosis of *Staphylococcus aureus* by cultured bovine aortic endothelial cells: model for postadherence events in endovascular infections." Infection and Immunity **54**(3): 833-6.
- Hanada, T., Y. Satomi, et al. (2009). "The amino-terminal region of Atg3 is essential for association with phosphatidylethanolamine in Atg8 lipidation." FEBS Letters **583**(7): 1078-83.
- Hanke, M. L., A. Angle, et al. (2012). "MyD88-dependent signaling influences fibrosis and alternative macrophage activation during *Staphylococcus aureus* biofilm infection." PLoS One **7**(8): e42476.
- Hart, P. D. and M. R. Young (1991). "Ammonium chloride, an inhibitor of phagosome-lysosome fusion in macrophages, concurrently induces phagosome-endosome fusion, and opens a novel pathway: studies of a pathogenic mycobacterium and a nonpathogenic yeast." Journal of Experimental Medicine **174**(4): 881-9.
- Harvie, E. A., J. M. Green, et al. (2013). "Innate immune response to *Streptococcus iniae* infection in zebrafish larvae." Infection and Immunity **81**(1): 110-21.
- Haslinger-Loffler, B., B. C. Kahl, et al. (2005). "Multiple virulence factors are required for *Staphylococcus aureus*-induced apoptosis in endothelial cells." Cell Microbiol **7**(8): 1087-97.
- He, C., C. R. Bartholomew, et al. (2009). "Assaying autophagic activity in transgenic GFP-Lc3 and GFP-Gabarap zebrafish embryos." Autophagy **5**(4): 520-6.
- Hegedus, Z., A. Zakrzewska, et al. (2009). "Deep sequencing of the zebrafish transcriptome response to mycobacterium infection." Molecular Immunology **46**(15): 2918-30.
- Herbomel, P., B. Thisse, et al. (1999). "Ontogeny and behaviour of early macrophages in the zebrafish embryo." Development **126**(17): 3735-45.

- Higgins, J., A. Loughman, et al. (2006). "Clumping factor A of *Staphylococcus aureus* inhibits phagocytosis by human polymorphonuclear leucocytes." FEMS Microbiology Letters **258**(2): 290-6.
- Hiramatsu, K., H. Hanaki, et al. (1997). "Methicillin-resistant *Staphylococcus aureus* clinical strain with reduced vancomycin susceptibility." Journal of Antimicrobial Chemotherapy **40**(1): 135-6.
- Hockemeyer, D., H. Wang, et al. (2011). "Genetic engineering of human pluripotent cells using TALE nucleases." Nature Biotechnology **29**(8): 731-4.
- Horsburgh, M. J., J. L. Aish, et al. (2002). "sigmaB modulates virulence determinant expression and stress resistance: characterization of a functional rsbU strain derived from *Staphylococcus aureus* 8325-4." Journal of Bacteriology **184**(19): 5457-67.
- Hosoi, S., T. Sakuma, et al. (2014). "Targeted mutagenesis in sea urchin embryos using TALENs." Development Growth and Differentiation **56**(1): 92-7.
- Howden, B. P. and M. L. Grayson (2006). "Dumb and dumber--the potential waste of a useful antistaphylococcal agent: emerging fusidic acid resistance in *Staphylococcus aureus*." Clinical Infectious Diseases **42**(3): 394-400.
- Howe, K., M. D. Clark, et al. (2013). "The zebrafish reference genome sequence and its relationship to the human genome." Nature **496**(7446): 498-503.
- Hu, Z., J. Zhang, et al. (2011). "Expression pattern and functions of autophagy-related gene atg5 in zebrafish organogenesis." Autophagy **7**(12): 1514-27.
- Hudson, M. C., W. K. Ramp, et al. (1995). "Internalization of *Staphylococcus aureus* by cultured osteoblasts." Microbial Pathogenesis **19**(6): 409-19.
- Hutchinson, S. A. and J. S. Eisen (2006). "Islet1 and Islet2 have equivalent abilities to promote motoneuron formation and to specify motoneuron subtype identity." Development **133**(11): 2137-47.
- Ichimura, Y., T. Kirisako, et al. (2000). "A ubiquitin-like system mediates protein lipidation." Nature **408**(6811): 488-92.
- Ip, W. K., A. Sokolovska, et al. (2010). "Phagocytosis and phagosome acidification are required for pathogen processing and MyD88-dependent responses to *Staphylococcus aureus*." Journal of Immunology **184**(12): 7071-81.
- Ishibashi, K., N. Fujita, et al. (2011). "Atg16L2, a novel isoform of mammalian Atg16L that is not essential for canonical autophagy despite forming an Atg12-5-16L2 complex." Autophagy **7**(12): 1500-13.
- Itakura, A. and O. J. McCarty (2013). "Pivotal role for the mTOR pathway in the formation of neutrophil extracellular traps (NETs) via regulation of autophagy." Am J Physiol Cell Physiol.
- Iwase, T., Y. Uehara, et al. (2010). "*Staphylococcus epidermidis* Esp inhibits *Staphylococcus aureus* biofilm formation and nasal colonization." Nature **465**(7296): 346-349.
- Jaber, N., Z. Dou, et al. (2012). "Class III PI3K Vps34 plays an essential role in autophagy and in heart and liver function." Proceedings of the

- National Academy of Sciences of the United States of America **109**(6): 2003-8.
- Jager, S., C. Bucci, et al. (2004). "Role for Rab7 in maturation of late autophagic vacuoles." Journal of Cell Science **117**(Pt 20): 4837-48.
- Jahreiss, L., F. M. Menzies, et al. (2008). "The itinerary of autophagosomes: from peripheral formation to kiss-and-run fusion with lysosomes." Traffic **9**(4): 574-87.
- Jarry, T. M. and A. L. Cheung (2006). "Staphylococcus aureus escapes more efficiently from the phagosome of a cystic fibrosis bronchial epithelial cell line than from its normal counterpart." Infection and Immunity **74**(5): 2568-77.
- Jarry, T. M., G. Memmi, et al. (2008). "The expression of alpha-haemolysin is required for Staphylococcus aureus phagosomal escape after internalization in CFT-1 cells." Cell Microbiol **10**(9): 1801-14.
- Jevons, P. M. (1961). "'Celbenin' - resistant Staphylococci." Br Med J. **1**(5219):b124-125.
- Jin, S. W., W. Herzog, et al. (2007). "A transgene-assisted genetic screen identifies essential regulators of vascular development in vertebrate embryos." Developmental Biology **307**(1): 29-42.
- Jin, T., M. Bokarewa, et al. (2004). "Staphylococcus aureus resists human defensins by production of staphylokinase, a novel bacterial evasion mechanism." Journal of Immunology **172**(2): 1169-76.
- Joshi, A. D. and M. S. Swanson (2011). "Secrets of a successful pathogen: legionella resistance to progression along the autophagic pathway." Front Microbiol **2**: 138.
- Joshi, G. S., J. S. Spontak, et al. (2011). "Arginine catabolic mobile element encoded speG abrogates the unique hypersensitivity of Staphylococcus aureus to exogenous polyamines." Molecular Microbiology **82**(1): 9-20.
- Jung, C. H., S. H. Ro, et al. (2010). "mTOR regulation of autophagy." FEBS Letters **584**(7): 1287-95.
- Kaatz, G. W., S. M. Seo, et al. (1993). "Efflux-mediated fluoroquinolone resistance in Staphylococcus aureus." Antimicrobial Agents and Chemotherapy **37**(5): 1086-94.
- Kabeya, Y., N. Mizushima, et al. (2000). "LC3, a mammalian homologue of yeast Apg8p, is localized in autophagosome membranes after processing." EMBO Journal **19**(21): 5720-8.
- Kahl, B. C., G. Belling, et al. (2003). "Thymidine-dependent small-colony variants of Staphylococcus aureus exhibit gross morphological and ultrastructural changes consistent with impaired cell separation." Journal of Clinical Microbiology **41**(1): 410-3.
- Kahl, B. C., M. Goulian, et al. (2000). "Staphylococcus aureus RN6390 replicates and induces apoptosis in a pulmonary epithelial cell line." Infection and Immunity **68**(9): 5385-92.
- Kaito, C., N. Akimitsu, et al. (2002). "Silkworm larvae as an animal model of bacterial infection pathogenic to humans." Microbial Pathogenesis **32**(4): 183-90.
- Kanther, M. and J. F. Rawls (2010). "Host-microbe interactions in the developing zebrafish." Current Opinion in Immunology **22**(1): 10-9.

- Katsuyama, T., A. Akhmedov, et al. (2013). "An efficient strategy for TALEN-mediated genome engineering in *Drosophila*." Nucleic Acids Res **41**(17): e163.
- Kay, J. E., L. Kromwel, et al. (1991). "Inhibition of T and B lymphocyte proliferation by rapamycin." Immunology **72**(4): 544-9.
- Kayath, C. A., S. Hussey, et al. (2010). "Escape of intracellular *Shigella* from autophagy requires binding to cholesterol through the type III effector, IcsB." Microbes Infect **12**(12-13): 956-66.
- Kennedy, A. D. and F. R. DeLeo (2009). "Neutrophil apoptosis and the resolution of infection." Immunologic Research **43**(1-3): 25-61.
- Keys, T. F. and W. L. Hewitt (1973). "Endocarditis due to *Micrococci* and *Staphylococcus epidermidis*." Archives of Internal Medicine **132**(2): 216-20.
- Kimura, S., T. Noda, et al. (2007). "Dissection of the autophagosome maturation process by a novel reporter protein, tandem fluorescent-tagged LC3." Autophagy **3**(5): 452-60.
- Kimura, S., T. Noda, et al. (2008). "Dynein-dependent movement of autophagosomes mediates efficient encounters with lysosomes." Cell Structure and Function **33**(1): 109-22.
- Kirkin, V., T. Lamark, et al. (2009). "A role for NBR1 in autophagosomal degradation of ubiquitinated substrates." Molecular Cell **33**(4): 505-16.
- Kissa, K. and P. Herbomel (2010). "Blood stem cells emerge from aortic endothelium by a novel type of cell transition." Nature **464**(7285): 112-5.
- Kissa, K., E. Murayama, et al. (2008). "Live imaging of emerging hematopoietic stem cells and early thymus colonization." Blood **111**(3): 1147-56.
- Klionsky, D. J., A. M. Cuervo, et al. (2007). "Methods for monitoring autophagy from yeast to human." Autophagy **3**(3): 181-206.
- Kobayashi, S. D., K. R. Braughton, et al. (2003). "Bacterial pathogens modulate an apoptosis differentiation program in human neutrophils." Proceedings of the National Academy of Sciences of the United States of America **100**(19): 10948-53.
- Kochl, R., X. W. Hu, et al. (2006). "Microtubules facilitate autophagosome formation and fusion of autophagosomes with endosomes." Traffic **7**(2): 129-45.
- Korczak, D. and C. Schoffmann (2010). "Medical and health economic evaluation of prevention- and control measures related to MRSA infections or -colonisations at hospitals." GMS Health Technol Assess **6**: Doc04.
- Koziel, J., A. Maciag-Gudowska, et al. (2009). "Phagocytosis of *Staphylococcus aureus* by macrophages exerts cytoprotective effects manifested by the upregulation of antiapoptotic factors." PLoS One **4**(4): e5210.
- Kriegeskorte, A., S. Konig, et al. (2011). "Small colony variants of *Staphylococcus aureus* reveal distinct protein profiles." Proteomics **11**(12): 2476-90.
- Kristian, S. A., M. Durr, et al. (2003). "MprF-mediated lysinylation of phospholipids in *Staphylococcus aureus* leads to protection against

- oxygen-independent neutrophil killing." Infection and Immunity **71**(1): 546-9.
- Kubica, M., K. Guzik, et al. (2008). "A potential new pathway for Staphylococcus aureus dissemination: the silent survival of S. aureus phagocytosed by human monocyte-derived macrophages." PLoS One **3**(1): e1409.
- Kugelberg, E., T. Norstrom, et al. (2005). "Establishment of a superficial skin infection model in mice by using Staphylococcus aureus and Streptococcus pyogenes." Antimicrobial Agents and Chemotherapy **49**(8): 3435-41.
- Kuma, A., M. Hatano, et al. (2004). "The role of autophagy during the early neonatal starvation period." Nature **432**(7020): 1032-6.
- Kyme, P., N. H. Thoennissen, et al. (2012). "C/EBPepsilon mediates nicotinamide-enhanced clearance of Staphylococcus aureus in mice." Journal of Clinical Investigation.
- Lam, G. Y., M. Cemma, et al. (2013). "Host and bacterial factors that regulate LC3 recruitment to Listeria monocytogenes during the early stages of macrophage infection." Autophagy **9**(7).
- Lam, S. H., H. L. Chua, et al. (2004). "Development and maturation of the immune system in zebrafish, Danio rerio: a gene expression profiling, in situ hybridization and immunological study." Developmental and Comparative Immunology **28**(1): 9-28.
- Langenau, D. M., A. A. Ferrando, et al. (2004). "In vivo tracking of T cell development, ablation, and engraftment in transgenic zebrafish." Proc Natl Acad Sci U S A **101**(19): 7369-74.
- Langheinrich, U. (2003). "Zebrafish: a new model on the pharmaceutical catwalk." Bioessays **25**(9): 904-12.
- Le Guyader, D., M. J. Redd, et al. (2008). "Origins and unconventional behavior of neutrophils in developing zebrafish." Blood **111**(1): 132-41.
- Lee, E., Y. Koo, et al. (2014). "Autophagy is essential for cardiac morphogenesis during vertebrate development." Autophagy **10**(4): 572-87.
- Lee, L. Y., Y. J. Miyamoto, et al. (2002). "The Staphylococcus aureus Map protein is an immunomodulator that interferes with T cell-mediated responses." Journal of Clinical Investigation **110**(10): 1461-71.
- Lei, Y., X. Guo, et al. (2013). "Generation of gene disruptions by transcription activator-like effector nucleases (TALENs) in Xenopus tropicalis embryos." Cell Biosci **3**(1): 21.
- Lei, Y., X. Guo, et al. (2012). "Efficient targeted gene disruption in Xenopus embryos using engineered transcription activator-like effector nucleases (TALENs)." Proceedings of the National Academy of Sciences of the United States of America **109**(43): 17484-9.
- Lerena, M. C. and M. I. Colombo (2011). "Mycobacterium marinum induces a marked LC3 recruitment to its containing phagosome that depends on a functional ESX-1 secretion system." Cell Microbiol **13**(6): 814-35.
- Levraud, J. P., P. Boudinot, et al. (2007). "Identification of the zebrafish IFN receptor: implications for the origin of the vertebrate IFN system." Journal of Immunology **178**(7): 4385-94.

- Levraud, J. P., O. Disson, et al. (2009). "Real-time observation of listeria monocytogenes-phagocyte interactions in living zebrafish larvae." Infection and Immunity **77**(9): 3651-60.
- Li, T., S. Huang, et al. (2011). "Modularly assembled designer TAL effector nucleases for targeted gene knockout and gene replacement in eukaryotes." Nucleic Acids Res **39**(14): 6315-25.
- Li, T., B. Liu, et al. (2012). "High-efficiency TALEN-based gene editing produces disease-resistant rice." Nature Biotechnology **30**(5): 390-2.
- Li, Y. J. and B. Hu (2012). "Establishment of Multi-Site Infection Model in Zebrafish Larvae for Studying Staphylococcus aureus Infectious Disease." J Genet Genomics **39**(9): 521-34.
- Lieschke, G. J., A. C. Oates, et al. (2001). "Morphologic and functional characterization of granulocytes and macrophages in embryonic and adult zebrafish." Blood **98**(10): 3087-96.
- Lin, B., S. Chen, et al. (2007). "Acute phase response in zebrafish upon Aeromonas salmonicida and Staphylococcus aureus infection: striking similarities and obvious differences with mammals." Molecular Immunology **44**(4): 295-301.
- Lindeman, R. E. and F. Pelegri (2010). "Vertebrate maternal-effect genes: Insights into fertilization, early cleavage divisions, and germ cell determinant localization from studies in the zebrafish." Molecular Reproduction and Development **77**(4): 299-313.
- Liou, W., H. J. Geuze, et al. (1997). "The autophagic and endocytic pathways converge at the nascent autophagic vacuoles." Journal of Cell Biology **136**(1): 61-70.
- Liu, S. and S. D. Leach (2011). "Zebrafish models for cancer." Annu Rev Pathol **6**: 71-93.
- Loewith, R., E. Jacinto, et al. (2002). "Two TOR complexes, only one of which is rapamycin sensitive, have distinct roles in cell growth control." Molecular Cell **10**(3): 457-68.
- Lopez-Munoz, A., M. P. Sepulcre, et al. (2011). "Evolutionary conserved pro-inflammatory and antigen presentation functions of zebrafish IFN γ revealed by transcriptomic and functional analysis." Molecular Immunology **48**(9-10): 1073-83.
- Lugo-Villarino, G., K. M. Balla, et al. (2010). "Identification of dendritic antigen-presenting cells in the zebrafish." Proceedings of the National Academy of Sciences of the United States of America **107**(36): 15850-5.
- Luong, T. T. and C. Y. Lee (2002). "Overproduction of type 8 capsular polysaccharide augments Staphylococcus aureus virulence." Infection and Immunity **70**(7): 3389-95.
- Ma, A. C., H. B. Lee, et al. (2013). "High Efficiency In Vivo Genome Engineering with a Simplified 15-RVD GoldyTALEN Design." PLoS One **8**(5): e65259.
- Maggini, S., E. S. Wintergerst, et al. (2007). "Selected vitamins and trace elements support immune function by strengthening epithelial barriers and cellular and humoral immune responses." British Journal of Nutrition **98 Suppl 1**: S29-35.

- Makky, K., J. Tekiela, et al. (2007). "Target of rapamycin (TOR) signaling controls epithelial morphogenesis in the vertebrate intestine." Developmental Biology **303**(2): 501-13.
- Mantovani, A., A. Sica, et al. (2004). "The chemokine system in diverse forms of macrophage activation and polarization." Trends Immunol **25**(12): 677-86.
- Mari, M., S. A. Tooze, et al. (2011). "The puzzling origin of the autophagosomal membrane." F1000 Biol Rep **3**: 25.
- Martinez, J., J. Almendinger, et al. (2011). "Microtubule-associated protein 1 light chain 3 alpha (LC3)-associated phagocytosis is required for the efficient clearance of dead cells." Proceedings of the National Academy of Sciences of the United States of America **108**(42): 17396-401.
- Mathias, J. R., B. J. Perrin, et al. (2006). "Resolution of inflammation by retrograde chemotaxis of neutrophils in transgenic zebrafish." Journal of Leukocyte Biology **80**(6): 1281-8.
- Maurin, M., H. Lepidi, et al. (1997). "Guinea pig model for *Staphylococcus aureus* native valve endocarditis." Antimicrobial Agents and Chemotherapy **41**(8): 1815-7.
- Mauthe, M., W. Yu, et al. (2012). "WIPI-1 Positive Autophagosome-Like Vesicles Entrap Pathogenic *Staphylococcus aureus* for Lysosomal Degradation." Int J Cell Biol **2012**: 179207.
- McVicker, G., T. K. Prajsnar, et al. (2014). "Clonal Expansion during *Staphylococcus aureus* Infection Dynamics Reveals the Effect of Antibiotic Intervention." PLoS Pathog **10**(2): e1003959.
- Meijer, W. H., I. J. van der Klei, et al. (2007). "ATG genes involved in non-selective autophagy are conserved from yeast to man, but the selective Cvt and pexophagy pathways also require organism-specific genes." Autophagy **3**(2): 106-16.
- Menzies, B. E. and I. Kourteva (2000). "*Staphylococcus aureus* alpha-toxin induces apoptosis in endothelial cells." FEMS Immunology and Medical Microbiology **29**(1): 39-45.
- Mestre, M. B. and M. I. Colombo (2012). "cAMP and EPAC are key players in the regulation of the signal transduction pathway involved in the alpha-hemolysin autophagic response." PLoS Pathog **8**(5): e1002664.
- Mestre, M. B. and M. I. Colombo (2012). "*Staphylococcus aureus* promotes autophagy by decreasing intracellular cAMP levels." Autophagy **8**(12): 1865-7.
- Mestre, M. B., C. M. Fader, et al. (2010). "Alpha-hemolysin is required for the activation of the autophagic pathway in *Staphylococcus aureus*-infected cells." Autophagy **6**(1): 110-25.
- Metlagel, Z., C. Otomo, et al. (2013). "Structural basis of ATG3 recognition by the autophagic ubiquitin-like protein ATG12." Proceedings of the National Academy of Sciences of the United States of America **110**(47): 18844-9.
- Miller, L. S., R. M. O'Connell, et al. (2006). "MyD88 mediates neutrophil recruitment initiated by IL-1R but not TLR2 activation in immunity against *Staphylococcus aureus*." Immunity **24**(1): 79-91.

- Miyazaki, S., Y. Matsumoto, et al. (2012). "Evaluation of *Staphylococcus aureus* virulence factors using a silkworm model." FEMS Microbiology Letters **326**(2): 116-24.
- Mizushima, N. (2007). "Autophagy: process and function." Genes and Development **21**(22): 2861-73.
- Mizushima, N., A. Kuma, et al. (2003). "Mouse Apg16L, a novel WD-repeat protein, targets to the autophagic isolation membrane with the Apg12-Apg5 conjugate." Journal of Cell Science **116**(Pt 9): 1679-88.
- Mizushima, N., H. Sugita, et al. (1998). "A new protein conjugation system in human. The counterpart of the yeast Apg12p conjugation system essential for autophagy." Journal of Biological Chemistry **273**(51): 33889-92.
- Mizushima, N., A. Yamamoto, et al. (2001). "Dissection of autophagosome formation using Apg5-deficient mouse embryonic stem cells." Journal of Cell Biology **152**(4): 657-68.
- Mizushima, N., A. Yamamoto, et al. (2004). "In vivo analysis of autophagy in response to nutrient starvation using transgenic mice expressing a fluorescent autophagosome marker." Molecular Biology of the Cell **15**(3): 1101-11.
- Mizushima, N., T. Yoshimori, et al. (2002). "Mouse Apg10 as an Apg12-conjugating enzyme: analysis by the conjugation-mediated yeast two-hybrid method." FEBS Letters **532**(3): 450-4.
- Molina, G. A., S. C. Watkins, et al. (2007). "Generation of FGF reporter transgenic zebrafish and their utility in chemical screens." BMC Dev Biol **7**: 62.
- Monteiro, R., C. Pouget, et al. (2011). "The gata1/pu.1 lineage fate paradigm varies between blood populations and is modulated by tif1gamma." EMBO Journal **30**(6): 1093-103.
- Moore, F. E., D. Reyon, et al. (2012). "Improved somatic mutagenesis in zebrafish using transcription activator-like effector nucleases (TALENs)." PLoS One **7**(5): e37877.
- Moscou, M. J. and A. J. Bogdanove (2009). "A simple cipher governs DNA recognition by TAL effectors." Science **326**(5959): 1501.
- Mostowy, S., L. Boucontet, et al. (2013). "The Zebrafish as a New Model for the In Vivo Study of *Shigella flexneri* Interaction with Phagocytes and Bacterial Autophagy." PLoS Pathog **9**(9): e1003588.
- Moy, T. I., A. R. Ball, et al. (2006). "Identification of novel antimicrobials using a live-animal infection model." Proceedings of the National Academy of Sciences of the United States of America **103**(27): 10414-9.
- Moy, T. I., A. L. Conery, et al. (2009). "High-throughput screen for novel antimicrobials using a whole animal infection model." ACS Chem Biol **4**(7): 527-33.
- Murai, M., A. Usui, et al. (1992). "Intracellular localization of *Staphylococcus aureus* within primary cultured mouse kidney cells." Microbiology and Immunology **36**(5): 431-43.
- Murayama, E., K. Kissa, et al. (2006). "Tracing hematopoietic precursor migration to successive hematopoietic organs during zebrafish development." Immunity **25**(6): 963-75.
- Nakagawa, I., A. Amano, et al. (2004). "Autophagy defends cells against invading group A *Streptococcus*." Science **306**(5698): 1037-40.

- Nakatogawa, H., Y. Ichimura, et al. (2007). "Atg8, a ubiquitin-like protein required for autophagosome formation, mediates membrane tethering and hemifusion." Cell **130**(1): 165-78.
- Nasevicius, A. and S. C. Ekker (2000). "Effective targeted gene 'knockdown' in zebrafish." Nature Genetics **26**(2): 216-20.
- Needham, A. J., M. Kibart, et al. (2004). "Drosophila melanogaster as a model host for Staphylococcus aureus infection." Microbiology **150**(Pt 7): 2347-55.
- Neely, M. N., J. D. Pfeifer, et al. (2002). "Streptococcus-zebrafish model of bacterial pathogenesis." Infection and Immunity **70**(7): 3904-14.
- Neyfakh, A. A., C. M. Borsch, et al. (1993). "Fluoroquinolone resistance protein NorA of Staphylococcus aureus is a multidrug efflux transporter." Antimicrobial Agents and Chemotherapy **37**(1): 128-9.
- Niethammer, P., C. Grabher, et al. (2009). "A tissue-scale gradient of hydrogen peroxide mediates rapid wound detection in zebrafish." Nature **459**(7249): 996-9.
- Nieto, C. and M. Espinosa (2003). "Construction of the mobilizable plasmid pMV158GFP, a derivative of pMV158 that carries the gene encoding the green fluorescent protein." Plasmid **49**(3): 281-5.
- Niggli, V. (2003). "Microtubule-disruption-induced and chemotactic-peptide-induced migration of human neutrophils: implications for differential sets of signalling pathways." Journal of Cell Science **116**(Pt 5): 813-22.
- Nishida, Y., S. Arakawa, et al. (2009). "Discovery of Atg5/Atg7-independent alternative macroautophagy." Nature **461**(7264): 654-8.
- Niu, H., M. Yamaguchi, et al. (2008). "Subversion of cellular autophagy by Anaplasma phagocytophilum." Cell Microbiol **10**(3): 593-605.
- Noda, T., N. Fujita, et al. (2008). "The Ubi brothers reunited." Autophagy **4**(4): 540-1.
- Noda, T. and Y. Ohsumi (1998). "Tor, a phosphatidylinositol kinase homologue, controls autophagy in yeast." Journal of Biological Chemistry **273**(7): 3963-6.
- Novick, R. P. (2003). "Autoinduction and signal transduction in the regulation of staphylococcal virulence." Molecular Microbiology **48**(6): 1429-49.
- Nozawa, T., C. Aikawa, et al. (2010). "The small GTPases Rab9A and Rab23 function at distinct steps in autophagy during Group A Streptococcus infection." Cell Microbiol **14**(8): 1149-65.
- Nulens, E., E. Broex, et al. (2008). "Cost of the meticillin-resistant Staphylococcus aureus search and destroy policy in a Dutch university hospital." Journal of Hospital Infection **68**(4): 301-7.
- Nüsslein-Volhard, C. and R. Sahm (2002). Zebrafish. Oxford, Oxford University Press.
- Nuzzo, I., M. R. Sanges, et al. (2000). "Apoptosis of human keratinocytes after bacterial invasion." FEMS Immunology and Medical Microbiology **27**(3): 235-40.
- O'Toole, R., J. Von Hofsten, et al. (2004). "Visualisation of zebrafish infection by GFP-labelled Vibrio anguillarum." Microbial Pathogenesis **37**(1): 41-6.
- Ogawa, M., Y. Yoshikawa, et al. (2011). "A Tecpr1-dependent selective autophagy pathway targets bacterial pathogens." Cell Host Microbe **9**(5): 376-89.

- Ogawa, M., T. Yoshimori, et al. (2005). "Escape of intracellular Shigella from autophagy." Science **307**(5710): 727-31.
- Ogryzko, N. V., E. E. Hoggett, et al. (2014). "Zebrafish tissue injury causes up-regulation of interleukin-1 and caspase dependent amplification of the inflammatory response." Dis Model Mech.
- Ogston, A. (1984). "Classics in infectious diseases. "On abscesses"." Reviews of Infectious Diseases **6**(1): 122-8.
- Ohsumi, Y. (1999). "Molecular mechanism of autophagy in yeast, *Saccharomyces cerevisiae*." Philosophical Transactions of the Royal Society of London. Series B: Biological Sciences **354**(1389): 1577-80; discussion 1580-1.
- Olson, M. E., H. Ceri, et al. (2002). "Biofilm bacteria: formation and comparative susceptibility to antibiotics." Canadian Journal of Veterinary Research **66**(2): 86-92.
- Ordas, A., Z. Hegedus, et al. (2011). "Deep sequencing of the innate immune transcriptomic response of zebrafish embryos to Salmonella infection." Fish Shellfish Immunol **31**(5): 716-24.
- Otto, M. (2008). "Staphylococcal biofilms." Current Topics in Microbiology and Immunology **322**: 207-28.
- Otto, M. (2013). "Community-associated MRSA: what makes them special?" International Journal of Medical Microbiology **303**(6-7): 324-30.
- Oviedo-Boyso, J., R. Cortes-Vieyra, et al. (2011). "The phosphoinositide-3-kinase-Akt signaling pathway is important for Staphylococcus aureus internalization by endothelial cells." Infection and Immunity **79**(11): 4569-77.
- Palha, N., F. Guivel-Benhassine, et al. (2013). "Real-time whole-body visualization of chikungunya virus infection and host interferon response in zebrafish." PLoS Pathog **9**(9): e1003619.
- Pankiv, S., T. H. Clausen, et al. (2007). "p62/SQSTM1 binds directly to Atg8/LC3 to facilitate degradation of ubiquitinated protein aggregates by autophagy." Journal of Biological Chemistry **282**(33): 24131-45.
- Papakyriacou, H., D. Vaz, et al. (2000). "Molecular analysis of the accessory gene regulator (agr) locus and balance of virulence factor expression in epidemic methicillin-resistant Staphylococcus aureus." Journal of Infectious Diseases **181**(3): 990-1000.
- Parikka, M., M. M. Hammaren, et al. (2012). "Mycobacterium marinum causes a latent infection that can be reactivated by gamma irradiation in adult zebrafish." PLoS Pathog **8**(9): e1002944.
- Patel, J. B., R. J. Gorwitz, et al. (2009). "Mupirocin resistance." Clinical Infectious Diseases **49**(6): 935-41.
- Patterson, H., A. Saralahti, et al. (2012). "Adult zebrafish model of bacterial meningitis in Streptococcus agalactiae infection." Developmental and Comparative Immunology **38**(3): 447-55.
- Peterson, R. T., B. A. Link, et al. (2000). "Small molecule developmental screens reveal the logic and timing of vertebrate development." Proceedings of the National Academy of Sciences of the United States of America **97**(24): 12965-9.
- Petiot, A., E. Ogier-Denis, et al. (2000). "Distinct classes of phosphatidylinositol 3'-kinases are involved in signaling pathways that

- control macroautophagy in HT-29 cells." Journal of Biological Chemistry **275**(2): 992-8.
- Piette, A. and G. Verschraegen (2009). "Role of coagulase-negative staphylococci in human disease." Veterinary Microbiology **134**(1-2): 45-54.
- Ponce de Leon, V., A. M. Merillat, et al. (2014). "Generation of TALEN-Mediated GR(dim) Knock-In Rats by Homologous Recombination." PLoS One **9**(2): e88146.
- Postma, B., M. J. Poppelier, et al. (2004). "Chemotaxis inhibitory protein of *Staphylococcus aureus* binds specifically to the C5a and formylated peptide receptor." Journal of Immunology **172**(11): 6994-7001.
- Pragman, A. A. and P. M. Schlievert (2004). "Virulence regulation in *Staphylococcus aureus*: the need for in vivo analysis of virulence factor regulation." FEMS Immunology and Medical Microbiology **42**(2): 147-54.
- Prajsnar, T. K., V. T. Cunliffe, et al. (2008). "A novel vertebrate model of *Staphylococcus aureus* infection reveals phagocyte-dependent resistance of zebrafish to non-host specialized pathogens." Cell Microbiol **10**(11): 2312-25.
- Prajsnar, T. K., R. Hamilton, et al. (2012). "A privileged intraphagocyte niche is responsible for disseminated infection of *Staphylococcus aureus* in a zebrafish model." Cell Microbiol.
- Prajsnar, T. K., S. A. Renshaw, et al. (2013). "Zebrafish as a novel vertebrate model to dissect enterococcal pathogenesis." Infection and Immunity.
- Prescott, L. M., J. P. Harley, et al. (1999). Microbiology. Boston, WCB/McGraw-Hill.
- Pressley, M. E., P. E. Phelan, 3rd, et al. (2005). "Pathogenesis and inflammatory response to *Edwardsiella tarda* infection in the zebrafish." Developmental and Comparative Immunology **29**(6): 501-13.
- Proctor, R. A. (2012). "Is there a future for a *Staphylococcus aureus* vaccine?" Vaccine **30**(19): 2921-7.
- Proikas-Cezanne, T. and H. Robenek (2011). "Freeze-fracture replica immunolabelling reveals human WIPI-1 and WIPI-2 as membrane proteins of autophagosomes." J Cell Mol Med **15**(9): 2007-10.
- Proikas-Cezanne, T., S. Ruckerbauer, et al. (2007). "Human WIPI-1 puncta-formation: a novel assay to assess mammalian autophagy." FEBS Letters **581**(18): 3396-404.
- Qazi, S. N., E. Counil, et al. (2001). "agr expression precedes escape of internalized *Staphylococcus aureus* from the host endosome." Infection and Immunity **69**(11): 7074-82.
- Qiu, Z., M. Liu, et al. (2013). "High-efficiency and heritable gene targeting in mouse by transcription activator-like effector nucleases." Nucleic Acids Res **41**(11): e120.
- Rammelkamp, M. (1942). "Resistances of *Staphylococcus aureus* to the action of penicillin." Proc Soc Exp Biol Med **51**:386-9.
- Redd, M. J., G. Kelly, et al. (2006). "Imaging macrophage chemotaxis in vivo: studies of microtubule function in zebrafish wound inflammation." Cell Motility and the Cytoskeleton **63**(7): 415-22.

- Remijnsen, Q., T. W. Kuijpers, et al. (2011). "Dying for a cause: NETosis, mechanisms behind an antimicrobial cell death modality." Cell Death and Differentiation **18**(4): 581-8.
- Renna, M., C. F. Bento, et al. (2013). "IGF-1 receptor antagonism inhibits autophagy." Human Molecular Genetics.
- Renna, M., M. Jimenez-Sanchez, et al. (2010). "Chemical inducers of autophagy that enhance the clearance of mutant proteins in neurodegenerative diseases." Journal of Biological Chemistry **285**(15): 11061-7.
- Renshaw, S. A., C. A. Loynes, et al. (2006). "A transgenic zebrafish model of neutrophilic inflammation." Blood **108**(13): 3976-8.
- Rhodes, J., A. Hagen, et al. (2005). "Interplay of pu.1 and gata1 determines myelo-erythroid progenitor cell fate in zebrafish." Dev Cell **8**(1): 97-108.
- Rigby, K. M. and F. R. DeLeo (2012). "Neutrophils in innate host defense against *Staphylococcus aureus* infections." Semin Immunopathol **34**(2): 237-59.
- Robertson, A. L., G. R. Holmes, et al. (2014). "A zebrafish compound screen reveals modulation of neutrophil reverse migration as an anti-inflammatory mechanism." Sci Transl Med **6**(225): 225ra29.
- Roca, F. J., I. Mulero, et al. (2008). "Evolution of the inflammatory response in vertebrates: fish TNF-alpha is a powerful activator of endothelial cells but hardly activates phagocytes." Journal of Immunology **181**(7): 5071-81.
- Rodriguez, I., B. Novoa, et al. (2008). "Immune response of zebrafish (*Danio rerio*) against a newly isolated bacterial pathogen *Aeromonas hydrophila*." Fish Shellfish Immunol **25**(3): 239-49.
- Rodvold, K. A. and K. W. McConeghy (2014). "Methicillin-resistant *Staphylococcus aureus* therapy: past, present, and future." Clinical Infectious Diseases **58** Suppl 1: S20-7.
- Romano, P. S., M. G. Gutierrez, et al. (2007). "The autophagic pathway is actively modulated by phase II *Coxiella burnetii* to efficiently replicate in the host cell." Cell Microbiol **9**(4): 891-909.
- Rooijackers, S. H., M. Ruyken, et al. (2005). "Immune evasion by a staphylococcal complement inhibitor that acts on C3 convertases." Nat Immunol **6**(9): 920-7.
- Rooijackers, S. H., W. J. van Wamel, et al. (2005). "Anti-opsonic properties of staphylokinase." Microbes Infect **7**(3): 476-84.
- Rounioja, S., A. Saralahti, et al. (2011). "Defense of zebrafish embryos against *Streptococcus pneumoniae* infection is dependent on the phagocytic activity of leukocytes." Developmental and Comparative Immunology.
- Rountree, P. and E. Thomson (1952). "INCIDENCE OF ANTIBIOTIC-RESISTANT STAPHYLOCOCCI IN A HOSPITAL." The Lancet **260**(6728): 262-265.
- Rupp, M. E., H. P. Holley, Jr., et al. (2007). "Phase II, randomized, multicenter, double-blind, placebo-controlled trial of a polyclonal anti-*Staphylococcus aureus* capsular polysaccharide immune globulin in treatment of *Staphylococcus aureus* bacteremia." Antimicrobial Agents and Chemotherapy **51**(12): 4249-54.

- Rusten, T. E., K. Lindmo, et al. (2004). "Programmed autophagy in the *Drosophila* fat body is induced by ecdysone through regulation of the PI3K pathway." *Dev Cell* **7**(2): 179-92.
- Saldanha, A. J. (2004). "Java Treeview--extensible visualization of microarray data." *Bioinformatics* **20**(17): 3246-8.
- Sanjuan, M. A., C. P. Dillon, et al. (2007). "Toll-like receptor signalling in macrophages links the autophagy pathway to phagocytosis." *Nature* **450**(7173): 1253-7.
- Santoro, J. and M. E. Levison (1978). "Rat model of experimental endocarditis." *Infection and Immunity* **19**(3): 915-8.
- Sarkar, S., R. A. Floto, et al. (2005). "Lithium induces autophagy by inhibiting inositol monophosphatase." *Journal of Cell Biology* **170**(7): 1101-11.
- Sarkar, S., G. Krishna, et al. (2008). "A rational mechanism for combination treatment of Huntington's disease using lithium and rapamycin." *Human Molecular Genetics* **17**(2): 170-8.
- Sarris, M., J. B. Masson, et al. (2012). "Inflammatory chemokines direct and restrict leukocyte migration within live tissues as glycan-bound gradients." *Current Biology* **22**(24): 2375-82.
- Scherr, T. D., C. E. Heim, et al. (2014). "Hiding in Plain Sight: Interplay between Staphylococcal Biofilms and Host Immunity." *Front Immunol* **5**: 37.
- Schiebler, M., K. Brown, et al. (2014). "Functional drug screening reveals anticonvulsants as enhancers of mTOR-independent autophagic killing of *Mycobacterium tuberculosis* through inositol depletion." *EMBO Mol Med* **7**(2): 127-39.
- Schnaith, A., H. Kashkar, et al. (2007). "Staphylococcus aureus subvert autophagy for induction of caspase-independent host cell death." *Journal of Biological Chemistry* **282**(4): 2695-706.
- Schroder, A., R. Kland, et al. (2006). "Live cell imaging of phagosome maturation in *Staphylococcus aureus* infected human endothelial cells: small colony variants are able to survive in lysosomes." *Med Microbiol Immunol* **195**(4): 185-94.
- Schroder, A., B. Schroder, et al. (2006). "Staphylococcus aureus fibronectin binding protein-A induces motile attachment sites and complex actin remodeling in living endothelial cells." *Molecular Biology of the Cell* **17**(12): 5198-210.
- Schwarz-Linek, U., J. M. Werner, et al. (2003). "Pathogenic bacteria attach to human fibronectin through a tandem beta-zipper." *Nature* **423**(6936): 177-81.
- Scott, D. F., J. M. Kling, et al. (1983). "Characterization of *Staphylococcus aureus* isolates from patients with toxic shock syndrome, using polyethylene infection chambers in rabbits." *Infection and Immunity* **39**(1): 383-7.
- Segal, B. H., T. L. Leto, et al. (2000). "Genetic, biochemical, and clinical features of chronic granulomatous disease." *Medicine* **79**(3): 170-200.
- Seglen, P. O. and P. Bohley (1992). "Autophagy and other vacuolar protein degradation mechanisms." *Experientia* **48**(2): 158-72.
- Seishima, M., G. Kato, et al. (2009). "Cytokine profile during the clinical course of toxic shock syndrome." *Clinical and Experimental Dermatology* **34**(8): e632-5.

- Shahnazari, S., W. L. Yen, et al. (2010). "A diacylglycerol-dependent signaling pathway contributes to regulation of antibacterial autophagy." Cell Host Microbe **8**(2): 137-46.
- Shan, Q., Y. Wang, et al. (2013). "Rapid and efficient gene modification in rice and *Brachypodium* using TALENs." Mol Plant **6**(4): 1365-8.
- Shimizu, S., S. Arakawa, et al. (2010). "Autophagy takes an alternative pathway." Autophagy **6**(2): 290-1.
- Shpilka, T., H. Weidberg, et al. (2011). "Atg8: an autophagy-related ubiquitin-like protein family." Genome Biol **12**(7): 226.
- Shrivastav, M., L. P. De Haro, et al. (2008). "Regulation of DNA double-strand break repair pathway choice." Cell Research **18**(1): 134-47.
- Sieprawska-Lupa, M., P. Mydel, et al. (2004). "Degradation of human antimicrobial peptide LL-37 by *Staphylococcus aureus*-derived proteinases." Antimicrobial Agents and Chemotherapy **48**(12): 4673-9.
- Sievers, F., A. Wilm, et al. (2011). "Fast, scalable generation of high-quality protein multiple sequence alignments using Clustal Omega." Mol Syst Biol **7**: 539.
- Sifri, C. D., J. Begun, et al. (2003). "Caenorhabditis elegans as a model host for *Staphylococcus aureus* pathogenesis." Infection and Immunity **71**(4): 2208-17.
- Silva, M. T. (2010). "When two is better than one: macrophages and neutrophils work in concert in innate immunity as complementary and cooperative partners of a myeloid phagocyte system." Journal of Leukocyte Biology **87**(1): 93-106.
- Simor, A. E., E. Phillips, et al. (2007). "Randomized controlled trial of chlorhexidine gluconate for washing, intranasal mupirocin, and rifampin and doxycycline versus no treatment for the eradication of methicillin-resistant *Staphylococcus aureus* colonization." Clinical Infectious Diseases **44**(2): 178-85.
- Sinha, B., P. P. Francois, et al. (1999). "Fibronectin-binding protein acts as *Staphylococcus aureus* invasin via fibronectin bridging to integrin alpha5beta1." Cell Microbiol **1**(2): 101-17.
- Smith, E. J., L. Visai, et al. (2011). "The Sbi protein is a multifunctional immune evasion factor of *Staphylococcus aureus*." Infection and Immunity **79**(9): 3801-9.
- Sokolovska, A., C. E. Becker, et al. (2013). "Activation of caspase-1 by the NLRP3 inflammasome regulates the NADPH oxidase NOX2 to control phagosome function." Nat Immunol **14**(6): 543-53.
- Sou, Y. S., S. Waguri, et al. (2008). "The Atg8 conjugation system is indispensable for proper development of autophagic isolation membranes in mice." Molecular Biology of the Cell **19**(11): 4762-75.
- Stachura, D. L., O. Svoboda, et al. (2013). "The zebrafish granulocyte colony-stimulating factors (Gcsfs): 2 paralogous cytokines and their roles in hematopoietic development and maintenance." Blood **122**(24): 3918-28.
- Starr, T., R. Child, et al. (2012). "Selective subversion of autophagy complexes facilitates completion of the *Brucella* intracellular cycle." Cell Host Microbe **11**(1): 33-45.

- Stephens, L., C. Ellson, et al. (2002). "Roles of PI3Ks in leukocyte chemotaxis and phagocytosis." Current Opinion in Cell Biology **14**(2): 203-13.
- Stranger-Jones, Y. K., T. Bae, et al. (2006). "Vaccine assembly from surface proteins of *Staphylococcus aureus*." Proceedings of the National Academy of Sciences of the United States of America **103**(45): 16942-7.
- Stromhaug, P. E. and P. O. Seglen (1993). "Evidence for acidity of prelysosomal autophagic/endocytic vacuoles (amphisomes)." Biochemical Journal **291** (Pt 1): 115-21.
- Sturgill-Koszycki, S. and M. S. Swanson (2000). "Legionella pneumophila replication vacuoles mature into acidic, endocytic organelles." Journal of Experimental Medicine **192**(9): 1261-72.
- Summerton, J. (1999). "Morpholino antisense oligomers: the case for an RNase H-independent structural type." Biochimica et Biophysica Acta **1489**(1): 141-58.
- Summerton, J. and D. Weller (1997). "Morpholino antisense oligomers: design, preparation, and properties." Antisense and Nucleic Acid Drug Development **7**(3): 187-95.
- Sung, Y. H., I. J. Baek, et al. (2013). "Knockout mice created by TALEN-mediated gene targeting." Nature Biotechnology **31**(1): 23-4.
- Swanson, J. A. and S. C. Baer (1995). "Phagocytosis by zippers and triggers." Trends in Cell Biology **5**(3): 89-93.
- Takaki, K., C. L. Cosma, et al. (2012). "An in vivo platform for rapid high-throughput antitubercular drug discovery." Cell Rep **2**(1): 175-84.
- Takemura-Uchiyama, I., J. Uchiyama, et al. (2013). "Evaluating efficacy of bacteriophage therapy against *Staphylococcus aureus* infections using a silkworm larval infection model." FEMS Microbiology Letters **347**(1): 52-60.
- Takeshige, K., M. Baba, et al. (1992). "Autophagy in yeast demonstrated with proteinase-deficient mutants and conditions for its induction." Journal of Cell Biology **119**(2): 301-11.
- Takeuchi, O., K. Hoshino, et al. (2000). "Cutting edge: TLR2-deficient and MyD88-deficient mice are highly susceptible to *Staphylococcus aureus* infection." Journal of Immunology **165**(10): 5392-6.
- Tanida, I., N. Minematsu-Ikeguchi, et al. (2005). "Lysosomal turnover, but not a cellular level, of endogenous LC3 is a marker for autophagy." Autophagy **1**(2): 84-91.
- Tanida, I., Y. S. Sou, et al. (2004). "HsAtg4B/HsApg4B/autophagin-1 cleaves the carboxyl termini of three human Atg8 homologues and delipidates microtubule-associated protein light chain 3- and GABAA receptor-associated protein-phospholipid conjugates." Journal of Biological Chemistry **279**(35): 36268-76.
- Tanida, I., E. Tanida-Miyake, et al. (2002). "Human Apg3p/Aut1p homologue is an authentic E2 enzyme for multiple substrates, GATE-16, GABARAP, and MAP-LC3, and facilitates the conjugation of hApg12p to hApg5p." Journal of Biological Chemistry **277**(16): 13739-44.
- Tanida, I., E. Tanida-Miyake, et al. (2001). "The human homolog of *Saccharomyces cerevisiae* Apg7p is a Protein-activating enzyme for

- multiple substrates including human Apg12p, GATE-16, GABARAP, and MAP-LC3." Journal of Biological Chemistry **276**(3): 1701-6.
- Tanida, I., T. Ueno, et al. (2004). "Human light chain 3/MAP1LC3B is cleaved at its carboxyl-terminal Met121 to expose Gly120 for lipidation and targeting to autophagosomal membranes." Journal of Biological Chemistry **279**(46): 47704-10.
- Tarkowski, A., L. V. Collins, et al. (2001). "Model systems: modeling human staphylococcal arthritis and sepsis in the mouse." Trends in Microbiology **9**(7): 321-6.
- Tarrand, J. J., P. R. LaSala, et al. (2012). "Dimethyl sulfoxide enhances effectiveness of skin antiseptics and reduces contamination rates of blood cultures." Journal of Clinical Microbiology **50**(5): 1552-7.
- Tassa, A., M. P. Roux, et al. (2003). "Class III phosphoinositide 3-kinase--Beclin1 complex mediates the amino acid-dependent regulation of autophagy in C2C12 myotubes." Biochemical Journal **376**(Pt 3): 577-86.
- Thakker, M., J. S. Park, et al. (1998). "Staphylococcus aureus serotype 5 capsular polysaccharide is antiphagocytic and enhances bacterial virulence in a murine bacteremia model." Infection and Immunity **66**(11): 5183-9.
- Thammavongsa, V., D. M. Missiakas, et al. (2013). "Staphylococcus aureus degrades neutrophil extracellular traps to promote immune cell death." Science **342**(6160): 863-6.
- Thurlow, L. R., M. L. Hanke, et al. (2011). "Staphylococcus aureus biofilms prevent macrophage phagocytosis and attenuate inflammation in vivo." Journal of Immunology **186**(11): 6585-96.
- Thurston, T. L., G. Ryzhakov, et al. (2009). "The TBK1 adaptor and autophagy receptor NDP52 restricts the proliferation of ubiquitin-coated bacteria." Nat Immunol **10**(11): 1215-21.
- Thwaites, G. E. and V. Gant (2011). "Are bloodstream leukocytes Trojan Horses for the metastasis of Staphylococcus aureus?" Nat Rev Microbiol **9**(3): 215-22.
- Tipper, D. J. and J. L. Strominger (1965). "Mechanism of action of penicillins: a proposal based on their structural similarity to acyl-D-alanyl-D-alanine." Proceedings of the National Academy of Sciences of the United States of America **54**(4): 1133-41.
- Tooze, J., M. Hollinshead, et al. (1990). "In exocrine pancreas, the basolateral endocytic pathway converges with the autophagic pathway immediately after the early endosome." Journal of Cell Biology **111**(2): 329-45.
- Tuchscher, L., E. Medina, et al. (2011). "Staphylococcus aureus phenotype switching: an effective bacterial strategy to escape host immune response and establish a chronic infection." EMBO Mol Med **3**(3): 129-41.
- Turlej, A., W. Hryniewicz, et al. (2011). "Staphylococcal cassette chromosome mec (Sccmec) classification and typing methods: an overview." Pol J Microbiol **60**(2): 95-103.
- Turner, R. D., E. C. Ratcliffe, et al. (2010). "Peptidoglycan architecture can specify division planes in Staphylococcus aureus." Nat Commun **1**: 26.

- Ulphani, J. S. and M. E. Rupp (1999). "Model of Staphylococcus aureus central venous catheter-associated infection in rats." Laboratory Animal Science **49**(3): 283-7.
- Underwood, B. R., S. Imarisio, et al. (2010). "Antioxidants can inhibit basal autophagy and enhance neurodegeneration in models of polyglutamine disease." Human Molecular Genetics **19**(17): 3413-29.
- Usui, A., M. Murai, et al. (1992). "Conspicuous ingestion of Staphylococcus aureus organisms by murine fibroblasts in vitro." Microbiology and Immunology **36**(5): 545-50.
- Valeva, A., I. Walev, et al. (1997). "Transmembrane beta-barrel of staphylococcal alpha-toxin forms in sensitive but not in resistant cells." Proceedings of the National Academy of Sciences of the United States of America **94**(21): 11607-11.
- van der Sar, A. M., B. J. Appelmeik, et al. (2004). "A star with stripes: zebrafish as an infection model." Trends in Microbiology **12**(10): 451-7.
- van der Sar, A. M., R. J. Musters, et al. (2003). "Zebrafish embryos as a model host for the real time analysis of Salmonella typhimurium infections." Cell Microbiol **5**(9): 601-11.
- van der Vaart, M., H. P. Spaank, et al. (2012). "Pathogen Recognition and Activation of the Innate Immune Response in Zebrafish." Adv Hematol **2012**: 159807.
- van Rijen, M., M. Bonten, et al. (2008) "Mupirocin ointment for preventing Staphylococcus aureus infections in nasal carriers." Cochrane Database of Systematic Reviews DOI: 10.1002/14651858.CD006216.pub2.
- van Rijen, M. M. and J. A. Kluytmans (2009). "Costs and benefits of the MRSA Search and Destroy policy in a Dutch hospital." European Journal of Clinical Microbiology and Infectious Diseases **28**(10): 1245-52.
- Varga, M., M. Sass, et al. (2014). "Autophagy is required for zebrafish caudal fin regeneration." Cell Death and Differentiation **21**(4): 547-56.
- Varshney, G. K., J. Lu, et al. "A large-scale zebrafish gene knockout resource for the genome-wide study of gene function." Genome Research **23**(4): 727-35.
- Vaudaux, P., P. Francois, et al. (2002). "Increased expression of clumping factor and fibronectin-binding proteins by hemB mutants of Staphylococcus aureus expressing small colony variant phenotypes." Infection and Immunity **70**(10): 5428-37.
- Veneman, W. J., O. W. Stockhammer, et al. (2013). "A zebrafish high throughput screening system used for Staphylococcus epidermidis infection marker discovery." BMC Genomics **14**(1): 255.
- Verdrengh, M. and A. Tarkowski (1997). "Role of neutrophils in experimental septicemia and septic arthritis induced by Staphylococcus aureus." Infection and Immunity **65**(7): 2517-21.
- Vergunst, A. C., A. H. Meijer, et al. (2010). "Burkholderia cenocepacia creates an intramacrophage replication niche in zebrafish embryos, followed by bacterial dissemination and establishment of systemic infection." Infection and Immunity **78**(4): 1495-508.
- Vlahos, C. J., W. F. Matter, et al. (1994). "A specific inhibitor of phosphatidylinositol 3-kinase, 2-(4-morpholinyl)-8-phenyl-4H-1-

- benzopyran-4-one (LY294002)." Journal of Biological Chemistry **269**(7): 5241-8.
- von Eiff, C. (2008). "Staphylococcus aureus small colony variants: a challenge to microbiologists and clinicians." International Journal of Antimicrobial Agents **31**(6): 507-10.
- von Eiff, C., K. Becker, et al. (2001). "Nasal carriage as a source of Staphylococcus aureus bacteremia. Study Group." New England Journal of Medicine **344**(1): 11-6.
- von Eiff, C., G. Peters, et al. (2006). "The small colony variant (SCV) concept -- the role of staphylococcal SCVs in persistent infections." Injury **37 Suppl 2**: S26-33.
- von Muhlinen, N., T. Thurston, et al. (2010). "NDP52, a novel autophagy receptor for ubiquitin-decorated cytosolic bacteria." Autophagy **6**(2): 288-9.
- Vos, M. C., M. D. Behrendt, et al. (2009). "5 years of experience implementing a methicillin-resistant Staphylococcus aureus search and destroy policy at the largest university medical center in the Netherlands." Infection Control and Hospital Epidemiology **30**(10): 977-84.
- Walker, S., P. Chandra, et al. (2008). "Making autophagosomes: localized synthesis of phosphatidylinositol 3-phosphate holds the clue." Autophagy **4**(8): 1093-6.
- Wang, D., L. E. Jao, et al. (2007). "Efficient genome-wide mutagenesis of zebrafish genes by retroviral insertions." Proceedings of the National Academy of Sciences of the United States of America **104**(30): 12428-33.
- Wang, F. D., Y. Y. Chen, et al. (2008). "Risk factors and mortality in patients with nosocomial Staphylococcus aureus bacteremia." American Journal of Infection Control **36**(2): 118-22.
- Wang, T. T., F. P. Nestel, et al. (2004). "Cutting edge: 1,25-dihydroxyvitamin D3 is a direct inducer of antimicrobial peptide gene expression." Journal of Immunology **173**(5): 2909-12.
- Wang, Z., S. Zhang, et al. (2008). "Response of complement expression to challenge with lipopolysaccharide in embryos/larvae of zebrafish Danio rerio: acquisition of immunocompetent complement." Fish Shellfish Immunol **25**(3): 264-70.
- Webster, P., I. J. JW, et al. (1998). "The agent of Human Granulocytic Ehrlichiosis resides in an endosomal compartment." Journal of Clinical Investigation **101**(9): 1932-41.
- Wefers, B., S. K. Panda, et al. (2013). "Generation of targeted mouse mutants by embryo microinjection of TALEN mRNA." Nat Protoc **8**(12): 2355-79.
- Wei, Y., S. Pattingre, et al. (2008). "JNK1-mediated phosphorylation of Bcl-2 regulates starvation-induced autophagy." Molecular Cell **30**(6): 678-88.
- Wertheim, H. F., M. C. Vos, et al. (2004). "Risk and outcome of nosocomial Staphylococcus aureus bacteraemia in nasal carriers versus non-carriers." Lancet **364**(9435): 703-5.
- Wesson, C. A., L. E. Liou, et al. (1998). "Staphylococcus aureus Agr and Sar global regulators influence internalization and induction of apoptosis." Infection and Immunity **66**(11): 5238-43.

- Wild, P., H. Farhan, et al. (2011). "Phosphorylation of the autophagy receptor optineurin restricts Salmonella growth." Science **333**(6039): 228-33.
- Williams, A., S. Sarkar, et al. (2008). "Novel targets for Huntington's disease in an mTOR-independent autophagy pathway." Nat Chem Biol **4**(5): 295-305.
- Williams, C. H. and C. C. Hong (2011). "Multi-step usage of in vivo models during rational drug design and discovery." Int J Mol Sci **12**(4): 2262-74.
- Williams, R. S., L. Cheng, et al. (2002). "A common mechanism of action for three mood-stabilizing drugs." Nature **417**(6886): 292-5.
- Wilson, E. B. and M. M. Hilferty (1931). "The Distribution of Chi-Square." Proceedings of the National Academy of Sciences of the United States of America **17**(12): 684-8.
- Wyman, C. and R. Kanaar (2006). "DNA double-strand break repair: all's well that ends well." Annual Review of Genetics **40**: 363-83.
- Wymann, M. P., G. Bulgarelli-Leva, et al. (1996). "Wortmannin inactivates phosphoinositide 3-kinase by covalent modification of Lys-802, a residue involved in the phosphate transfer reaction." Molecular and Cellular Biology **16**(4): 1722-33.
- Xia, H. G., L. Zhang, et al. (2010). "Control of basal autophagy by calpain1 mediated cleavage of ATG5." Autophagy **6**(1): 61-6.
- Xiao, A., Z. Wang, et al. (2013). "Chromosomal deletions and inversions mediated by TALENs and CRISPR/Cas in zebrafish." Nucleic Acids Res.
- Yamada, Y., N. N. Suzuki, et al. (2007). "The crystal structure of Atg3, an autophagy-related ubiquitin carrier protein (E2) enzyme that mediates Atg8 lipidation." Journal of Biological Chemistry **282**(11): 8036-43.
- Yamaguchi, H., I. Nakagawa, et al. (2009). "An initial step of GAS-containing autophagosome-like vacuoles formation requires Rab7." PLoS Pathog **5**(11): e1000670.
- Yamatake, K., M. Maeda, et al. (2007). "Role for gingipains in Porphyromonas gingivalis traffic to phagolysosomes and survival in human aortic endothelial cells." Infection and Immunity **75**(5): 2090-100.
- Yan, M., S. J. Pamp, et al. (2013). "Nasal microenvironments and interspecific interactions influence nasal microbiota complexity and S. aureus carriage." Cell Host Microbe **14**(6): 631-40.
- Yang, L., L. Bu, et al. (2014). "Functional characterization of mannose-binding lectin in zebrafish: Implication for a lectin-dependent complement system in early embryos." Developmental and Comparative Immunology **46**(2): 314-22.
- Yaniv, K., S. Isogai, et al. (2006). "Live imaging of lymphatic development in the zebrafish." Nature Medicine **12**(6): 711-6.
- Yoder, J. A. (2009). "Form, function and phylogenetics of NITRs in bony fish." Developmental and Comparative Immunology **33**(2): 135-44.
- Yoong, P. and V. J. Torres (2013). "The effects of Staphylococcus aureus leukotoxins on the host: cell lysis and beyond." Current Opinion in Microbiology **16**(1): 63-9.

- Yoshikawa, Y., M. Ogawa, et al. (2009). "Listeria monocytogenes ActA-mediated escape from autophagic recognition." Nat Cell Biol **11**(10): 1233-40.
- Yoshimori, T. (2006). "Autophagy vs. Group A Streptococcus." Autophagy **2**(3): 154-5.
- Yoshimoto, K., H. Hanaoka, et al. (2004). "Processing of ATG8s, ubiquitin-like proteins, and their deconjugation by ATG4s are essential for plant autophagy." Plant Cell **16**(11): 2967-83.
- Zetola, N., J. S. Francis, et al. (2005). "Community-acquired methicillin-resistant Staphylococcus aureus: an emerging threat." Lancet Infect Dis **5**(5): 275-86.
- Zhang, L., J. Yu, et al. (2007). "Small molecule regulators of autophagy identified by an image-based high-throughput screen." Proceedings of the National Academy of Sciences of the United States of America **104**(48): 19023-8.
- Zhang, Y., F. Zhang, et al. (2013). "Transcription activator-like effector nucleases enable efficient plant genome engineering." Plant Physiology **161**(1): 20-7.
- Zheng, Y. T., S. Shahnazari, et al. (2009). "The adaptor protein p62/SQSTM1 targets invading bacteria to the autophagy pathway." Journal of Immunology **183**(9): 5909-16.
- Zhou, C., W. Zhong, et al. (2012). "Monitoring autophagic flux by an improved tandem fluorescent-tagged LC3 (mTagRFP-mWasabi-LC3) reveals that high-dose rapamycin impairs autophagic flux in cancer cells." Autophagy **8**(8): 1215-26.
- Zu, Y., X. Tong, et al. (2013). "TALEN-mediated precise genome modification by homologous recombination in zebrafish." Nat Methods **10**(4): 329-31.

Appendix 1

A

atg5_zebrafish	1	MIMADDDKDLRDVWFGRIPACFTLSPDEETTEREAEPYLLPRVSYLTLVTDKVKKHFLK	60
atg5_human	1	--MTDDKDLRDVWFGRIPCTFTLYQDEITEREAEPYLLPRVSYLTLVTDKVKKHFK	58
		*:*****:**** ** ***** *	
atg5_zebrafish	61	VMKAEDVEEMWFEHGTPLKWHYPIGLFDLHASNSALPWNITVHFKNPEQDLLHCSTN	120
atg5_human	59	VMRQEDISEIWFYEGTPLKWHYPIGLFDLASSALPWNITVHFKSEPEKDLLHCPSK	118
		**:.*:	
atg5_zebrafish	121	SVIEAHFMSCIKADALKHKQVINDMQKDKHQLWMGLQNDKFDQFWAMNRKLMYPTPE	180
atg5_human	119	DAIEAHFMSCMKADALKHKSQVINEMQKDKHQLWMGLQNDRFQDFWAINRKLMEYPAE	178
		..*****:*****:****:*****:*****:*****:*****:*****:*****:	
atg5_zebrafish	181	EGGFRYIPFRYIQTMSDRPFIQTLFRPVSSEGOALTLGDLLKELFPAAIED--EPKFKVQ	238
atg5_human	179	ENGFRIYIPFRYIQTTERPFIQKLRPVAADGQLHTLGDLLKEVCPSAIDPEDGKKNQV	238
		* ***** :*****:****:*****:**** *****: *:*: ** **	
atg5_zebrafish	239	MIHGIEPLETPIQWLSEHLSHPDNFLHISIIIPASD	275
atg5_human	239	MIHGIEPMLBTPLQWLSEHLSYDPNFLHISIIIPQPTD	275
		*****:****:*****:*****:***** *:*	

B

atg7_zebrafish	1	----MAESSLKLQFAPFCSALEAGFWHQLTQKKLNEYRLDESPKNIKGYYYNGDAVGLP	55
atg7_human	1	MAAATGDPGLSKLQFAPFSSALDVGFWHELQKKLNEYRLDEAPKDIKGYYYNGDSAGLP	60
		. *****:****:*****:*****:*****:*****:*****:*****:*****:	
atg7_zebrafish	56	ARLTLEFSAPFDADGPTPARCCPASGTLVYNTTLEAPKSTDKKALLDKAANEIWSAIQSCA	115
atg7_human	61	ARLTLEFSAPFMSAPTPARCCPAIGTLVYNTTLESPKTDKLLLEQAANEIWSIKSGT	120
		***** .***** *****:****:**** *:*:*****:****:****:	
atg7_zebrafish	116	ALEDSSILNKFI LLTFADLKKYHFYWFPCPALCFVGIQLLRAPLSLEQHFSDKQISSL	175
atg7_human	121	ALENPVLNKFLLTFADLKKYHFYWFPCPALCLPESLPLIQGPVGLDQRFSLKQIEAL	180
		: **:*****:*****:****: *.: *:*:*:*:*:* *:*:*:	
atg7_zebrafish	176	Q SAYDNLCASGTTAVPHFLKYSEESVEVAPLKEINLSPFDLKNYTTIYIFQDPCTLPQ	235
atg7_human	181	ECAYDNLCQEGVTALPYFLIKYDENMVLVSLKHYSDFFQGRTKITIG-VYDPCNLAQ	239
		:.*****:*.***:***:***: * * * * .** * . * * . * * * * *	
atg7_zebrafish	236	HPGWPLRNLVLLAKKWSQLDVVEVLCFRDRTQGVRSVQHSIIFQLRLSDPAPSAEAL	295
atg7_human	240	HPGWPLRNLVLAHRWSSSQSVEVLCFRDRTQGVARDVAHSIIFEVKLEPMAFSPDCP	299
		:*****:*** *:*:*:*:*: *:	
atg7_zebrafish	296	VOIHWKMIHSIQGNSAFVSECQKVRLEASSVDLNLKLMRWLVPALDLEKVVSTRCL	355
atg7_human	300	KAVGWKNQKGMGPRMVNLSECMDPKRLAESSVDLNLKLMRWLVPALDLEKVVSVKCL	359
		: * * * * . * * . :*** ***** *****:*****:*****:*****:***	
atg7_zebrafish	356	LLGAGTLGCNVARTLMGWVRHITFVDNAKISYSNPVROPLYEFEDCLSG-KSKALAAVD	414
atg7_human	360	LLGAGTLGCNVARTLMGWVRHITFVDNAKISYSNPVROPLYEFEDCLGGKPKALAAVD	419
		*****:*****:*****:*****:*****:*****:*****:*****:*****:*****:	
atg7_zebrafish	415	RLKKIIPPGVNAEGFNMSIPMPGHPVNFSDLTVAQAQDVEQLKLISEHDVVFLMDTRE	474
atg7_human	420	RLQKIPPGVNAEGFNMSIPMPGHPVNFSSVLEQARRDVEQLEQLIESHDVVFLMDTRE	479
		::*****:*****:*****:****: *:*:*****:****:*****:*****:*****:	
atg7_zebrafish	475	SRWLPVIAASQRKLI VNAALGFDTFVVMRHGLKPKRDSGSGFL--RHKLISGYVYRSSL	532
atg7_human	480	SRWLPVIAASKRKL VINAALGFDTFVVMRHGLKPKKQQAQGLCPNHVPVADLLGSSL	539
		*****:*****:***:*****:*****:*****:*****:*****:*****:*****:*****:	
atg7_zebrafish	533	FSNIPGHRGCGYFCNDVVAPGDSTRDRTLQDQCTVSRPGLAVIAGALAVELMVSVLQHP	592
atg7_human	540	FANIPGYKLGCGYFCNDVVAPGDSTRDRTLQDQCTVSRPGLAVIAGALAVELMVSVLQHP	599
		*:*****:*****:*****:*****:*****:*****:*****:*****:*****:*****:	
atg7_zebrafish	593	GGYAVASSDDRMNEPPTSLGLVPHQIRGFLSRFDNVLPASLAFDKCTACSPVILENYER	652
atg7_human	600	GGYAIASSDDRMNEPPTSLGLVPHQIRGFLSRFDNVLPVSLAFDKCTACSSKVLQYER	659
		:**:*****:*****:*****:*****:*****:*****:*****:*****:*****:	
atg7_zebrafish	653	EGFQFLAKVFNSSHSFLEDLTGLTLLHQETQAAEMWSTTEDQRK	697
atg7_human	660	EGFNFLLAKVFNSSHSFLEDLTGLTLLHQETQAAEI-WDMSDETI	703
		:**:*****:*****:*****:*****:*****:*****:*****:*****:*****:	

